Εθνικό Μετσόβιο Πολυτεχνείο

Σχολή Πολιτικών Μηχανικών

Τομέας Γεωτεχνικής

National Technical University of Athens

School of Civil Engineering

Geotechnical Division

Diploma Thesis by

ITALOS MARIOS

Supervised by

Assistant Professor N. Gerolymos

ΜΗ ΓΡΑΜΜΙΚΗ ΣΕΙΣΜΙΚΗ ΑΠΟΚΡΙΣΗ ΕΔΑΦΙΚΟΥ ΣΧΗΜΑΤΙΣΜΟΥ: ΣΥΓΚΡΙΣΗ ΚΑΤΑΣΤΑΤΙΚΩΝ ΠΡΟΣΟΜΟΙΩΜΑΤΩΝ

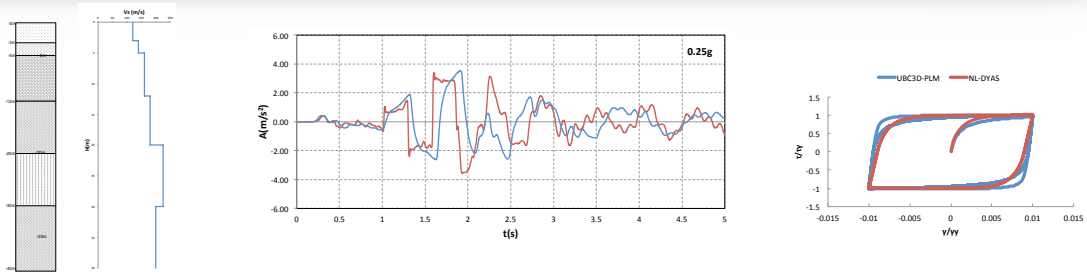

NON LINEAR SEISMIC RESPONSE OF SOIL DEPOSITS: A COMPARATIVE STUDY OF CONSTITUTIVE MODELS

Διπλωματική εργασία

ΙΤΑΛΟΥ ΜΑΡΙΟΥ

Επιβλέπων:

Επίκουρος Καθηγητής Ν. Γερόλυμος

Αθήνα, Ιούλιος 2015 ***Athens, July 2015***

Στην οικογένεια μου και στην Ζωή

Acknowledgements

Upon completing this diploma thesis I would like to thank my professor mr. N. Gerolymos for his immense help and guidance throughout the preparing of this thesis. His help and knowledge have been a valuable asset and working with him was a unique opportunity. He selfishly offered his knowledge and his time to surpass any obstacle and for all the above I am greatful.

I would also like to thank my family for all their support through this 5 year degree. They stood by me on every step in my life in both successes and failures. I promise their efforts and legacy will not go in vain.

TABLE OF CONTENTS

Περίληψη

Στην παρούσα διπλωματική γίνεται αναφορά σε τρία καταστατικά προσομοιώματα, για την μη γραμμική μονοδιάστατη ανάλυση της σεισμικής απόκρισης πολύστρωτου εδαφικού σχηματίσμού καθώς και εκθετικα σκληρυνόμενου μοντέλου.

Τα δύο εκ των ανωτέρω αφορούν ενα παλιό και ενα καινούργιο τροποποιημένο μοντέλο σε αντιπαραβολή με ενα διαφορετικό προσομοίωμα. Το πρωτότυπο αφορά το μοντέλο BWGG το οποίο είχε ώς βάση το μοντέλο Bouc Wen ενώ το νεότερο μοντέλο εφαρμόζει το “smooth hysteresis hypothesis” το οποίο αποκαλείται BWGG modified. Η συγκριση επικεντρώνεται μεταξύ των BWGG modified και του UBCSAND. Το τελευταίο (UBCSAND) έχει ευρεία εφαρμογή σε έργα μηχανικού καθώς εφαρμόζεται σε δημοφιλής εμπορικούς κώδικες όπως το FLAC και το PLAXIS είναι εξιδικευμένο σε απόκριση αμμώδους εδαφικού σχηματισμού σε συνθήκες ρευστοποίησης.

Στην διπλωματική αυτή τίθεται το ερώτημα του εαν δεν υπάρχουν συνθήκες ρευστοποίησης τότε, κατα πόσο ένα ευρέως διαδεδομένο εμπορικώς προσομοίωμα μπορεί να ανταπεξέλθει σε αντιπαραβολή με προσομοίωμα καταξιωμένο σε τέτοιες συνθήκες και επιβεβαιωμένα σε συγκρισεις με διεθνή βιβλιογραφια (BWGG modified)

Στο δεύτερο κεφάλαιο γίνεται παρουσίαση των προσομοιωμάτων καθώς και των νόμων που τους διέπουν. Γίνεται αναφορά στο Masing Criterion.

Στο τρίτο κεφάλαιο γίνεται ρύθμιση και βαθμονόμηση των παραμέτρων που θα χρησιμοποιηθούν για σύγκριση των προσομοιωμάτων. Ακολουθούν δοκιμες για την βαθμονόμηση και προτείνετε μέθοδος επιλογής των παραμέτρων ώστε τα προσομοιώματα να καταστούν ισοδύναμα ούτως ώστε να καταστούν κατα το δυνατόν συγκρίσημα. Η μέθοδος βασίζεται τόσο στην χρήση των καμπύλων Ishibashi & Chang όσο και σε ορισμένες παραδοχές και αποκλεισμό παραμέτρων μετά απο δοκιμές. Η ταυτοποίηση του νέου μοντέλου και του UBC3D-PLM είναι πρακτικώς αδύνατη, δια το λόγο αυτό παρουσιάζεται μεθοδολογία επαλήθευσης και επικύρωσης του UBC3D-PLM μέσω του αρχικού προσομοιώματος BWGG σε επιπεδο βρόγχων.

Στο τέταρτο κεφάλαιο αναπτύσσονται 2 πειραματικές διατάξεις εδαφικών στυλών 40 μέτρων βάθους. Η πρώτη αφορά πολύστρωτο εδαφικό σχηματισμό ενω η δεύτερη αφορά σχηματισμό που μεταβάλλεται με το βάθος εκθετικά. Οι δύο σχηματισμοί υποβάλλονται σε διαδοχικές δοκιμες με το ζεύγος υστερητικών κωδίκων ("NL-DYAS" που αφορά την μέθοδο BWGG και τον κώδικα "NL-DYAS modified" που αφορά το new smooth hysteresis model) σε σχέση με την μέθοδο UBCSAND που εφαρμόζεται στον κώδικα "UBC3D-PLM" με έμφαση στο ζεύγος "NL-DYAS modified" και "UBC3D-PLM". Οι πειραματικές διατάξεις υποβάλλονται τα επιταχυνσιογραφήματα του Αιγίου(1995) 0.39g, της Λευκάδας (2003) με 0.42g, και τον πιό καταστροφικό αυτο του Kobe(1995) με 0.68g. Στόχος είναι η επαλήθευση και η επικύρωση του UBCSAND προσομοιώματος υποβάλλοντας το σε έλεγχους ορθότητας της μαθηματικής προσέγγισης του, αλλά καί στην ορθότητα του σε επίπεδο φυσικής των αποτελεσμάτων (μετακινήσεις κλπ.). Τα αποτελέσματα παρουσιάζουν τα επιταχυνσιογραφήματα και σύγκριση των βρόγχων διατμητικής τάσης-παραμόρφωσης για επιλεγμένα διαφορετικά βάθη των δύο σχηματισμών για διάφορα σενάρια έντασης των επιταχυνσιογραφημάτων καθώς και συγκρίσεις σε επίπεδο φασμάτων απόκρισης, επιταχυνσιογραφημάτων και περιβάλλουσων μετακινήσεων, τάσεων, διατμητικών παραμορφώσεων. Η σύγκριση γίνεται τόσο σε μικροσκοπικό επίπεδο (βρόγχοι) όσο και μακροσκοπικό (επίπεδο σχεδιασμού - φάσματα και περιβάλλουσες).

CHAPTER 1

Introduction

1.1 Scope

In this thesis three constitutive models are compared and an optimization and calibration methodology for their parameters is proposed in order to equate and make them compareable. The constitutive models compared are “BWGG “(Gerolymos and Gazetas - 2004), “BWGG modified” (Gerolymos and Gazetas - Modified by Gerolymos and Parpottas - 2014) and UBCSAND.

The goal of this thesis is to verify and validate UBCSAND model which is a widely used constitutive model in engineering projects as it is also incorporated in popular commercial codes like FLAC and PLAXIS. In order to achieve that it is verified against NLDYAS and validated against NLDYAS modified models which are thoroughly and intensively tested in international literature and they are accepted to be a reliable metric.

The calibration and optimization for the choice of the parameters is done for the 5th cycle of prescribed cyclic strains on an experimental arithmetic 1-dimensional formation with the UBC3D-PLM model. With the use of the Ishibashi and Chang curves parameters comparable matching is achieved for the three models and particularly for the UBC3D-PLM (UBCSAND) and NLDYAS modified (BWGG modified) pair.

The original model is based on the ‘Bouc-Wen’ hysteresis model, which was developed for the non-linear one-dimensional ground response analysis of layered soil deposits. The model reproduces the nonlinear hysteretic behaviour of a variety of soils, and possesses considerable flexibility to represent complex patterns of cyclic behaviour such as stiffness decay and loss of strength due to buildup of porewater pressure, cyclic mobility, and load induced anisotropy. It also has the ability of simultaneously generating realistic modulus and damping versus strain curves, by a simple calibration of only three of its parameters. The model is implemented into the NL-DYAS code through an explicit finite–difference algorithm.

The modified version “BWGG modified” was developed in order to improve some weaknesses of the earlier version by using the smooth hysteresis model and produce more realistic results.

Lastly the UBCSAND model is based upon a completely different approach into the solution of the 1 dimensional non linear models. It is a plasticity-based model rather than hysteretic like the other two are based hence the need for a choice of parameters able to justify a reliable comparison upon them. Additionally the UBCSAND model is specialized in liquifaction scenarios and the use for non liquifaction is still investigated. The model used is implemented into the commercial code Plaxis plugin UBC3D-PLM that gives the ability to simulate complex problems with overlaying structures and also 3D. These reasons justify the need to verify that the UBC3D-PLM constitutive model is versatile and able to provide suitable engineering problem solutions in non liquifaction situations (majority of cases), thus it is compared with proven models in that field.

1.2 Layout

The second chapter deals with the laws that each of the three models represent as well as present and compare them. The reader is then introduced to the sophisticated BWGG Winkler model developed by Gerolymos and Gazetas, which is essentially a Winkler – based macro-element model and is briefly compared to the recently developed smooth hysteresis model by Gerolymos and Parpottas. The two models above are then compared to the UBCSAND plasticity-based model by Puebla et al.(1997) with emphasis into the comparison of the improved BWGG modified new smooth hysteresis model against UBCSAND.

The third chapter deals with the optimization and calibration that result into the parameter choice methodology proposed in order to have a comparable match between the three models. The commercial code Plaxis 2D via an extension plugin for soil tests (“UBC3D-PLM”) is used to create stress-strain loops for exact prescribed strains out of which the 5th loop gives the final data needed.

The optimization results are presented, where the parameters are originally calibrated based on the Ishibaashi and Zhang curves by using an optimization MATLAB code developed by Parpottas in 2014 and subscequently the rest of the parameters are chosen based on a simple methodology. A new MATLAB code was developed in order to produce the relevant G/G_{max} - γ and ξ-γ charts and those are compared to justify the choice of the parameters. Some tests were also ran for NLDYAS parameters.

In the fourth chapter the hysteresis code (“NL-DYAS modified” code based on the new smooth hysteresis model) and UBCSAND model are compared with emphasis on the comparison of the improved “NL-DYAS modified” and UBCSAND. Two experimental profiles of soil columns 40 meters deep are developed. The first represents a multilayered soil profile while the second an exponentially hardening profile relative to depth. The two profiles are then subjected on three different seismic excitations Aegion (1995) 0.39g, Lefkadas (2003) με 0.42g, and the more destructive one of Kobe (1995) με 0.68g. The results are presenting the excitations and comparison of the stress-strain loops for different selected depths for the two soil profiles and for different scaled excitation intensities.

CHAPTER 2

Constitutive Models

2.1 Introduction

Constitutive Modeling is the mathematical description of how materials respond to various loadings. In this thesis emphasis is given into the dynamic behavior of sand soil elements under cyclic loading. The hysteresis loop is the way stress is connected with strain as the result of this very behavior.

One-dimensional nonlinear constitutive models for soils are mostly of an empirical nature. They are not a result fundamental physic laws but often result of simplified expressions meant to reproduce with an engineering accuracy a relevant set of of experimental stress strain relationships.

Multiple models have been developed over the years some of which are

- Viscoelastic models combined with equivalent linear analysis methods
- Hysteresis or non linear cyclic models
- Models based on the theory of plasticity

Viscoelastic constitutive equations of stress-strain are defined by two parameters that define the shear modulus and damping of the soil. Viscoelastic models are mostly used to describe cyclic response of the soil in small strains ($<10^{-5}$), whereas with proper equal-linear methods of analyses the method can be expanded to approach the non linear response of the soil in mediocre strains ($<10^{-3}$).

As a result viscoelastic constitutive models are failing to efficiently and accurately describe the soil response in strains greater than 10^{-3} due to the fact that they are affected dearly by the deformation amplitude but also from the number of cycles and the exact relation between stress and strain.

In order to describe more more complex behaviors like ‘relaxation’, strength degradation during multiple cycles of loading unreloading and reloading as well as permanent soil distortion and cyclic mobility, non linear hysteresis constitutive models are more appropriate.

Hysteresis constitutive models are described by two types of curves.

A. monotonic loading curve

B. the loading-unloading-reloading law

For the monotonic loading curve numerous constitutive models have been proposed but getting into further detail is not subject of this thesis.

For cyclic loading, involving unloading and reloading cycles, most available hysteresis models are based on the Masing hypothesis (‘‘criterion’’). Many such models do not fit the experimental G : γ and ξ : γ curves simultaneously — often overestimating the hysteretic damping at large strains. In addition, in many cases they model rather crudely the shape of experimental stress–strain loops.

To avoid some of these drawbacks Gerolymos and Gazetas adopted the model developed by Bouc and Wen. This model consists of a first order nonlinear differential expression that relates input (strain or displacement) to output (stress or force) and is called BWGG.

The Gerolymos and Gazetas model has been later improved by Gerolymos and Parpotas 2014 in order to simulate soil behavior more realistically rather than fundamentally changing the whole concept of the model and additionally approach all possible combinations of G : γ and ξ : γ curves with more accuracy.

In this thesis emphasis is given into the comparison of the BWGG modified and UBC3D-PLM models. We predefine parameters into the two constitutive models, the modified model by Gerolymos and Parpotas called (Smooth Hysteresis model or NLDYAS modified) and the model UBC3D-PLM, a generalized version of the original UBCSAND which uses an elastic plastic formulation in order to make them comparable and then see how the two correlate. The original version of BWGG is also compared above the two.

One major disadvantage of non-linear (hysteresis) cyclic models is the fact that it is difficult for them to simulate the behavior of numerous stress route. For this reason multiple constitutive simulations are based on plasticity theory.

2.2 Masing Hypothesis “Criterion”

The Masing model describes the unloading-reloading behavior curve of almost the whole of soil hysteresis constitutive model and has the following characteristics.

- At the initial Loading the stress-strain curve is described by the monotonic loading curve, $\tau=F(\gamma)$
- At the unloading phase, the stress strain curve is given by the equation

$$\frac{\tau-\tau_r}{2}=F\left(\frac{\gamma-\gamma r}{2}\right) \tag{2.1}$$

(for unloading that occurs at stress strain point (τ_r,γ_r)

- The unloading-reloading curve is a reversed copy of the respective curve in monotonic loading and the shear modulus on unloading is a match of that of the initial loading.
- If during the loading or unloading the maximun previous strain is exceeded and the monotonic loading curve is crossed by the unloading or reloading curve then the monotonic loading curve is followed.
- Loss of energy is completely independent to the rate of stress enforcement.

Non Linear cyclic models where Masing criterion is used in unloading reloading the ratio of hysteretic damping is defined as follows:

$$\xi = \frac{1}{4\pi}\frac{\Delta W}{W} \tag{2.2}$$

where:

$$W = \frac{1}{2}\gamma_r \tau(\gamma_r) \qquad , \qquad \Delta W = 8\left(\int_0^{\gamma r} \tau(\gamma)\, d\gamma - W\right) \tag{2.3}$$

thus:

$$\xi = \frac{2}{\pi}\left(\frac{2\int_0^{\gamma r} \tau(\gamma)\, d\gamma}{\gamma_r \tau(\gamma_r)} - 1\right) \tag{2.4}$$

The greatest benefits of hysteresis models compared to viscoelastic models is the ability to realisticly correlate the soil stregth with loading cycles and development of excess pore pressures as of course happens in reality.

The models can simulate effectively the remnant strains (“hardening) as well as correlating different mechanical characteristics (such as shear modulus and strength) with the time history also rather than only the running strain value.

2.3 Elastic -Perfectly Plastic Model

The elastic - perfectly plastic model is the elementary model of the hysteresis family. It is suitable for the describing of the dynamic behavior of metals in small strain values and for a low number of cycles. Nevertherless due to its simplicity it is widely used for the recycling behavior of the soil.

According to the elastic-perfectly plastic model the shear modulus remains stable during the loading untill the yield stress whereas it becomes equal to zero.

The main downside is the fact that it ignores plasticity for values lower than the yield strain and for that reason the hysteretic damping beyond that level is calculated as zero. On the other hand once the stress reaches the yield stress the damping value is exagarrated. That behavior is not valid in a realistic model and is evident from a multitude of experimental data.

The ratio of the shear modulus and hysteresis damping compared to plasticity of damping μ, for a soil that its cyclic behavior is described by the elastic-perfectly plastic model is given via the following equations:

$$\frac{G}{G_{\max}} = \frac{1}{\mu} \tag{2.5}$$

and:

$$\xi = \frac{2}{\pi}\left(1 - \frac{1}{\mu}\right) \tag{2.6}$$

where:

$$\mu = \frac{\gamma}{\gamma_y} \qquad \mu \geq 1 \tag{2.7}$$

Result of the above is:

$$\mu \to \infty \Rightarrow \xi = \frac{2}{\pi} \tag{2.8}$$

Conclusively it is noticed that models using the Masing hypothesis as their unloading-reloading criterion can reach a maximum hysteretic damping equal to $2/\pi$ which is a high value of 63.7%. However this is contradicted by laboratory calculated dampings which rarely exceed the 30% mark, furtherly showing the need for more realistic approaches to that issue.

2.4 Models

The models this thesis empasizes onto are the ”BWGG modified” model and the UBC3D-PLM model which is basicly a generalized model of the UBCSAND model. Those two are optimized and calibrated based on literature methodologies, reports and additionally proposed methodologies presented at chapter 3.

The original BWGG model is also brought into comparison at the final stage in order to have a better understanding of the whole scope of the weaknesses and strong points of each of the constitutive models.

2.4.1 BWGG Model

With published constituitive models for soils incapable of realistically describing the cyclic soil behavior on large strain the need emerged for a new phenomenological constitutive model which is an extention of Wen model.

The disadvantages of the models were:

- Inconcistency with experimental G/Gmax-γ and ξ-γ data. (for example the hysteretic damping is overestimated)
- Only small to medium strain levels can allow them to properly model the shape of various experimental stress-strain loops of soil behavior

BWGG not only avoids the above but also allows for considerable flexibility in representing complex non-linear characteristics of cyclic behavior such as, stiffness decay, loss of strength and relaxation due to pore-water pressure development, non-symmetric behavior with loading direction.

2.4.1.1 NLDYAS Code

BWGG is incorporated into NL-DYAS code for the non-linear one-dimensional ground response analysis of layered sites. The code accepts soil profiles and excitations and produces detailed information regarding accellerations,displacements, stress and strains depending on the depth of the soil profile and also provides the maximum value of each characteristic.

2.4.2 UBC SAND

UBCSAND is a fully coupled effective stress dynamic analysis procedure for modeling seismic liquefaction. An elastic plastic formulation is used for the constitutive model UBCSAND in which the yield loci are radial lines of constant stress ratio and the flow rule is non-associated. This is incorporated into the 2D version of FLAC by modifying the existing Mohr-Coulomb model.

Its formulation is based on classical plasticity theory with a hyperbolic strain hardening rule, based on the Duncan-Chang approach with modifications

The model UBC3D-PLM admittetely follows closely the UBCSAND model introduced by Puebla et al. (1997), Beaty and Byrne (1998). The original model is a 2-D model developed for the prediction of liquefaction in sandy soils.

The main difference between the UBCSAND model and the UBC3D model is the latter generalized 3-D formulation.

2.4.1.1 UBC3D-PLM Code

Plaxis Bv took the the UBCSAND model and implemented a generalized formula into the Plaxis code and is called UBC3D-PLM. UBC3D-PLM is an abbrevation of the words UBCSAND 3D Plaxis Liquefaction Code and is an addon of the commercial code plaxis.

2.4.3 New Hysteresis Model

The “BWGG modified” or New Smooth Hysteresis Model is simulating the soil behavior more realistically compared to its counterpart.

As it is noticed by multiple analyses the unloading and reloading curves are characterized by a decreased shear modulus in contrast with Bouc-Wen model which keeps the same shear modulus as on the initial monotonic loading curve which is wrong and unrealistic.

2.4.1.1 NLDYAS modified

The model is implemented into the latest version of BWGG as an improved version of Bouc-Wen model. It essentially obeys the same rules in order to run but the optimization parameters are less as the process is now simplified. Less parameters are required into the input for it to run and core equations are modified too.

2.4.4 Comparison of methods

Prior to the detailed analyses in order to produce detailed results we expect that UBC3D-PLM beeing a plasticity based model following the rules prior to the genesis of BWGG should overestimate the hysteresis damping.

A challenge is presented in the fact that UBC3D-PLM is built to be a 3D model. Additionally it is proven for a fact that UBCSAND is specialized into liquefaction scenarios. In order to compare it reliably with a 1D model which BWGG and BWGG modified a lot of prequisities have to be accepted as well as a thorough optimization process.

Additionally the UBC3D-PLM model follows the old hysteresis rules that BWGG came in to improve so in order for those to be comparable we have to force them to be equal in a way that the comparison results are reliable. The process upon which this is achieved is presented into Chapter 3 and includes a verification and a validation process.

Figures

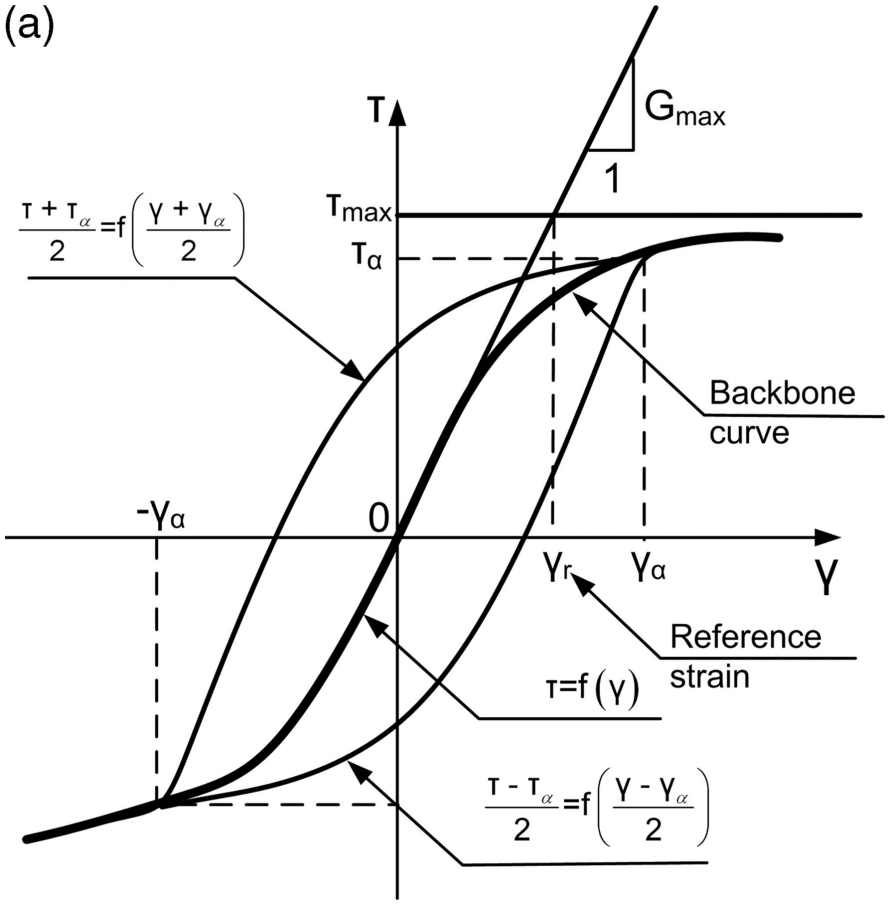

Figure 2.1 *a) Masing criterion with backbone curve and rule of unloading/reloading*

CHAPTER 3

Calibration - Optimization

3.1 Introduction

In this Chapter the optimization process followed in order to proceed to the analyses is presented in detail.

3.2 Parameters in discussion

3.2.1 Shear modulus reduction and hysteretic damping growth curves

To analyze the seismic response of soils the equivalent-linear method is often used. According to this method the nonlinear cyclic behavior of soils can be approached with the utilization of only two dynamic parameters. Those parameters are the secant shear modulus (which is calculated as the average gradient of the stress strain curve) and the hysteretic damping ration (which is calculated as the area of the hysteretic stress strain loop).

In this thesis the equivalent-linear method is used in order to process the experimental data and extract the two main dynamic parameters as per the γ (strain value).

The G/Gmax-γ and ξ-γ curves are the main source of comparison in this thesis resulting by the hysteresis loops produced by each method.

Seed & Idriss (1970) suggested some curves for the secant shear modulus and the damping ratio to strain for sands, gravel and non cohesive slurry stain. According to Seed & Idrisses findings sands behave very similarly to gravel in terms of cyclic behavior. The Secant shear modulus and the hysteretic damping ratio however according to them was a related only to the width of the shear strain.

Following researches however has brought to attention the fact that the shear modulus and hysteretic damping are affected by a multitute of other parameters out of which the following are the most important:

- average effective stress

- pore index
- Plasticity Index (not relevant for sands and these thesis)

Other parameters that can significantly affect non-cohesive materials but are not investigated in this thesis are:

- saturation rate
- number of load cycles.

Iwasaki et al (1978) and Kokushu et al (1980) have suggested that the depth and as a result effective stresses have a tremendous influence in the shear modulus and hysteretic damping values. The greater the average effective stress:

- The G/Gmax-γ curve is moving upwards
- The ξ-γc curve is movind downwards
- the ξ ratio is growing less after N load cycles for a locked value of strain.

Evident by literature the PI (=Plasticity index) is very important for cohesive materials like clay but in our case effective stress influence is similarly important for non cohesive materials like sands as in our case.

Subsequently if we consider the shear modulus ration equation on a hyperbolic model with n=2 we have:

$$\frac{G}{G_{\max}} = \frac{1}{1+\frac{\gamma}{\gamma_y}} \tag{3.1}$$

Where γ_y is the yield strain which means it sets the boundary after which the plasticity strains behavior overrules the elasticity behavior. Raising the γ_y value leads in raise of the soil strength.

As it is proven by laboratory and on site measurements the raise of the max shear modules is corellated directly with the exponential growth of the effective stress, concequently the γ_y parameter is approached by the following:

$$\gamma_y = A\sigma_o{}^m \quad m \geq 0 \tag{3.2}$$

So as a concequence by replacing the value of γ_y with :

$$\frac{G}{G_{\max}} = \frac{1}{1+\frac{\gamma}{A\sigma_o{}^m}} \tag{3.3}$$

It was proposed by shibata and Soelarno (1975) that:

$$A=0.001,\ m=0.5 \tag{3.4}$$

The influence of the average effective stress is significant and should not be ignored if a realistic analysis is to be achieved.

Subsequently the choice of an experimental curve set is presented in order to proceed with the optimizations and calibration nesessary in order to accurately run the subsequent analyses.

3.2.1.1 Ishibashi & Chang Curves

There are numerous methodologies that can be followed in order to optimize the parameters for the analyses. Primarily the optimization of parameters for non-linear hysteretic models is based on :

- Laboratory tests such as triaxal loading, cyclic shear loading test etc.
- empirical equations for the secant shear modulus and the hysteretic damping ratio from international literature.

The second methodology tends to be prefered instead of the first due to the fact that laboratory tests results tend to be not as reliable as the empirical equations. Laboratory speciments are limited and are unable to provide a broad understanding of how different soil types under different situations might really react. Additionally laboratory situations might not represent precisely the real nature behavior of the speciment. On the other hand empirical equations are the result of hundreds or even thousands of subsequent tests upon a broad spectrum of of soil types and profiles.

The curves of choice (Ishibashi & Chang) for chapter 4 optimizations and this thesis, have been used extensively in previous optimization efforts for “NLDYAS” and “NLDYAS modified”.

Ishibashi & Chang (1993) have suggested the following equations to describe the Gsec-γc, ξ-γc curves. Their suggestion takes into account the influence of the Plasticity index and the average effective stress into the alteration of the shear modulus and hysteretic damping ration. In our case the plasticity index is equal to zero (PI=0) but that does not limit the use of the curves.

The main equation is:

$$\frac{G}{G_{\max}} = K\left(\gamma, PI\right)\left(\sigma'_m\right)^{m(\gamma,PI)-mo} \tag{3.5}$$

where:

$$K(\gamma,PI)=0.5\left\{1+\tanh\left[\ln\left(\frac{0.000102+n(PI)}{\gamma}\right)^{0.492}\right]\right\} \tag{3.6}$$

$$m(\gamma,PI)-m_o=0.272\left\{1-\tanh\left[\ln\left(\frac{0.000556}{\gamma}\right)^{0.4}\right]\right\}e^{\left[-0.0145(PI)^{1.3}\right]} \tag{3.7}$$

$$n(PI)=\begin{cases}0 & , \quad PI=0\\ 3.37\times10^{-6}(PI)^{1.404} & , \quad 0\le PI15\\ 7.0\times10^{-7}(PI)^{1.976} & , \quad 15\le PI70\\ 2.7\times10^{-5}(PI)^{1.115} & , \quad PI\ge 70\end{cases} \tag{3.8}$$

and:

$$\xi=0.333\frac{1+\exp\left[-0.0145(PI)^{1.3}\right]}{2}\left[0.586\left(\frac{G}{G_{\max}}\right)^2-1.547\frac{G}{G_{\max}}+1\right] \tag{3.9}$$

3.2.2 "NLDYAS" Parameters

The program NL–DYAS computes the response of a semi–infinite horizontally layered soil deposit overlying a uniform (flexible) half–space subjected to vertically propagating shear waves. The analysis is done in the time domain.

NLDYAS parameters that are due to be optimized or calculated/suggested are presented and briefly explained below. The laws that govern as well as the fundamental equations that will subsequently be used into the optimization process are also presented. An overview of the input files

The code needs two input files for it to execute and produce results. The first is an input file with detailed soil characteristics and the second one would be the respective seismic excitation accellerogram.

The first input file consist of:

Option 1: Consists of the dynamic soil properties. Material number and identification information for model parameters (b, n, A, α, s1, s2, x). Each line accomodates one material

Where:

b(I): Parameter that controls the shape of the unloading–reloading curve

n(I): Parameter that governs the sharpness of the transition from the linear to nonlinear range during initial virgin loading

A(I): Must be taken equal to 1

α(I): Parameter that controls the post yielding shear stiffness

s_1(I): Parameter that controls the reversal shear stiffness

s_2(I): The characteristic value of strain ductility, γ / γ_y, beyond of which the stiffness degradation initiates

x(I): If x = 1 the parameters s_1 and s_2 are taken into consideration in the analysis. If x = 0 then parameters s_1 and s_2 are ignored

Option 2: Consists of Identification information for the soil profile. That includes the parameters (I (H, ρ, Vs, γ_y, η_c). Each line accomodates one layer with its unique identification number and material type.

Where:

H(I): Layer thickness (the distance between two consecutive soil nodes). H(1) is always taken equal to 0

ρ(I): Mass density of the soil layer

V_s(I): Shear wave velocity of the soil layer

γ_y(I): The value of shear strain at "initiation of yielding" in the soil

η_c(I): The viscoelastic constant of the soil layer. Is related to the equivalent material hysteretic damping by $\xi = \eta_c \omega / 2G$, where ξ is the material damping, ω is the cyclic frequency of the motion, and G is the shear modulus of the soil layer. To avoid numerical instabilities a lowermost value of 0.06% ρV_r^2 is recommended for η_c .

Option 3: Dynamic rock properties of the halfspace. In this part parameters C_{rock} , x_2 are defined

where:

C_{rock} : Is the rock dashpot coefficient accounting for the partial transmission of the downward–travelling stress waves that reach the soil–rock boundary, through the rock halfspace (radiation damping). Is given by $C_{rock} = \rho_r V_r$. Where ρ_r and V_r are the mass density and the shear wave velocity of the rock, respectively.

x_2 : If x_2 = 1 then rock outcrop motion is considered (the rock base is considered as flexible – with radiation damping). If x_2 = 0 the within motion is considered (the rock base is considered as rigid – no radiation damping)

Option 4: Input motion preferences. On this part the second input file name is defined. The number of acceleration values to be read, the time interval between acceleration values and the scaling factor to adjust/multiply each acceleration value are presented.

The optimization process that follows on chapter 4 essentially is the base to generate the respective soil input file as it gives the complete information that would be used later to generate the soil characteristics.

In general the input values are sets of PI and σ'_o values.

PI = Plasticity index

σ'_o = effective stresses (relevant to depth)

the optimization results give us

γ_y^{-1} = yield strain exponential factor -1 (small values are easier to present if factor is -1)

b, n, s1, s2 are explained above.

From the above mentioned parameters optimization tables are created such as **table (3.1)** which shows the optimization results of V.Drosos for NLDYAS

3.2.3 "NLDYAS modified" Parameters

"NLDYAS modified" parameters that are due to be optimized or calculated/suggested are identical to the original version. The differences are presented below.

In general the input values are a set of PI and σ'o values similarily to the original version. For better accuracy some parameters are neglected in this model (α,s_2) and b=g=0.5 pre-defined.

From the above mentioned parameters optimization tables are created such as **table (3.2)** which shows the optimization results of Gerolymos and Parpotas for the new optimization method.

The NL-DYAS modified code needs the same concept input files (two input files one with soil characteristics and one with the excitation).

The output also exports the surface spectrum.

3.2.4 UBC3D-PLM Parameters

UBC3D-PLM that are due to be optimized or calculated/suggested are presented and briefly explained below. The laws that govern as well as the fundamental equations that will subsequently be used into the optimization process are also presented:

The elastic behaviour which occurs within the yield surface is governed by a non-linear rule. Two parameters control this non-linear behaviour; the elas- tic bulk modulus K and the elastic shear modulus G. These two moduli are stress dependent and the relationships are given in the following equations:

$$K = K_B^e P_A \left(\frac{p}{\mathrm{P_{r\,ef}}} \right)^{me} \tag{3.10}$$

$$G = K_G^e P_A \left(\frac{p}{\mathrm{P_{r\,ef}}} \right)^{ne} \tag{3.11}$$

where K_B^e and K_G^e are the bulk and the shear modulus respectively at a reference stress level. The factors *ne* and *me* are parameters define the rate of stress dependency of stiffness. In the literature, the reference stress level (p_{ref}) is commonly taken as the atmospheric pressure (P_A=100 kPa) but in our later calculations we can adjust that to the proper value in order to adjust the parameters depending on the confining pressure that exists in larger depths.

Pure elastic behaviour is predicted by the model during the unloading process

The input parameters of the UBC3D are summarized bellow:

- ϕ_{cv} is the constant volume friction angle
- ϕ_p is the peak friction angle
- c is the cohesion of the soil
- K_B^e is the elastic bulk modulus of the soil in a reference level of 100 kPa. It can be derived from a drained triaxial test with a confining pressure of 100 kPa. When data from a triaxial test with a different confining pressure are available, it can be corrected using **3.10**
- K_G^e is the elastic shear modulus of the soil in a reference level of 100 kPa. It can be related with the K_B^e using the Poison ratio as shown in the optimization at chapter 3.4.

- K_G^p is the plastic shear modulus and has to be extracted after curve fit
- me is the elastic bulk modulus index and has a default value of 0.5
- ne is the elastic shear modulus index and has a default value of 0.5
- np is the plastic shear modulus index and has a default value of 0.5
- R_f is the failure ratio n_f / n_{ult}
- P_A is the atmospheric pressure

• fac_{hard} is the densification factor. It is a multiplier that controls the scaling of the plastic shear modulus during secondary loading. Above 1 the K_G^p becomes higher and the behaviour stiffer and bellow 1 the K_G^p becomes lower and the behaviour softer

• $N1_{60}$ is the corrected SPT value of the soil.

• fac_{post} Fitting parameter to adjust post liquefaction behaviour

3.3 Optimization

An optimization process was followed based on previous work on optimization for BWGG and BWGG modified as well as reports for the UBC3D-PLM model. Several assumptions and simplifications were also made in order to achieve the relevant comparability.

3.3.1 Equating BWGG modified and UBC3D-PLM

BWGG modified and UBC3D-PLM have a different methodology and follow different rules so for that reason if we dont equate them to be relevant then the comparison G/Gmax-γ and ξ-γ curves will have no meaning whatsoever and no scientific value.

To start the equation process we will list the leading parameters of the process.

From the Ishibashi & Chang curve fitting process we are able to get γ_y-1, n and s_1 with only a set of PI and σ_o' known. Since though the individual depths and soil density will be known and since we only consider sandy profiles the parameters are easily calculated.

The equation process is explained below.

For "NLDYAS" and "NLDYAS modified" the simple stress-strain ratio is giving us the shear modulus as follows:

$$\frac{\tau_y}{\gamma_y} = G_{\max} \Rightarrow \tau_y = G_{\max}\ \gamma_y \tag{3.12}$$

For UBC3D-PLM:

$$\tau_y = \sigma_{vo}' \sin\varphi \tag{3.13}$$

From the () and () we have:

$$\left.\begin{array}{l} \tau_y = G_{\max}\gamma_y \\ \tau_y = \sigma_{vo}'\sin\varphi \end{array}\right\} \Rightarrow \quad \sin\varphi = \frac{G_{\max}\gamma_y}{\sigma_{vo}'} \tag{3.14}$$

From equation () and the curve fitting from ishibashi & Chang we have what is needed to proceed.

3.3.2 "BWGG" Parameters

The optimization process followed takes in mind the curve fitting by Ishibashi & Chang and the work done by V.Drosos and Gerolymos.

The main equation that calculates the shear stress is shown below

$$\tau_{i+1} = \tau_i + \frac{\gamma_{i+1} - \gamma_i}{\gamma_y} \cdot eta \cdot \left\{1 - \left|\tau_i\right|^n \left[b + g \cdot sign\left[\left(\gamma_{i+1} - \gamma_i\right) \cdot \tau_i\right]\right]\right\} \tag{3.15}$$

where:

$$eta = \frac{s_1 + \left[a\left(\mu_{\max} - 1\right) + s_2\right]}{s_1 + \mu_{\max}} \tag{3.16}$$

and:

$$\tau_p = \tau_i \quad if \quad (\gamma_{i+1} - \gamma_i) \cdot (\gamma_i - \gamma_i) > 0 \tag{3.17}$$

$$\mu_{\max} = \max\left(\frac{\gamma_o}{\gamma_y}, s_2\right) \tag{3.18}$$

τ_i, τ_{i+1}: previous and following stress respectively

γ_y: yield strain (optimization parameter)

The preliminary simplified optimization results in the following table for BWGG with x=0.

3.3.3 "BWGG modified" Parameters

PI	σ_o'	γ_y^{-1}	b	n	s_1	s_2
0	10	3500	0.50	0.60	1.00	0.00
0	50	1400	0.50	0.60	1.00	0.00
0	100	900	0.50	0.60	1.00	0.00
0	200	500	0.50	0.60	1.00	0.00
0	400	300	0.50	0.60	1.00	0.00
0	1000	200	0.50	0.60	1.00	0.00

Table 3.3 *Proposed optimization results for BWGG*

The optimization process followed takes in mind the curve fitting by Ishibashi & Chang and the work done by Parpotas and Gerolymos and results in the following table for BWGG modified.

The improved equation that calculates the shear stress is shown below:

$$\tau_{i+1} = \tau_i + \frac{\gamma_{i+1} - \gamma_i}{\gamma_y} \cdot eta \cdot \left\{ 1 - \left(\left| \frac{\tau_i - \tau_p}{1 - sign(\gamma_{i+1} - \gamma_i) \cdot \tau_p} \right| \right) \right\}^n \tag{3.19}$$

PI	σ_o'	γ_y^{-1}	n	s_1
0	10	2537.644	0.536	4
0	50	961.116	0.454	4
0	100	637.226	0.457	4
0	200	432.904	0.495	4
0	400	302.268	0.583	4
0	1000	203.6	1.326	3.235

Table 3.4 *Optimization results for BWGG modified*

This version accepts b=g=0.5 and neglects α,s2

PI	σ_o'	γ_y^{-1}	b	n	s_1	s_2
0	10	3500	0.60	0.40	2.20	0.10
0	50	1400	0.60	0.40	2.20	0.10
0	100	900	0.60	0.40	2.10	0.20
0	200	500	0.60	0.40	2.10	0.20
0	400	300	0.60	0.45	2.10	0.20
0	1000	200	0.60	0.70	2.00	0.20
15	10	1400	0.60	0.50	1.30	0.10
15	50	800	0.60	0.50	1.30	0.10
15	100	600	0.60	0.60	1.30	0.10
15	200	500	0.60	0.60	1.30	0.10
15	400	400	0.60	0.65	1.30	0.10
15	1000	300	0.60	0.75	1.30	0.10
30	10	600	0.60	0.80	1.00	0.00
30	50	500	0.60	0.80	1.00	0.00
30	100	400	0.60	0.80	1.00	0.00
30	200	400	0.60	1.00	1.10	0.00
30	400	400	0.60	1.20	1.20	0.00
30	1000	400	0.60	1.20	1.20	0.00
50	10	400	0.60	1.20	0.90	0.00
50	50	350	0.60	1.20	0.90	0.00
50	100	350	0.60	1.20	0.90	0.00
50	200	420	0.60	1.20	0.90	0.00
50	400	320	0.60	1.20	0.90	0.00
50	1000	280	0.60	1.20	0.90	0.00
100	10	160	0.60	1.20	0.80	0.00
100	50	160	0.60	1.20	0.80	0.00
100	100	150	0.60	1.20	0.80	0.00
100	200	150	0.60	1.20	0.80	0.00
100	400	150	0.60	1.20	0.80	0.00
100	1000	150	0.60	1.20	0.80	0.00
200	10	70	0.60	1.20	0.80	0.00
200	50	70	0.60	1.20	0.80	0.00
200	100	70	0.60	1.20	0.80	0.00
200	200	70	0.60	1.20	0.80	0.00
200	400	70	0.60	1.20	0.80	0.00
200	1000	70	0.60	1.20	0.80	0.00

Table 3.1 *Optimization results table as proposed by V.Drosos for NLDYAS*

PI	σ_o'	γ_y^{-1}	n	s_1
0	10	2537.644	0.536	4
0	50	961.116	0.454	4
0	100	637.226	0.457	4
0	200	432.904	0.495	4
0	400	302.268	0.583	4
0	1000	203.6	1.326	3.235
15	10	1509.635	0.676	3.361
15	50	888.688	0.757	3.134
15	100	711.283	0.843	2.958
15	200	572.34	0.979	2.759
15	400	464.352	1.205	2.548
15	1000	387.749	2.749	2.176
30	10	730.657	0.826	2.078
30	50	572.781	0.951	1.97
30	100	517.001	1.029	1.919
30	200	467.859	1.132	1.865
30	400	425.775	1.276	1.814
30	1000	383.322	1.596	1.773
50	10	329.631	0.782	1.545
50	50	305.566	0.841	1.5
50	100	296.133	0.872	1.481
50	200	287.387	0.907	1.464
50	400	279.48	0.949	1.448
50	1000	270.692	1.017	1.434
100	10	117.201	0.696	1.252
100	50	116.962	0.699	1.249
100	100	116.871	0.701	1.249
100	200	116.777	0.702	1.248
100	400	116.686	0.703	1.247
100	1000	116.564	0.705	1.246
200	10	53.43	0.683	1.189
200	50	53.367	0.683	1.187
200	100	53.367	0.683	1.187
200	200	53.359	0.683	1.187
200	400	53.359	0.683	1.187
200	1000	53.355	0.682	1.187

Table 3.2 *Optimization results table as proposed by Gerolymos and Parpottas for NLDYAS modified.*

3.3,3,1 Role of rock outcrop motion for NLDYAS modified

On the next chapter a comparison is made between x=1 or x=0 for one of the experimental soil profiles that was created. The results are presented on chart. After that analysis rock outcrop motion that was pick was x=0 which means that after the halfspace the sub terrain considered as rigid – no radiation damping as that is believed to be more realistic and match the analyses of UBC3D-PLM.

3.3.4 UBC3D-PLM parameters

For this optimization the UBC3D-PLM Soiltest plugin is used. An sample soil profile is defined and tests are run to understand the role of each parameter.

First of all some parameters are pre-defined in order to minimize the unknown parameters and be able to run the optimizations

The admissions and simplifications made are presented below:

The values of ϕcv constant volume friction angle and ϕp peak friction angle are considered equal between them and equal to the ϕ angle of equation (3.13)

$$\varphi_{cv} = \varphi_p \tag{3.20}$$

The elastic shear modulus (K_G^e) and plastic shear modulus (K_G^P) behave like springs in series. For that reason the equivalent shear modulus reacts like a series of springs consisting of the elastic shear modulus and the plastic shear modulus.

$$G_{\max} = \frac{K_G^e \times K_G^p}{K_G^e + K_G^p} \tag{3.21}$$

Elastic bulk modulus for a typical poisson ratio is connected to the elastic shear modulus as follows:

$$\frac{K_B^e}{K_G^e} = \frac{2(1+\nu')}{3(1-2\nu')} \tag{3.22}$$

It is accepted in this thesis that:

$$K_B^e = 0.7 K_G^e \tag{3.23}$$

$$PA = 100 \tag{3.24}$$

The connection between the constitutive models was presented in 3.4.1 as below:

$$\sin\varphi = \frac{G_{\max}\gamma_y}{\sigma_{vo}'} \tag{3.24}$$

The remaining parameters are chosen as below:

$$Rf = 1 \tag{3.25}$$

$$np = 0.5 \tag{3.26}$$

$$N_1(60) = 40 \tag{3.27}$$

It is also accepted that:

$$K_G^{e} = K_G^{p} \tag{3.28}$$

thus:

$$G_{\max} = \frac{K_G^{e}}{2} \tag{3.29}$$

Into the program the reference values are entered. That means if the confinining effective stress σ_{vo}' is different than the PA = 100kpa value then a correction is needed that is achieved via a modification of the starting KGe or KGp respectively. The result is presented:

$$K_G^{e}{}_{ref} = K_G^{e}\left(\frac{PA}{\sigma_{vo}'}\right)^{0.5} \tag{3.30}$$

3.3.4.1 Role of various parameters

A choice of different parameters were picked in order to define their role and how they affect the resulting G/G_{max}-γ and ξ-γ curves.

The contesting parameters that are believed to have impact and their role is to be determined are the values of ϕcv constant volume friction angle and ϕp peak friction angle that are from now on ϕ as they are considered equal , the elastic shear modulus (K_G^e) and plastic shear modulus (K_G^P) between them ratio and the the plastic shear modulus index np which is a random sample from the default 0.5 parameters.

For the optimization process a set of PI and σ_{vo}' pairs was optimized as per Ishibashi & Chang as shown in the table below:

PI	σ_o'	γ_y^{-1}	n	s_1
0	10	2537.644	0.536	4
0	50	961.116	0.454	4
0	100	637.226	0.457	4
0	200	432.904	0.495	4
0	400	302.268	0.583	4

Table 3.5 *Optimization results for UBC3D-PLM parameter role optimization*

3.3.4.2 Role of φ

To define how ϕ affects the resulting G/G_{max}-γ and ξ-γ curves we pre-define ϕ values at ϕ=30, 35, 40, 45 and we perform a test for each of them for four different soil depth/ confinement scenarios σ_{vo}'=10, 50, 100, 200.

The value of γ_y^{-1} is known from the optimization process and by concidering $K_G^e=K_G^p$ and by following the procedure in 3.3.4 for seting parameters and correcting the $K_{G\,ref}^e$ values where nessessary we run analyses via the UBC3D-PLM soiltest plugin.

We generate hysteresis loops and we run the test for 5 cycles for 6 prescribed strains thus 0.001%, 0.01%, 0.1%, 1%, 10% and 100%.

The results are presented in the figure section where ϕ is shown not to change the curves.

3.3.4.3 Role of np

To define how a random parameter like np that in most cases is set at 0.5 affects the resulting G/G_{max}-γ and ξ-γ curves we pre-define np values at np=0.2, 0.4, 0.6, 0.8 and we perform a test for each of them for three different soil depth/confinement scenarios σ_{vo}'=50, 100, 200 we a fixed ϕ value at 35° since we know that the ϕ value is not altering our results

The value of γ_y^{-1} is known from the optimization process and by concidering $K_G^e=K_G^p$ and by following the procedure in 3.3.4 for setting parameters and correcting the $K_G^e{}_{ref}$ values where nessessary we run analyses via the UBC3D-PLM soiltest plugin.

We generate hysteresis loops and we run the test for 5 cycles for 6 prescribed strains thus 0.001%, 0.01%, 0.1%, 1%, 10% and 100%.

The results are presented in the figure section where np does not change the curves. For that reason the np and other parameters are from now on set at 0.50 default value.

3.3.4.4 Role of K_G^e and K_G^p

To determine the role of the K_G^e/K_G^p ratio and how it affects the resulting G/G_{max}-γ and ξ-γ curves we pre-define three different K_G^e/K_G^p ration as shown below:

$$\frac{K_G{}^e}{K_G{}^p} = 1$$

$$\frac{K_G{}^e}{K_G{}^p} = \frac{1}{2}$$

$$\frac{K_G{}^e}{K_G{}^p} = 2$$

A test is performed for each of them for a fixed soil depth/confinement scenario σ_{vo}'=200 and a fixed ϕ value at 35° since we know that the ϕ value is not altering our results and focus is desired on only how the ratio affects the curves.

The value of γ_y^{-1} is known from the optimization process and by concidering the three ratio scenarios and by following the procedure in 3.3.4 for setting parameters and correcting the $K_G^e{}_{ref}$ values where nessessary as well as generate the appropriate values for K_G^e and K_G^p according to their ratio we run analyses via the UBC3D-PLM soiltest plugin.

We generate hysteresis loops and we run the test for 5 cycles for 6 prescribed strains thus 0.001%, 0.01%, 0.1%, 1%, 10% and 100%.

The results are presented in the figure section where the role of the ratio is clearly shown.

3.4. Calibration

3.4.1 G/Gsec-γ and ξ-γ curve MATLAB program

A MATLAB program was developed due to calculate and produce the G/G_{max}-γ and ξ-γ curves out of the outputs of the UBC3D-PLM soiltest by counting the 5th cycle details after which we consider the soil stabilized.

The program is presented below and takes as input a 12 column stress-strain raw excel input that has stress-strain pairs side by side for 6 prescribed strains thus 0.001%, 0.01%, 0.1%, 1%, 10% and 100%:

```
%%%%%%%%%%%%%%%%%%%%%%%%%%%%%%%%%%%%%%%%%%%%%%%%%%%%%%%%%%%%%%%%%%%%%%%%%%%%%%%
%                                  Diploma Thesis                                %
%                                       by                                       %
%                                 Italos Marios                                  %
%                          National Technical University Athens                  %
%                             Supervisor:Nikos Gerolymos                         %
%%%%%%%%%%%%%%%%%%%%%%%%%%%%%%%%%%%%%%%%%%%%%%%%%%%%%%%%%%%%%%%%%%%%%%%%%%%%%%%

%import plaxis export from UBC3D-PLM soiltest
x = xlsread ('INPUT-FILE-NAME.xlsx');

%correction of data
xcor = x/10^14;
areacalc = [0 0 0 0 0 0];
%get number of lines0
xdim = size(xcor)
h = xdim(1);
l=0;
%save t and g in own tables.
   g(:,1) = xcor(:,1);
   t(:,1) = xcor(:,2);
   g(:,2) = xcor(:,3);
   t(:,2) = xcor(:,4);
   g(:,3) = xcor(:,5);
   t(:,3) = xcor(:,6);
   g(:,4) = xcor(:,7);
   t(:,4) = xcor(:,8);
   g(:,5) = xcor(:,9);
   t(:,5) = xcor(:,10);
   g(:,6) = xcor(:,11);
   t(:,6) = xcor(:,12);

for j=1:6
l=1;
    for i=1:h

       if i>2;
%difference between (i+1)-i  and i-(i-1)
```

```
          dt1(i-2,j)=g(i-1,j)-g(i-2,j);
          dt3(i-2,j)=g(i,j)-g(i-1,j);
%multiplied dt1*dt3 gives us a change in direction
          if (dt1(i-2,j)*dt3(i-2,j))<0;
            l=l+1;  %peak count
            peak(l,j)=i-1; %save peak counter
          end
       end
    end
end

for j=1:6
    %count only 5th loop
    for i=peak(9,j):peak(11,j)-1;

    areacalc(j) = areacalc(j) + (t(i+1,j)+t(i,j))*(g(i+1,j)-g(i,j))/2;
%calculate area with integration

    end
end


for j=1:6
%calculate ksi and Gsec and starting Go
Gsec(j) = abs((t(peak(11,j),j)-t(peak(10,j),j))/(g(peak(11,j),j)-
g(peak(10,j),j))) ;
areacalcel(j) = abs(t(peak(11,j),j)*g(peak(11,j),j))/2
ksi(j) = areacalc(j)/areacalcel(j)*(1/(4*pi));
%G1 = Gsec/Gostat logos Gsec/Go
G1(j)=abs(Gsec(j)/Gmax);
end

%normalization of Go/Gmax with Gmax from data
Gmax=max(Gsec);
GGmax=Gsec/Gmax;

%graph plot for input data.
%plot(xcor(:,1), xcor(:,2));
%hold on;

%Exports Data to text
fid2 = fopen('GGo-Ksi-plaxis-output.txt', 'w');

fprintf(fid2,'Go/Gsec\n');
fprintf(fid2,'%f %f %f %f %f %f\n',GGmax);
fprintf(fid2,'Ksi\n');
fprintf(fid2,'%f %f %f %f %f %f\n',ksi);
fprintf(fid2,'Gmax\n');
fprintf(fid2,'%f\n',Gmax);
fprintf(fid2,'gmax\n');
fprintf(fid2,'%f %f %f %f %f %f\n',g(peak(9),:));
fprintf(fid2,'tmax\n');
fprintf(fid2,'%f %f %f %f %f %f\n',t(peak(9),:));
fprintf(fid2,'Gsec\n');
fprintf(fid2,'%f %f %f %f %f %f\n',Gsec);
fclose(fid2);

%%%%%%%%%%%%%%%%%%%%%%END OF PROGRAM%%%%%%%%%%%%%%%%%%%%%%%%%%%%
```

3.4.2 Comparison of New Smooth Hysteresis model "NLDYAS modified" and "UBC3D-PLM" model

This stage features a comparison of UBC3D-PLM and NLDYAS modifed that are a product of the proposed optimization process as featured above for the UBC3D-PLM model and as proposed by Parpotas and Gerolymos for NLDYAS modified.

The figures (3.28) to (3.33) present a comparison of G/G_{max}-γ and ξ-γ curves for three (3) different load scenarios (σvo'=50kpa, σvo'=100kpa, σvo'=200kpa) and a comparison is also made for the hysteretic loops for the σvo'=50 and σvo'=200kpa load scenarios for 6 prescribed strains thus 0.001%, 0.01%, 0.1%, 1%, 10% and 100%.

3.4.3 Verification of "NLDYAS" and "UBC3D-PLM" model

This stage features a verification run between UBC3D-PLM and NLDYAS old. The verification is run that in order to show that reproducing UBC3D-PLM with NLDYAS is possible with setting the NLDYAS parameter that deactivates s1 and s2, (x=0) and the parameter n=0.60 (with b=g=0.5). The loops are presented at the figure section and show a considerable matching between the two models.

The new model "NLDYAS modified" is an improved version of the old version since it has a considerable match with bibliography and experimental data from Ishibashi & Chang's curves. For that reason the loops have a smaller total area to have a maximum ξ of around 32.7% which is remotely right and on par of experimental data. Additionally on the unloading phase there is no elasticity on contrary of NLDYAS old and UBC3D-PLM that return elasticly untill 0.

3.5. Optimization and Calibration commentary

The proposed methodology is deemed sufficient to get a fairly good understanding on the weaknesses and advantages of each method. It is also providing a fairly accurate and simplified method of equating the two constitutive models.

It appears that although G/G_{max}-γ arent very different the hysteretic damping curves ξ-γ are highly overestimated from UBC3D-PLM which is also expected.

Althought "NLDYAS modified" is fundamedally different than UBC3D-PLM the differences and especially the impro

In the next chapter dynamic analyses where run on two expiremental soil profiles in order to get a better understanding of how each method works.

Figures

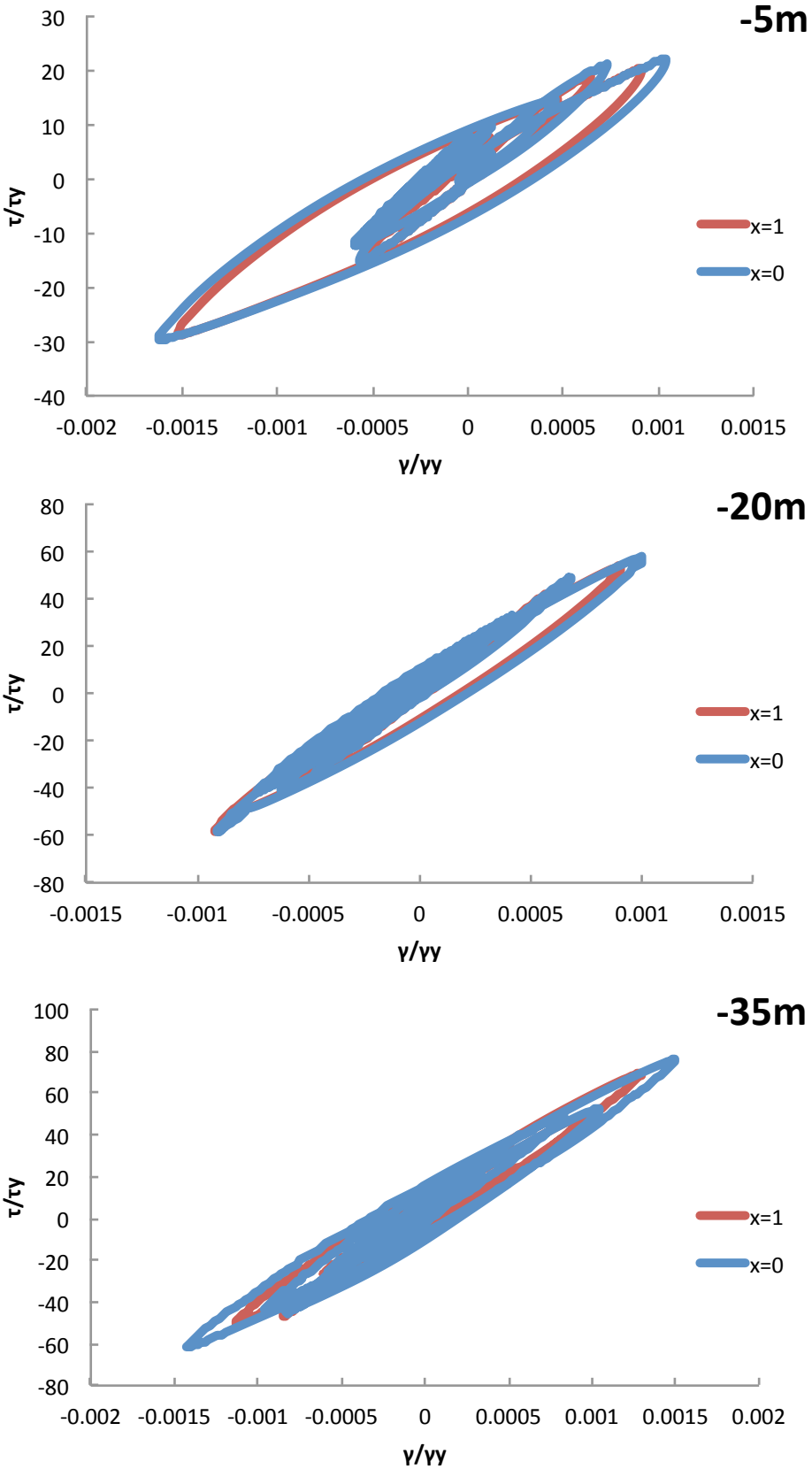

Figure 3.1: Role of rock outcrop motion. *τ-τ/γ - γ-γy charts for x=1 (rock outcrop motion activated, rigid) or x=0 (rock outcrop motion deactivated) on "NL-DYAS modified". Application on* ***Experimental Layered Soil*** *in depths -35m, -20m, -5m respectively for the Aegion 0.39g excitation. x=0 means rock base is rigid meaning no radiation damping.*

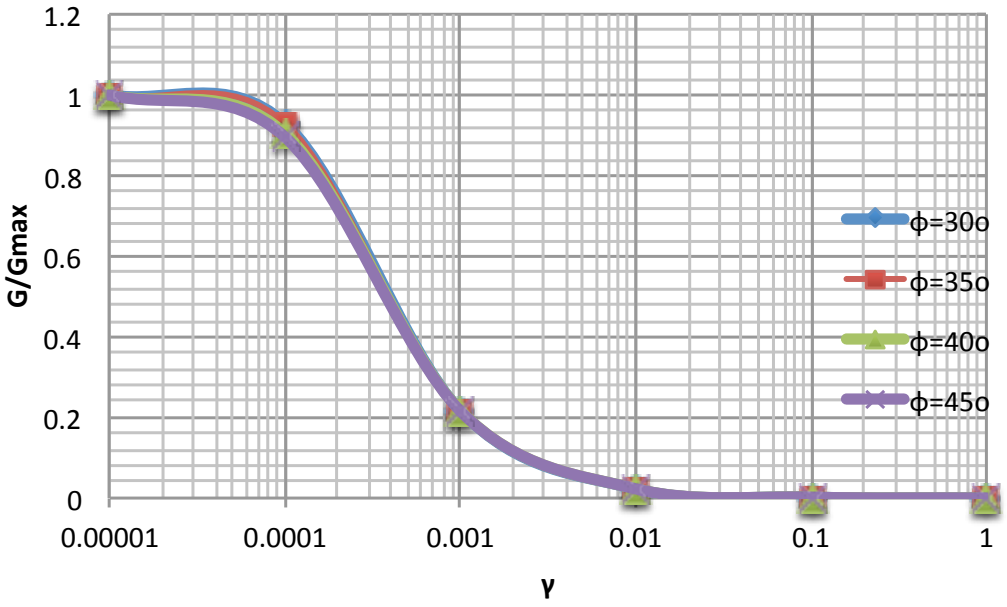

Figure 3.2 ***Role of φ angle.*** *UBC3D-PLM triaxial soiltest for 4 different φ values. Comparison of the 4 different G/Gmax - γ charts for a fixed load of* ***σv'=10kpa****.*

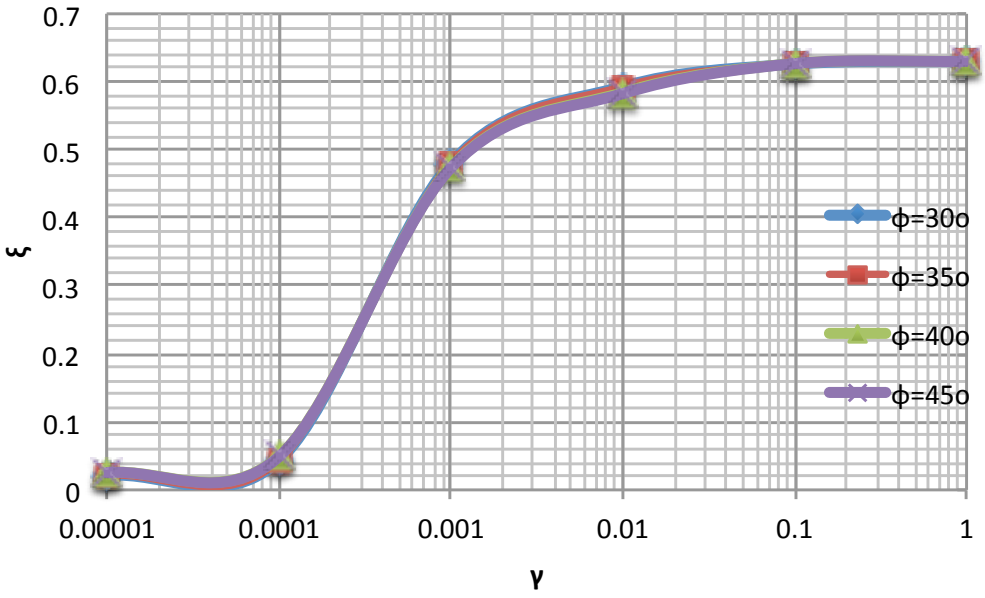

Figure 3.3 ***Role of φ angle.*** *UBC3D-PLM triaxial soiltest for 4 different φ values. Comparison of the 4 different ξ - γ charts for a fixed load of* ***σv'=10kpa****.*

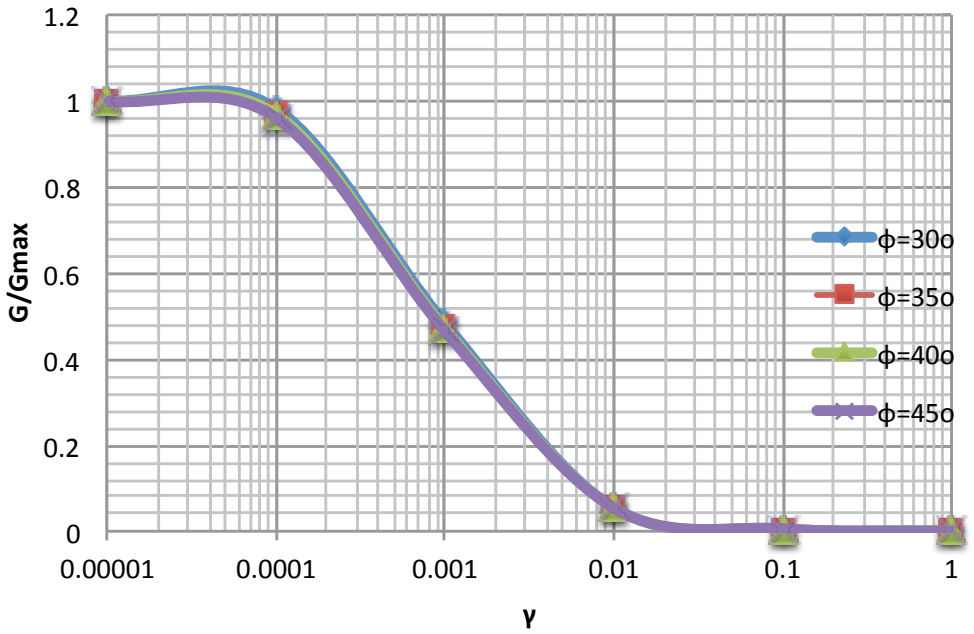

Figure 3.4 Role of φ angle. *UBC3D-PLM triaxial soiltest for 4 different φ values. Comparison of the 4 different G/Gmax - γ charts for a fixed load of* ***σv'=50kpa****.*

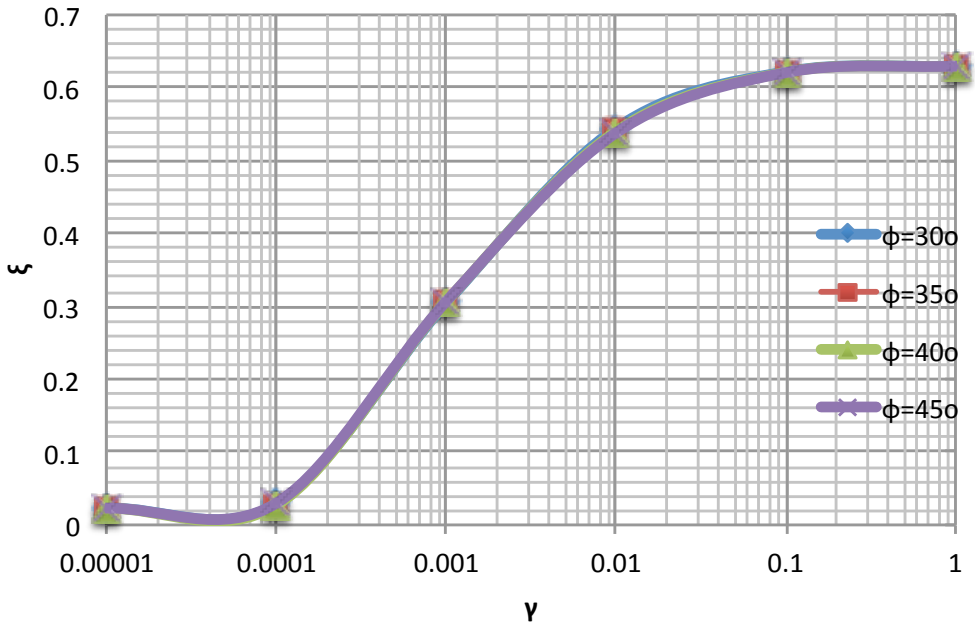

Figure 3.5 Role of φ angle. *UBC3D-PLM triaxial soiltest for 4 different φ values. Comparison of the 4 different ξ - γ charts for a fixed load of* ***σv'=50kpa****.*

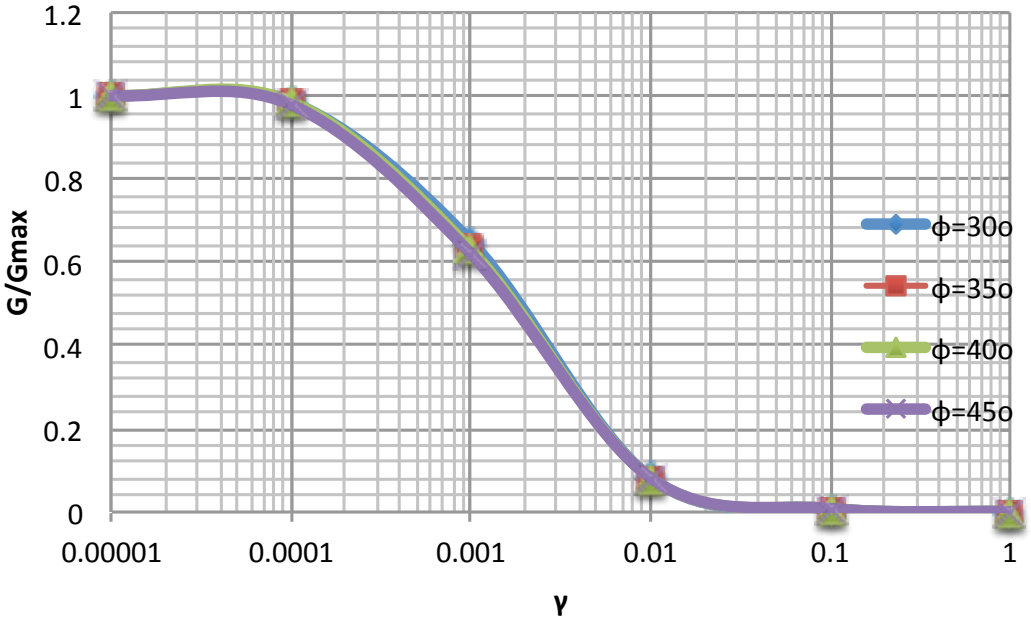

Figure 3.6 Role of φ angle. *UBC3D-PLM triaxial soiltest for 4 different φ values. Comparison of the 4 different G/Gmax - γ charts for a fixed load of* ***σv'=100kpa****.*

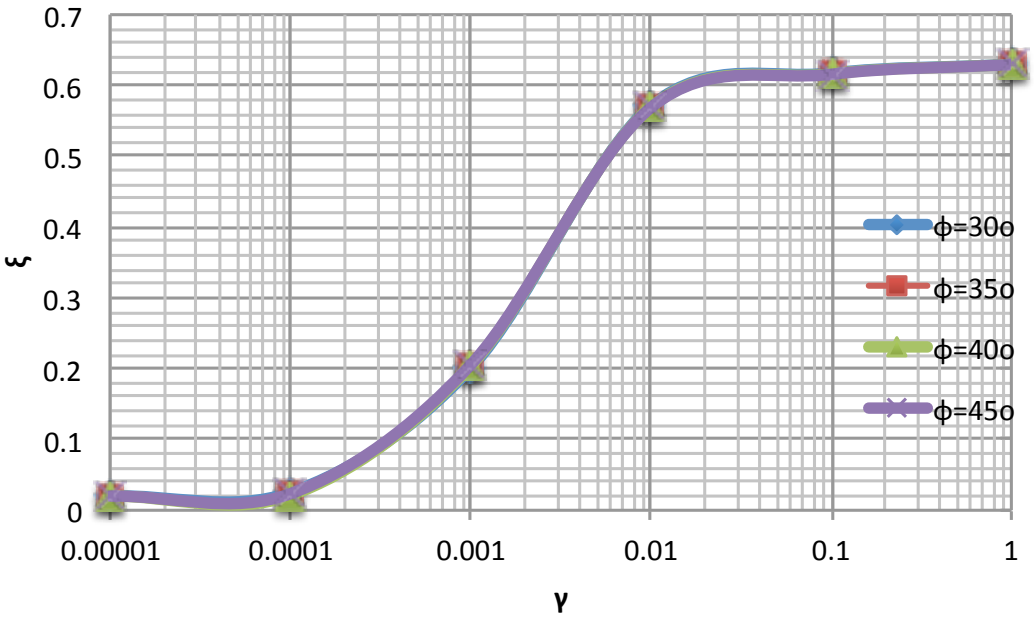

Figure 3.7 Role of φ angle. *UBC3D-PLM triaxial soiltest for 4 different φ values. Comparison of the 4 different ξ - γ charts for a fixed load of* ***σv'=100kpa****.*

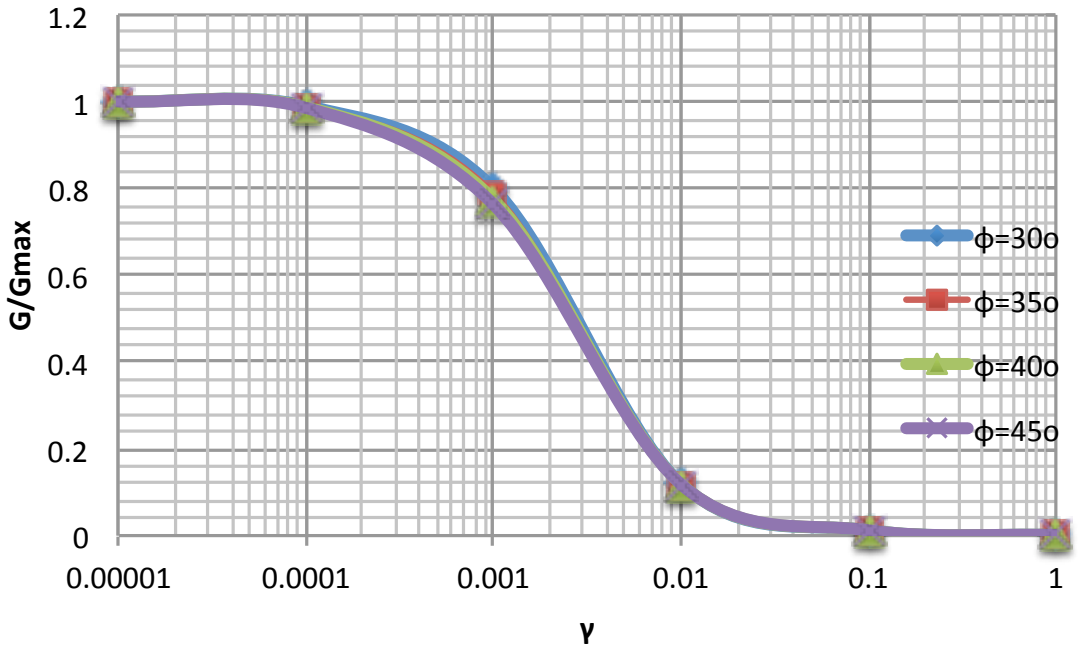

Figure 3.8 Role of φ angle. *UBC3D-PLM triaxial soiltest for 4 different φ values. Comparison of the 4 different G/Gmax - γ charts for a fixed load of* ***σv'=200kpa****.*

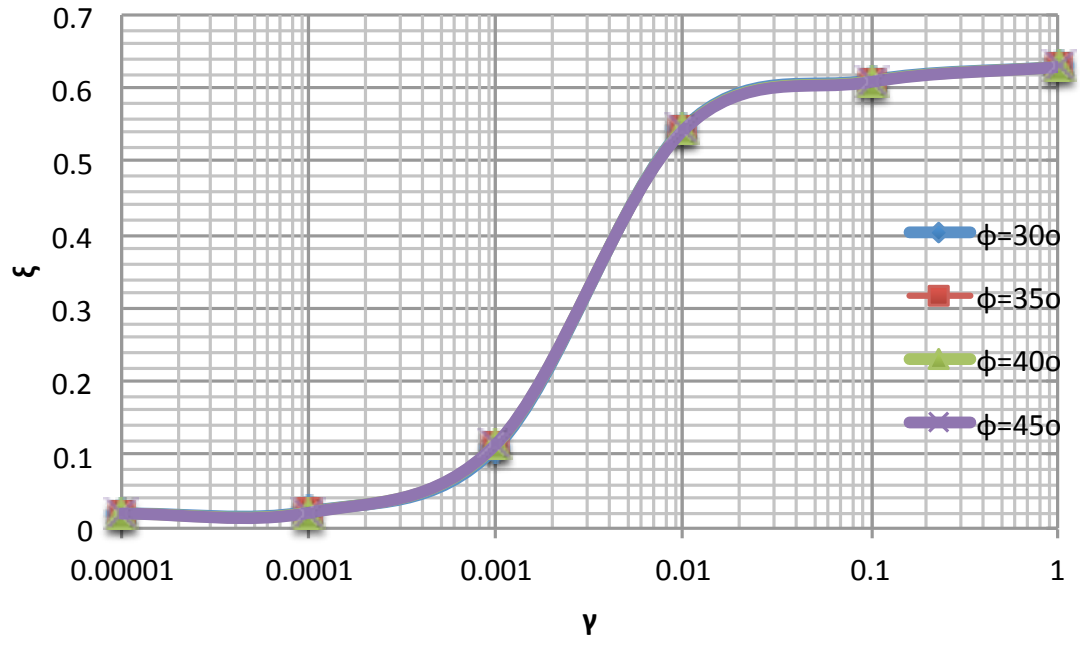

Figure 3.9 Role of φ angle. *UBC3D-PLM triaxial soiltest for 4 different φ values. Comparison of the 4 different ξ - γ charts for a fixed load of* ***σv'=200kpa****.*

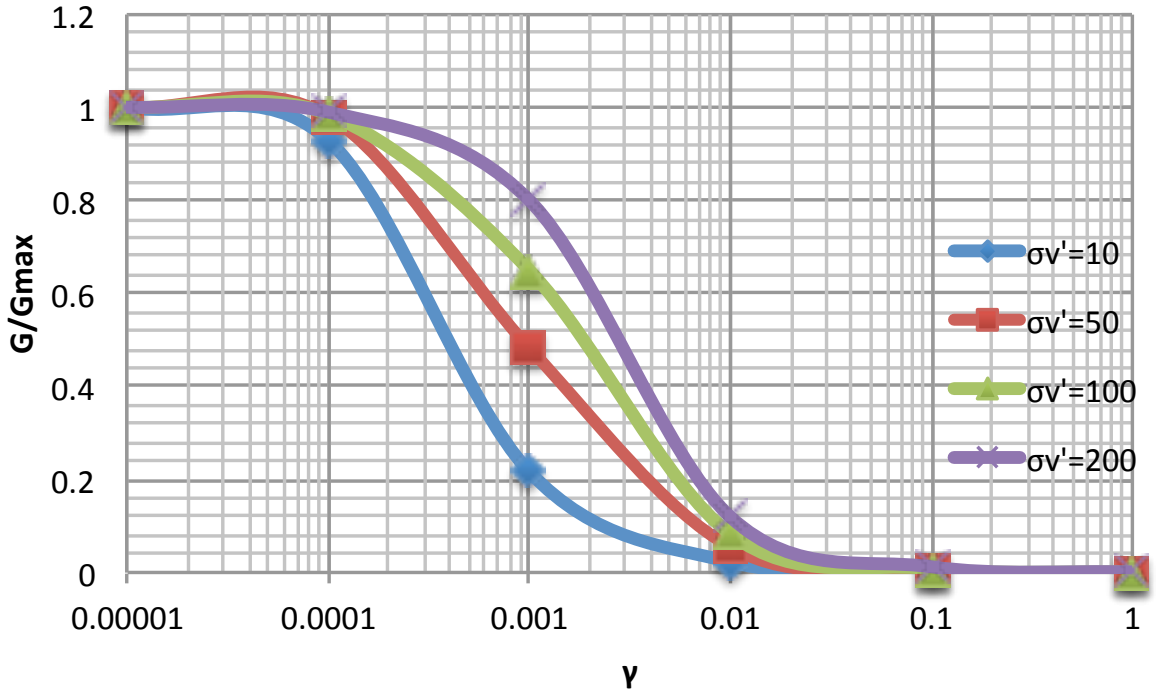

Figure 3.10 Role of φ angle. *UBC3D-PLM triaxial soiltest for 4 different φ values. Comparison of the 4 different G/Gmax - γ charts for the 4 fixed load scenarios of* ***σv'=10kpa, σv'=50kpa, σv'=100kpa, σv'=200kpa*** *and the same φ value.*

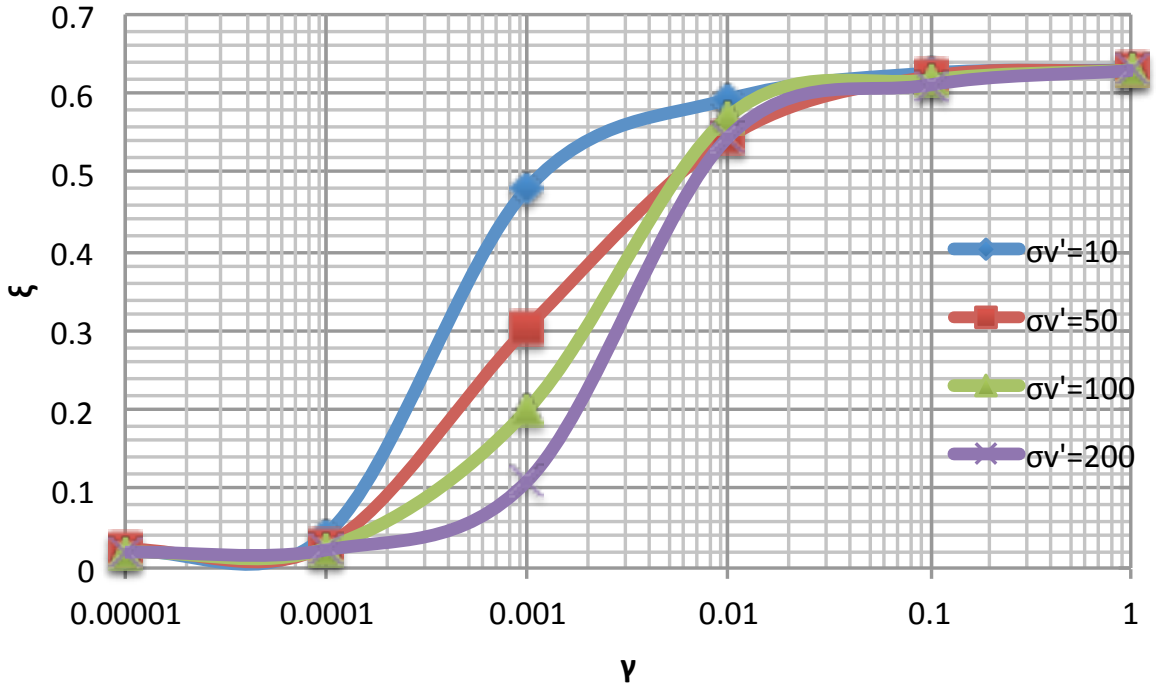

Figure 3.11 Role of φ angle. *UBC3D-PLM triaxial soiltest for 4 different φ values. Comparison of the 4 different ξ - γ charts for the 4 fixed load scenarios of* ***σv'=10kpa, σv'=50kpa, σv'=100kpa, σv'=200kpa*** *and the same φ value.*

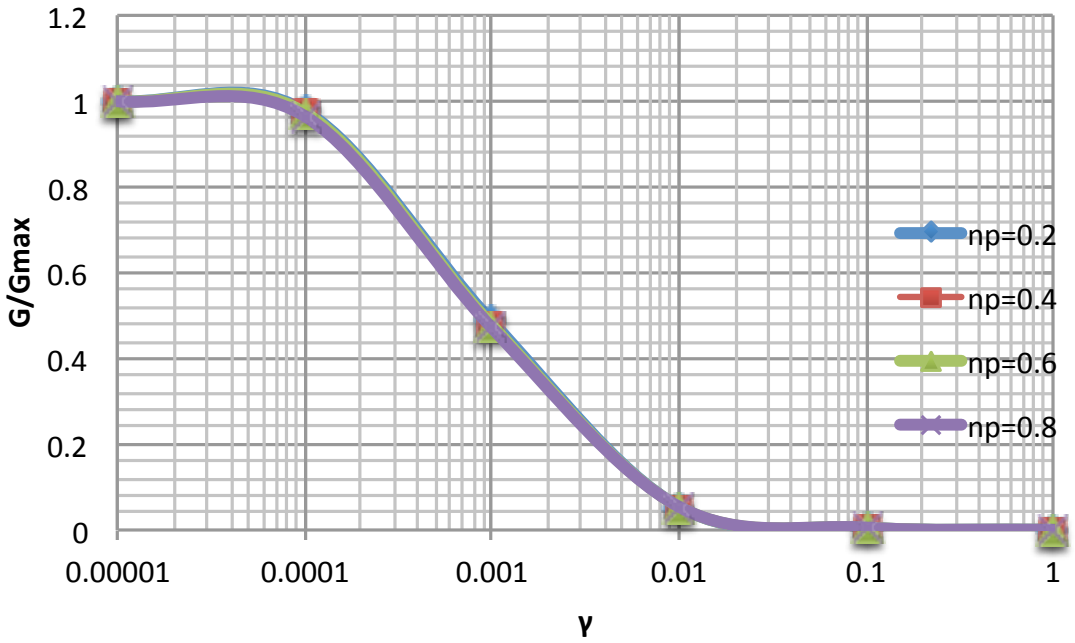

Figure 3.12 ***n_p role.*** *UBC3D-PLM triaxial soiltest for 4 different* ***n_p*** *values. Comparison of the 4 different G/Gmax - γ charts for a fixed load of σv'=50kpa.*

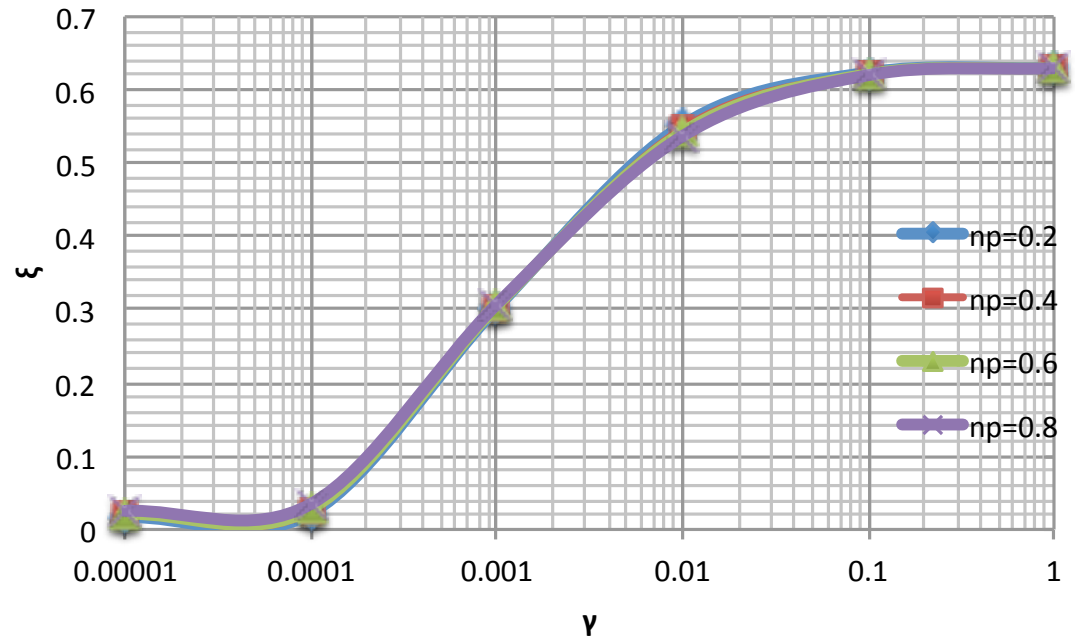

Figure 3.13 ***n_p role.*** *UBC3D-PLM triaxial soiltest for 4 different* ***n_p*** *values. Comparison of the 4 different ξ - γ charts for a fixed load of σv'=50kpa.*

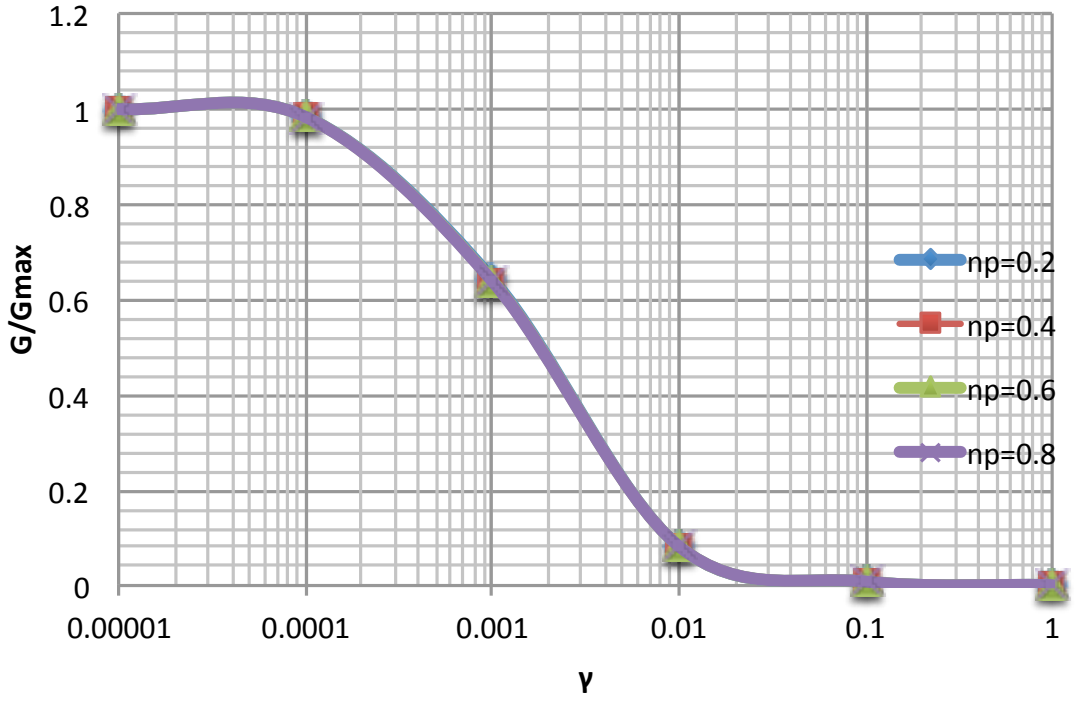

Figure 3.14 ***n_p role.*** *UBC3D-PLM triaxial soiltest for 4 different* ***n_p*** *values. Comparison of the 4 different G/Gmax - γ charts for a fixed load of σv'=100kpa.*

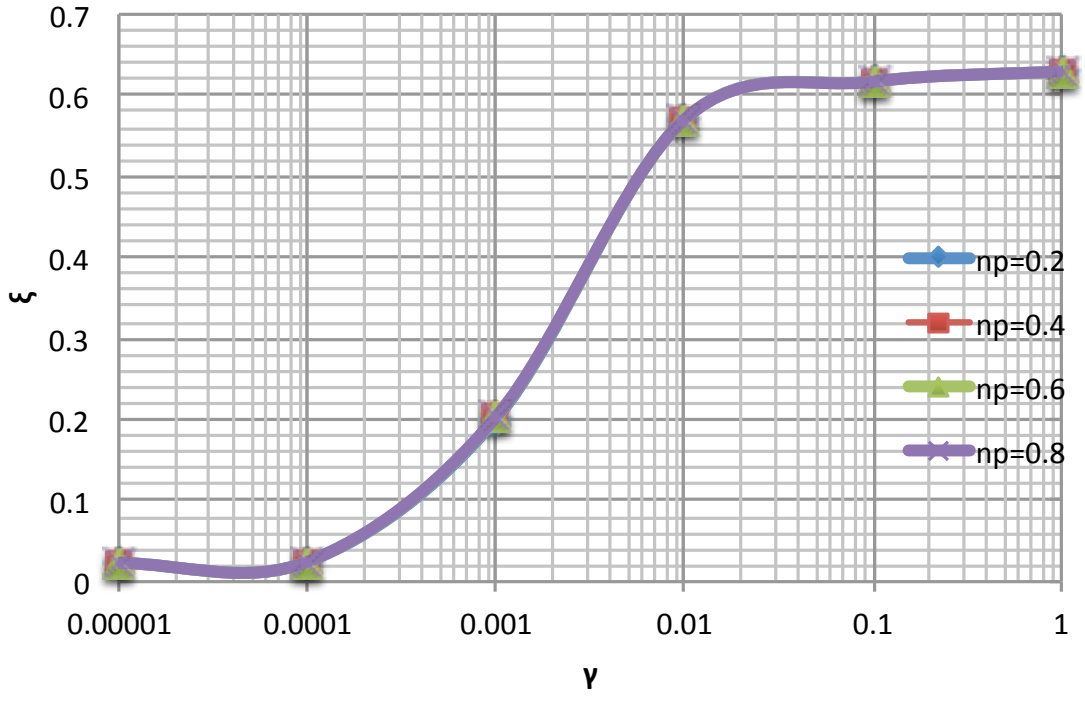

Figure 3.15 ***n_p role.*** *UBC3D-PLM triaxial soiltest for 4 different* ***n_p*** *values. Comparison of the 4 different ξ - γ charts for a fixed load of σv'=100kpa.*

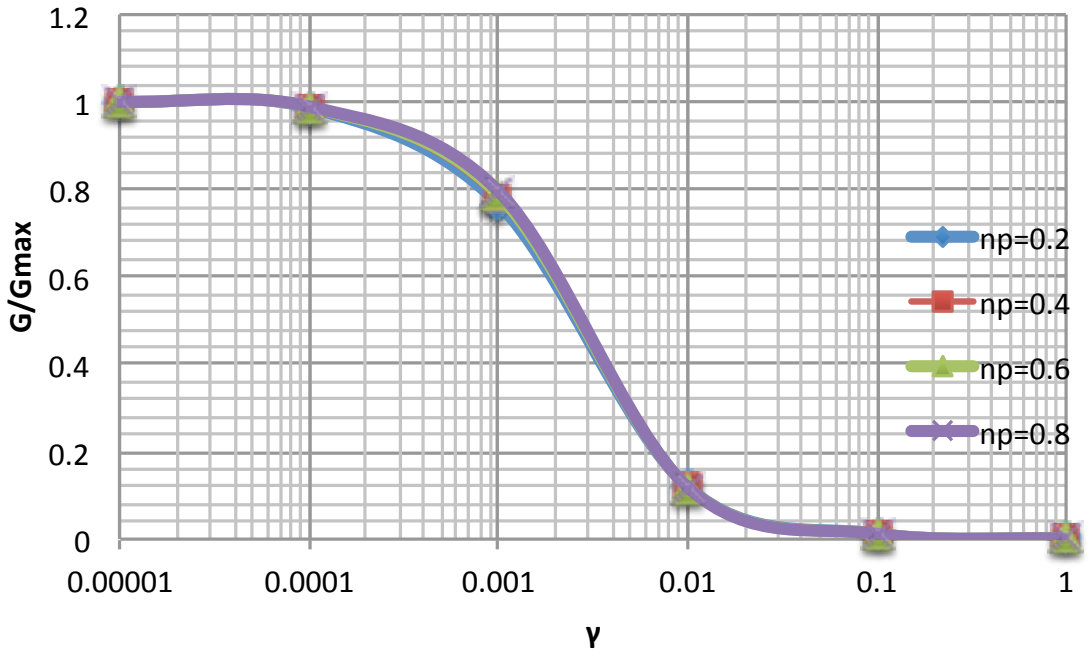

Figure 3.16 n_p role. *UBC3D-PLM triaxial soiltest for 4 different n_p values. Comparison of the 4 different G/Gmax - γ charts for a fixed load of σv'=200kpa.*

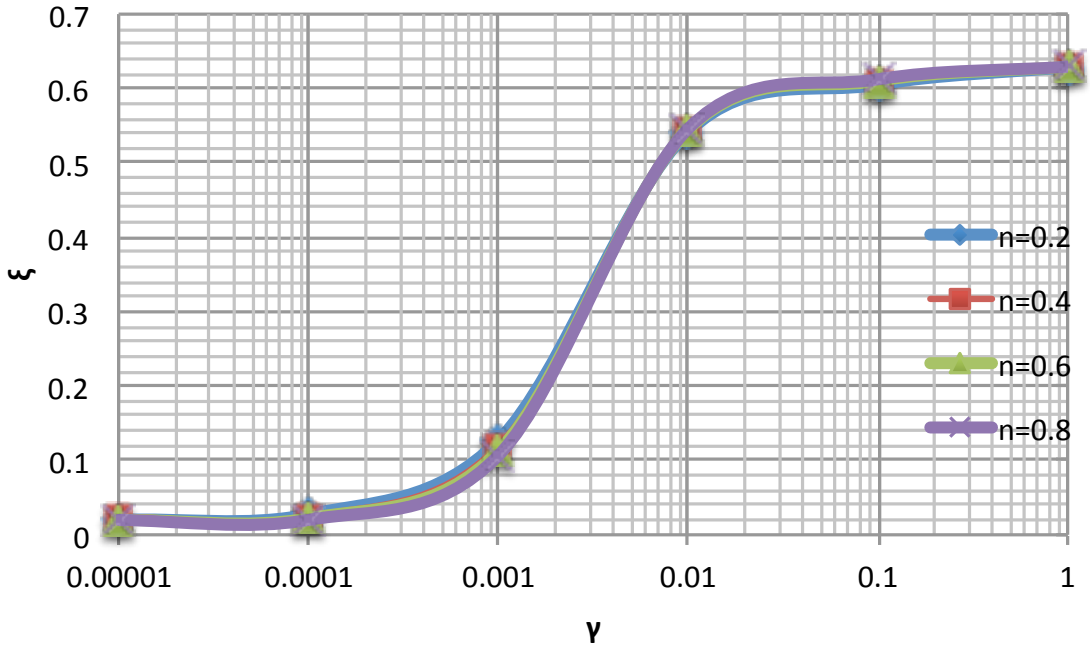

Figure 3.17 n_p role. *UBC3D-PLM triaxial soiltest for 4 different n_p values. Comparison of the 4 different ξ - γ charts for a fixed load of σv'=200kpa.*

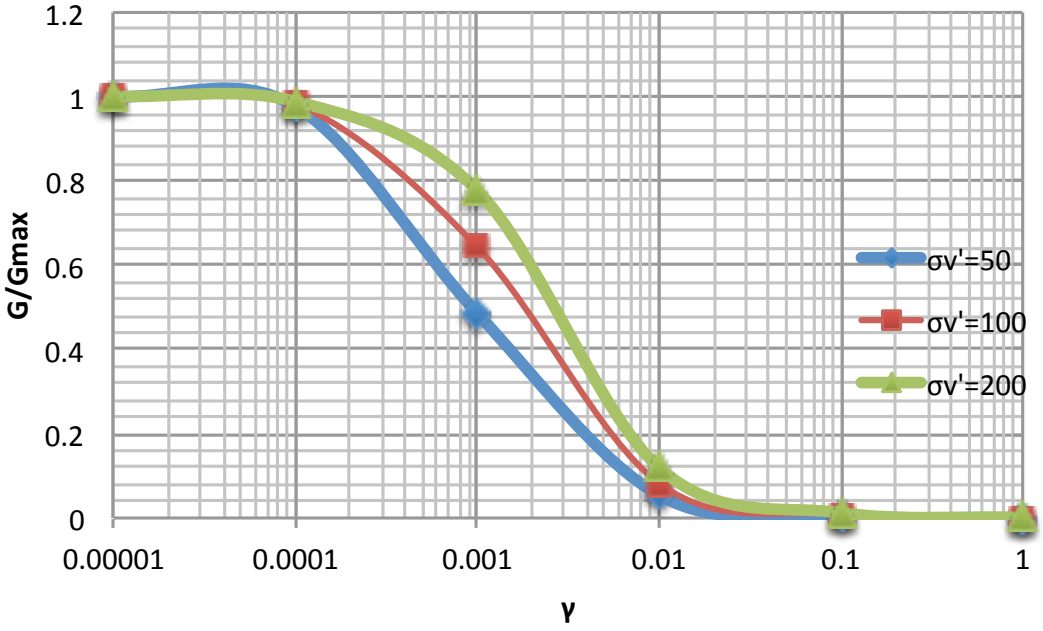

Figure 3.18 n_p role. *UBC3D-PLM triaxial soiltest for 3 different n_p values. Comparison of the 3 different G/Gmax - γ charts for the 3 fixed load scenarios of* ***σv'=50kpa, σv'=100kpa, σv'=200kpa*** *and the same n_p value.*

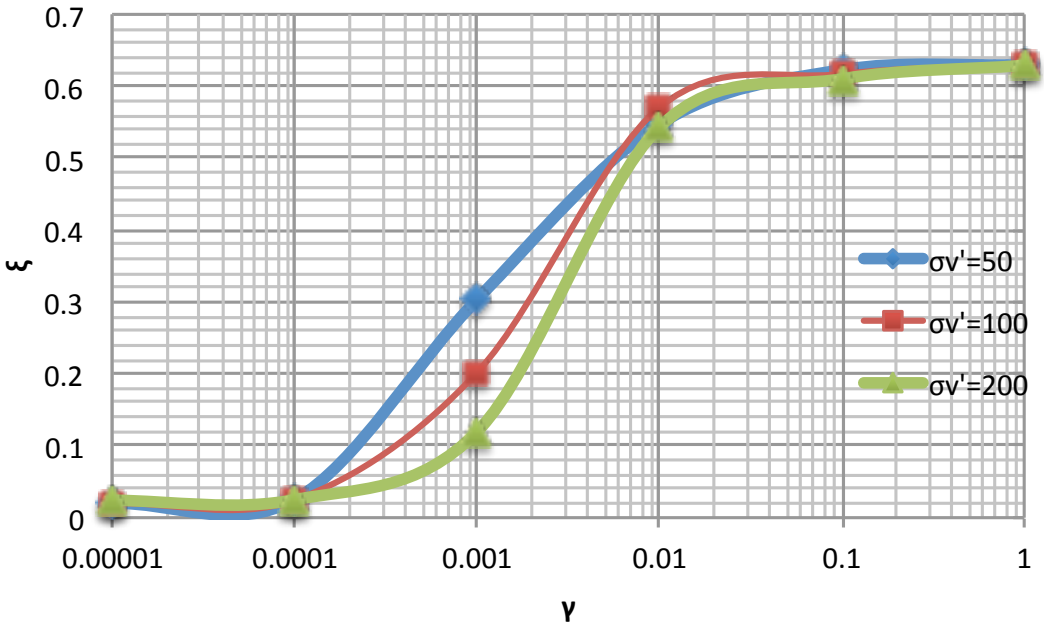

Figure 3.19 n_p role. *UBC3D-PLM triaxial soiltest for 3 different n_p values. Comparison of the 3 different ξ - γ charts for the 3 fixed load scenarios of* ***σv'=50kpa, σv'=100kpa, σv'=200kpa*** *and the same n_p value.*

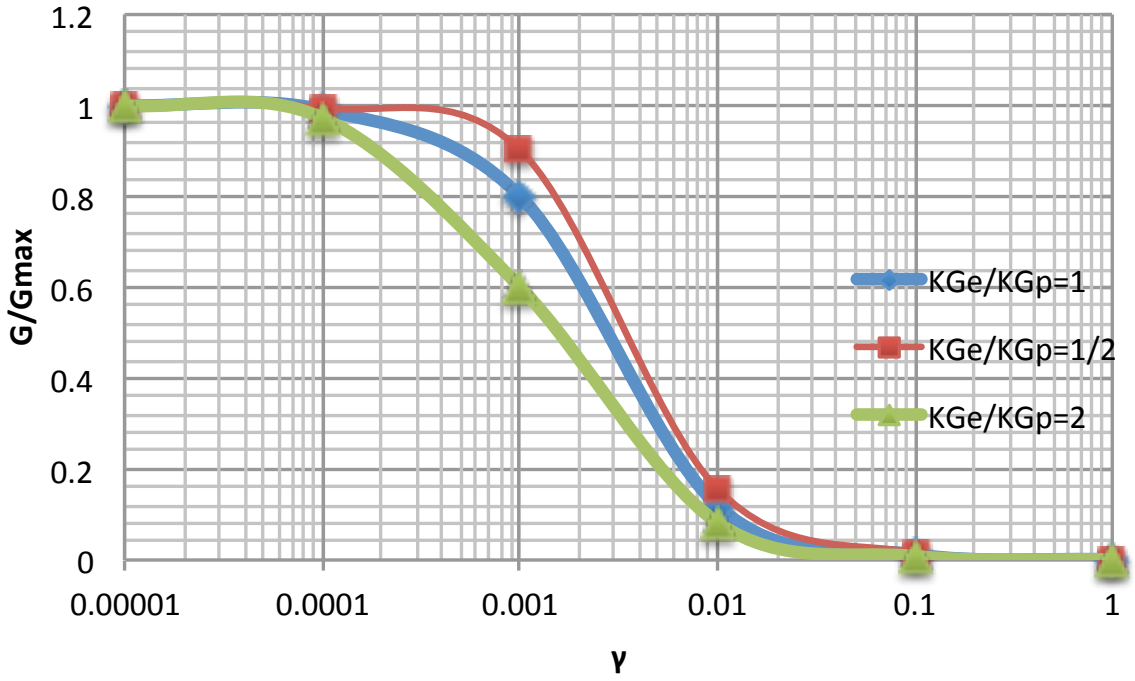

Figure 3.20 KG role. *G/Gmax - γ chart comparison for φ=30º and different ratios of KGe/KGp resulting from UBC3D-PLM triaxal soiltest.*

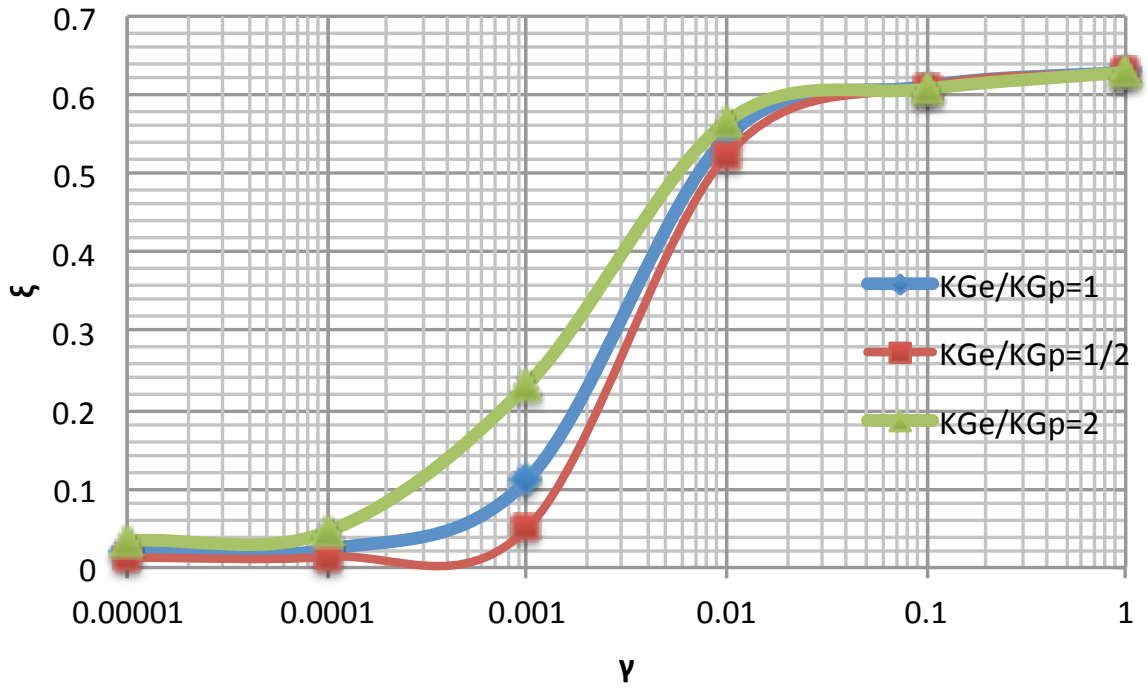

Figure 3.21 KG role. *ξ - γ chart comparison for φ=30º and different ratios of KGe/KGp resulting from UBC3D-PLM triaxal soiltest.*

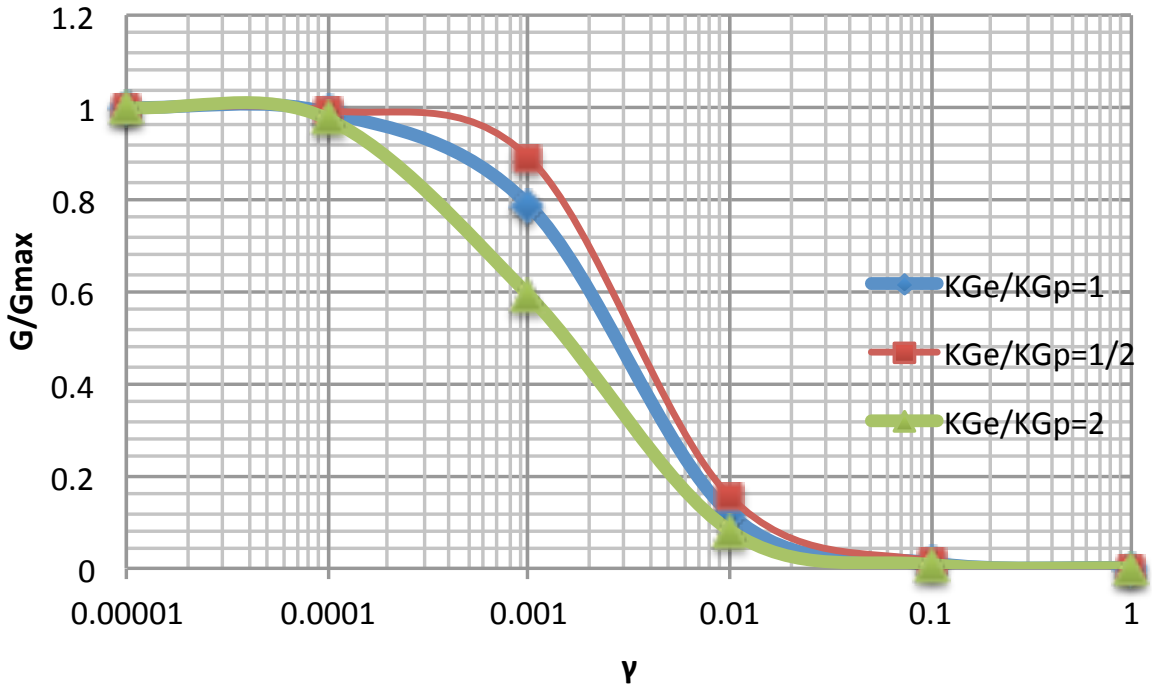

Figure 3.22 KG role. *G/Gmax - γ chart comparison for φ=35º and different ratios of KGe/KGp resulting from UBC3D-PLM triaxal soiltest.*

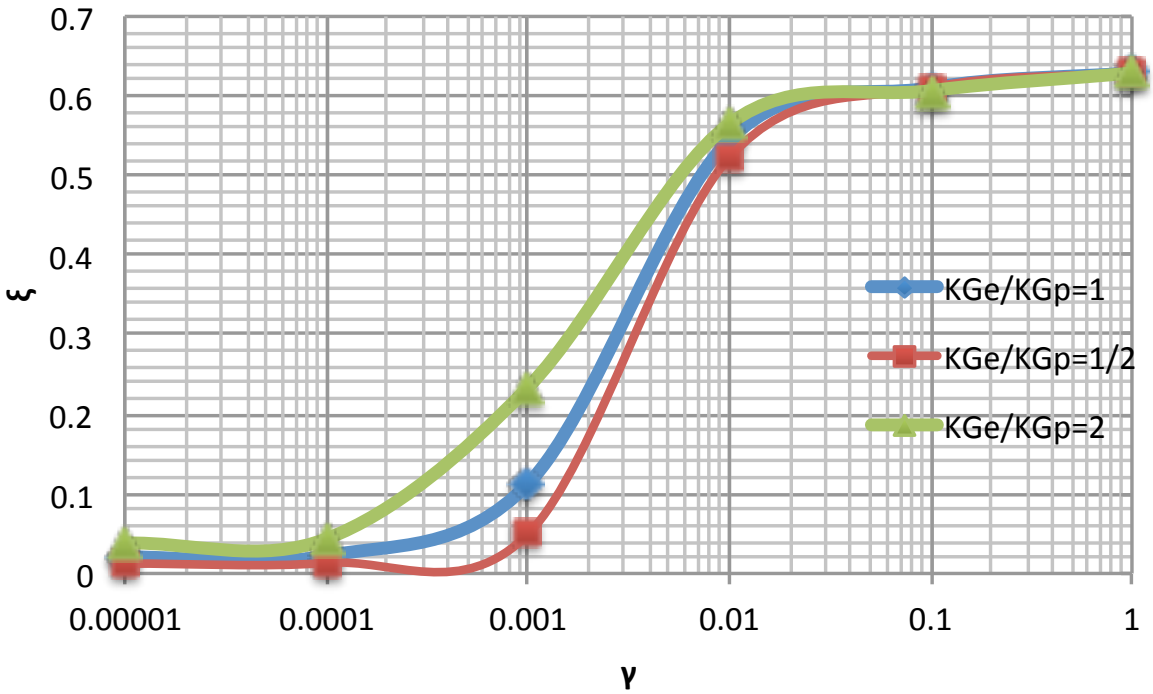

Figure 3.23 KG role. *ξ - γ chart comparison for φ=35º and different ratios of KGe/KGp resulting from UBC3D-PLM soiltest.*

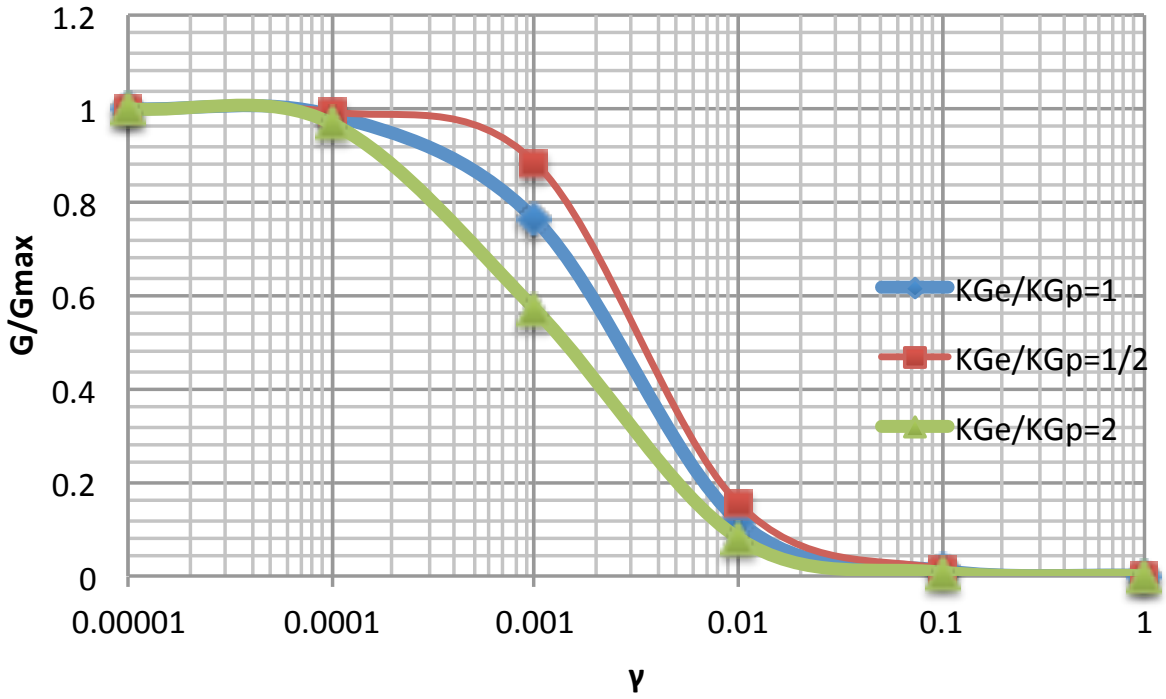

Figure 3.24 KG role. *G/Gmax - γ chart comparison for φ=40° and different ratios of KGe/KGp resulting from UBC3D-PLM soiltest.*

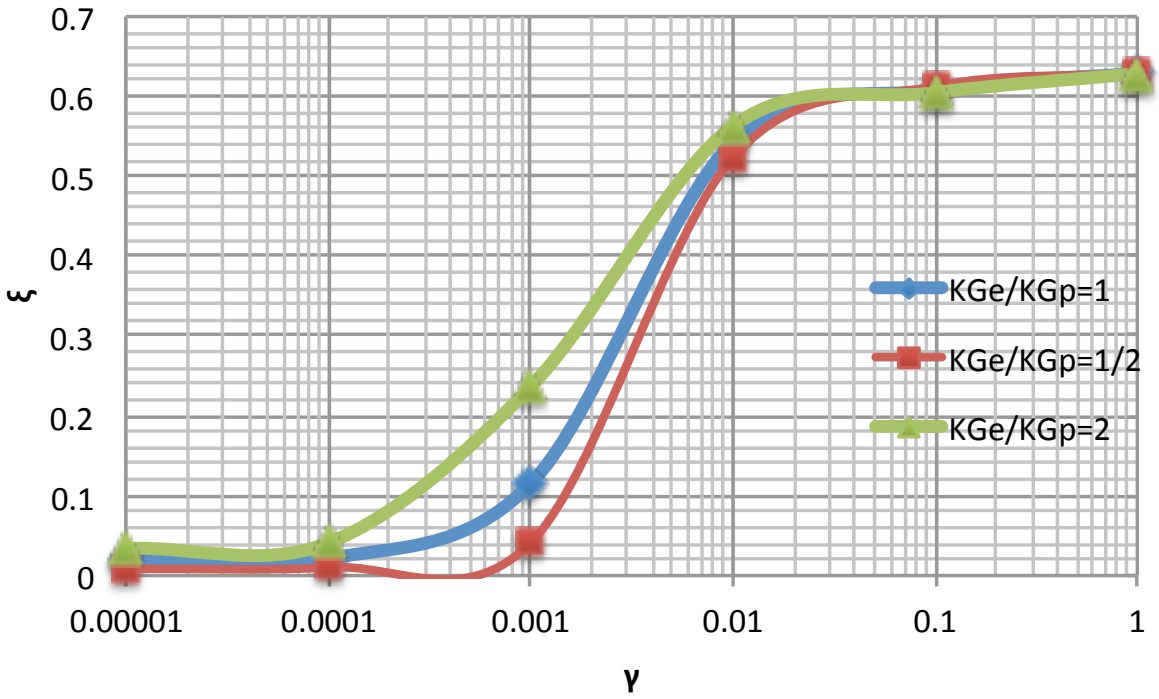

Figure 3.25 KG role. *ξ - γ chart comparison for φ=40° and different ratios of KGe/KGp resulting from UBC3D-PLM soiltest.*

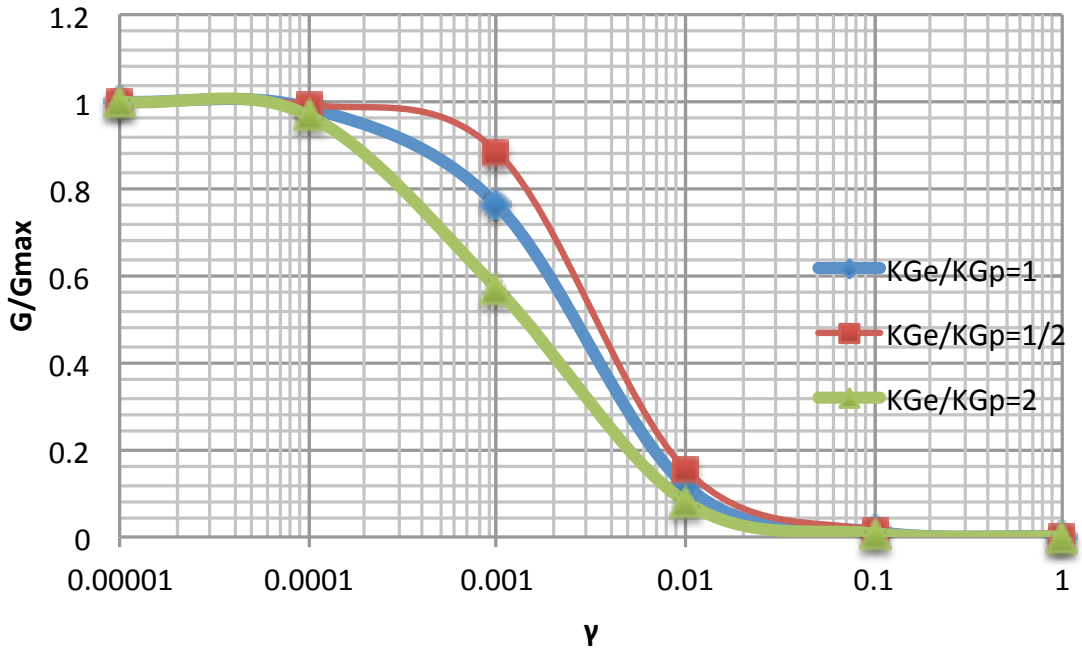

Figure 3.26 KG role. *G/Gmax - γ chart comparison for φ=45° and different ratios of KGe/KGp resulting from UBC3D-PLM soiltest.*

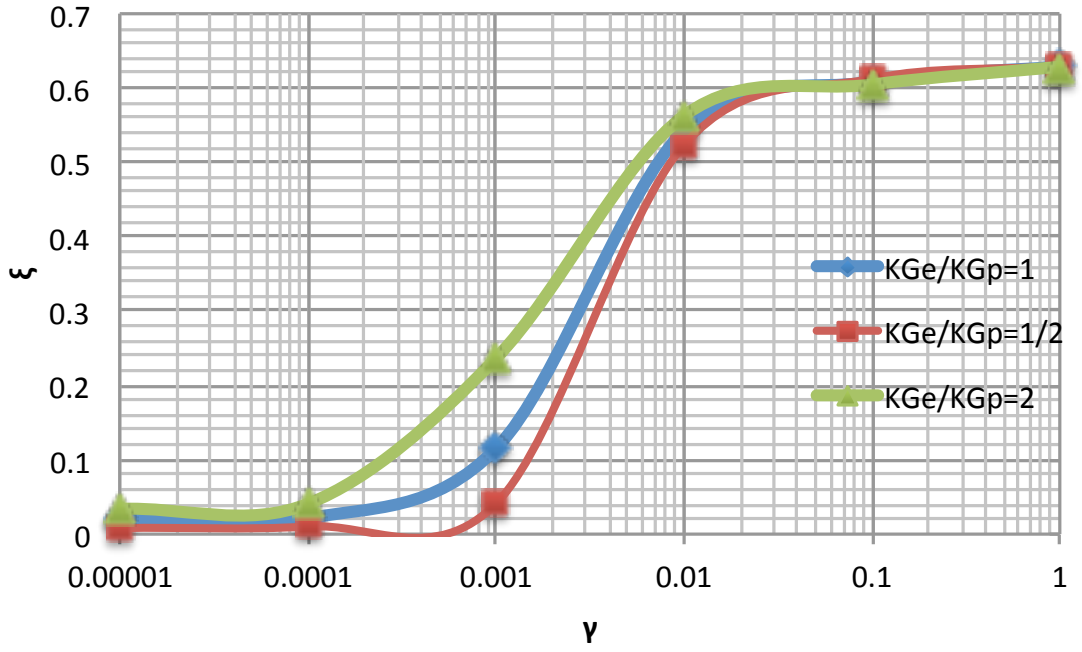

Figure 3.27 KG role. *ξ - γ chart comparison for φ=45° and different ratios of KGe/KGp resulting from UBC3D-PLM soiltest.*

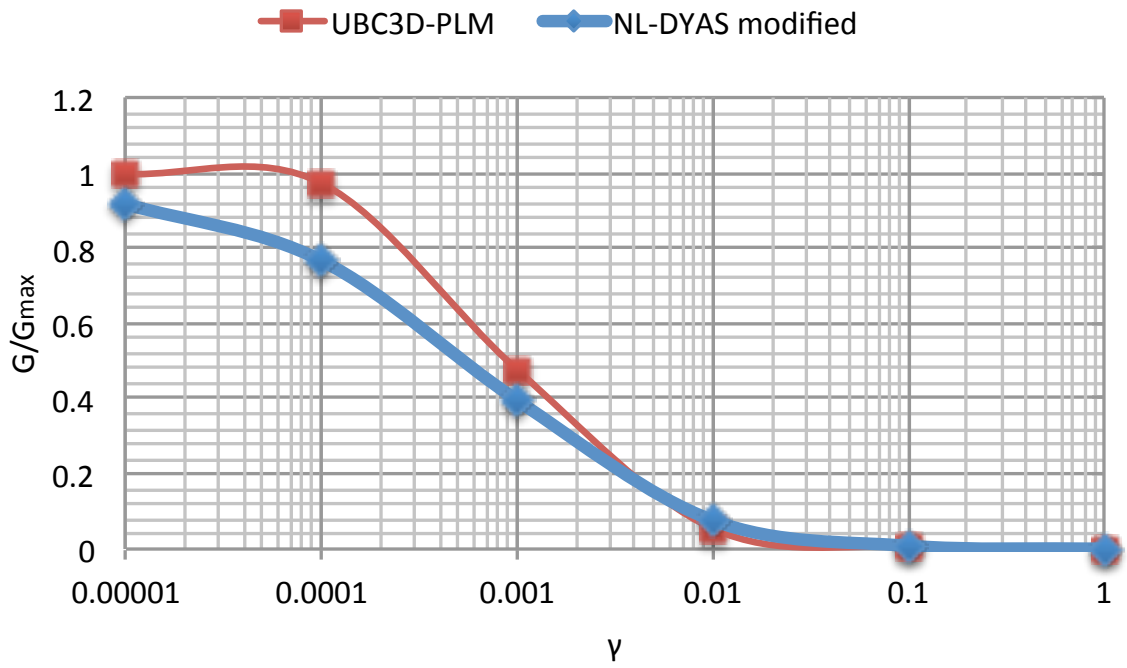

Figure 3.28 . *G/Gmax - γ chart for fixed load of* ***σv'=50kpa****. Comparison between UBC3D-PLM and NL-DYAS modified with equated parameters*

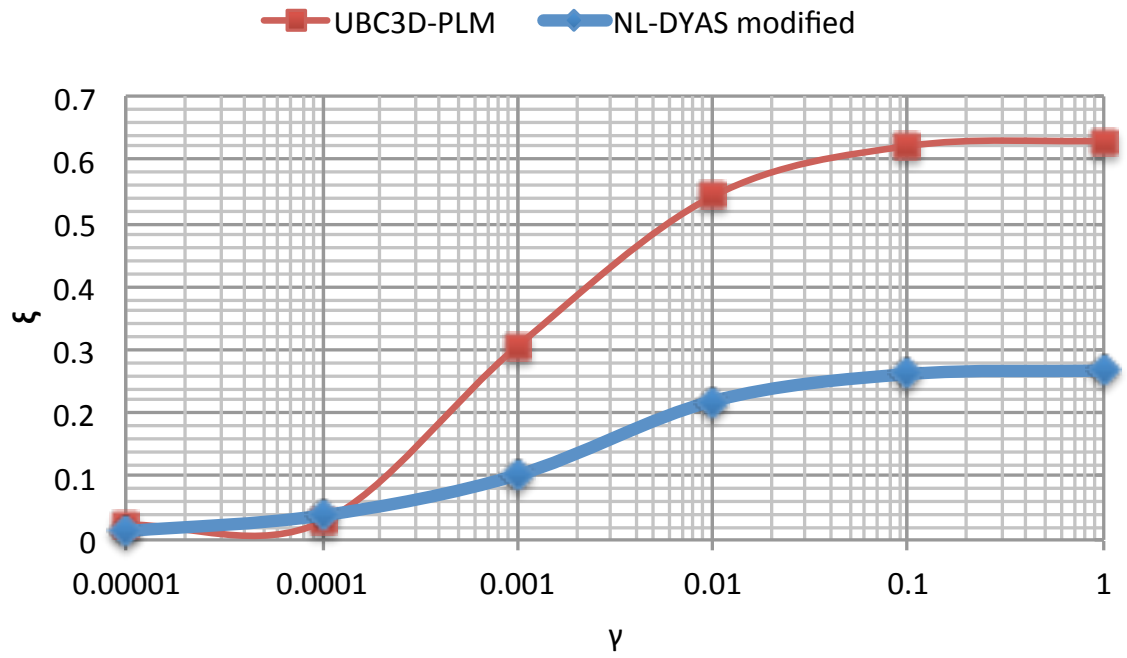

Figure 3.29 . *ξ - γ chart for fixed load of* ***σv'=50kpa****. Comparison between UBC3D-PLM and NL-DYAS modified with equated parameters*

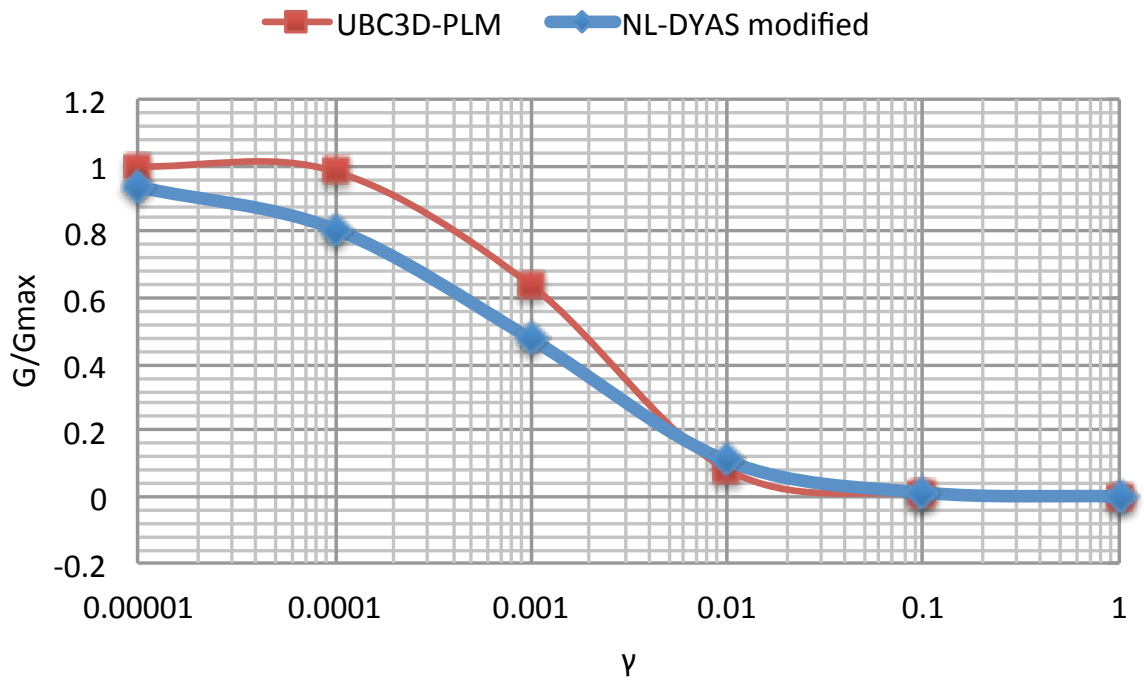

Figure 3.30 *G/Gmax - γ chart for fixed load of* ***σv'=100kpa*** *between UBC3D-PLM and NL-DYAS modified with equated parameters.*

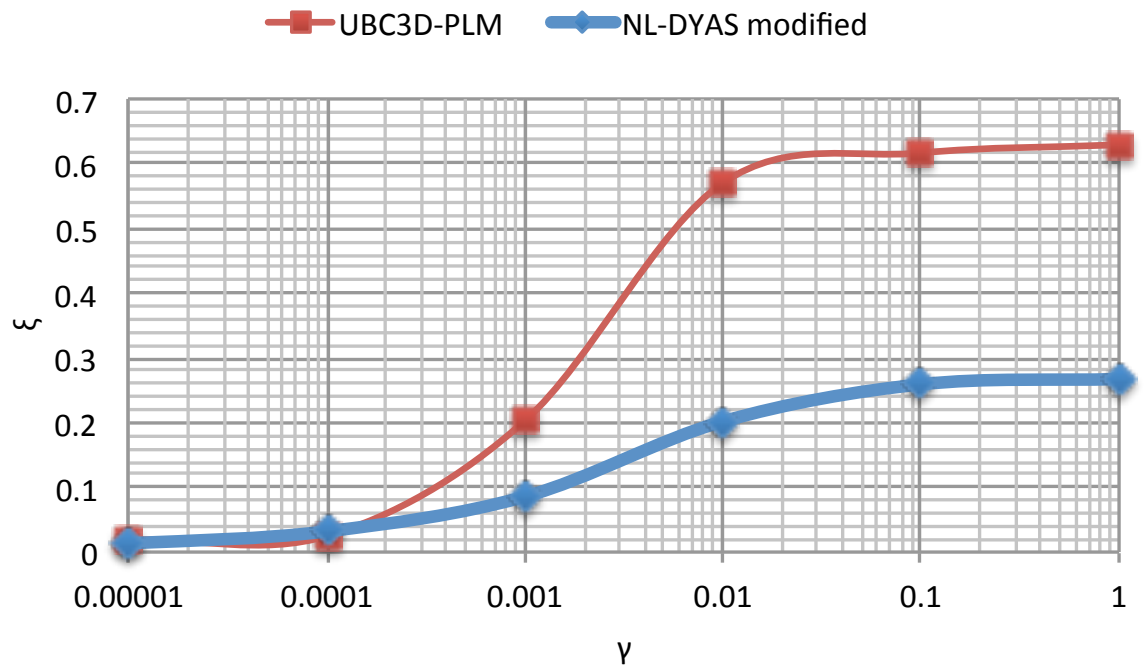

Figure 3.31 *ξ - γ chart for fixed load of* ***σv'=100kpa*** *between UBC3D-PLM and NL-DYAS modified with equated parameters.*

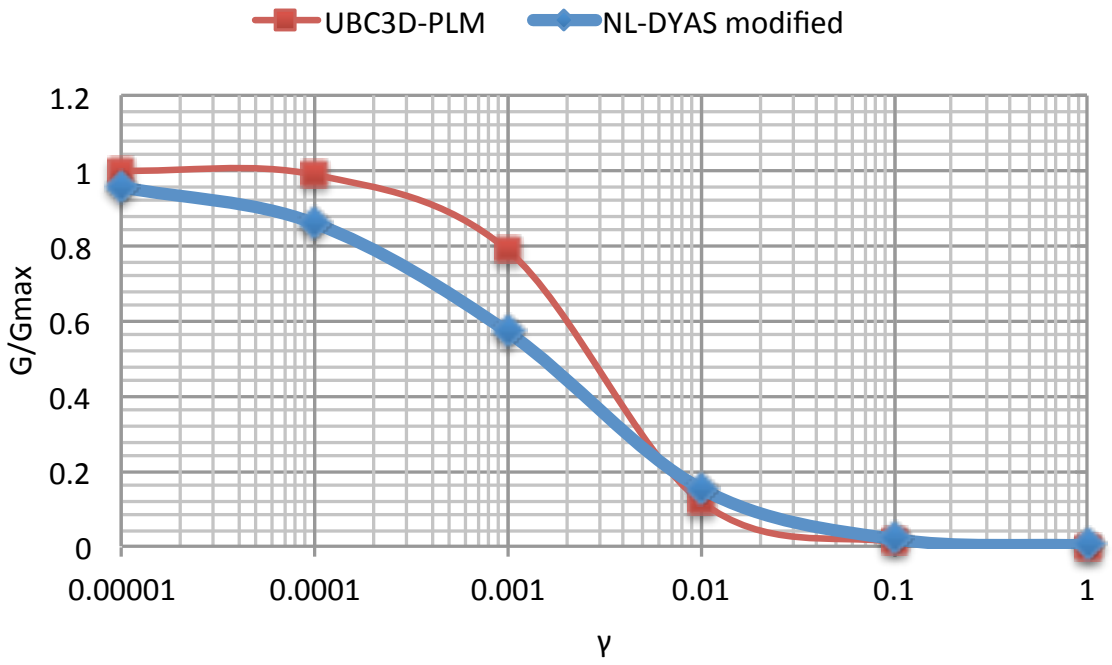

Figure 3.32 *G/Gmax - γ chart for fixed load of* ***σv'=200kpa*** *between UBC3D-PLM and NL-DYAS modified with equated parameters.*

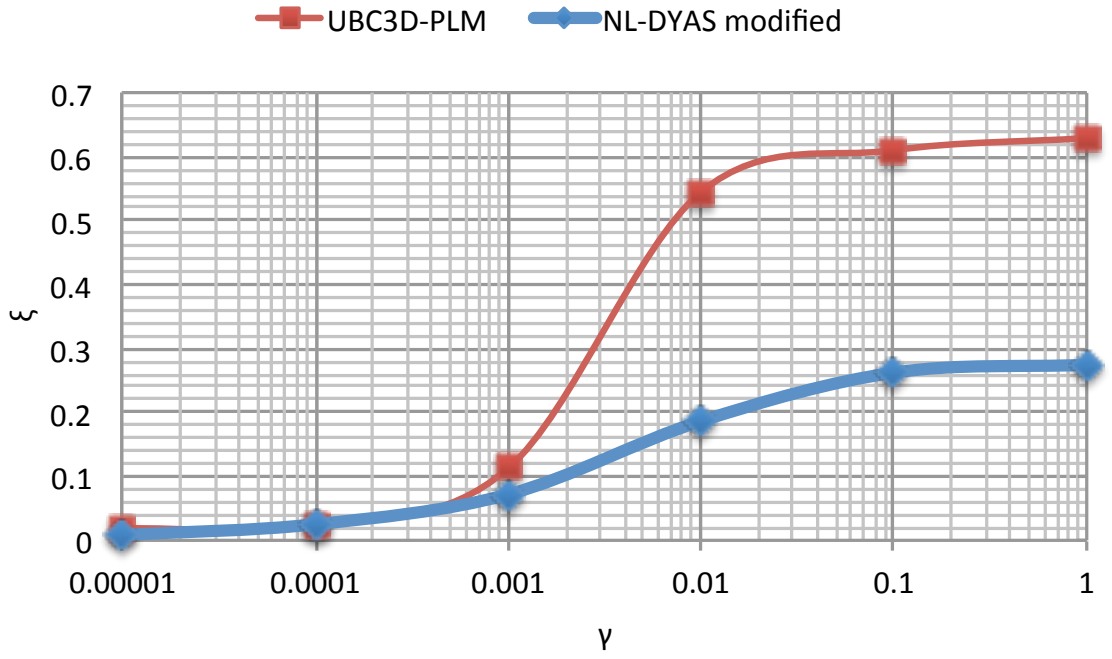

Figure 3.33 *ξ - γ chart for fixed load of* ***σv'=200kpa*** *between UBC3D-PLM and NL-DYAS modified with equated parameters.*

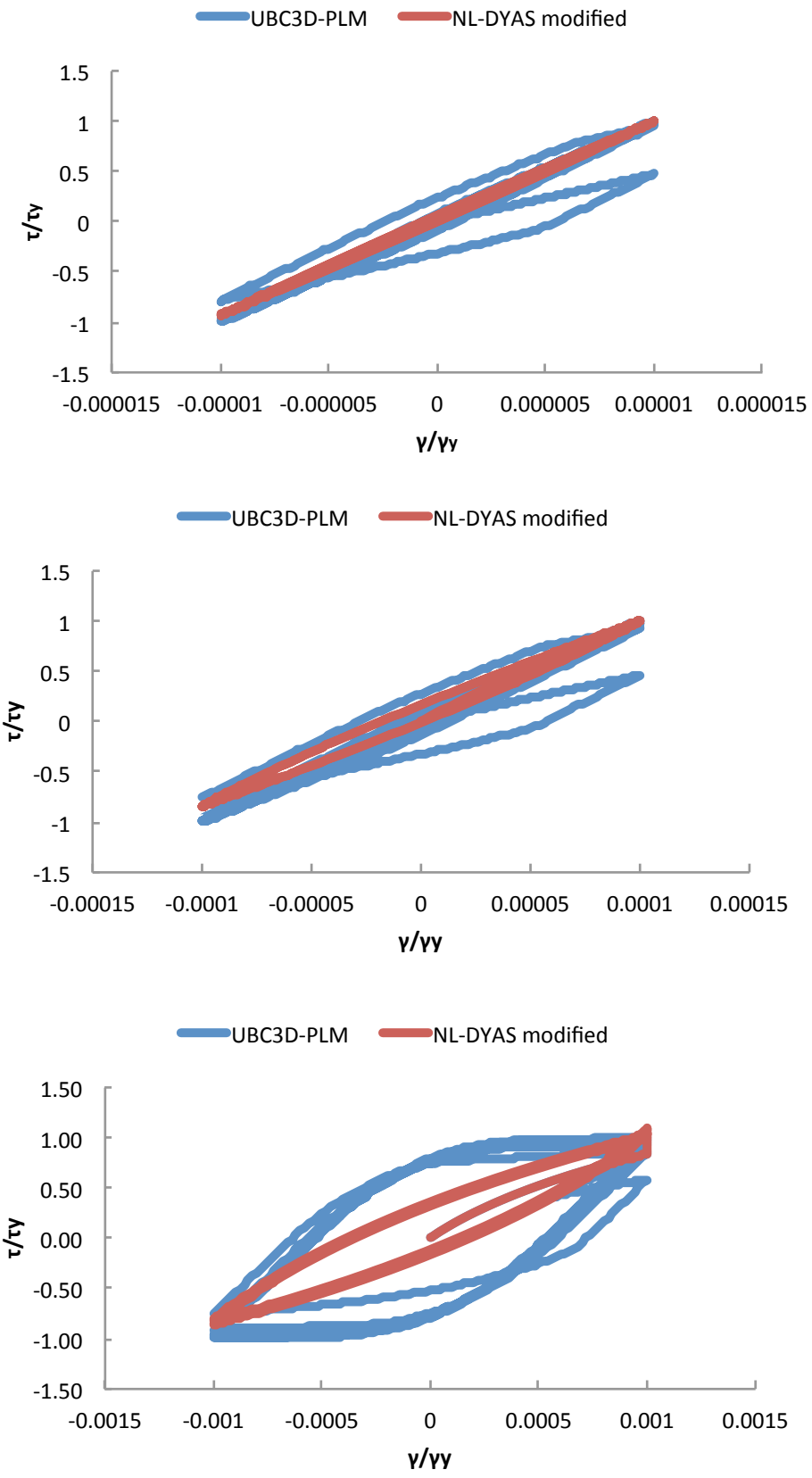

Figure 3.34 *Individual normalized stress-strain Loops for* ***σv'=50kpa*** *for strains 10^{-5}, 10^{-4}, 10^{-3} respectively. Comparison between NLDYAS modified and UBC3D-PLM with proposed optimization process parameters.*

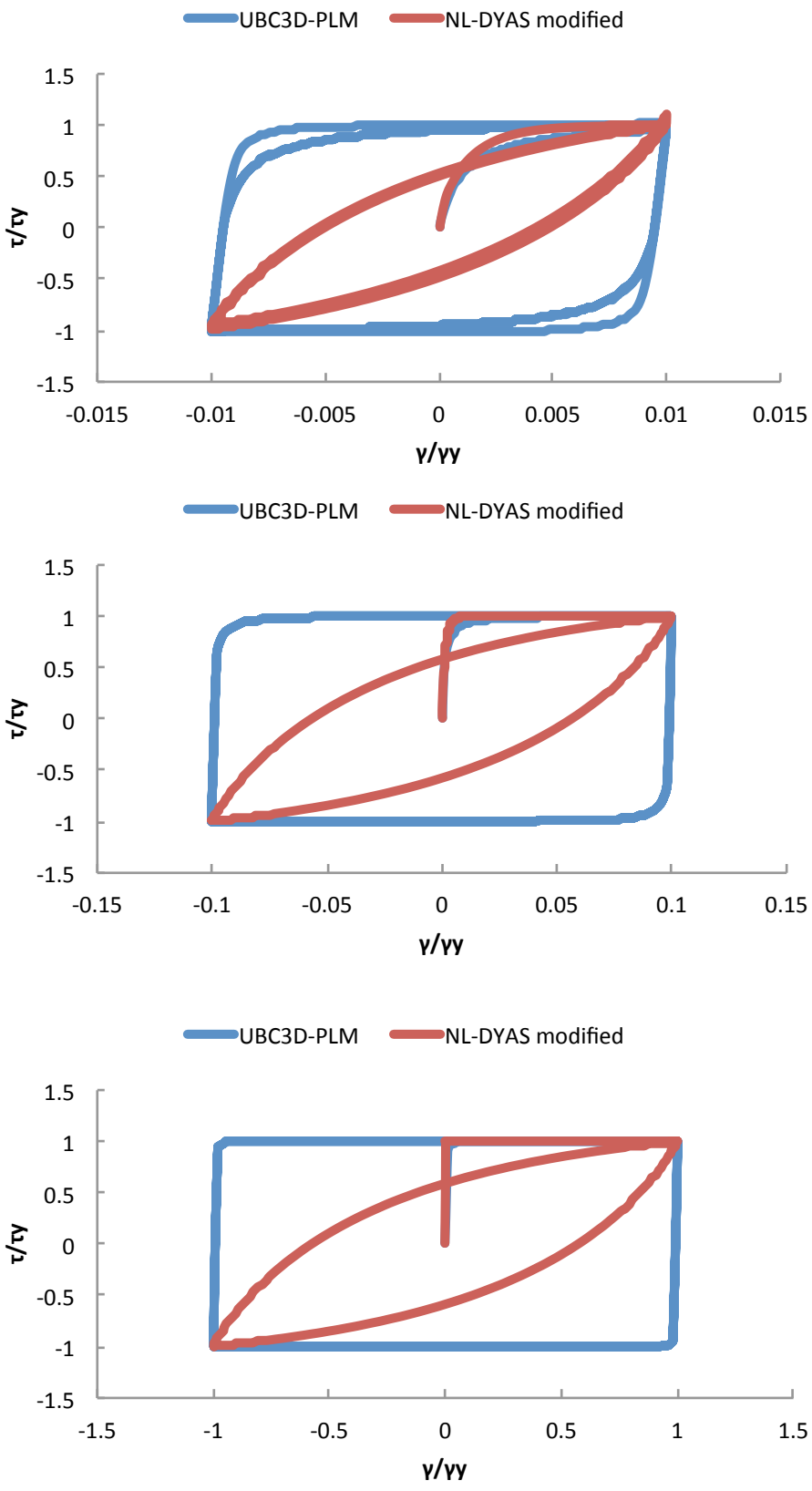

Figure 3.35 *Individual normalized stress-strain Loops for* ***σv'=50kpa*** *for strains 10^{-2}, 10^{-1}, 10^{-0} respectively. Comparison between NLDYAS modified and UBC3D-PLM with proposed optimization process parameters.*

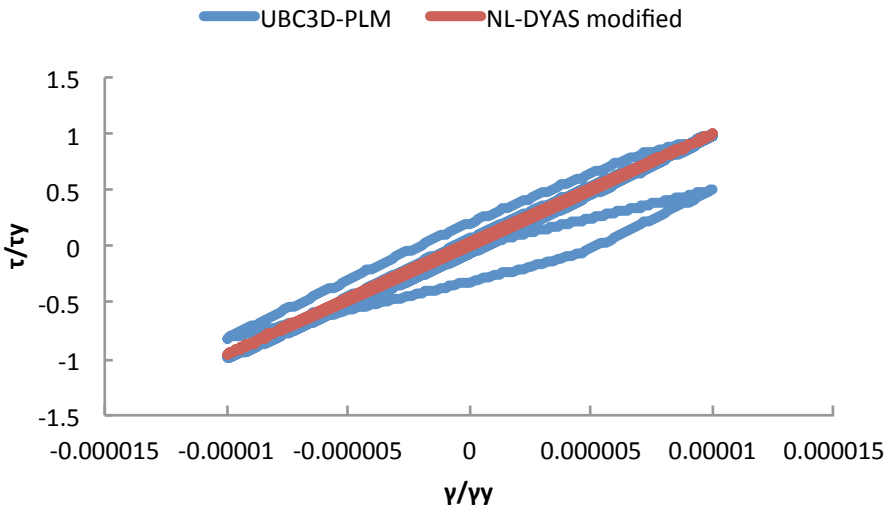

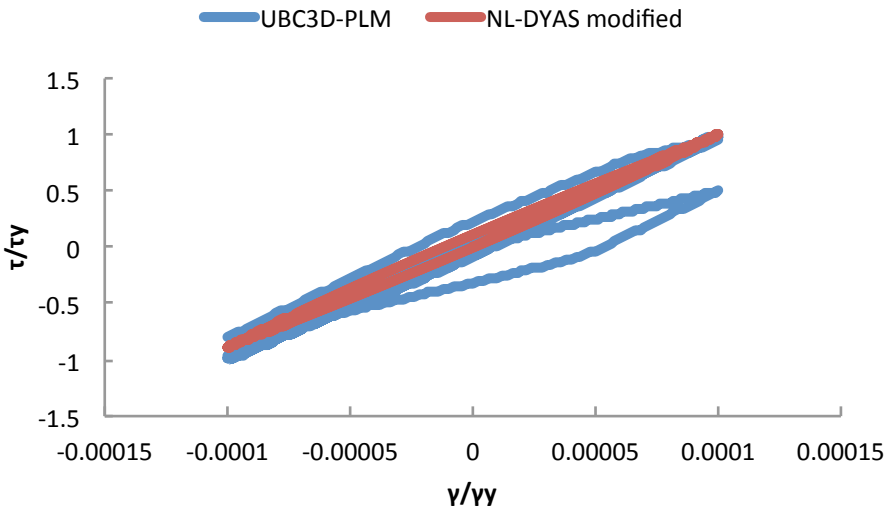

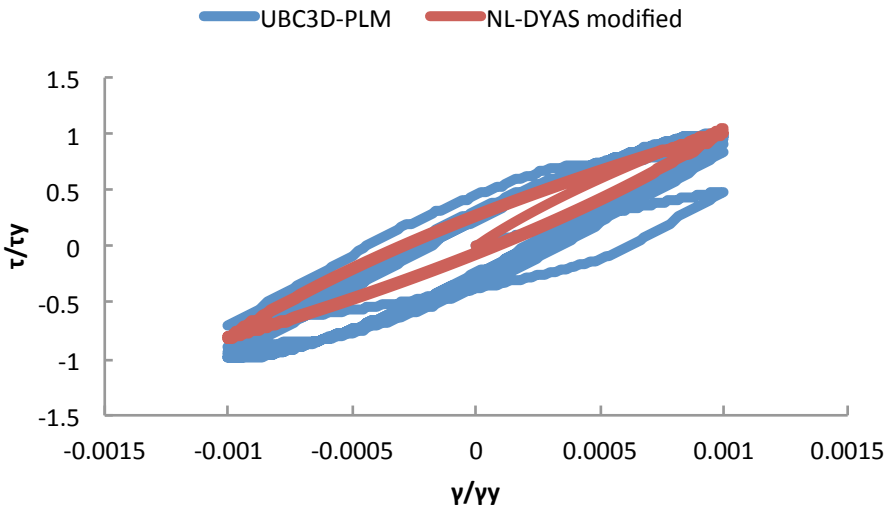

Figure 3.36 *Individual normalized stress-strain Loops for* ***σv'=200kpa*** *for strains 10^{-5}, 10^{-4}, 10^{-3} respectively. Comparison between NLDYAS modified and UBC3D-PLM with proposed optimization process parameters.*

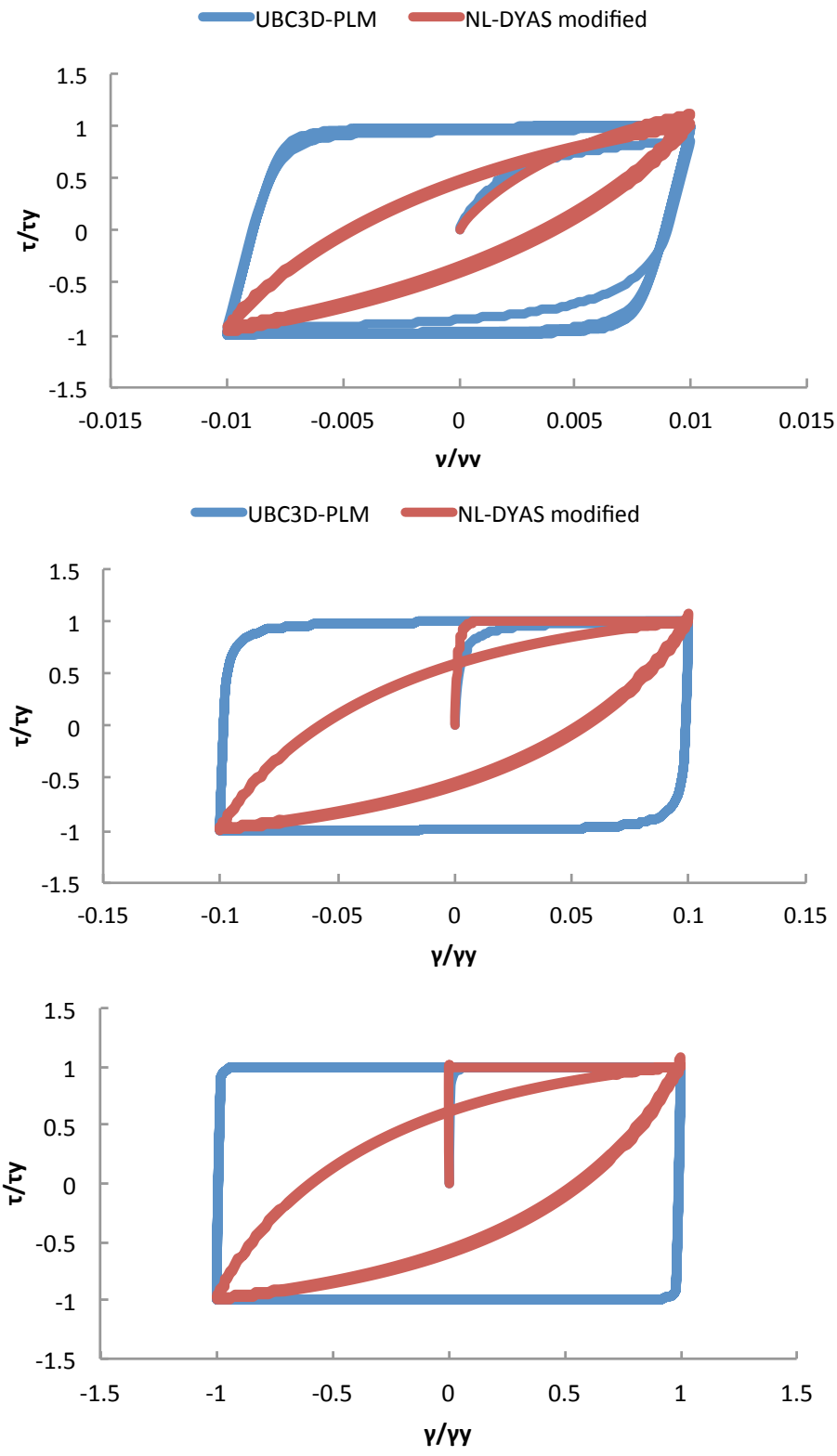

Figure 3.37 *Individual normalized stress-strain Loops for* ***σv'=200kpa*** *for strains 10^{-2}, 10^{-1}, 10^{-0} respectively. Comparison between NLDYAS modified and UBC3D-PLM with proposed optimization*

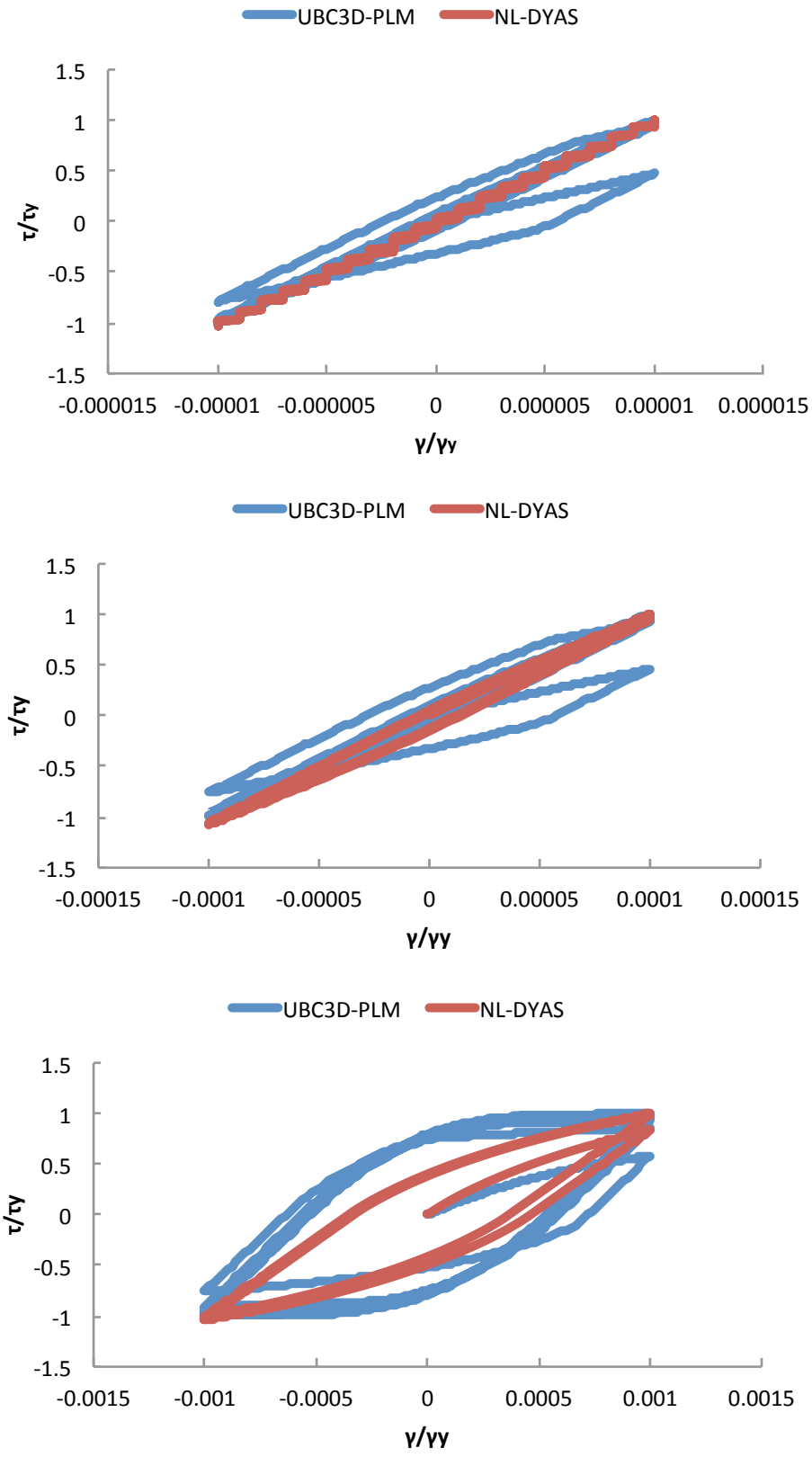

Figure 3.38 *Individual normalized stress-strain Loops for* ***σv'=50kpa*** *for strains 10^{-5}, 10^{-4}, 10^{-3}respectively for NLDYAS to match UBC3D-PLM. Possible match with x=0 and n=0.60*

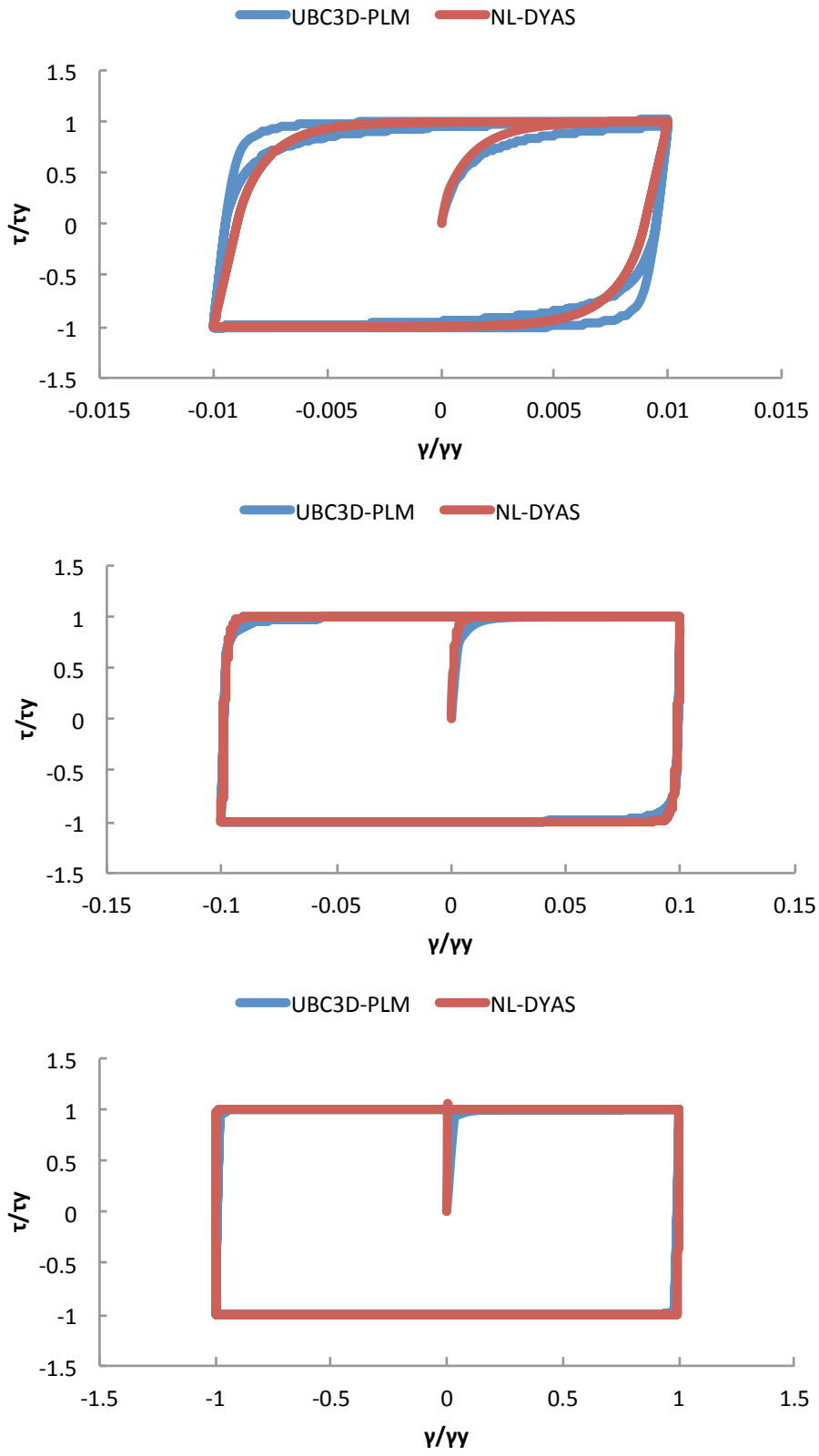

Figure 3.39 *Individual normalized stress-strain Loops for* ***σv'=50kpa*** *for strains 10^{-5}, 10^{-4}, 10^{-3}respectively for NLDYAS to match UBC3D-PLM. Possible match with x=0 and n=0.60*

CHAPTER 4

Soil Profile Analyses

4.1 Introduction

For the analyses two experiemental soil profiles were developed. The first is a layered one and the second an exponentially hardening soil profile following an exponentially increased shear wave velocity equation. The figures (4.1) and (4.2) show the two profiles and their respective Vs (shear wave velocity)

The two profiles consist of an individual 40m depth column each and further details are presented below.

The two profiles have had the accelleration of Aegion 1993 (0.39g), Kobe 1993 (0.68g) and Lefkada 2003 (0.42g) imposed and data has been gathered in order to form stress-strain charts for 3 different depths -5m, -20m, -35m.

The excitations were scaled to 0.05g, 0.25g and 0.60g. The 0.05g excitation gives a good idea of how elastic behavior is for each model, 0.25g is a fair excitation intensity and at 0.60g we have an intense excitation.

The analyses have been repeated for the two soil profiles, for three depths, with NLDYAS modified and UBC3D-PLM, for three seismic excitations and three seismic intensities.

At first a verification is ran against a soil scenario with NLDYAS old version against UBC3D-PLM. The verification was run at a loop level with success on chapter 3 and it is now run at a macroscale to show that we can reproduce as needed the UBCSAND model hence the need to compare it on a validation basis against NLDYAS modified.

The data are gathered and compared in the figure section.

4.2 Experimental Layered soil profile

The layered soil profile has a soil density of ρ=1.8Mpa/m3

The individual layer details are presented in the table below

Layer	Thickness	Depth	Vs m/s	ρs
1	3	3	120	1.8
2	2	5	140	1.8
3	7	12	160	1.8
4	8	20	180	1.8
5	10	30	225	1.8
6	10	40	200	1.8

Table 4.1 : *Layered Soil profile details*

We calculate and optimize from Ishibashi & Change parameters for each layer midpoint effective stress.

Furthermore we have:

Layer	PI	σvo	n	s1	γγ-1
1	0	27	0.428	7.267	1540.1
2	0	72	0.429	7.36	875.2
3	0	153	0.46	7.005	566.1
4	0	288	0.518	6.345	393.1
5	0	450	0.602	5.54	303.4
6	0	630	0.728	4.657	250.3

Table 4.2 : *Layered Soil optimization results for "NLDYAS modified"*

From:

$$Go = \rho \times Vs^2$$

and the equations at section 3.3.4 we can generate the soil profile inputs for UBC3D-PLM and from the table 4.2 the input files for NLDYAS and NLDYAS modified are generated.

4.3 Experimental Exponentially hardened soil profile

The exponential soil profile has a soil density of ρ=1.8Mpa/m3

The exponential profile is divided into 5m layers for a better handling in the analyses.

For the exponential soil the rule that derives the figure () results is $Vs=100xZ^{0.25}$ with a minimum Vs value of 95 m/s for z=0

The individual 5m divided layers are presented in the table below.

Layer	Thickness	Depth	Vs m/s	ρs
1	5	5	123.8	1.8
2	5	10	163.7	1.8
3	5	15	187.3	1.8
4	5	20	204.1	1.8
5	5	25	217.5	1.8
6	5	30	228.8	1.8
7	5	35	238.6	1.8
8	5	40	247.4	1.8

Table 4.3 : Exponential Soil profile details

The optimization results are presented below

Layer	PI	σvo	n	s1	γγ-1
1	0	45	0.423	7.386	1148.5
2	0	135	0.452	7.093	608.5
3	0	225	0.490	6.653	453.4
4	0	315	0.531	6.212	373.2
5	0	405	0.577	5.764	322.5
6	0	495	0.630	5.316	287.2
7	0	585	0.692	4.875	261.0
8	0	675	0.768	4.443	240.9

Table 4.4 : Exponential Soil profile optimization details for NLDYAS modified

4.4 Analyses Results commentary

4.4.1 NLDYAS results

NLDYAS is compared against UBC3D-PLM in a one load scenario in order to verify the loops. The results are presented in the figure section.

4.4,2 NLDYAS modified results

NLDYAS modified results are presented in the figure section.

4.4.3 UBC3D-PLM results

UBC3D-PLM results are presented in the figure section.

4.5 Comparison of methods

NLDYAS modified and UBC3D-PLM are compared in all scenarios and also compared on accellerograph stage, surface spectrums. Displacement, stresses and deformations maximums are also compared.

Whats obvious from the analyses has been that the full equation of the two models is not easily accomplishable without suppressing the laws that each constitutive model represents.

On the other hand even though the loops and the accellerographs have some reseblance but no scientific matching we notice the following

- UBC3D-PLM produces some kind of hardening behavior while the other models not.
- As far as displacement and strasses are concerned there is a fair match in both models
- The surface spectrum for NLDYAS modified has a lower peak but is affecting a higher value of T.

Figures

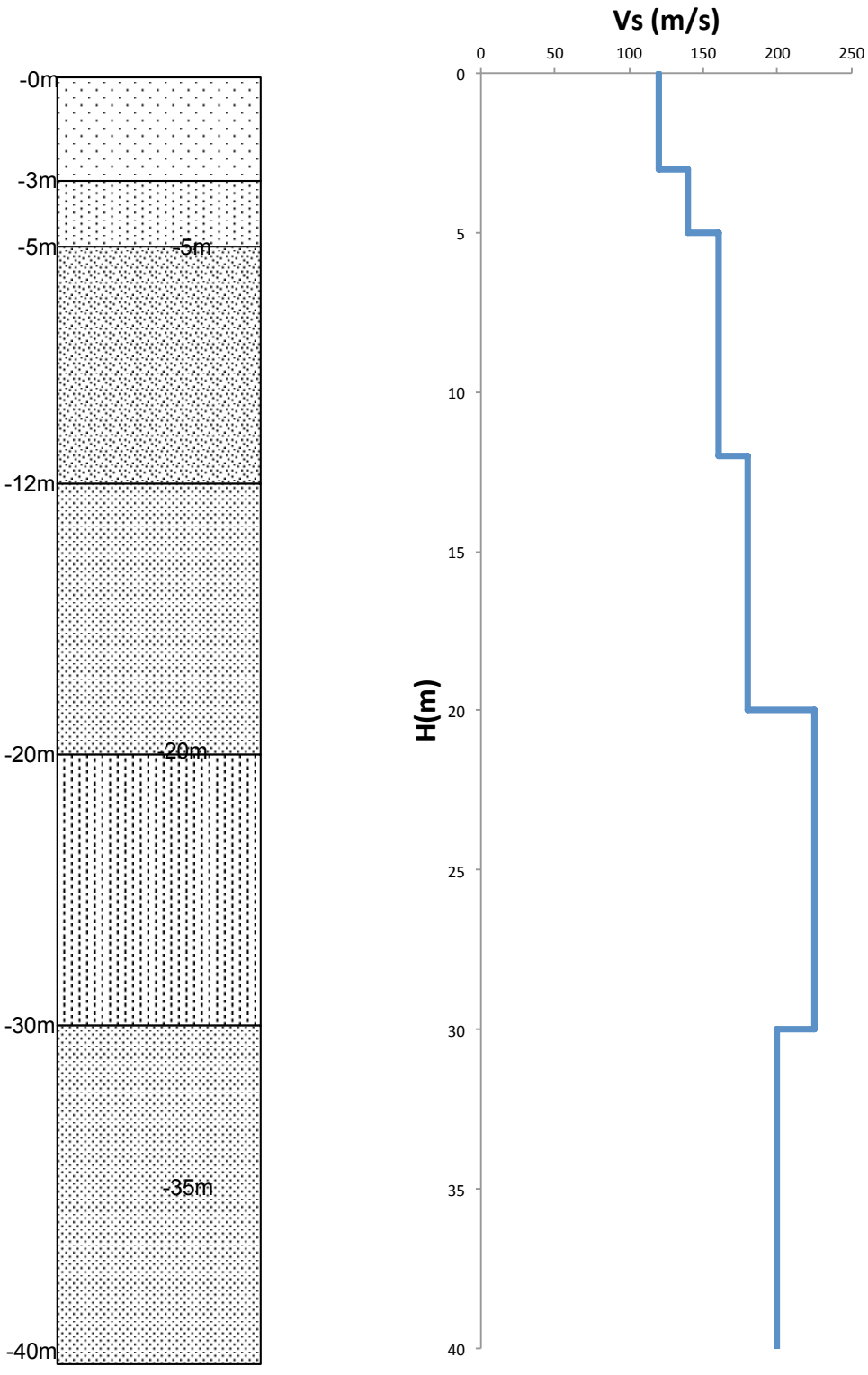

Figure 4.1 Experimental Soil profile. *Layered Soil Profile.*

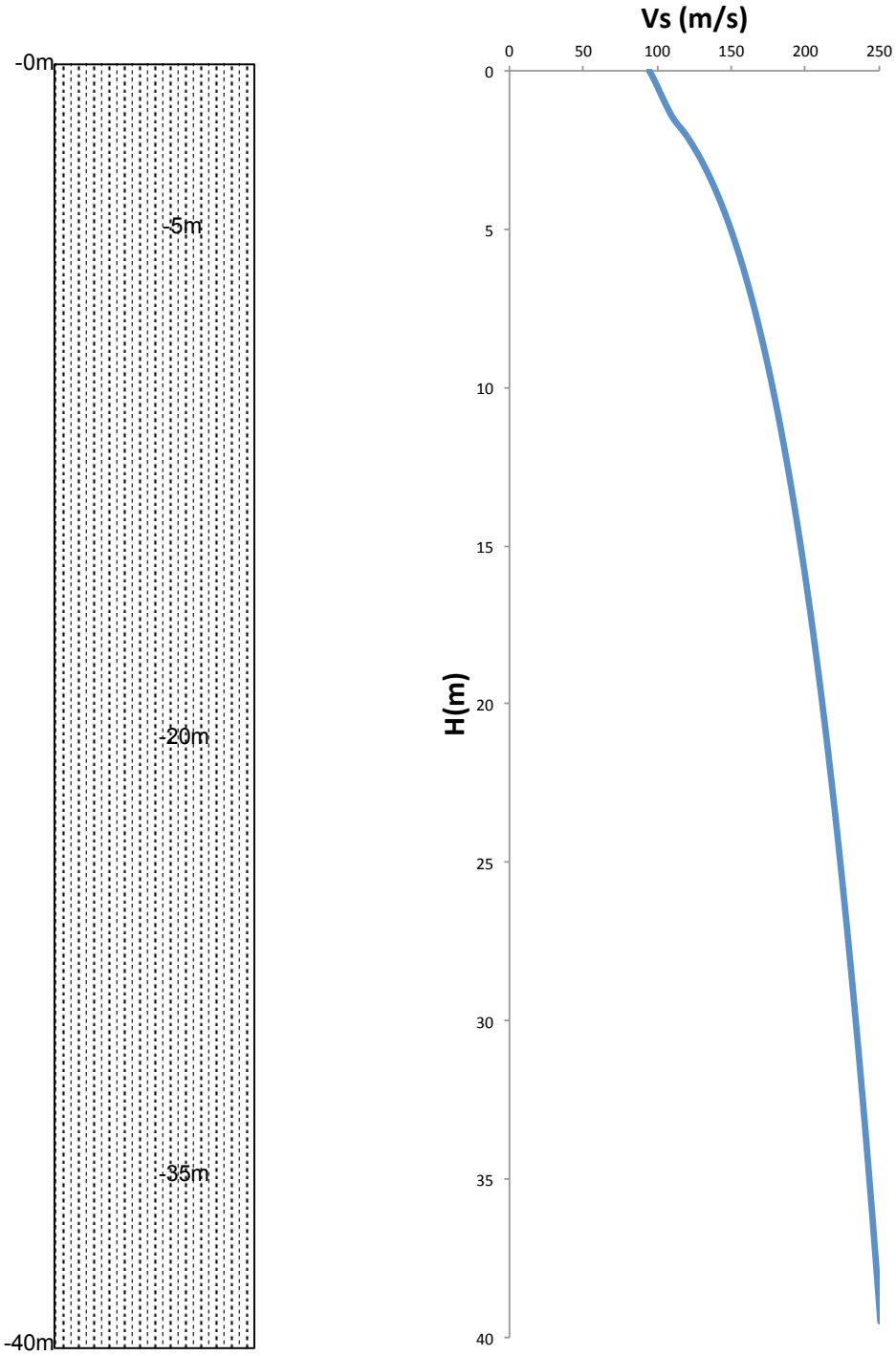

Figure 4.2 Experimental Soil profile. *Exponential Soil Profile.*

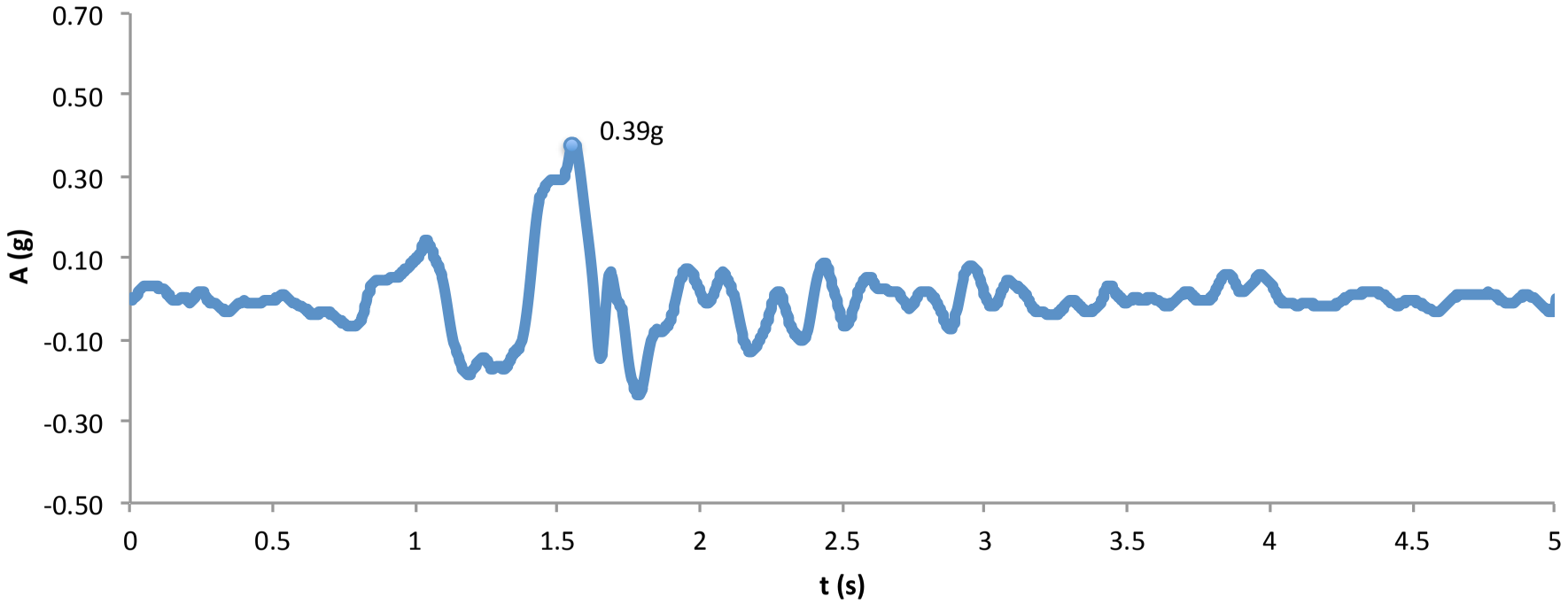

Figure 4.3 *Recorded Accelleration time histories for Aegion 1995 (0.39g)*

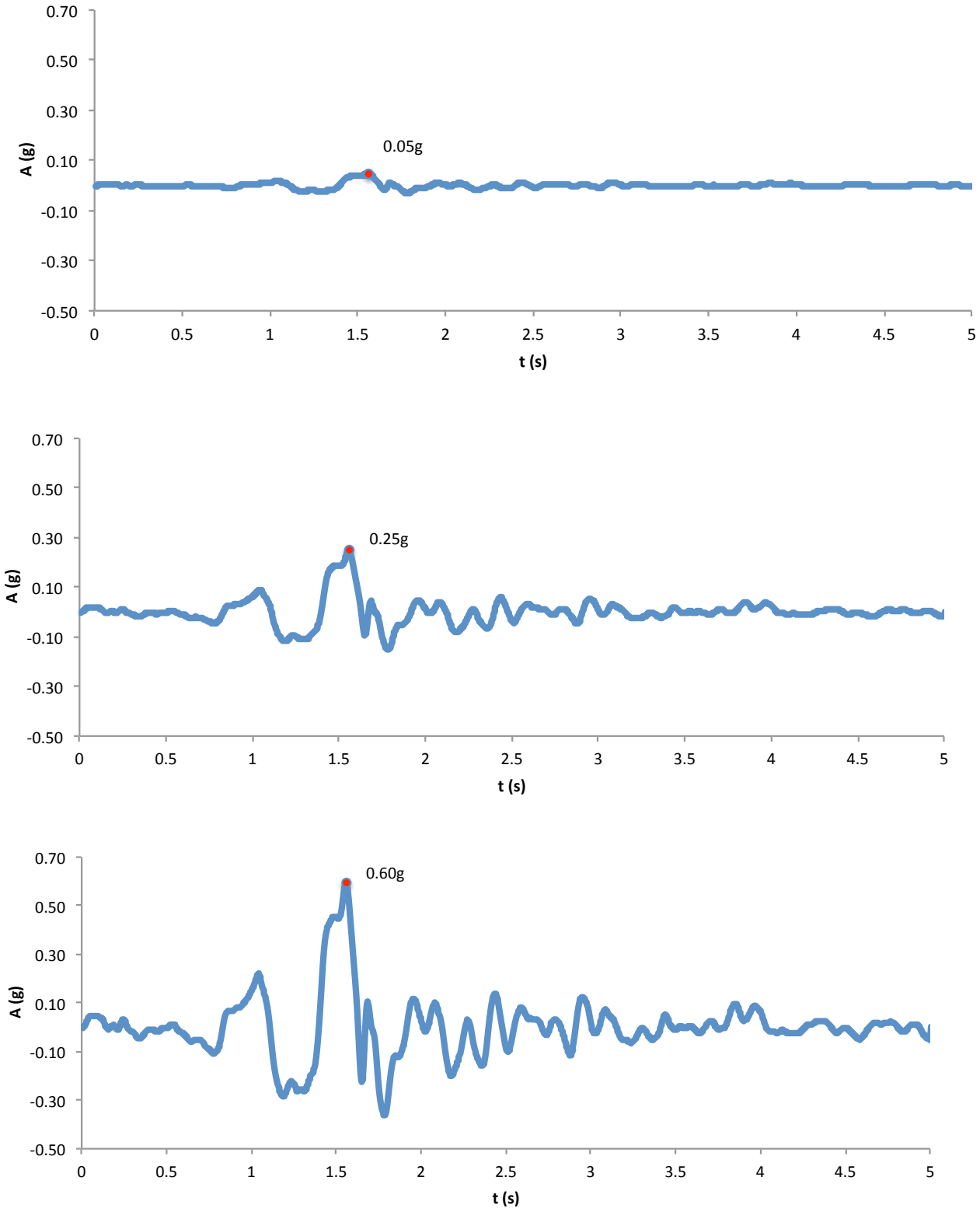

Figure 4.4 *Acceleration time histories for Aegion 1995 (0.39g) scaled to 0.05g, 0.25g, 0.60g*

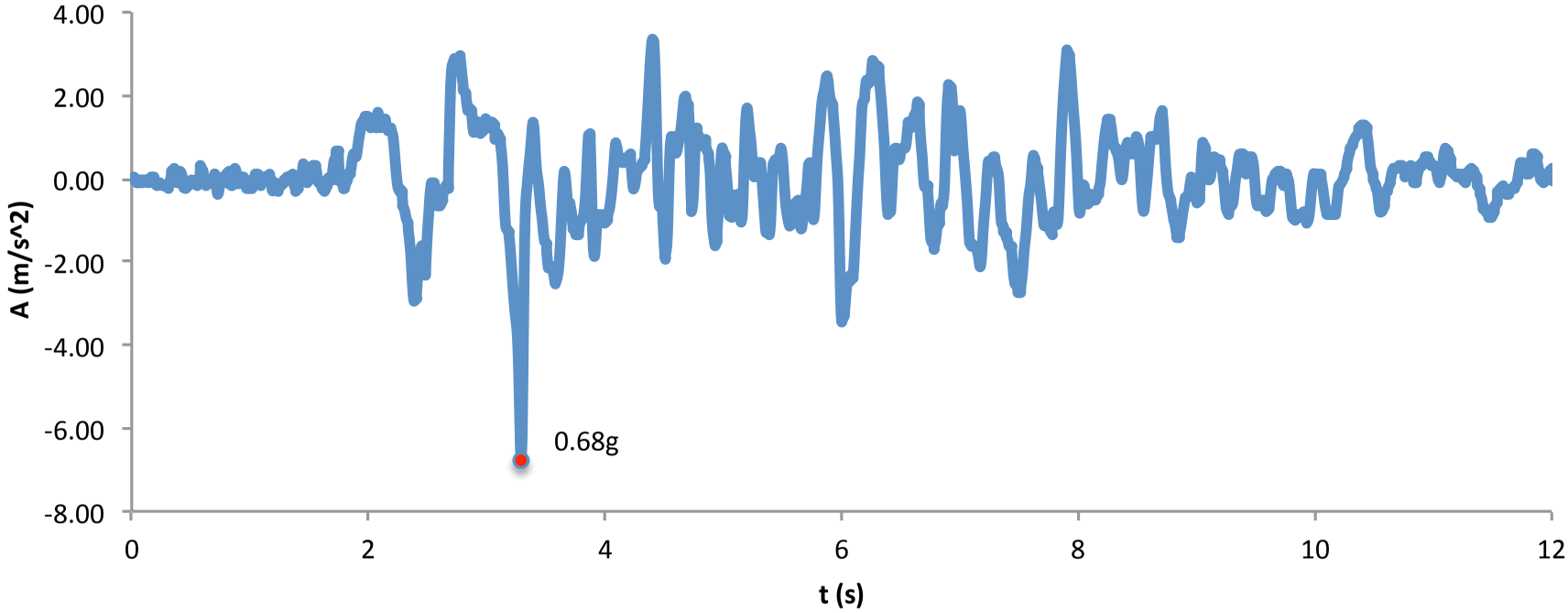

Figure 4.5 *Recorded Accelleration time histories for Kobe 1995 (0.68g)*

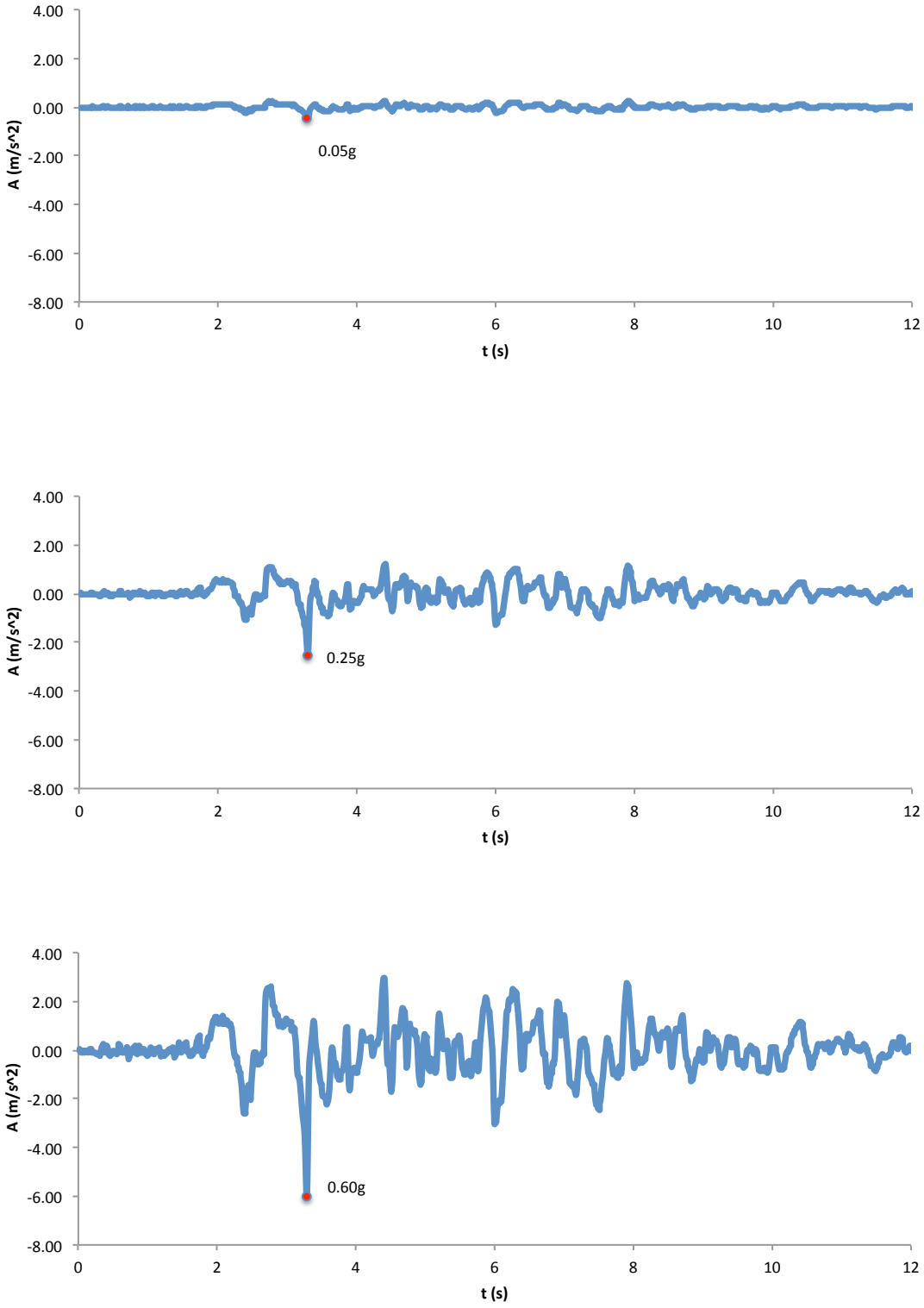

Figure 4.6 *Acceleration time histories for Kobe 1995 (0.68g) scaled to 0.05g, 0.25g, 0.60g*

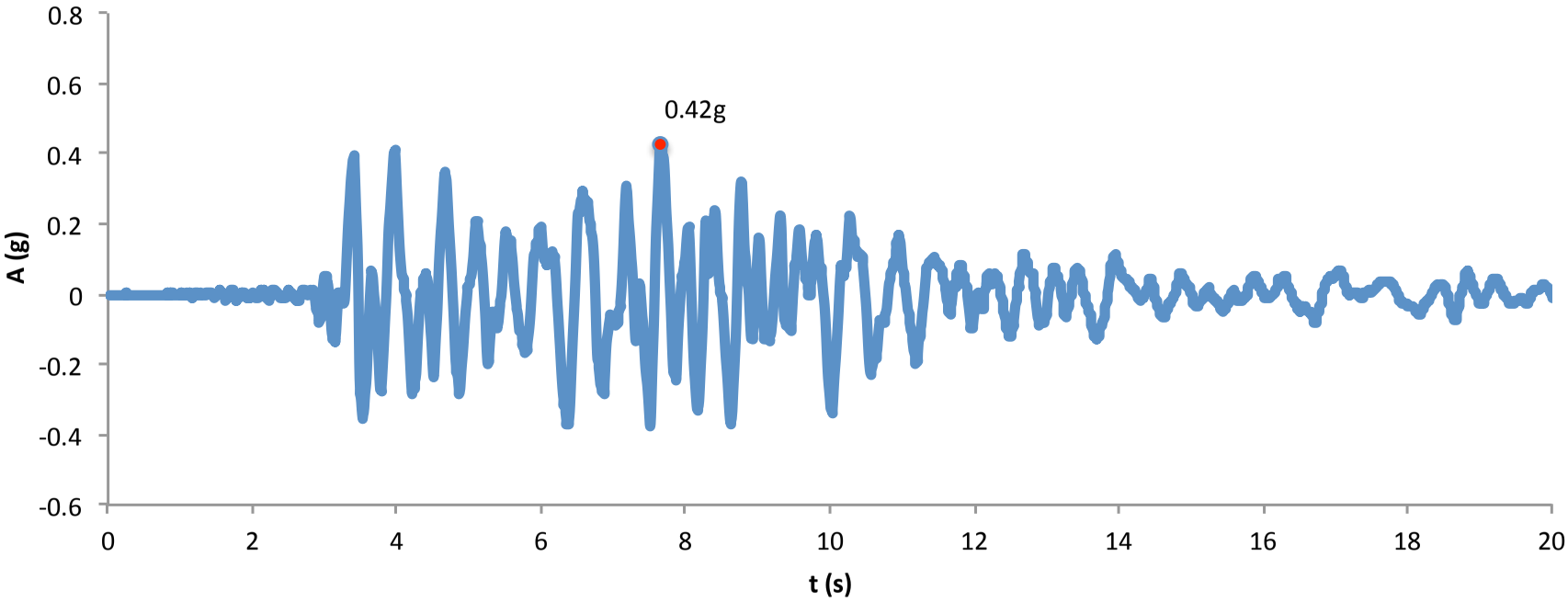

Figure 4.7 *Recorded Accelleration time histories for Lefkada 2003 (0.42g)*

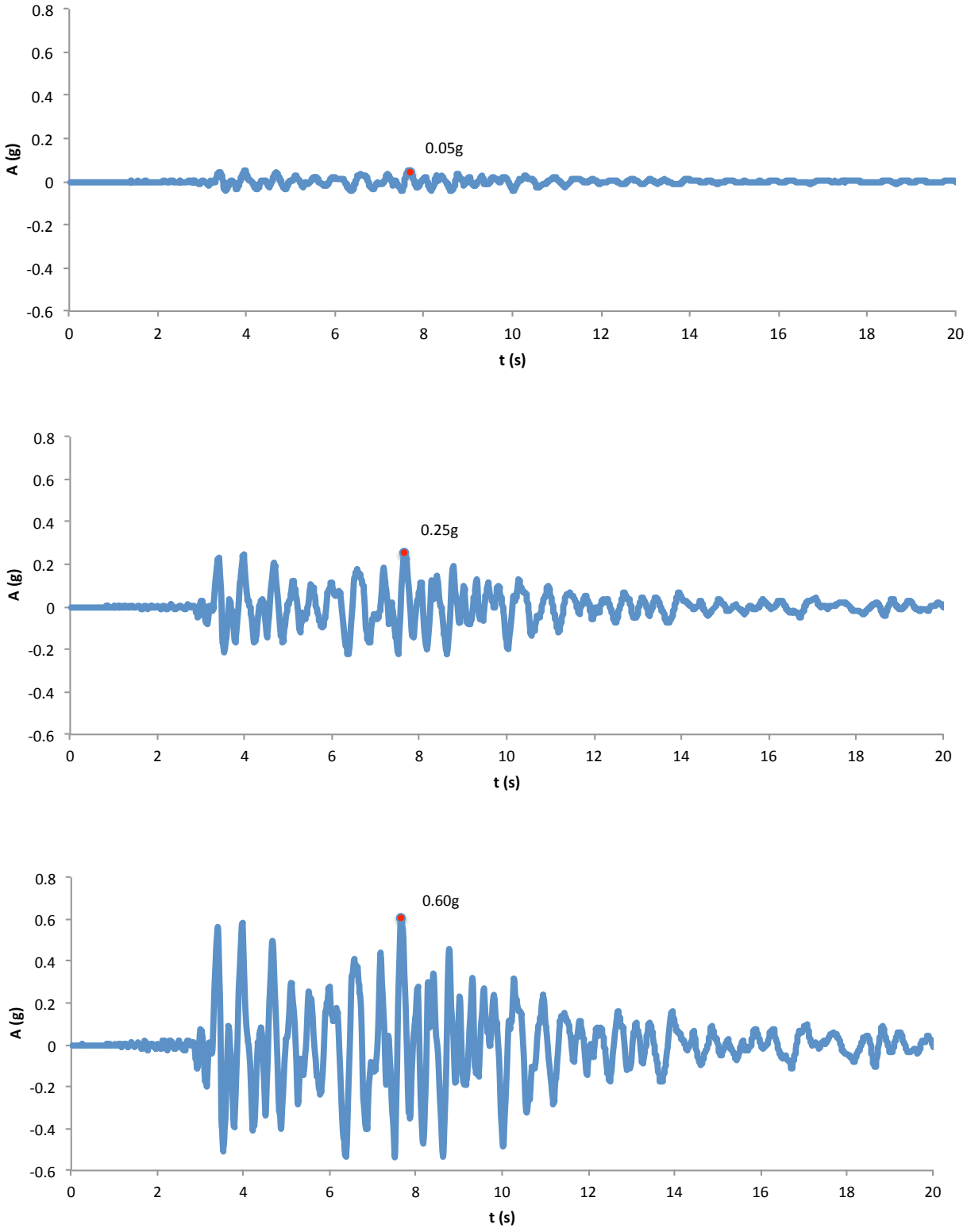

Figure 4.8 *Acceleration time histories for Lefkada 2003 (0.42g) scaled to 0.05g, 0.25g, 0.60g*

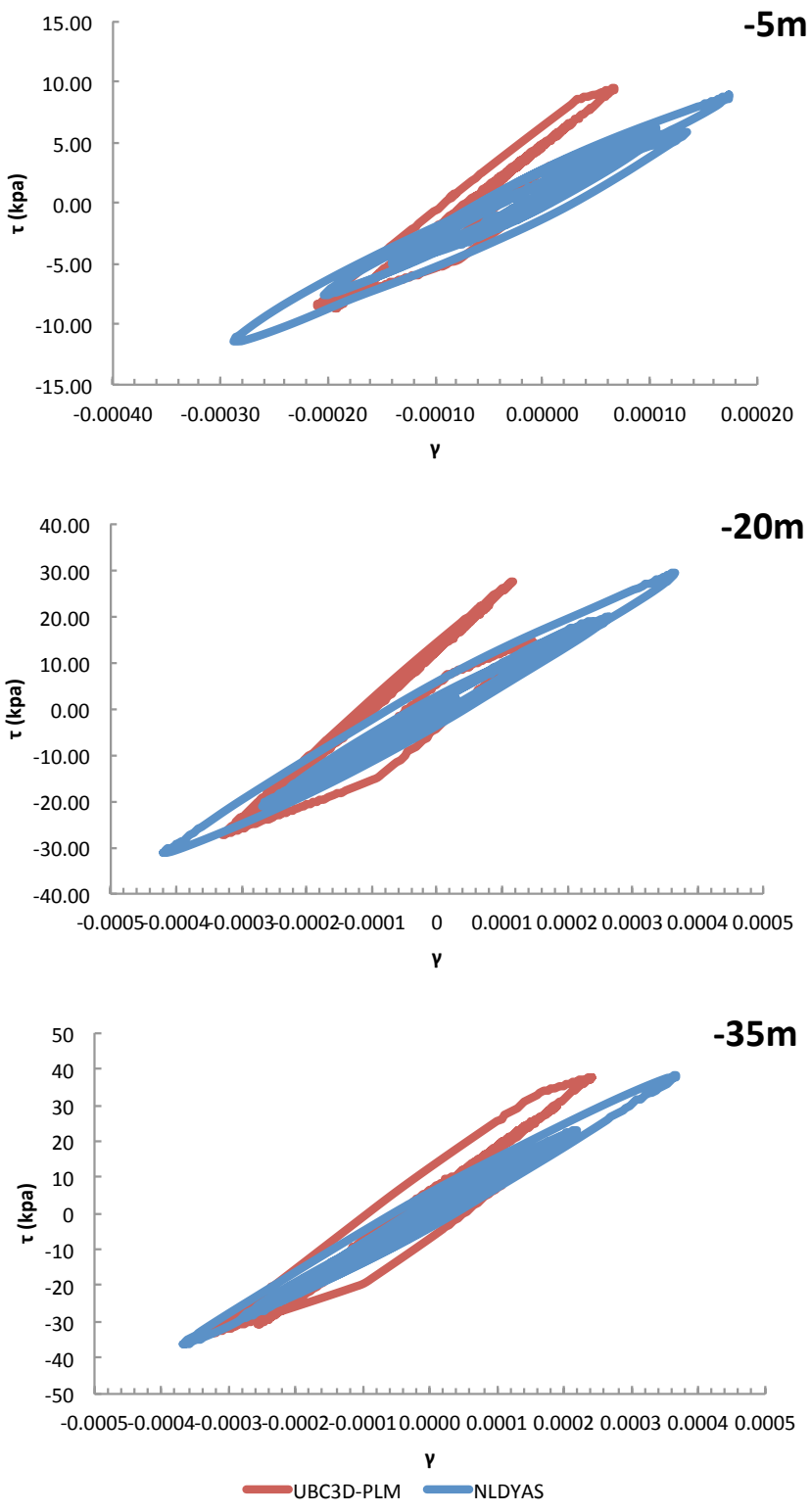

Figure 4.9 Validation soil τ-γ loops. *Validation of UBC3D-PLM model by comparing it against the old NLDYAS model with n=0.60, x=0 for s1 and s2 and b=g=0.5. Soil for the tests is the Exponential soil layer for Aegion excitation under a 0.05g scaling*

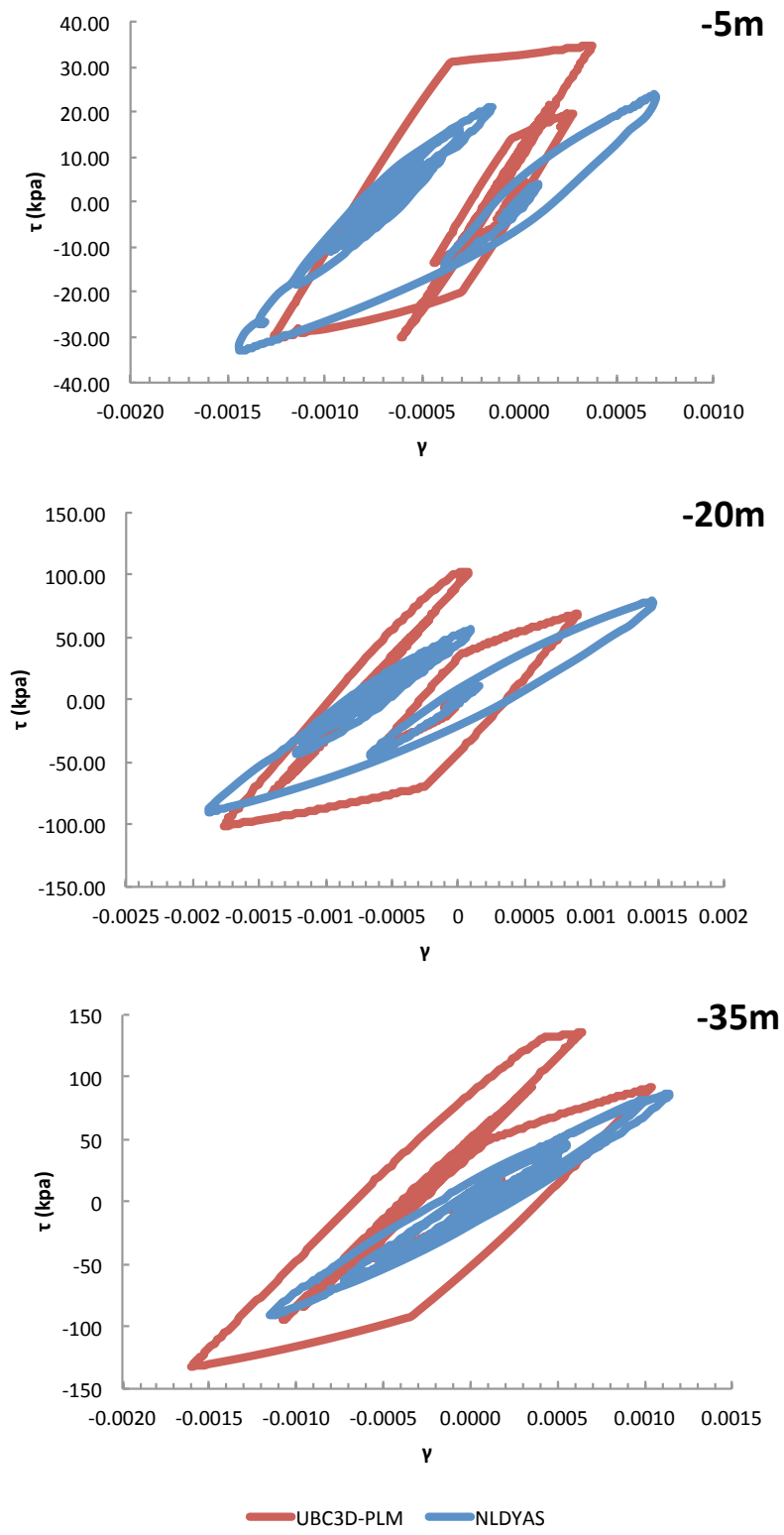

Figure 4.10 Validation soil τ-γ loops. *Validation of UBC3D-PLM model by comparing it against the old NLDYAS model with n=0.60, x=0 for s1 and s2 and b=g=0.5. Soil for the tests is the Exponential soil layer for Aegion excitation under a 0.25g scaling*

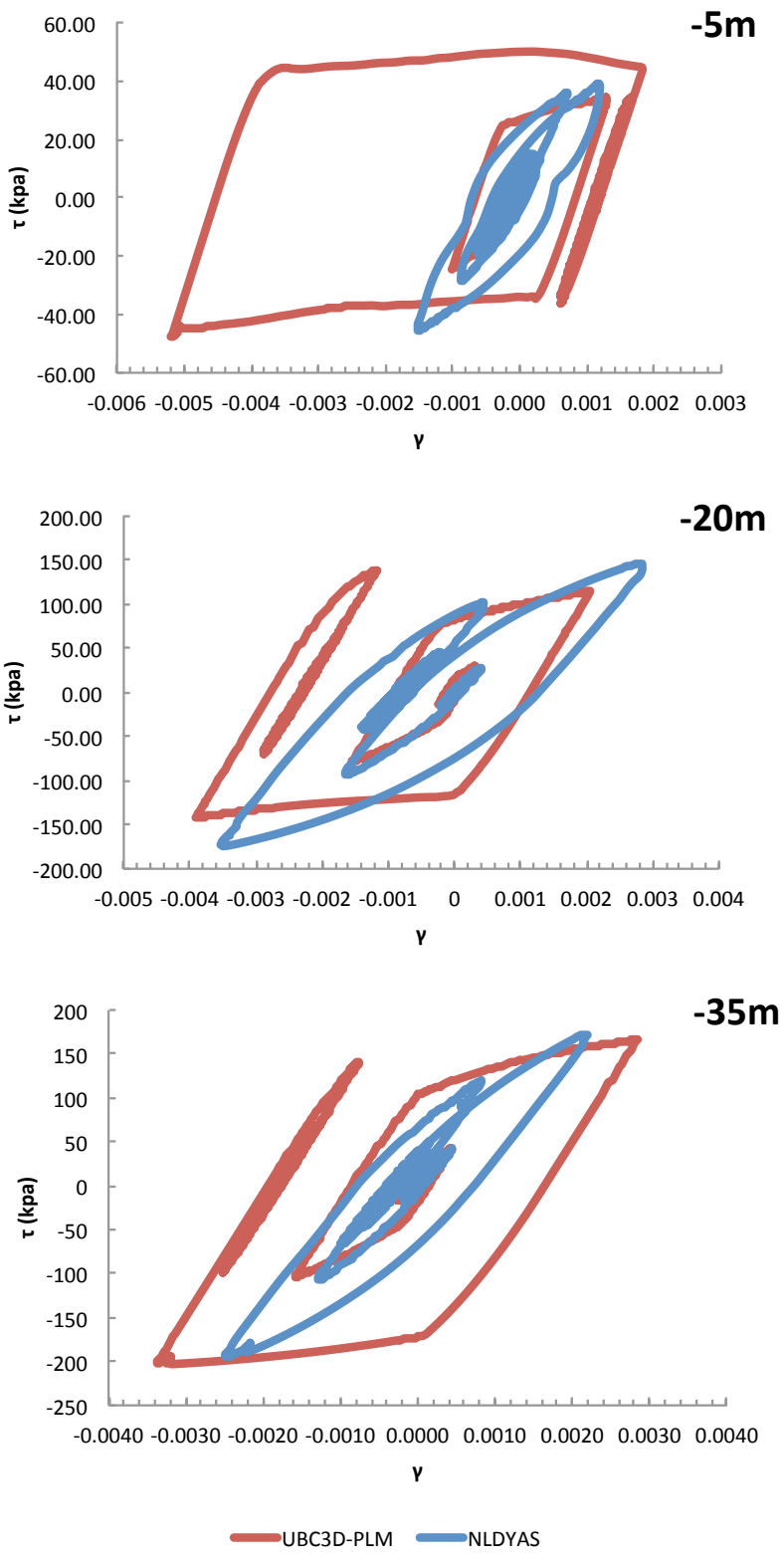

Figure 4.11 Validation soil τ-γ loops. *Validation of UBC3D-PLM model by comparing it against the old NLDYAS model with n=0.60, x=0 for s1 and s2 and b=g=0.5. Soil for the tests is the Exponential soil layer for Aegion excitation under a 0.60g scaling*

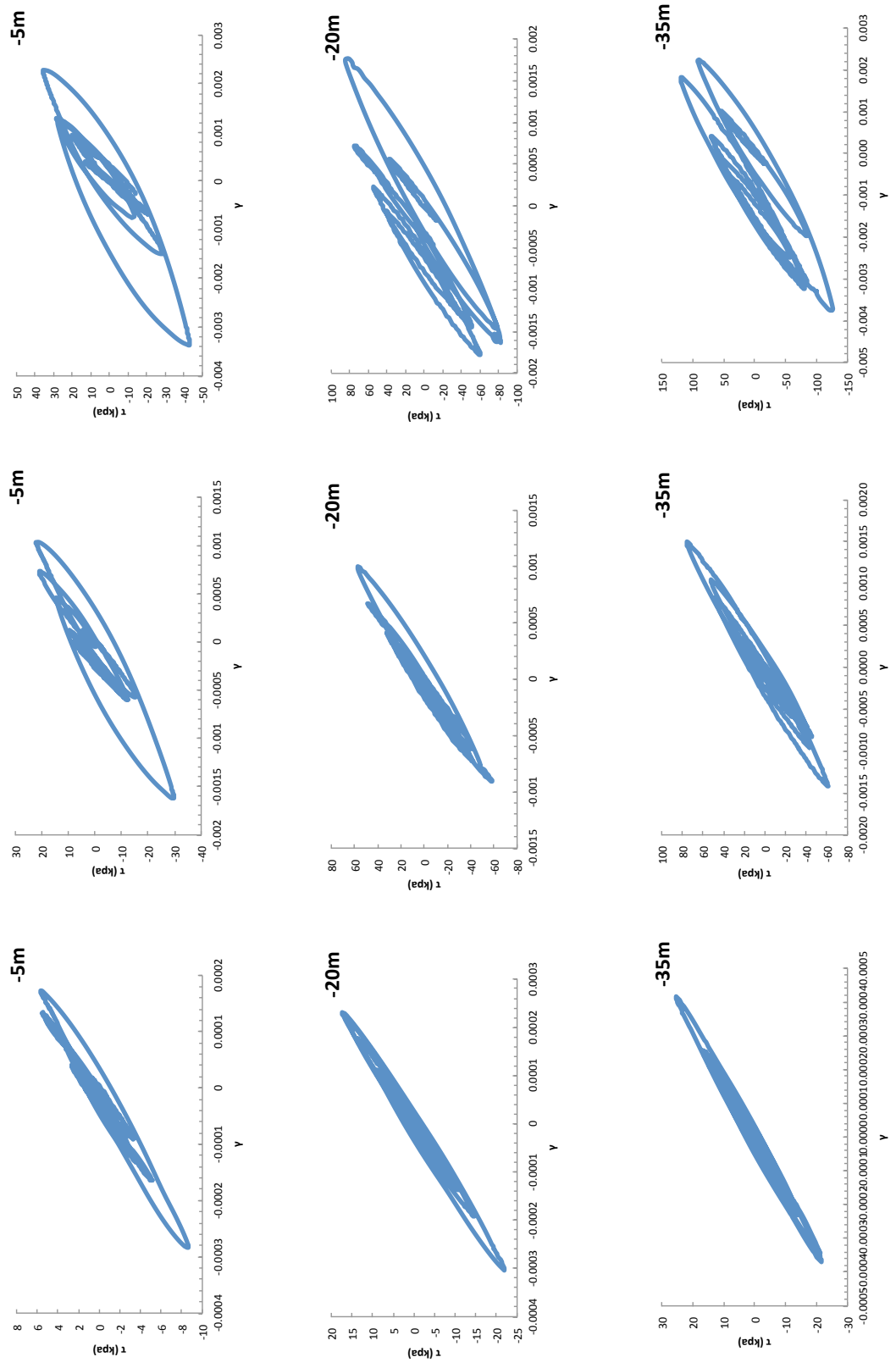

Figure 4.12 τ-γ loops. *Analyses results for the* ***Layered Soil profile*** *with* ***"NL-DYAS modified"*** *code for the* ***Aegion excitation*** *for 0.05g, 0.25g, 0.60g respectively from left to right and for different depths.*

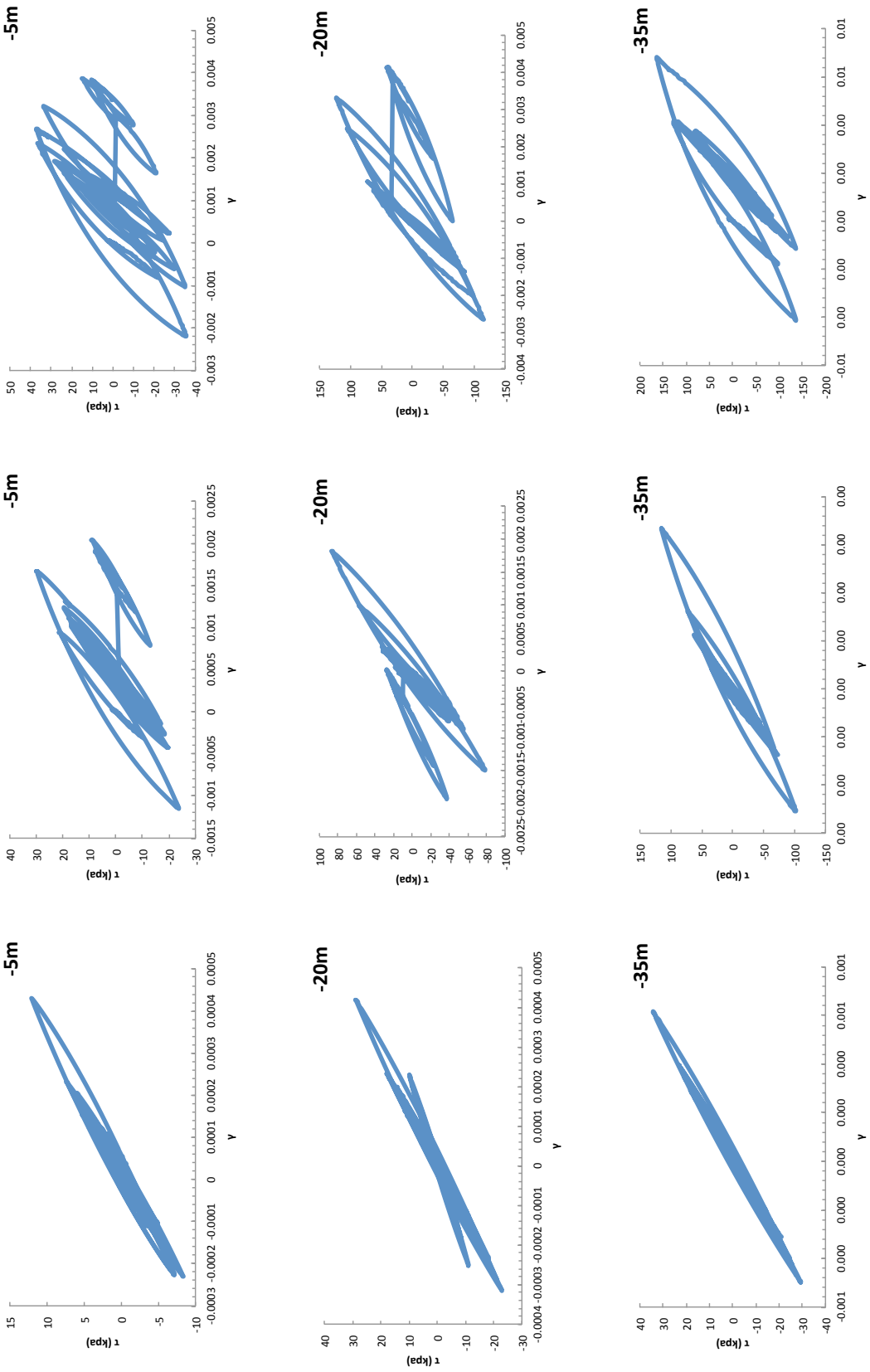

Figure 4.13 τ-γ loops. *Analyses results for the* ***Layered Soil profile*** *with* ***"NL-DYAS modified"*** *code for the* ***Kobe excitation*** *for 0.05g, 0.25g, 0.60g respectively from left to right and for different depths.*

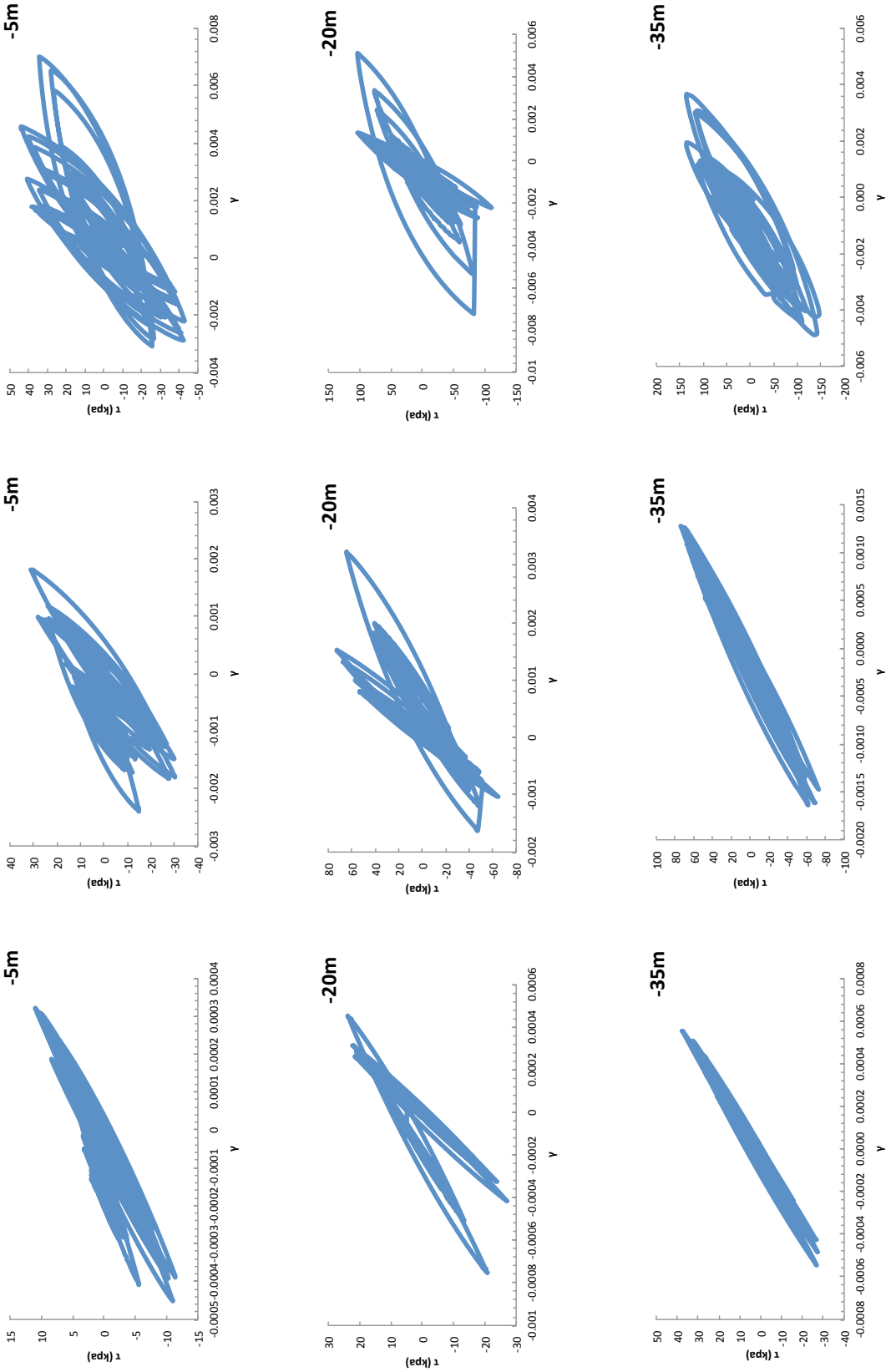

Figure 4.14 τ-γ loops. *Analyses results for the* ***Layered Soil profile*** *with* ***"NL-DYAS modified"*** *code for the* ***Lefkada excitation*** *for 0.05g, 0.25g, 0.60g respectively from left to right and for different*

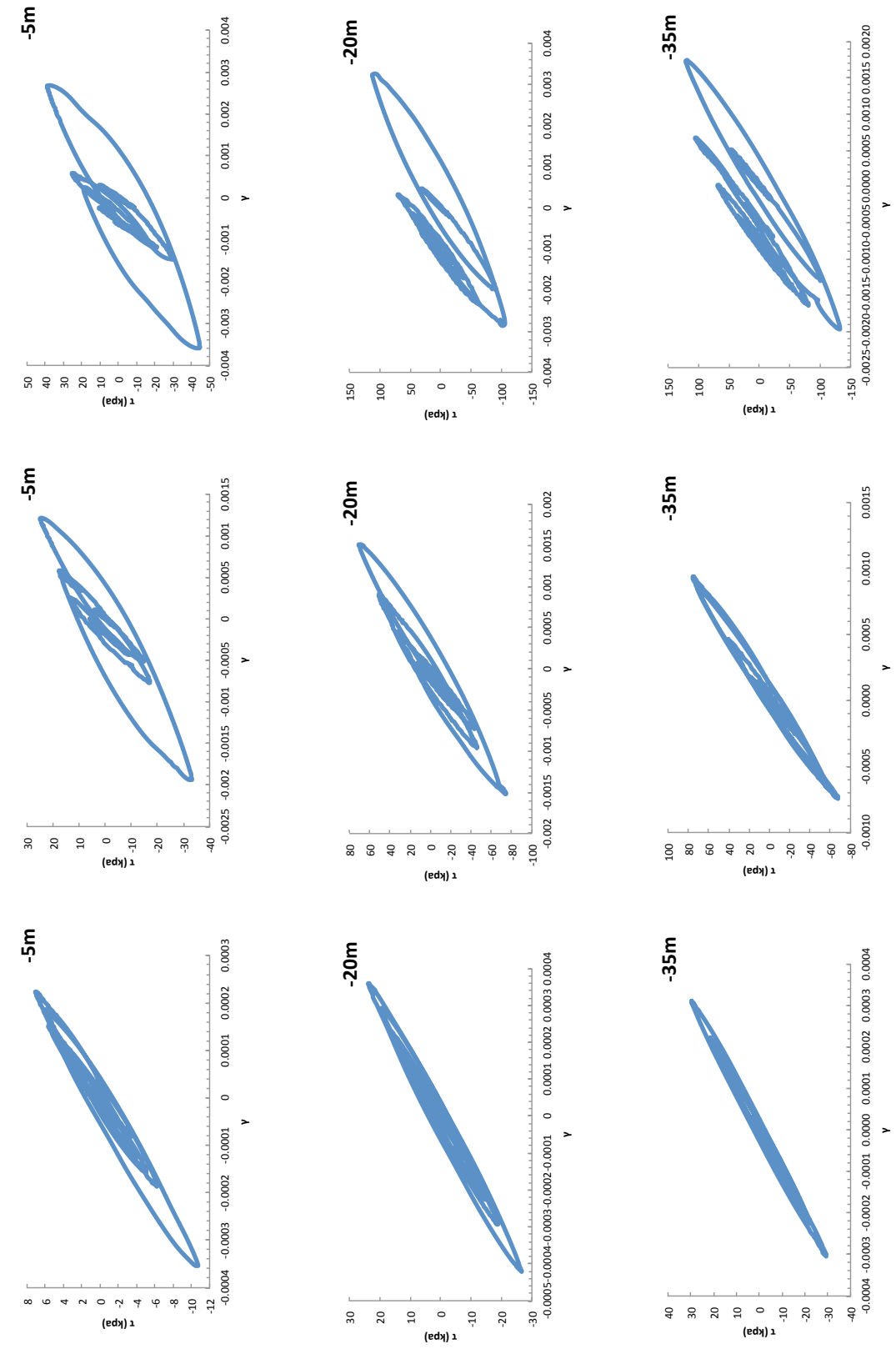

Figure 4.15 τ-γ loops. *Analyses results for the* ***Exponential Soil profile*** *with* ***"NL-DYAS modified"*** *code for the* ***Aegion excitation*** *for 0.05g, 0.25g, 0.60g respectively from left to right and for different depths.*

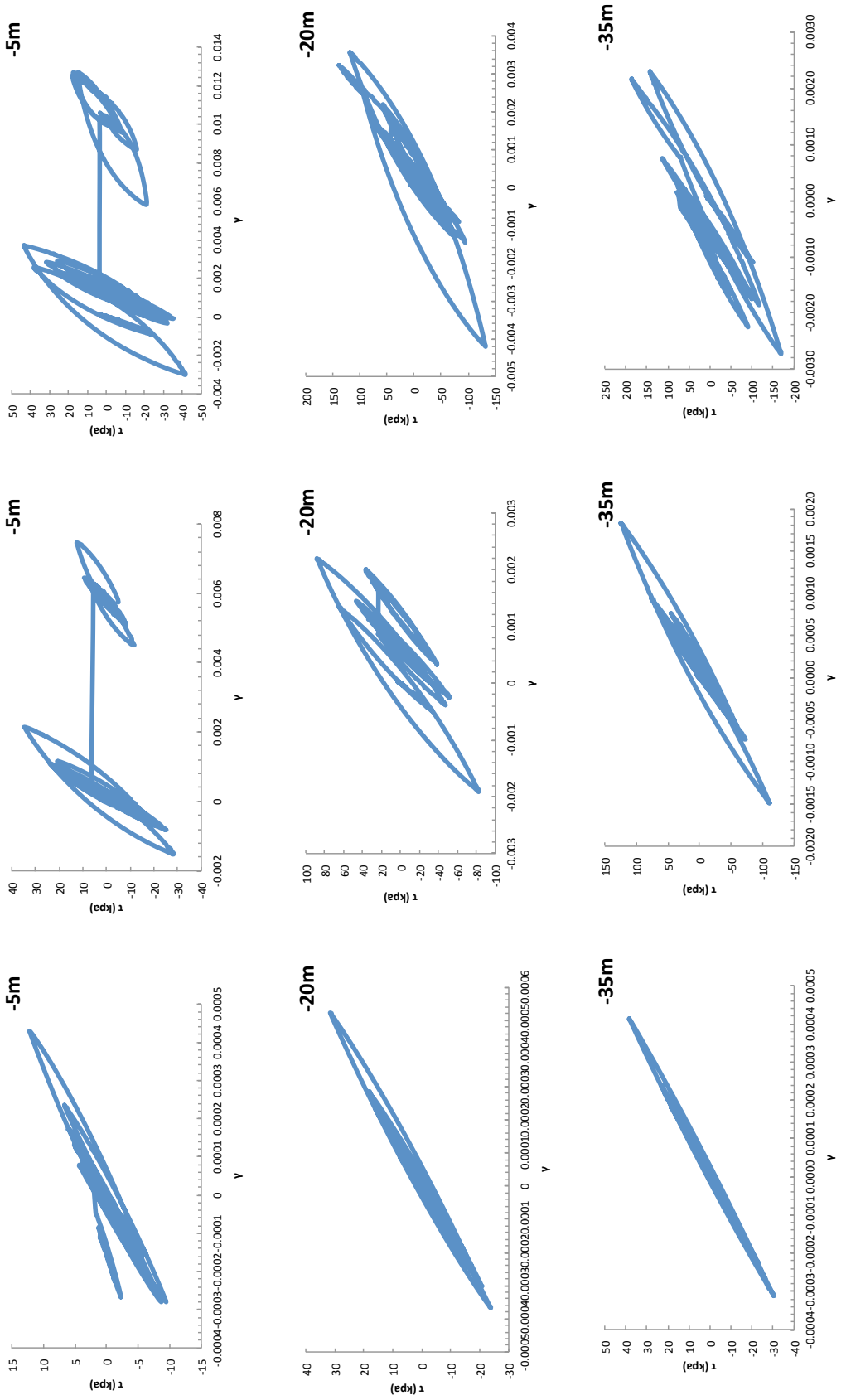

Figure 4.16 τ-γ loops. *Analyses results for the* ***Exponential Soil profile*** *with* ***"NL-DYAS modified"*** *code for the* ***Kobe excitation*** *for 0.05g, 0.25g, 0.60g respectively from left to right*

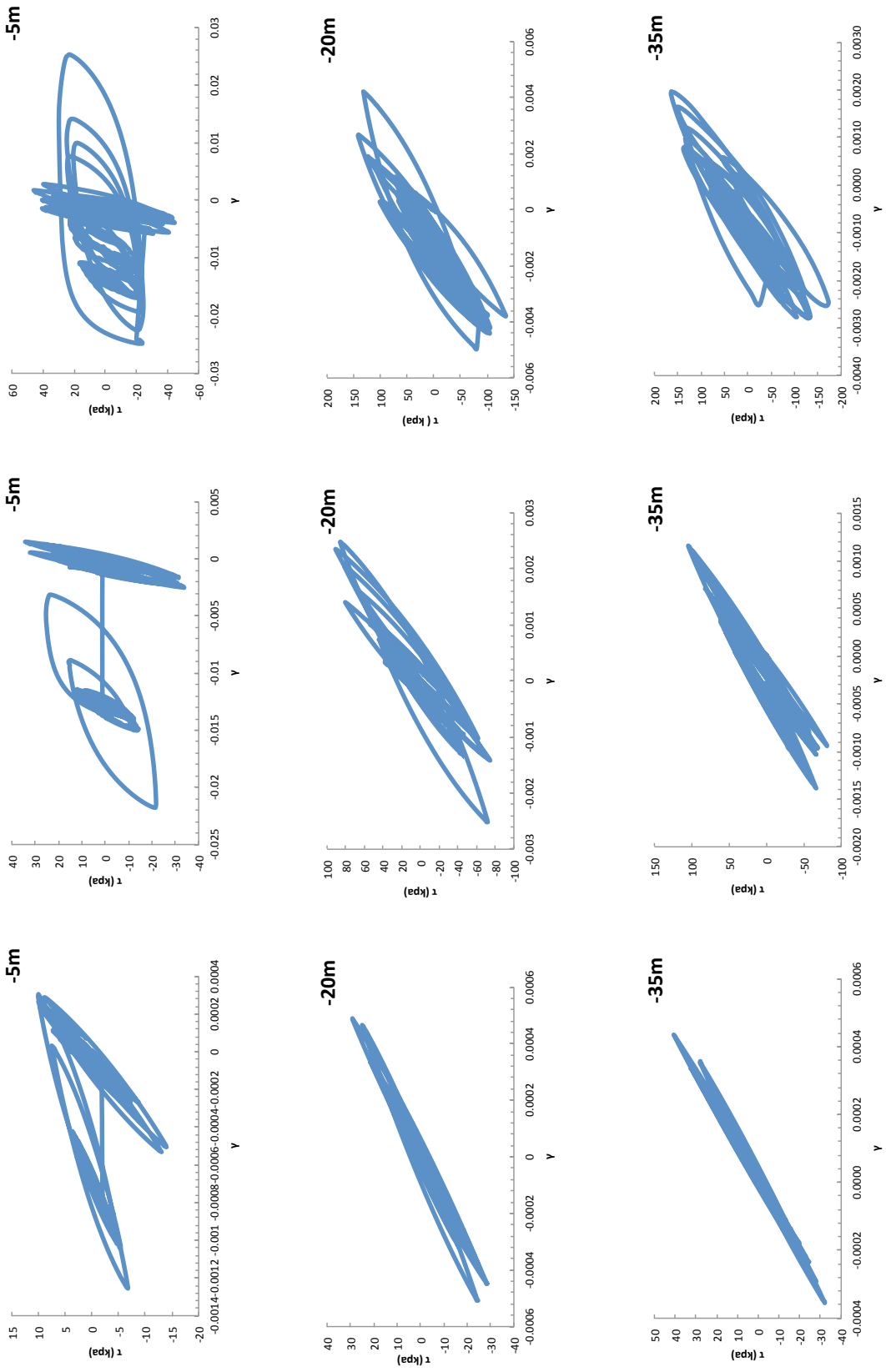

Figure 4.17 τ-γ loops. *Analyses results for the* ***Exponential Soil profile*** *with* ***"NL-DYAS modified"*** *code for the* ***Lefkada excitation*** *for 0.05g, 0.25g, 0.60g respectively from left to right and for different depths.*

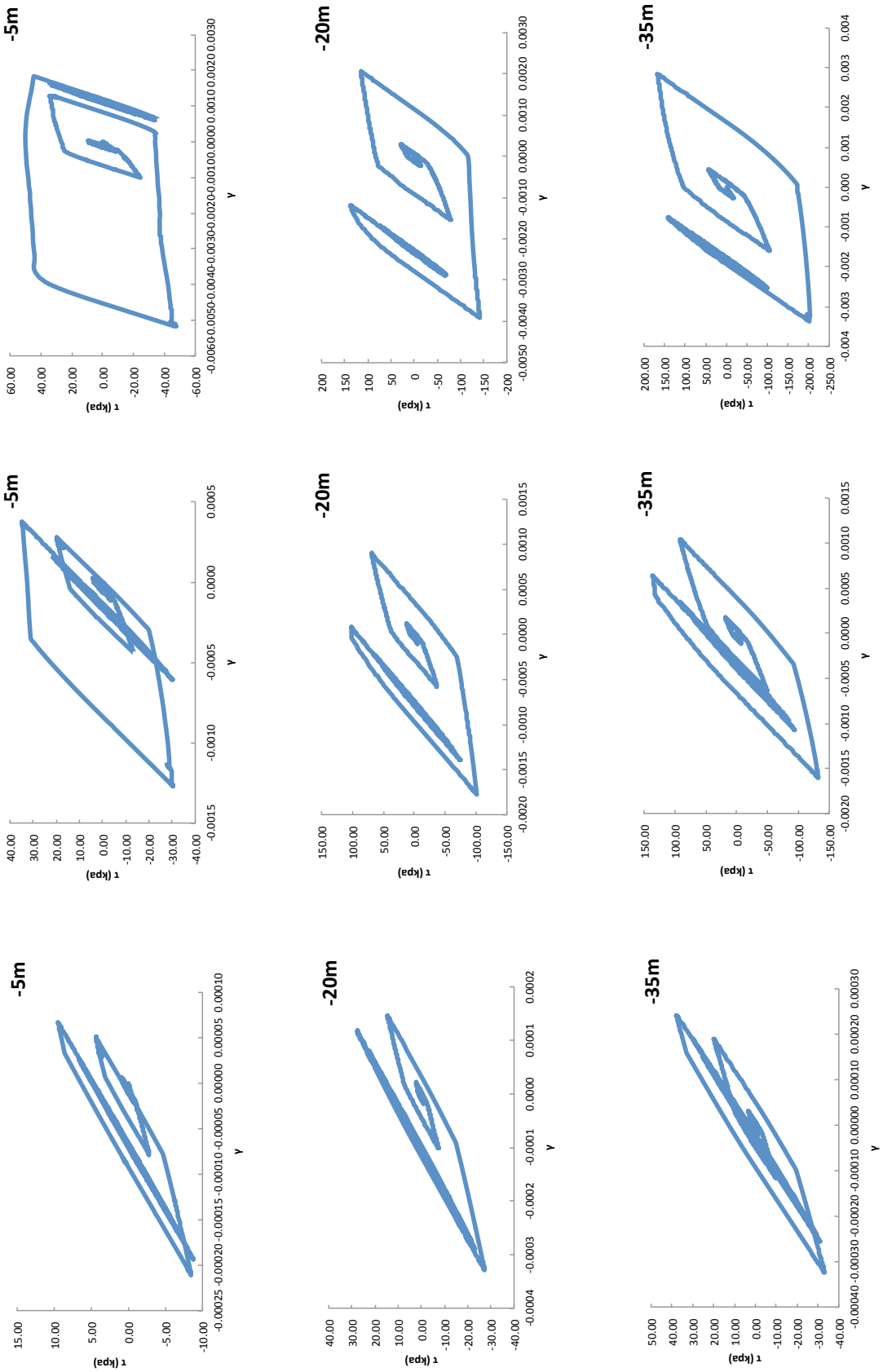

Figure 4.18 τ-γ loops. *Analyses results for the* ***Layered Soil profile*** *with* ***"UBC3D-PLM"*** *code for the* ***Aegion excitation*** *for 0.05g, 0.25g, 0.60g respectively from left to right and for different depths.*

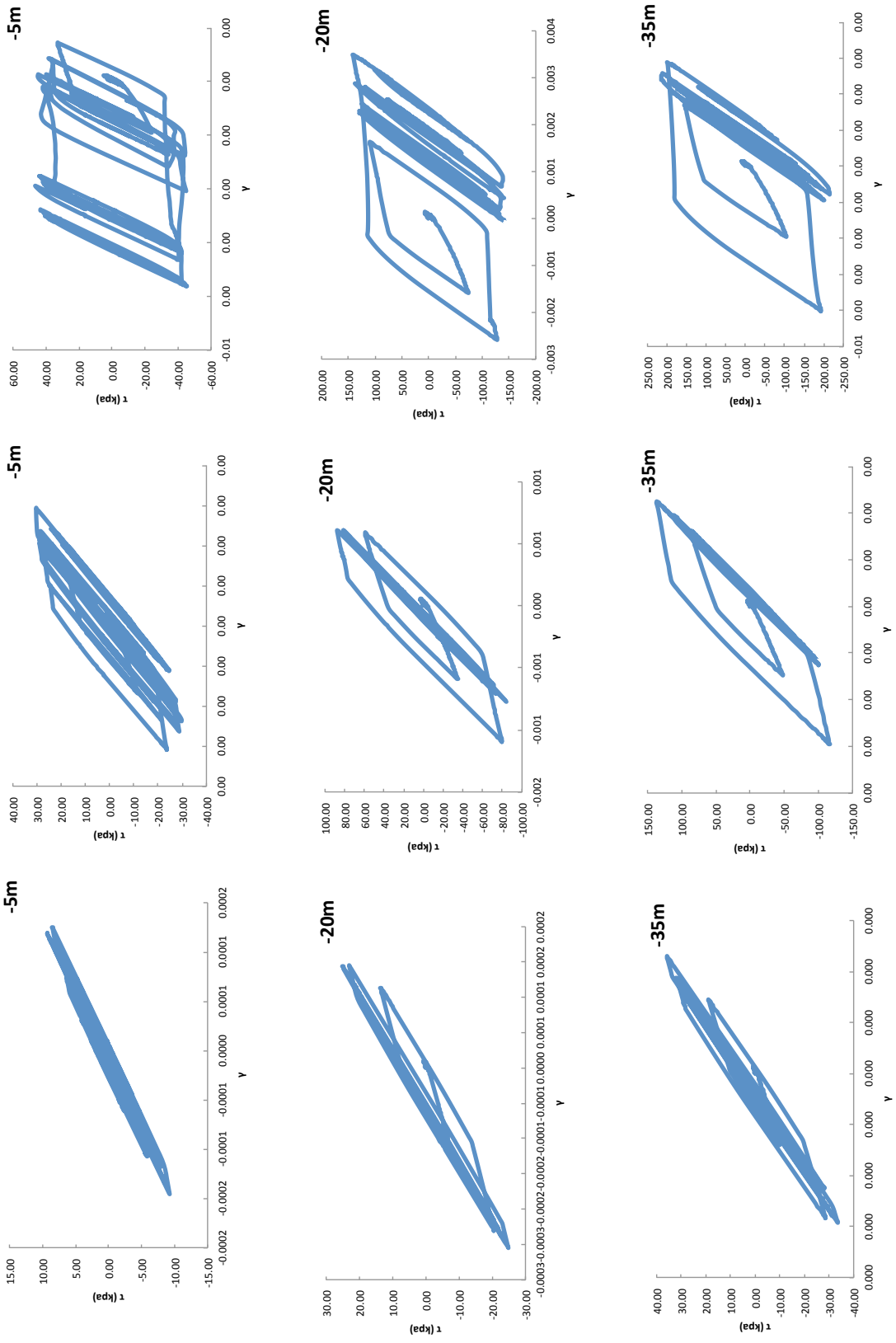

Figure 4.19 τ-γ loops. *Analyses results for the* ***Layered Soil profile*** *with* ***"UBC3D-PLM"*** *code for the* ***Kobe excitation*** *for 0.05g, 0.25g, 0.60g respectively from left to right and for different depths.*

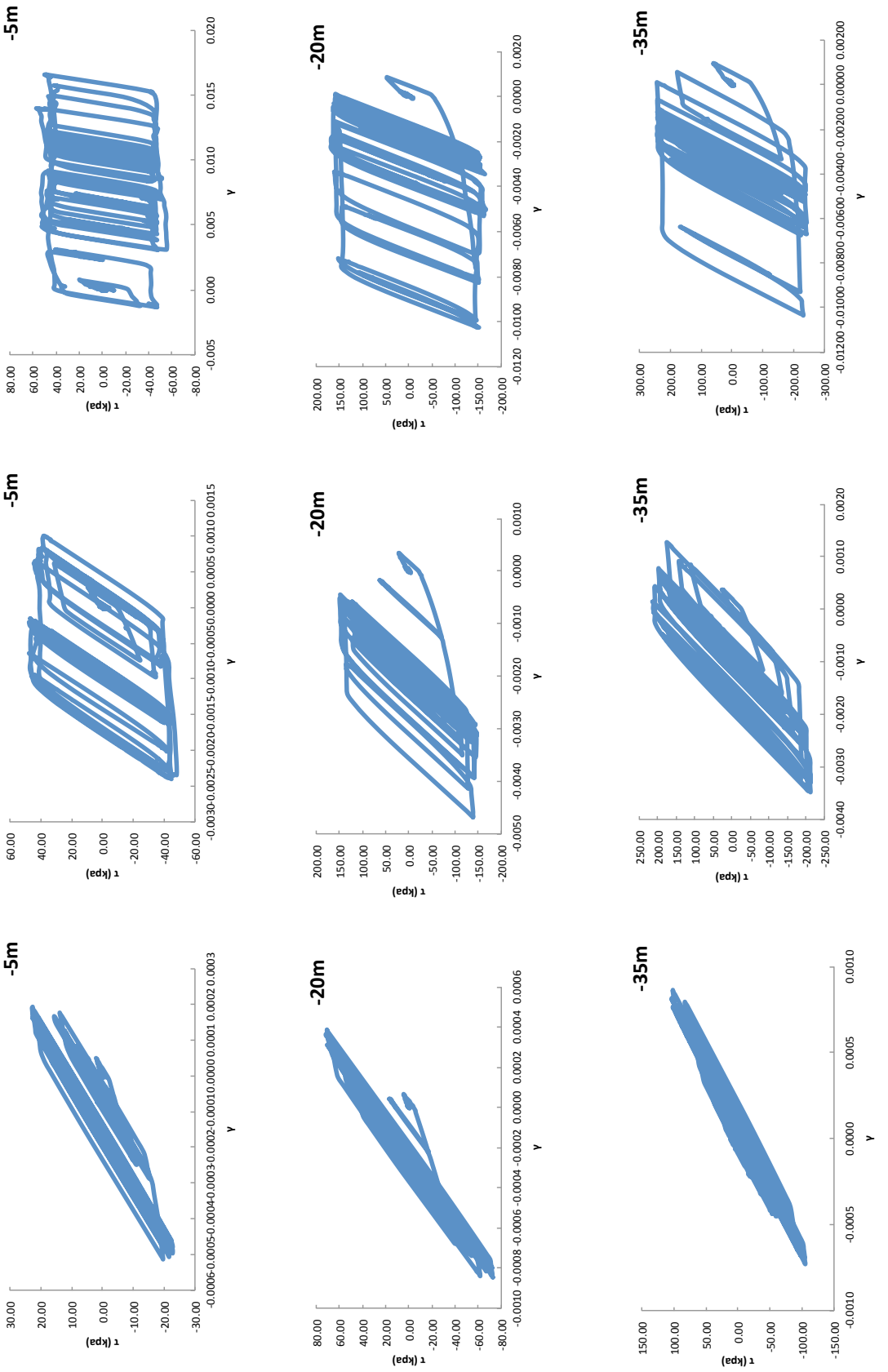

Figure 4.20 τ-γ loops. *Analyses results for the* ***Layered Soil profile*** *with* ***"UBC3D-PLM"*** *code for the* ***Lefkada excitation*** *for 0.05g, 0.25g, 0.60g respectively from left to right and for different depths.*

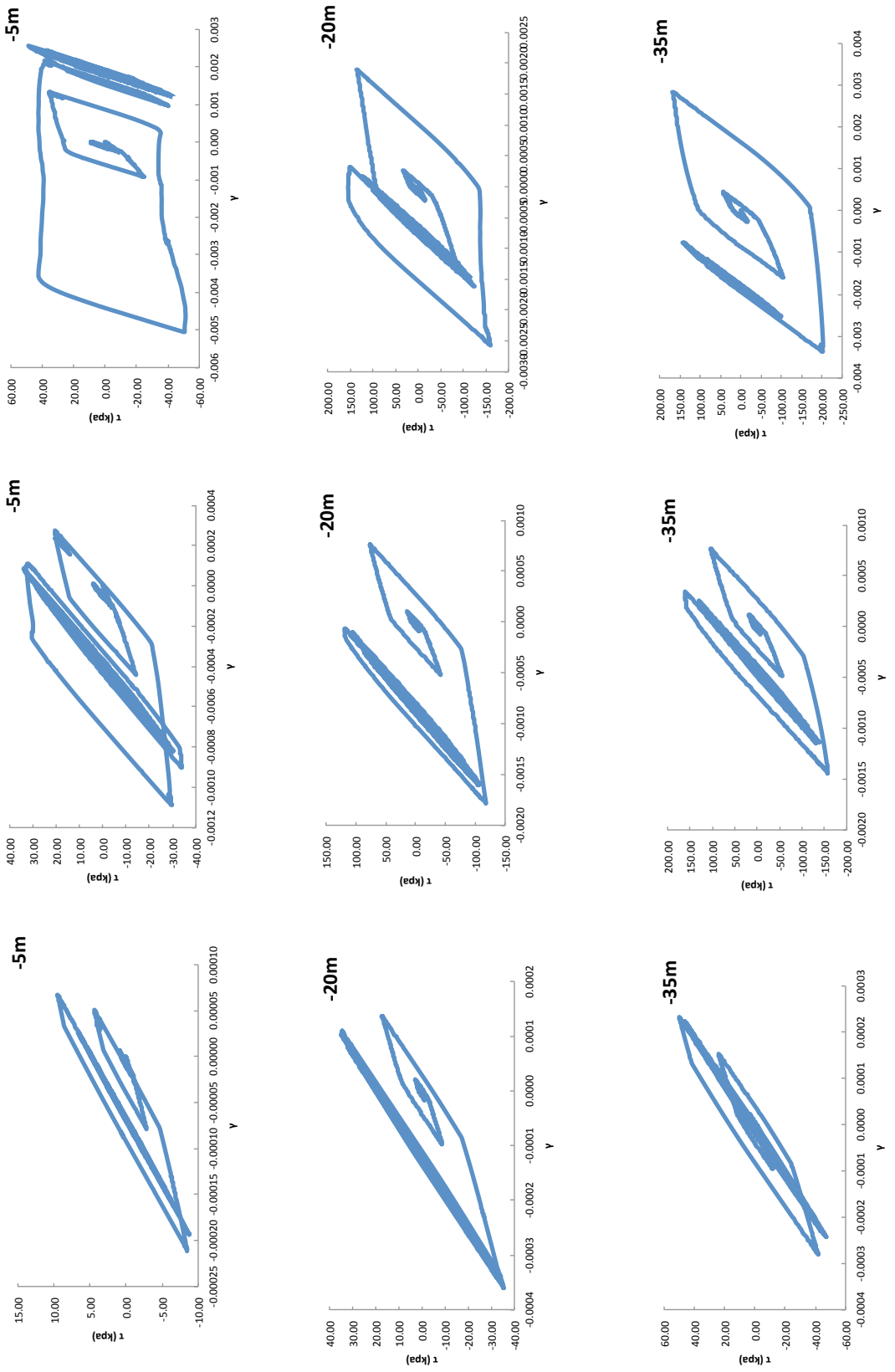

Figure 4.21 τ-γ loops. *Analyses results for the* ***Exponential Soil profile*** *with* ***"UBC3D-PLM"*** *code for the* ***Aegion excitation*** *for 0.05g, 0.25g, 0.60g respectively from left to right and for different depths.*

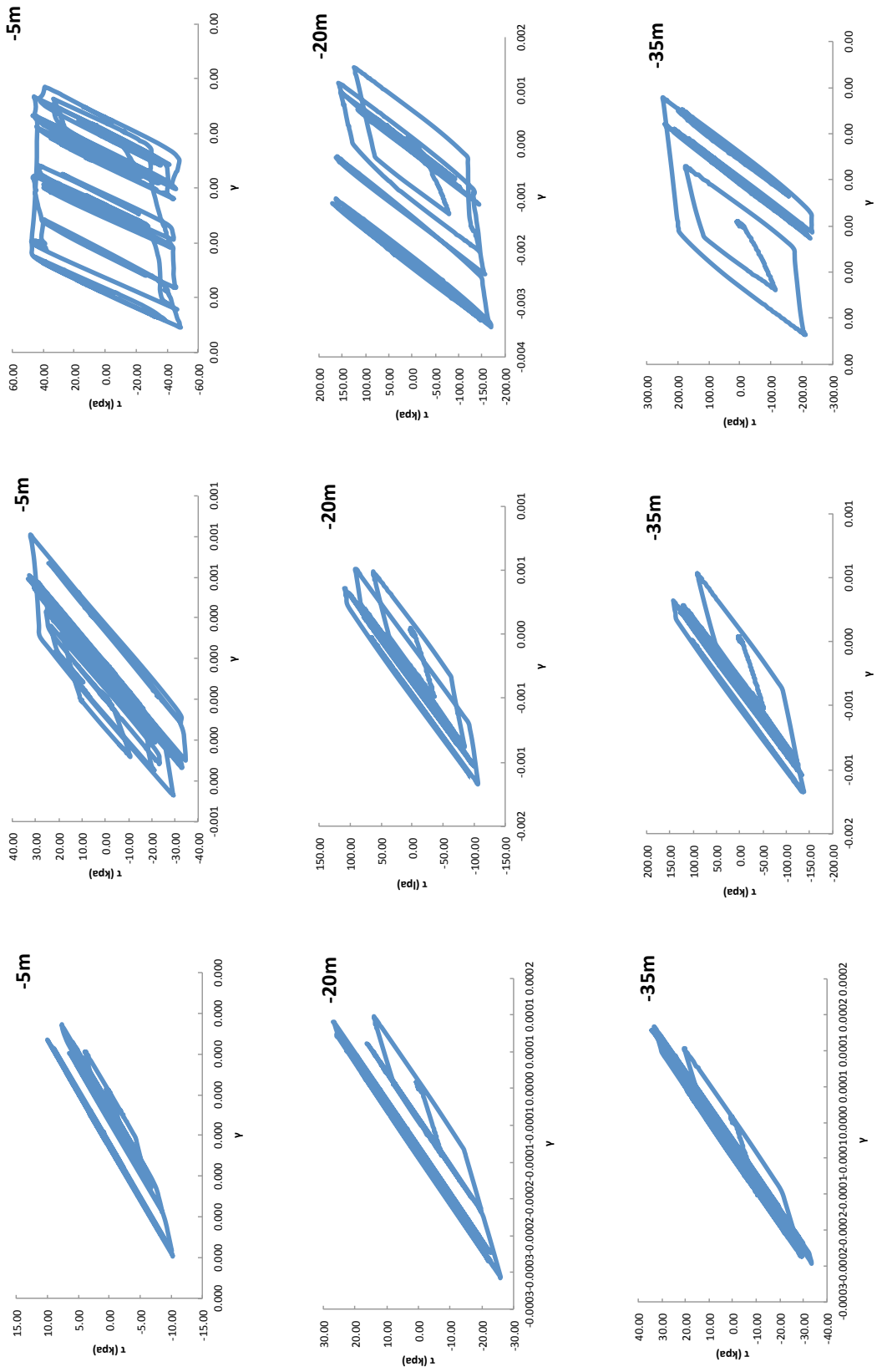

Figure 4.22 τ-γ loops. *Analyses results for the* ***Exponential Soil profile*** *with* ***"UBC3D-PLM"*** *code for the* ***Kobe excitation*** *for 0.05g, 0.25g, 0.60g respectively from left to right and for different depths.*

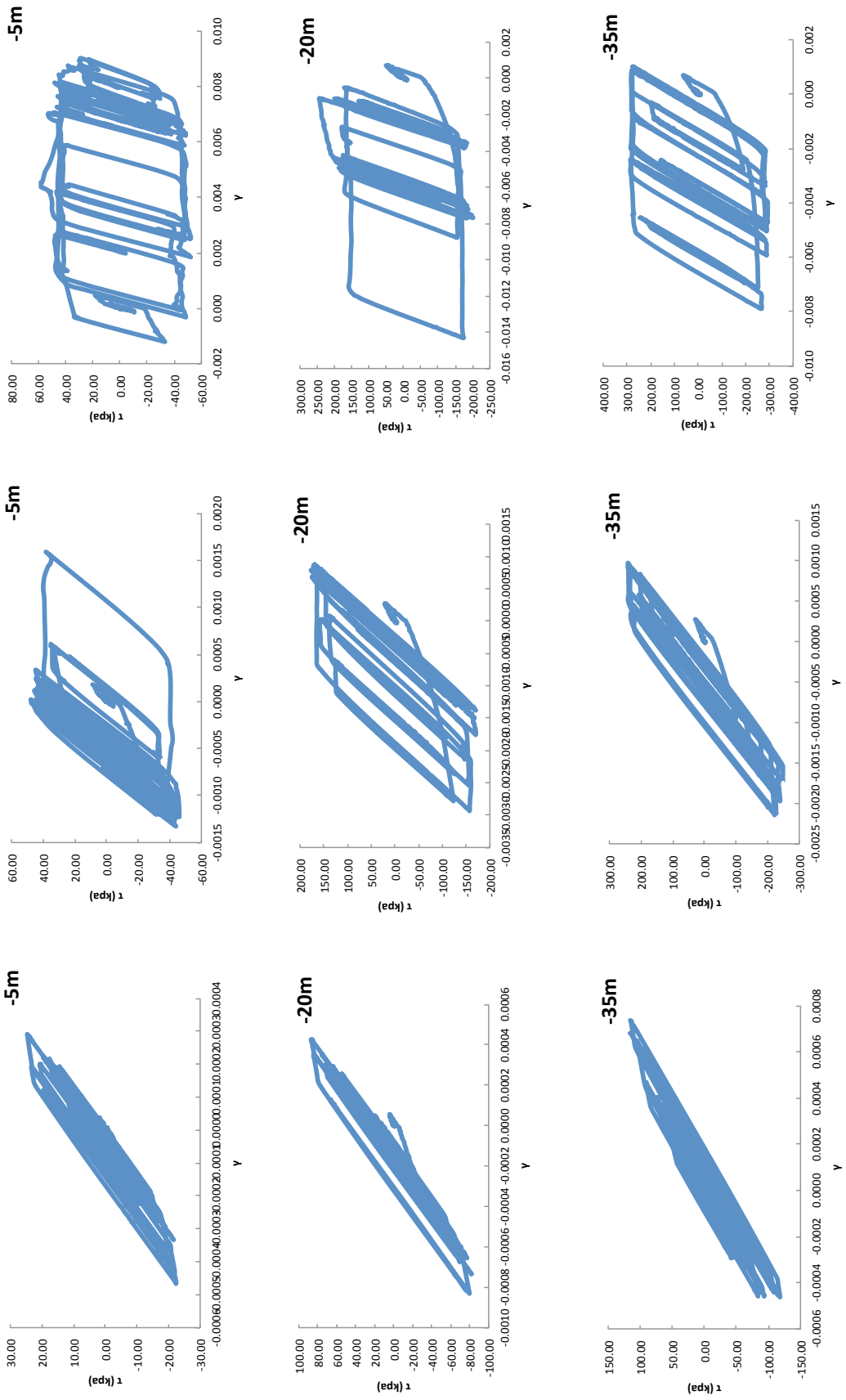

Figure 4.23 τ-γ loops. *Analyses results for the* ***Exponential Soil profile*** *with* ***"UBC3D-PLM"*** *code for the* ***Lefkada excitation*** *for 0.05g, 0.25g, 0.60g respectively from left to right and for different depths.*

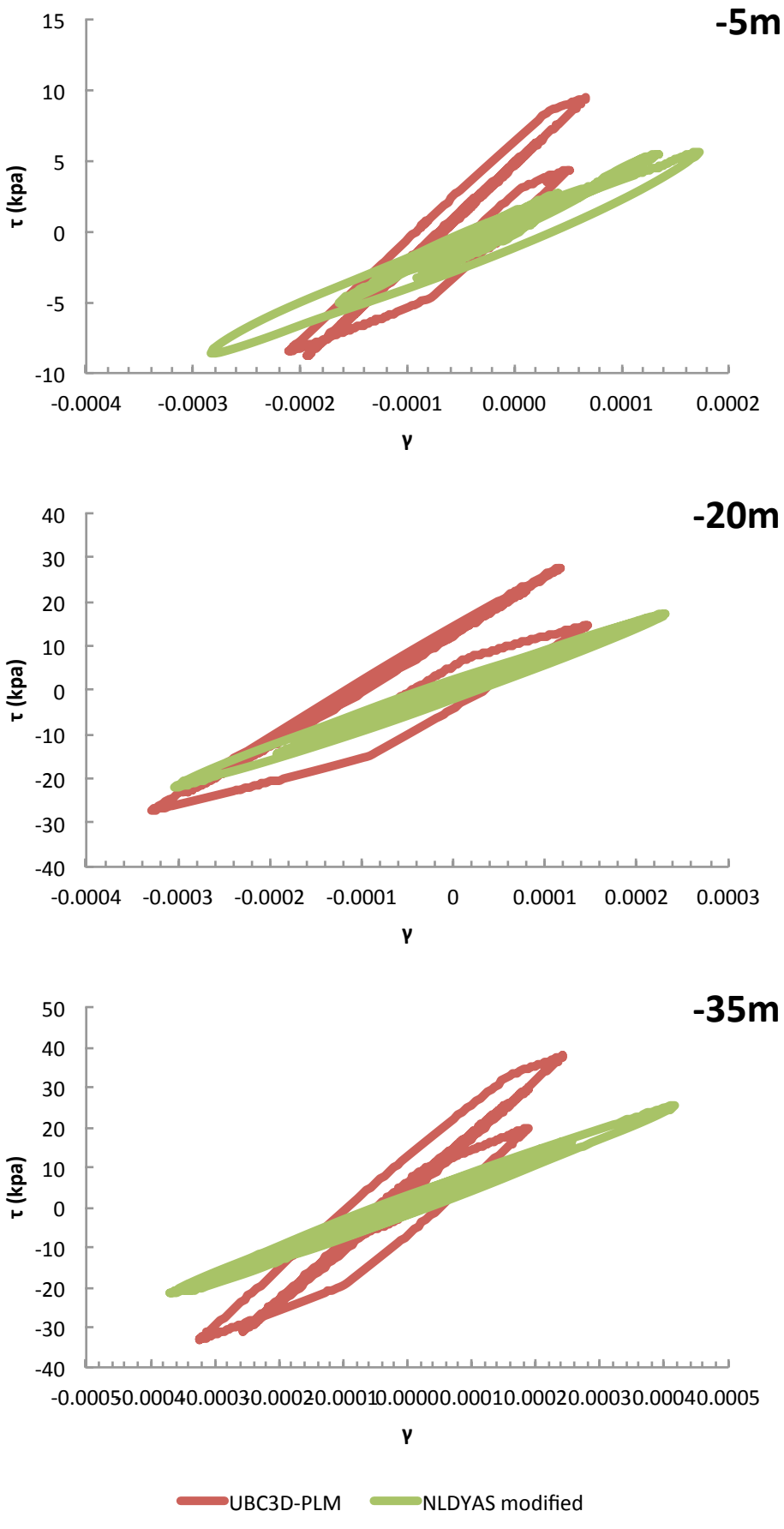

Figure 4.24 τ-γ loops. *Comparison results for the* ***Layered Soil profile*** *between* ***"UBC3D-PLM"*** *code and* ***"NLDYAS-modified"*** *for the* ***Aegion excitation*** *for 0.05g, for different depths.*

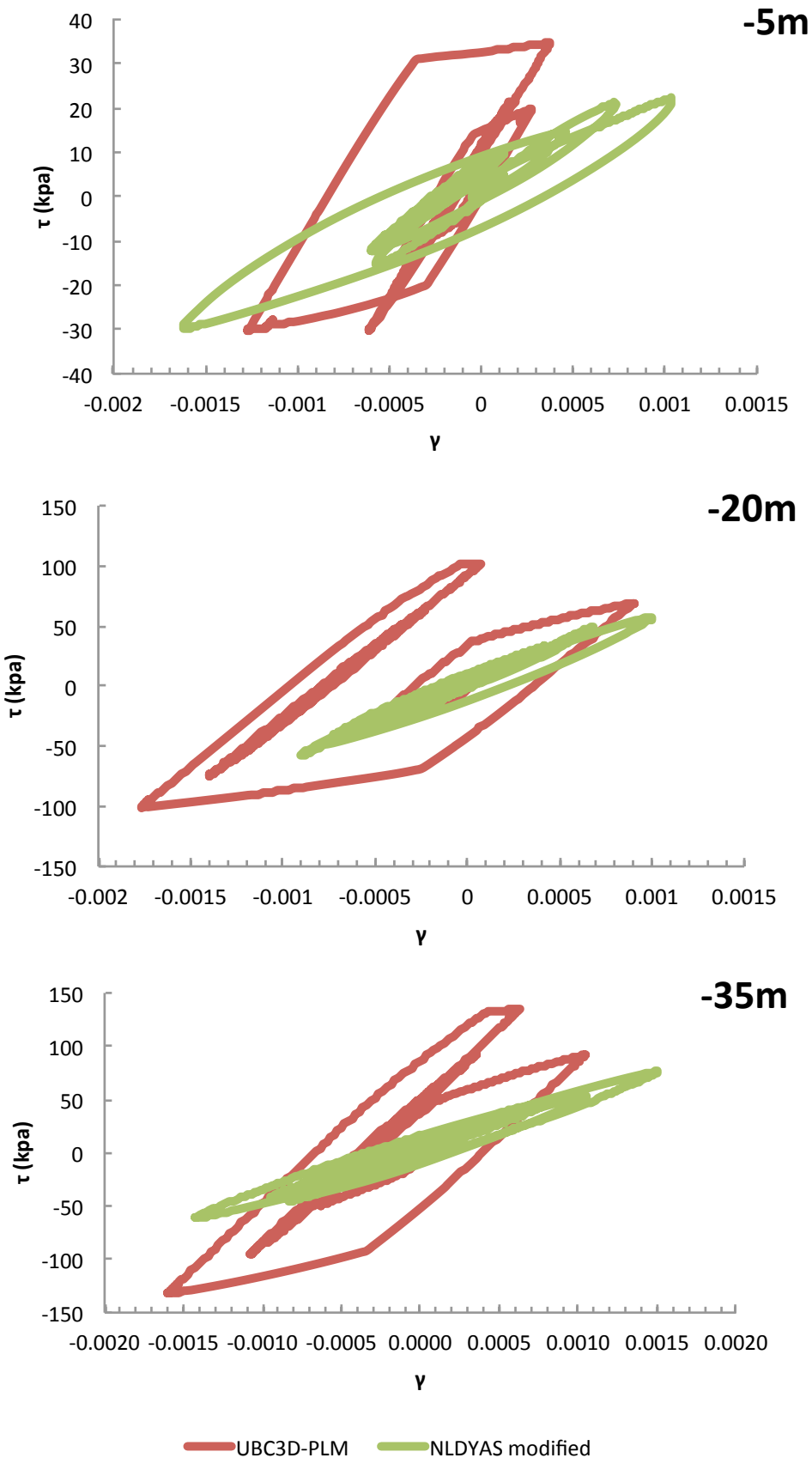

Figure 4.25 τ-γ loops. *Comparison results for the* ***Layered Soil profile*** *between* ***"UBC3D-PLM"*** *code and* ***"NLDYAS-modified"*** *for the* ***Aegion excitation*** *for 0.25g, for different depths.*

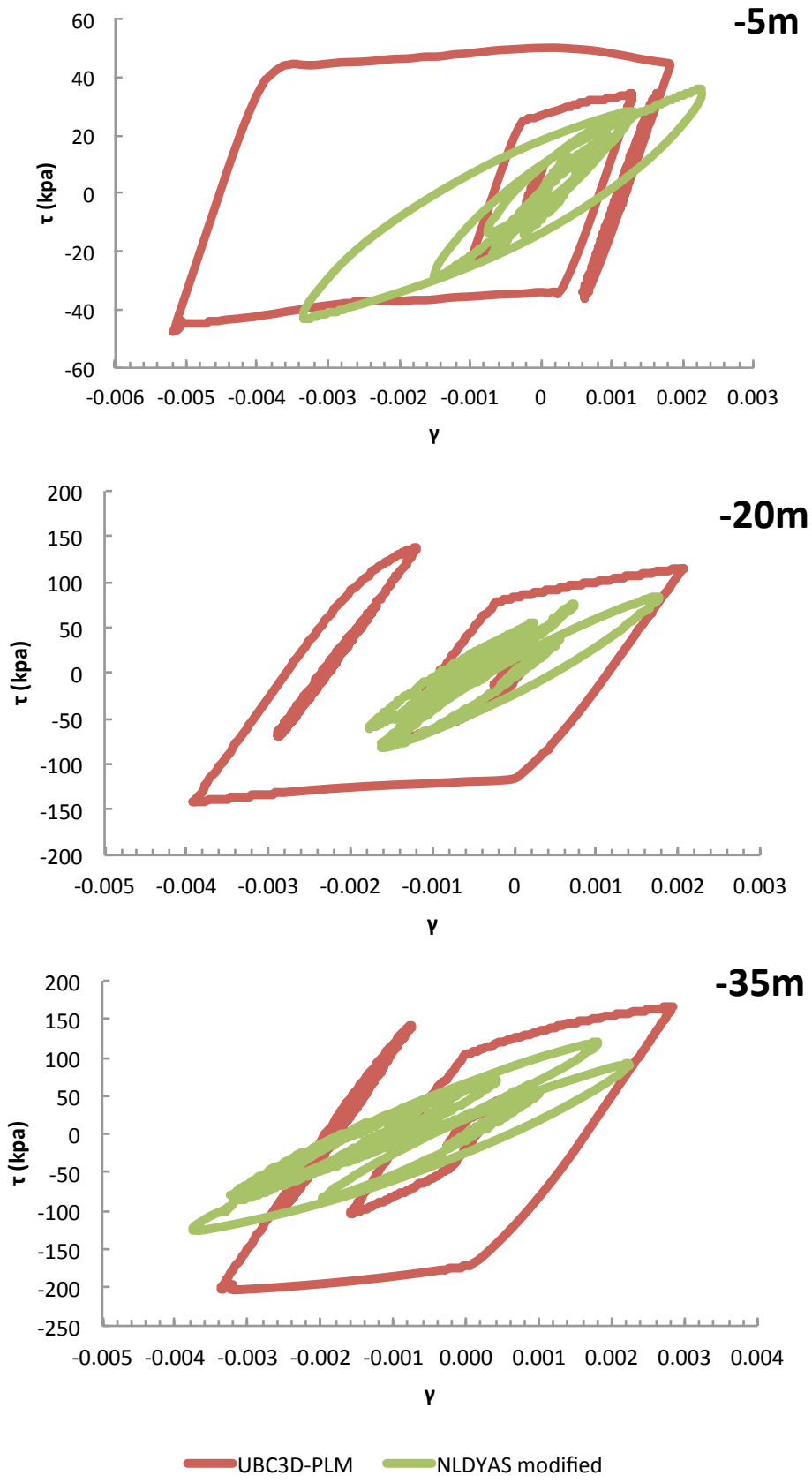

Figure 4.26 τ-γ loops. *Comparison results for the* ***Layered Soil profile*** *between* ***"UBC3D-PLM"*** *code and* ***"NLDYAS-modified"*** *for the* ***Aegion excitation*** *for 0.60g, for different depths.*

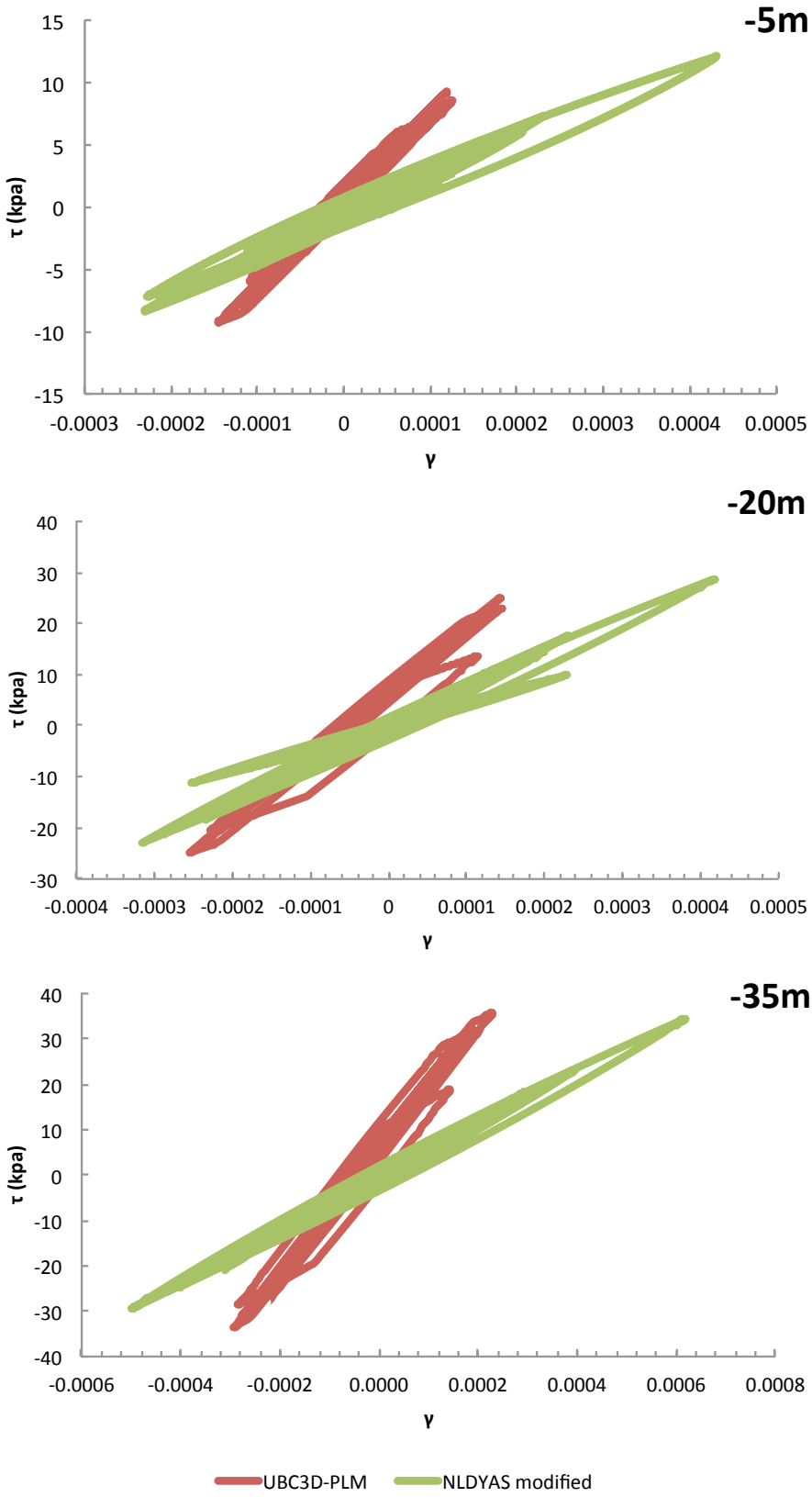

Figure 4.27 τ-γ loops. *Comparison results for the* ***Layered Soil profile*** *between* ***"UBC3D-PLM"*** *code and* ***"NLDYAS-modified"*** *for the* ***Kobe excitation*** *for 0.05g, for different depths.*

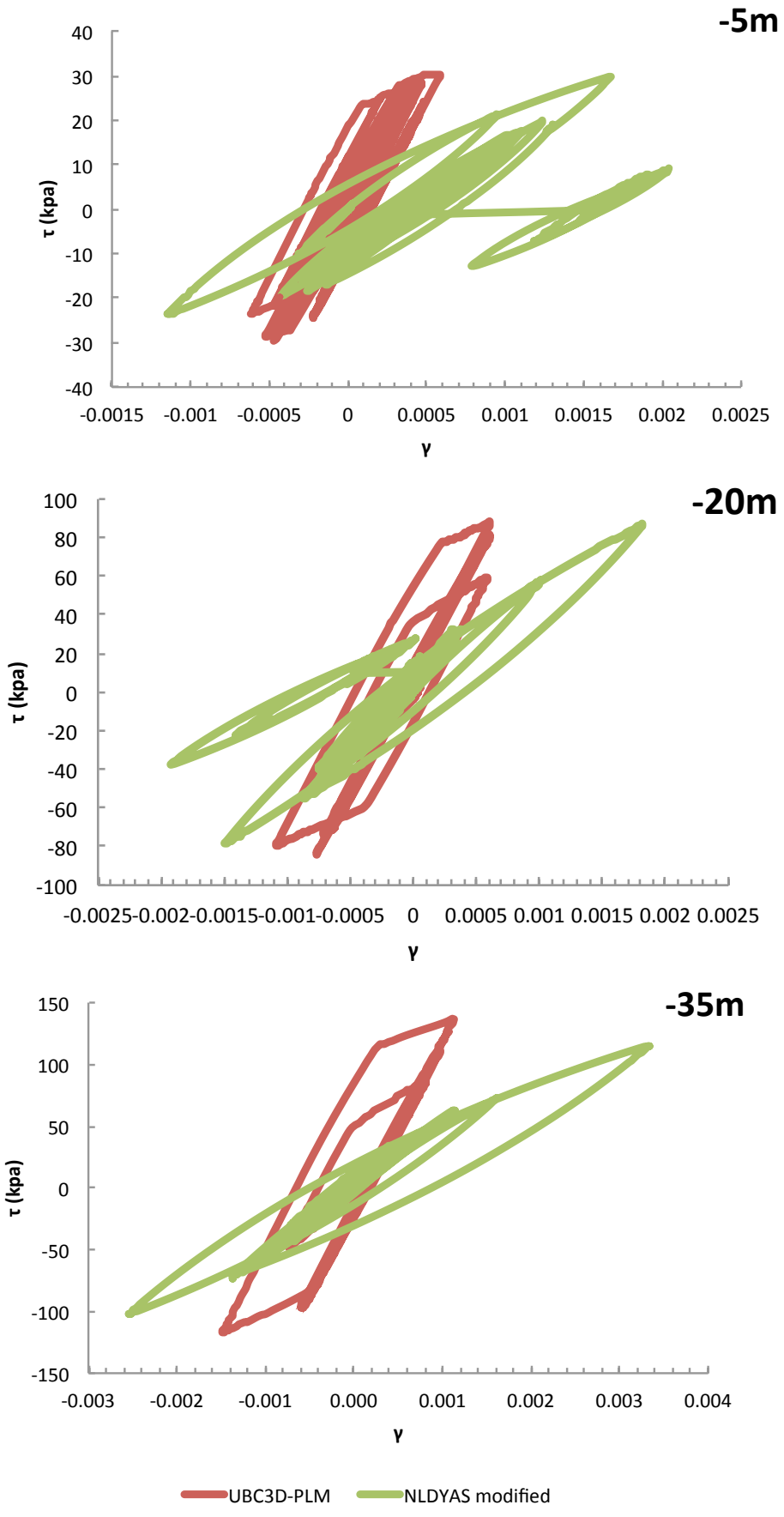

Figure 4.28 τ-γ loops. *Comparison results for the* ***Layered Soil profile*** *between* ***"UBC3D-PLM"*** *code and* ***"NLDYAS-modified"*** *for the* ***Kobe excitation*** *for 0.25g, for different depths.*

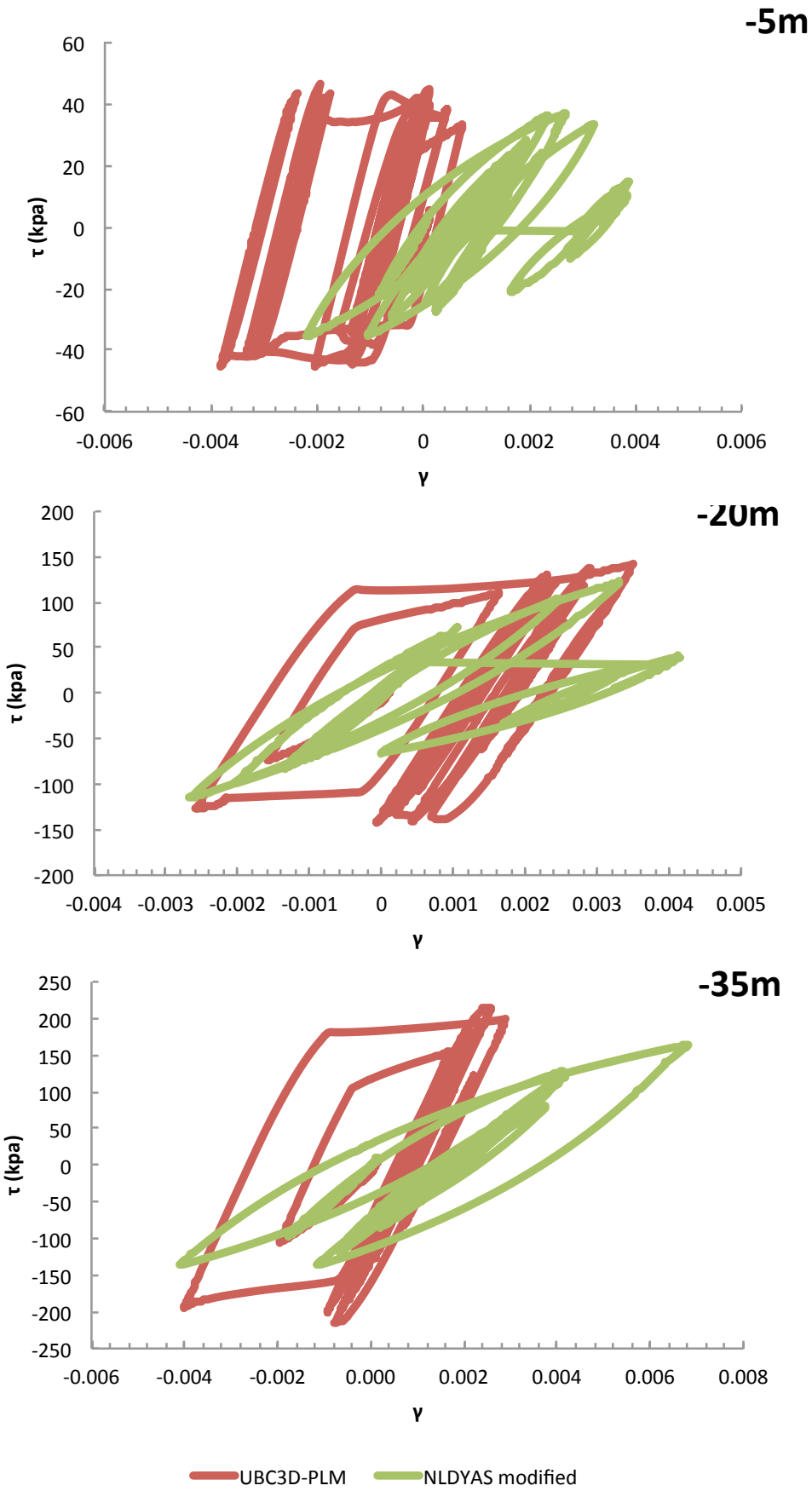

Figure 4.29 τ-γ loops. *Comparison results for the* ***Layered Soil profile*** *between* ***"UBC3D-PLM"*** *code and* ***"NLDYAS-modified"*** *for the* ***Kobe excitation*** *for 0.60g, for different depths.*

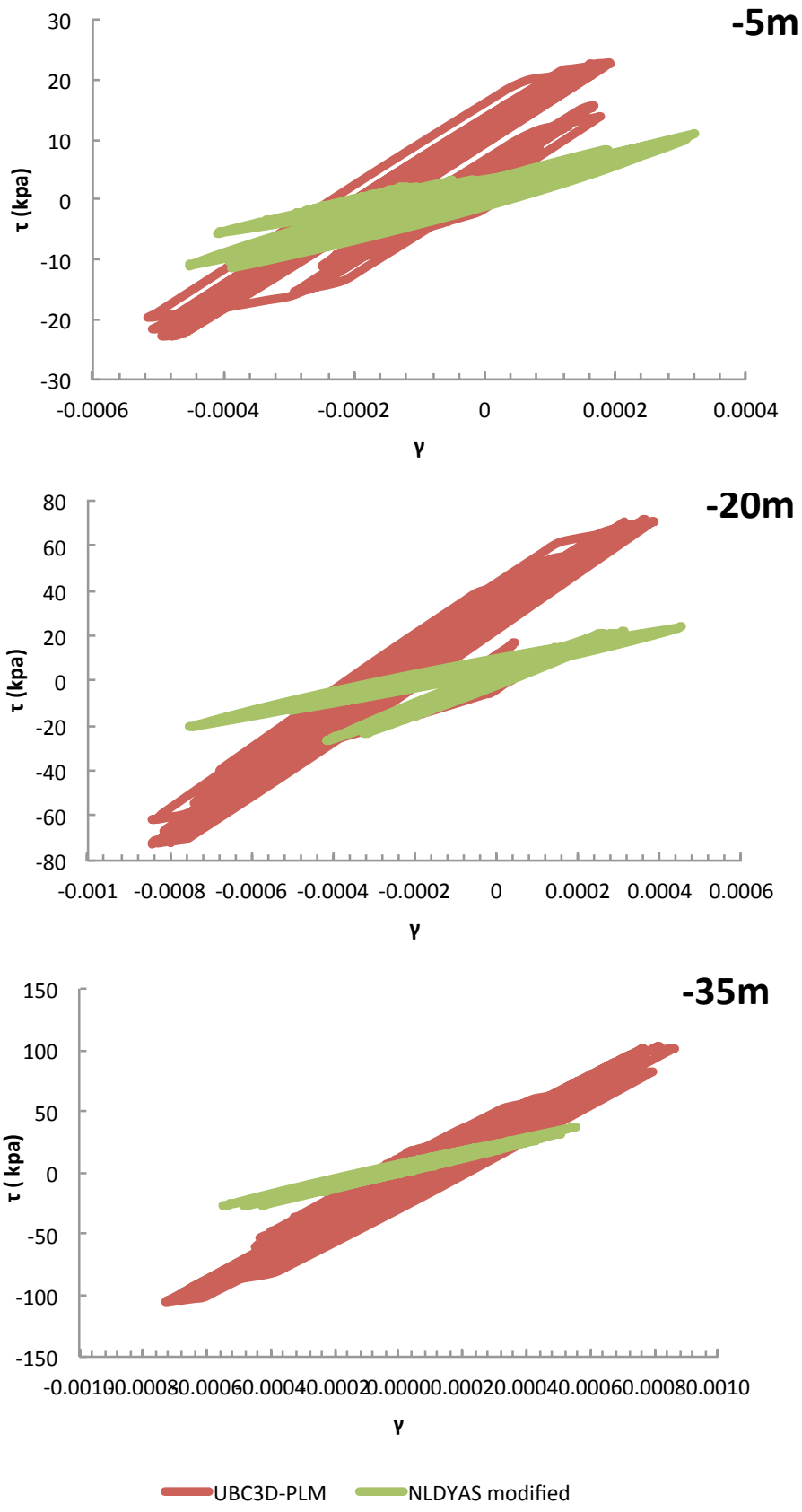

Figure 4.30 τ-γ loops. *Comparison results for the* ***Layered Soil profile*** *between* ***"UBC3D-PLM"*** *code and* ***"NLDYAS-modified"*** *for the* ***Lefkada excitation*** *for 0.05g, for different depths.*

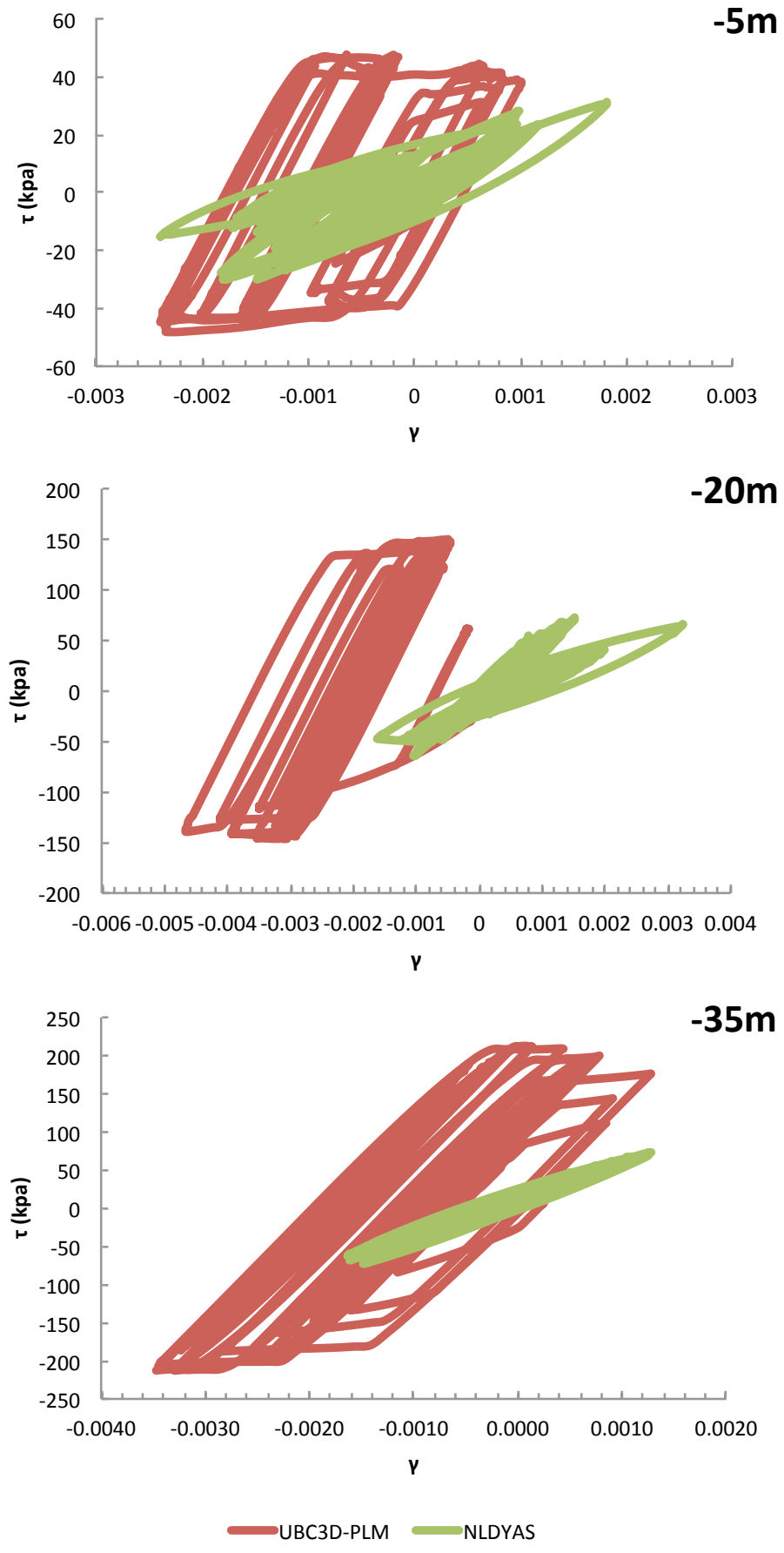

Figure 4.31 τ-γ loops. *Comparison results for the* ***Layered Soil profile*** *between* ***"UBC3D-PLM"*** *code and* ***"NLDYAS-modified"*** *for the* ***Lefkada excitation*** *for 0.25g, for different depths.*

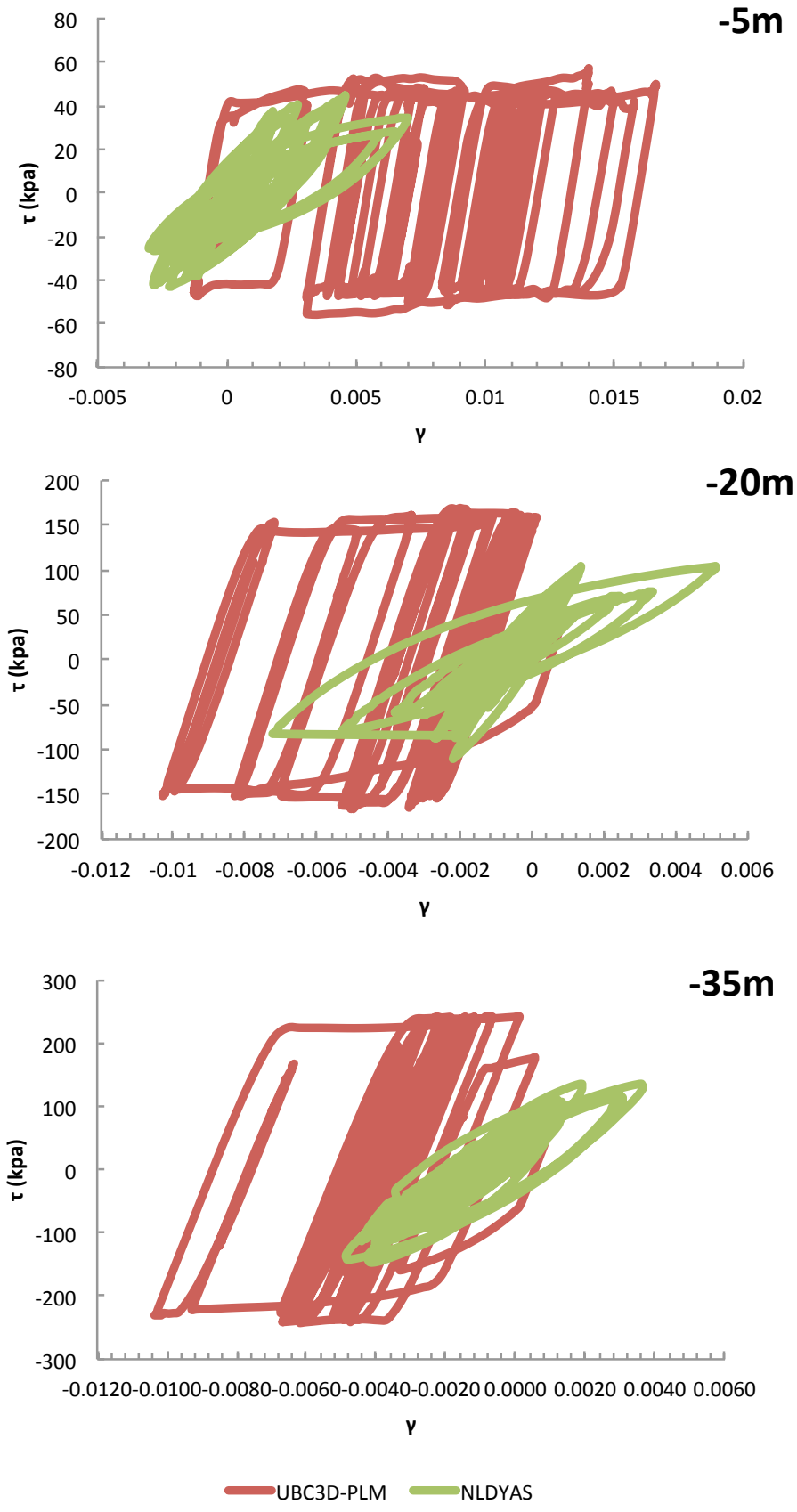

Figure 4.32 τ-γ loops. *Comparison results for the* ***Layered Soil profile*** *between* ***"UBC3D-PLM"*** *code and* ***"NLDYAS-modified"*** *for the* ***Lefkada excitation*** *for 0.60g, for different depths.*

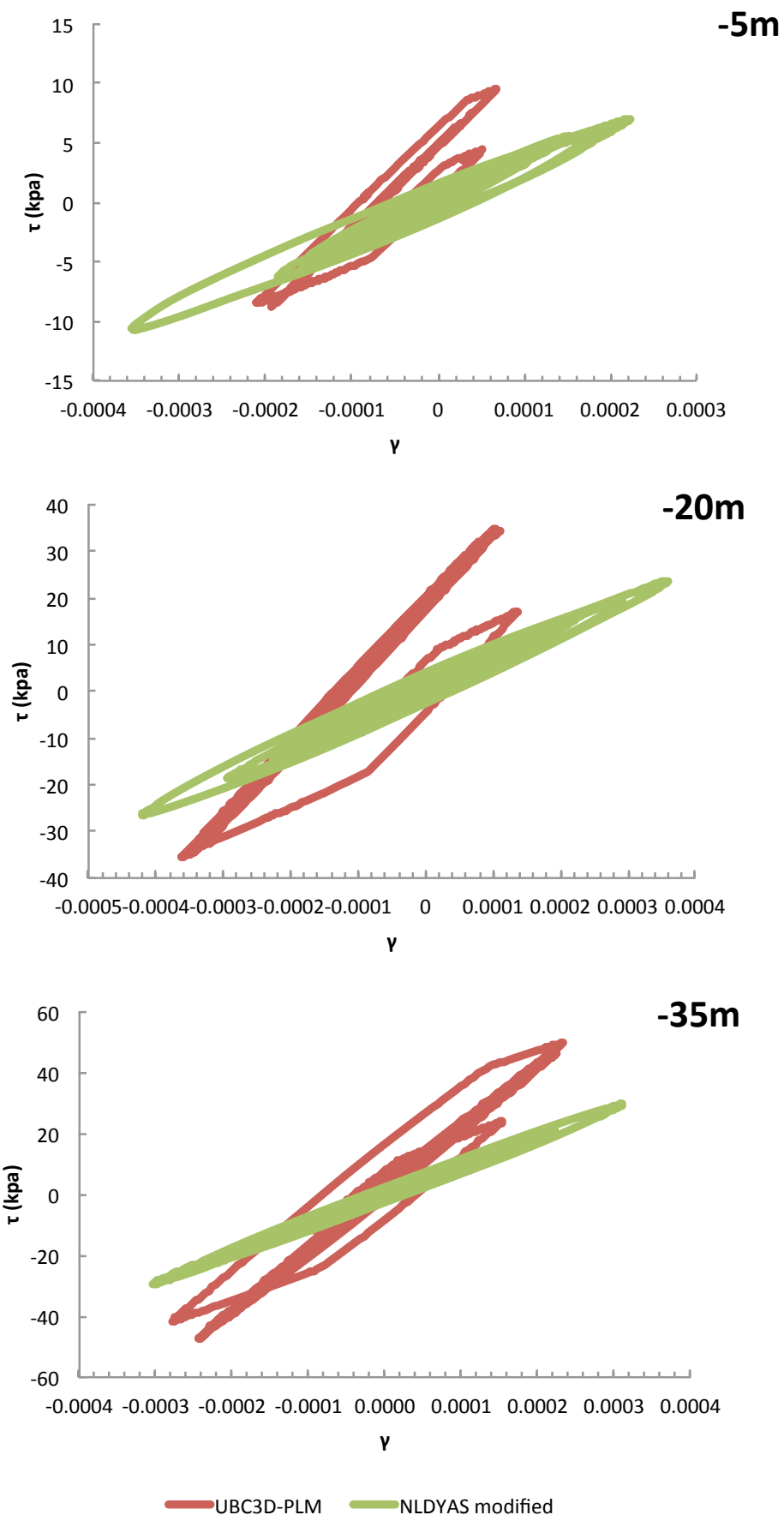

Figure 4.33 τ-γ loops. *Comparison results for the* ***Exponential Soil profile*** *between* ***"UBC3D-PLM"*** *code and* ***"NLDYAS-modified"*** *for the* ***Aegion excitation*** *for 0.05g, for different depths.*

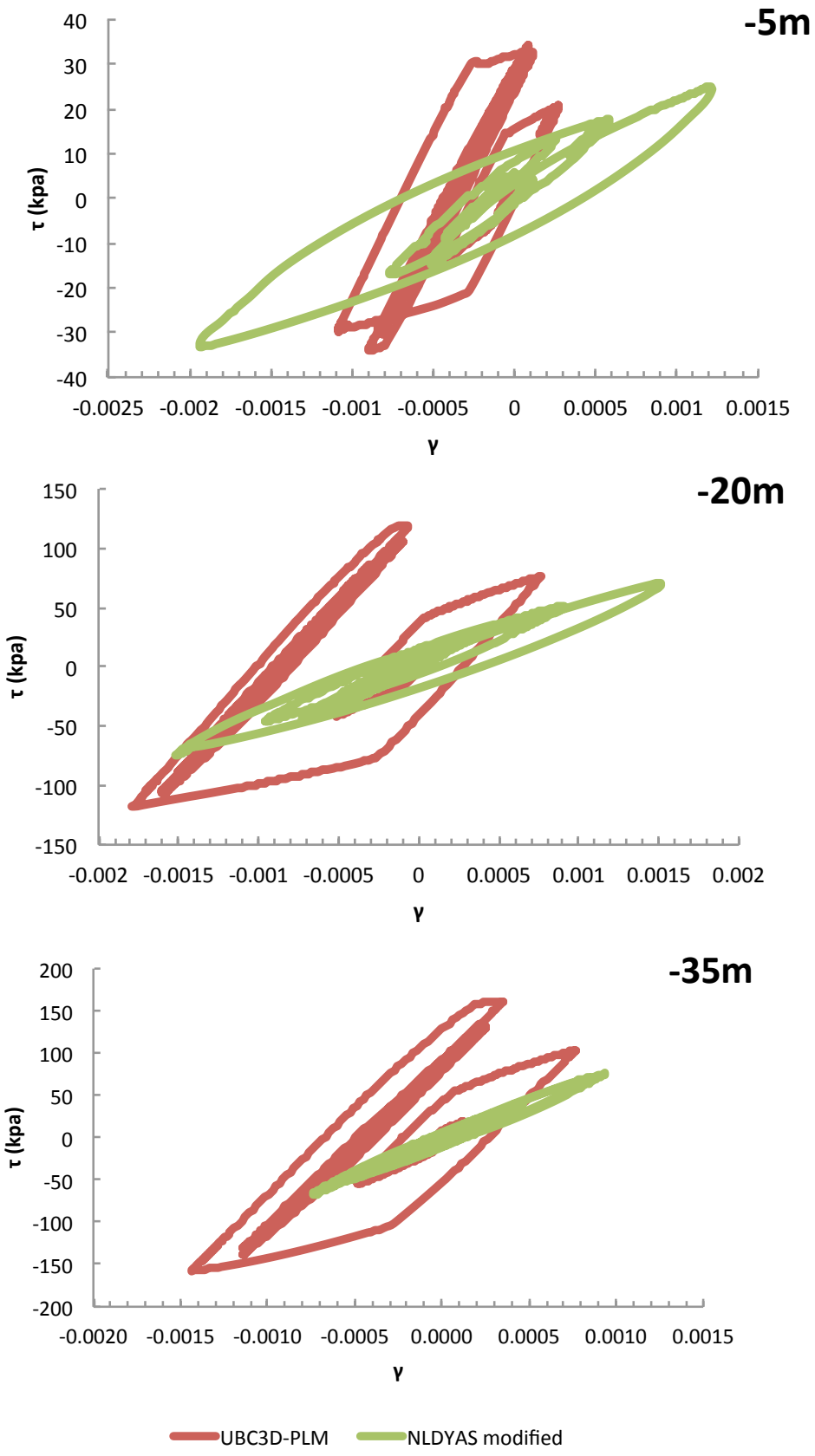

Figure 4.34 τ-γ loops. *Comparison results for the* ***Exponential Soil profile*** *between* ***"UBC3D-PLM"*** *code and* ***"NLDYAS-modified"*** *for the* ***Aegion excitation*** *for 0.25g, for different depths.*

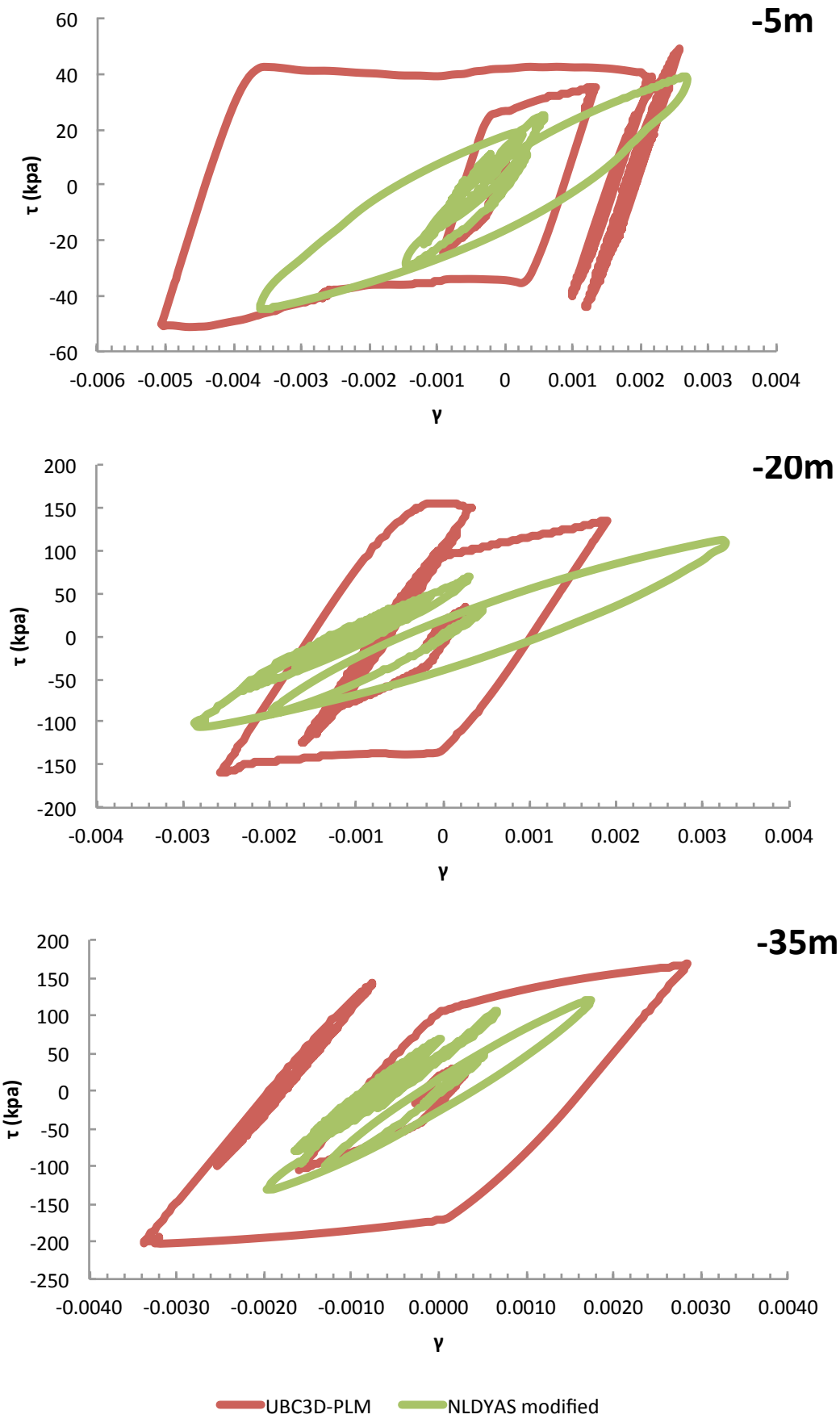

Figure 4.35 τ-γ loops. *Comparison results for the* ***Exponential Soil profile*** *between* ***"UBC3D-PLM"*** *code and* ***"NLDYAS-modified"*** *for the* ***Aegion excitation*** *for 0.60g, for different depths.*

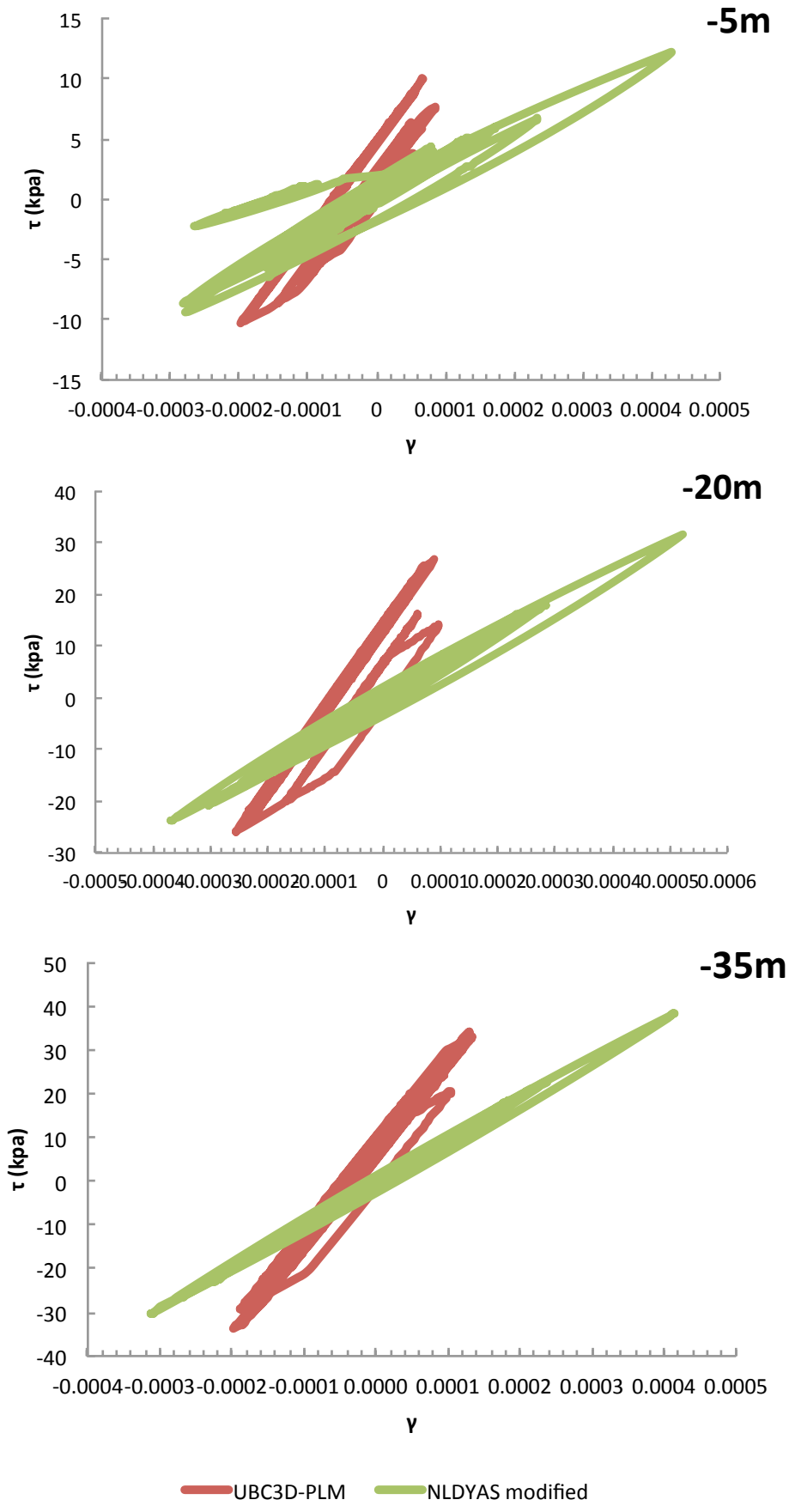

Figure 4.36 τ-γ loops. *Comparison results for the* ***Exponential Soil profile*** *between* ***"UBC3D-PLM"*** *code and* ***"NLDYAS-modified"*** *for the* ***Kobe excitation*** *for 0.05g, for different depths.*

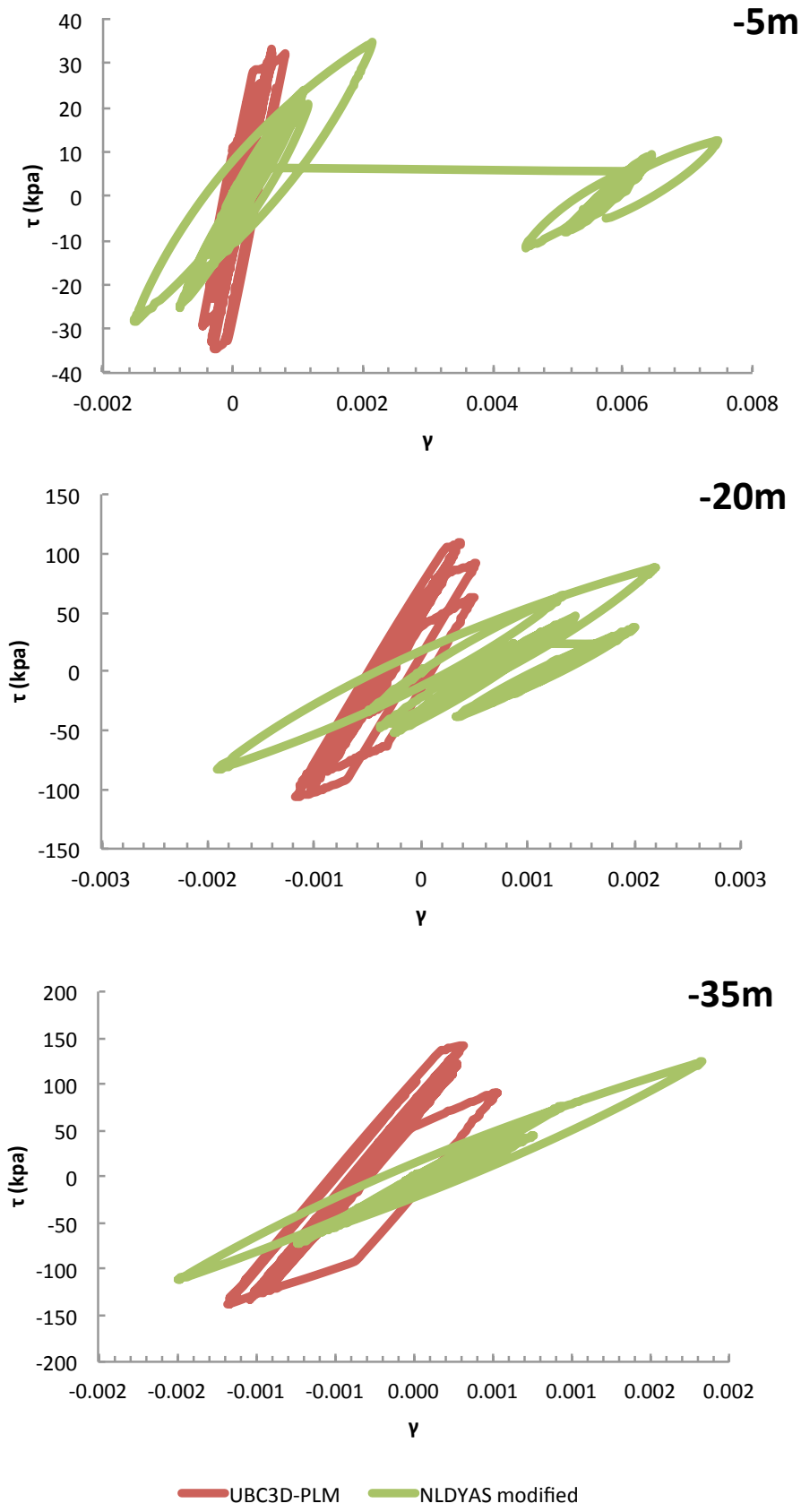

Figure 4.37 τ-γ loops. *Comparison results for the* ***Exponential Soil profile*** *between* ***"UBC3D-PLM"*** *code and* ***"NLDYAS-modified"*** *for the* ***Kobe excitation*** *for 0.25g, for different depths.*

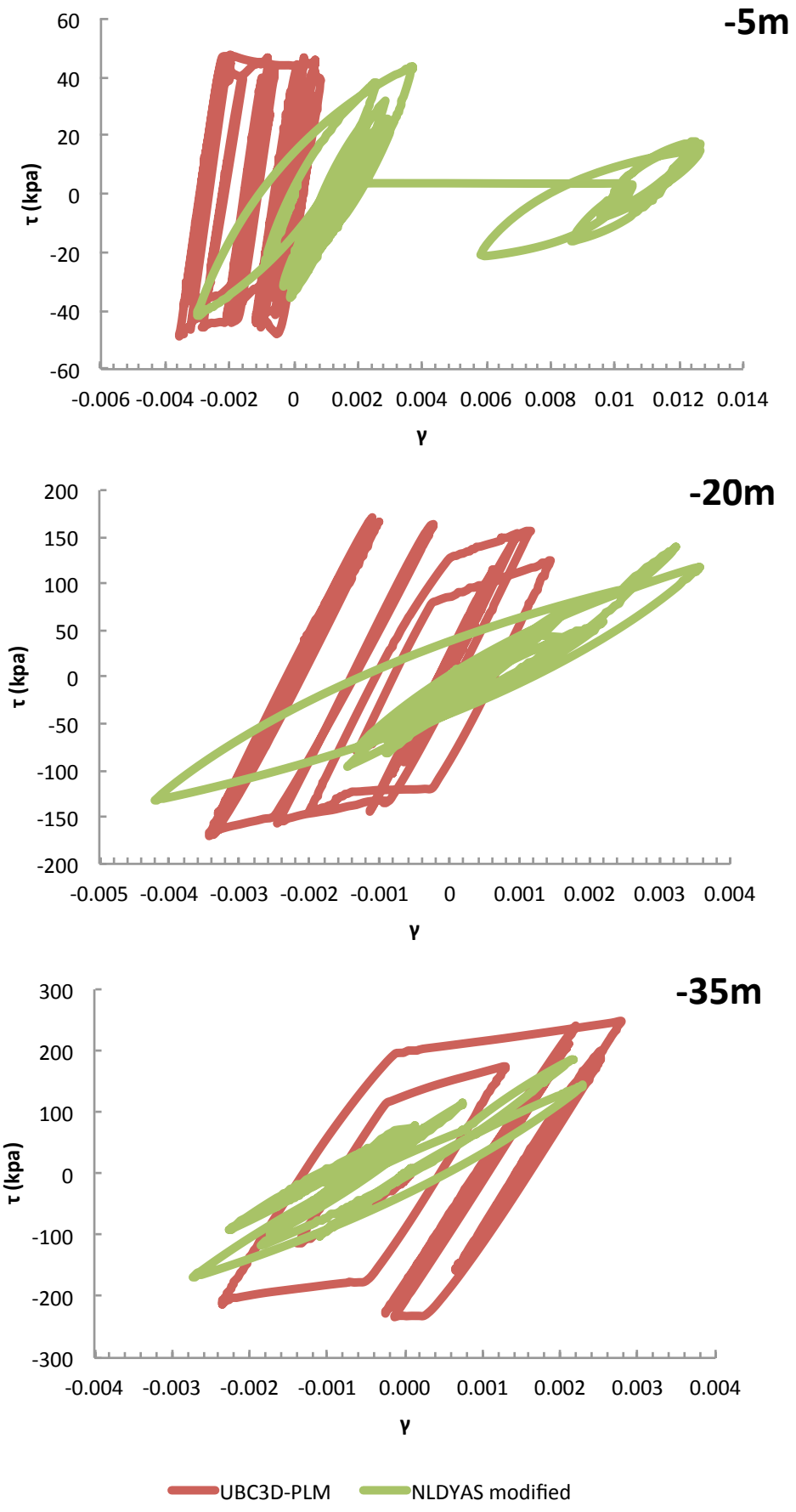

Figure 4.38 τ-γ loops. *Comparison results for the* ***Exponential Soil profile*** *between* ***"UBC3D-PLM"*** *code and* ***"NLDYAS-modified"*** *for the* ***Kobe excitation*** *for 0.60g, for different depths.*

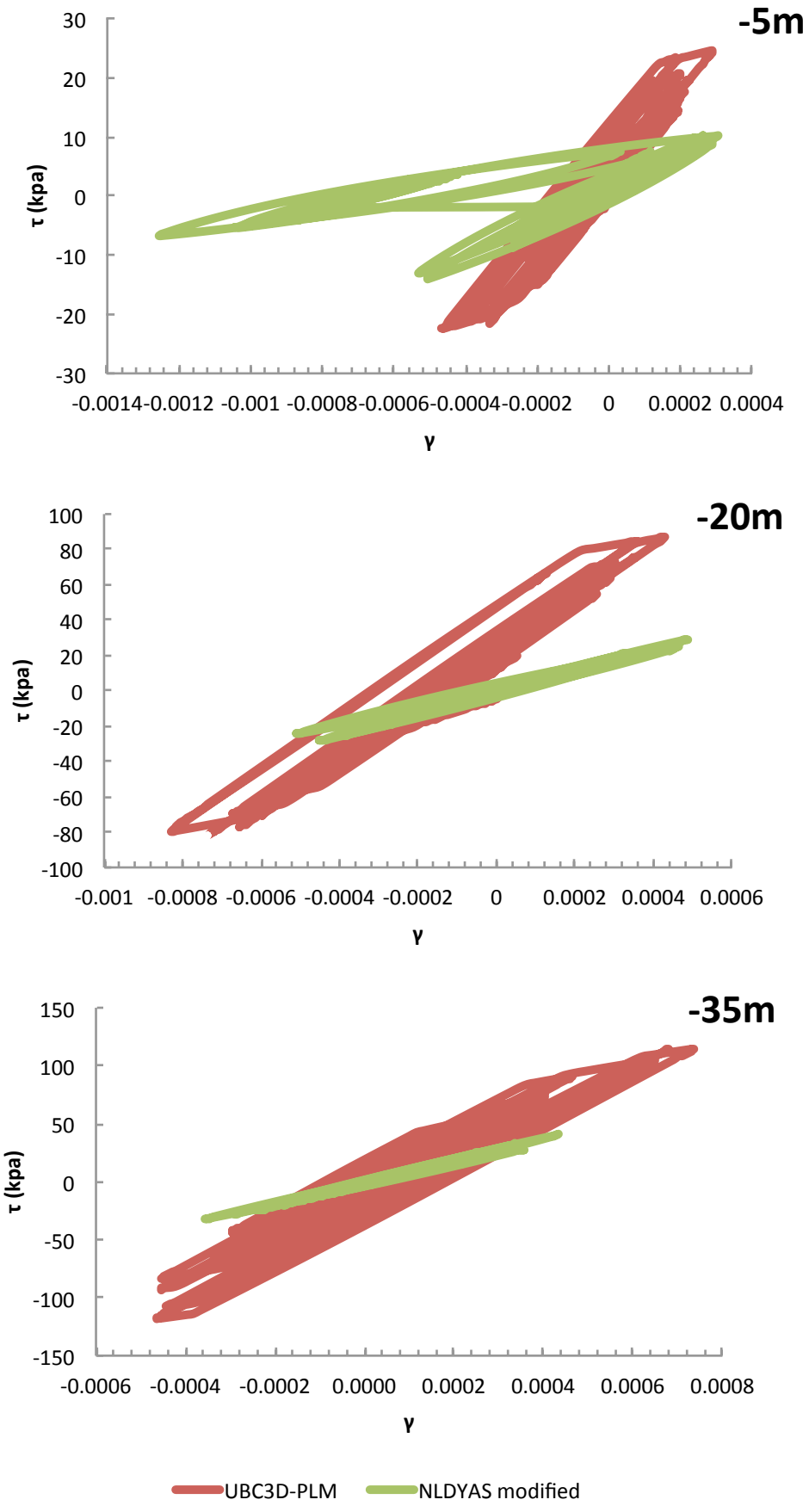

Figure 4.39 τ-γ loops. *Comparison results for the* ***Exponential Soil profile*** *between* ***"UBC3D-PLM"*** *code and* ***"NLDYAS-modified"*** *for the* ***Lefkada excitation*** *for 0.05g, for different depths.*

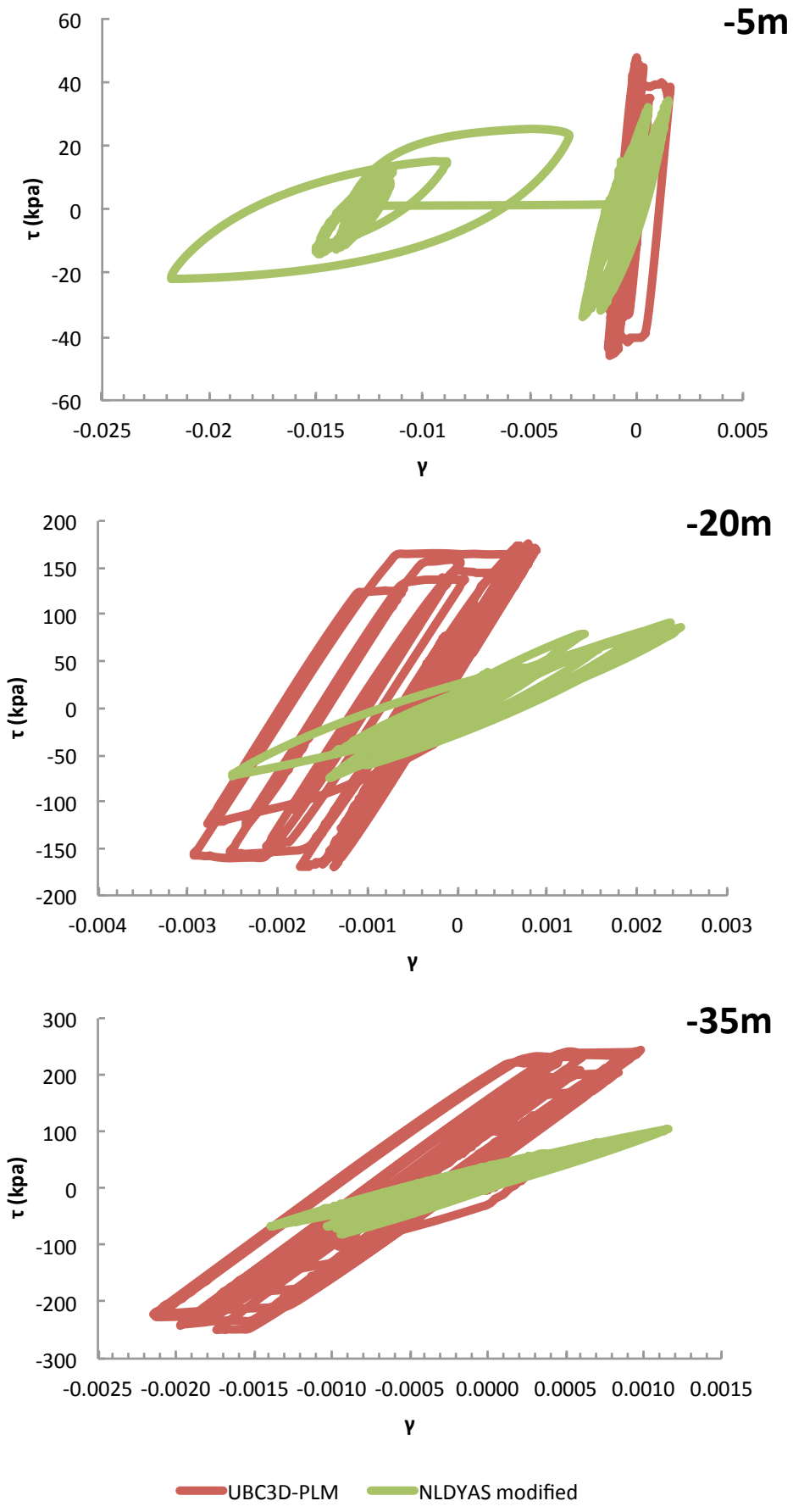

Figure 4.40 τ-γ loops. *Comparison results for the* ***Exponential Soil profile*** *between* ***"UBC3D-PLM"*** *code and* ***"NLDYAS-modified"*** *for the* ***Lefkada excitation*** *for 0.25g, for different depths.*

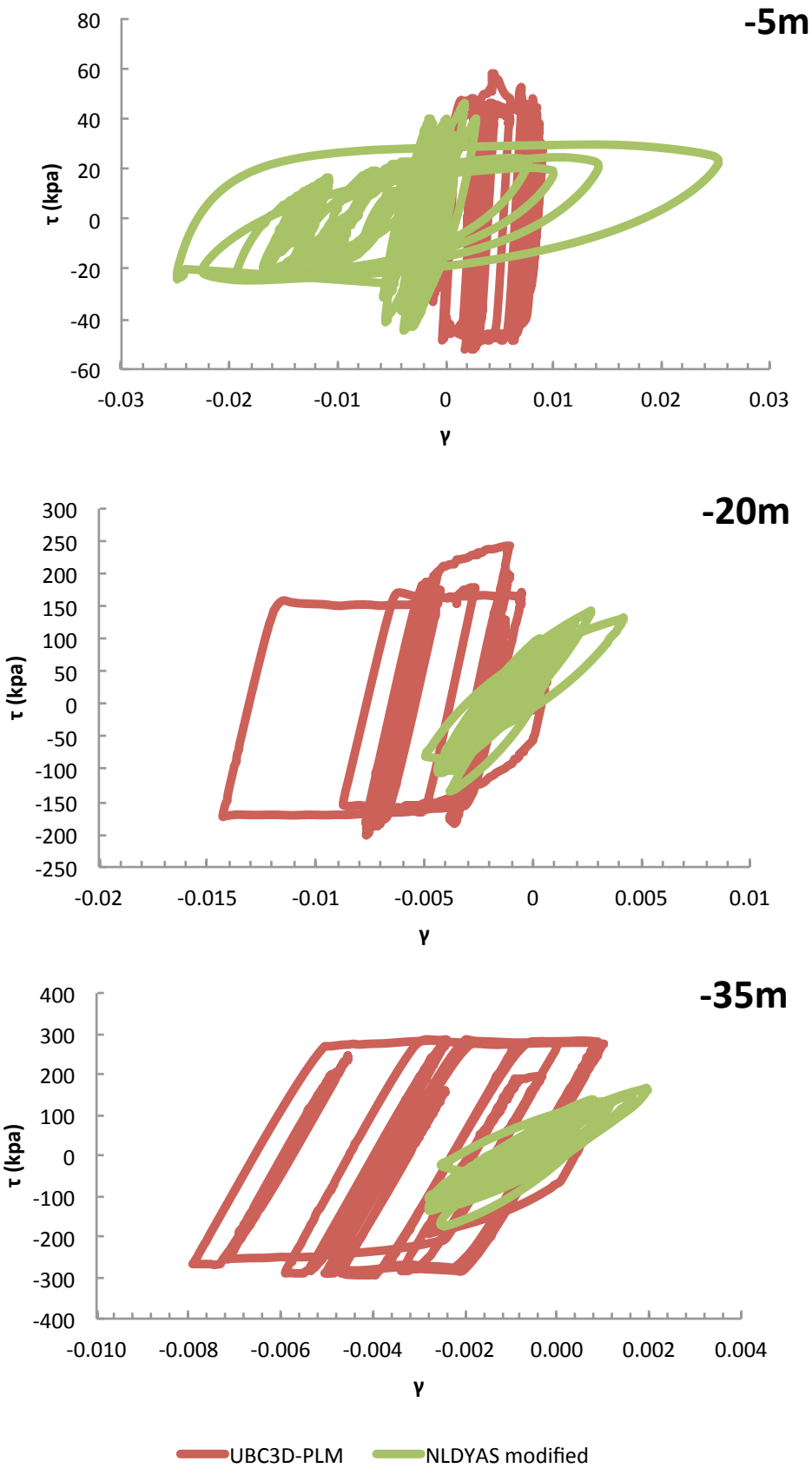

Figure 4.41 τ-γ loops. *Comparison results for the* ***Exponential Soil profile*** *between* ***"UBC3D-PLM"*** *code and* ***"NLDYAS-modified"*** *for the* ***Lefkada excitation*** *for 0.60g, for different depths.*

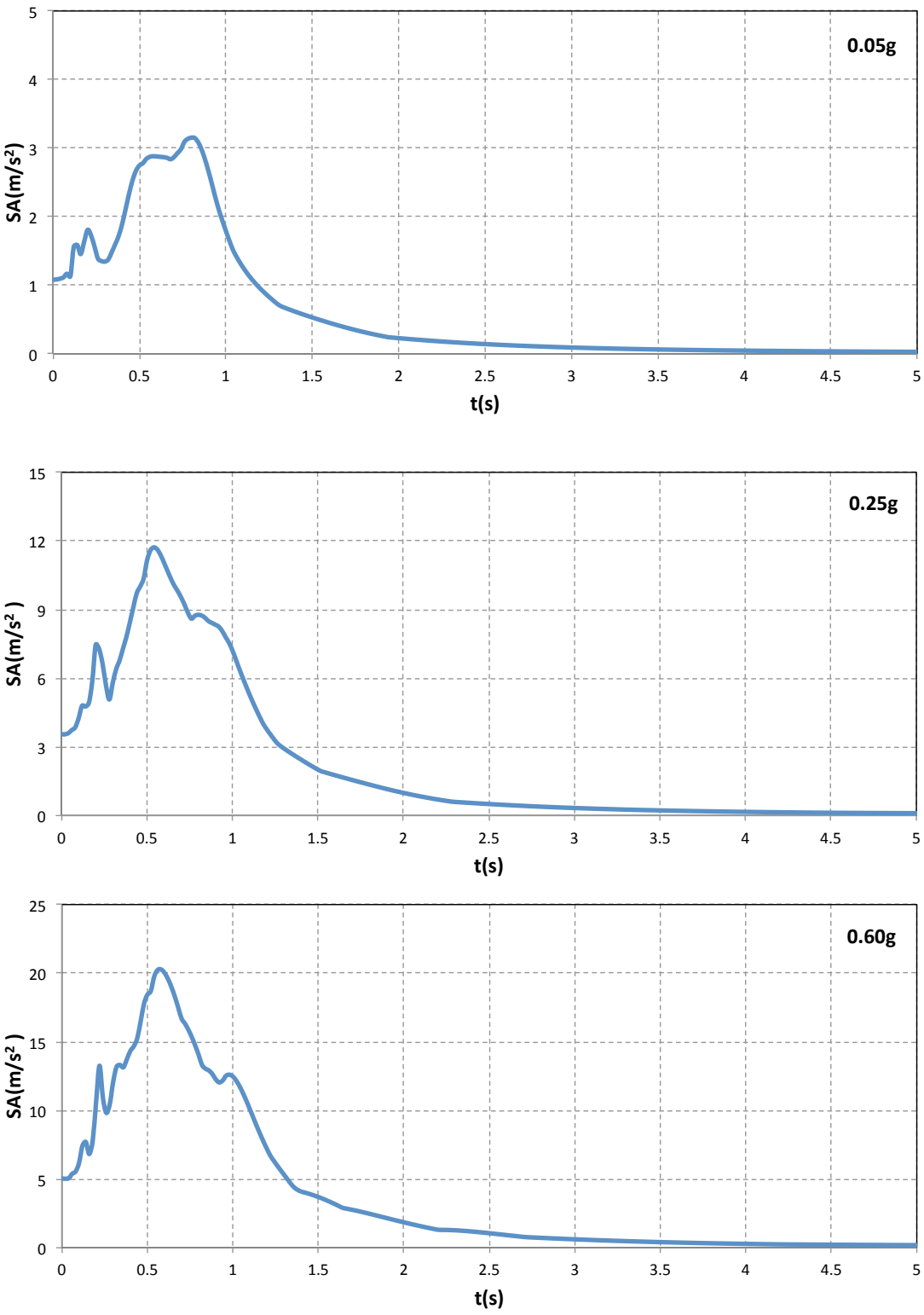

Figure 4.42 PSA Spectrums. *Surface spectrums for the* ***Layered Soil Profile*** *analysed with* ***"NLDYAS-modified"*** *for the* ***Aegion excitation*** *for 0.05g, 0.25g and 0.60g*

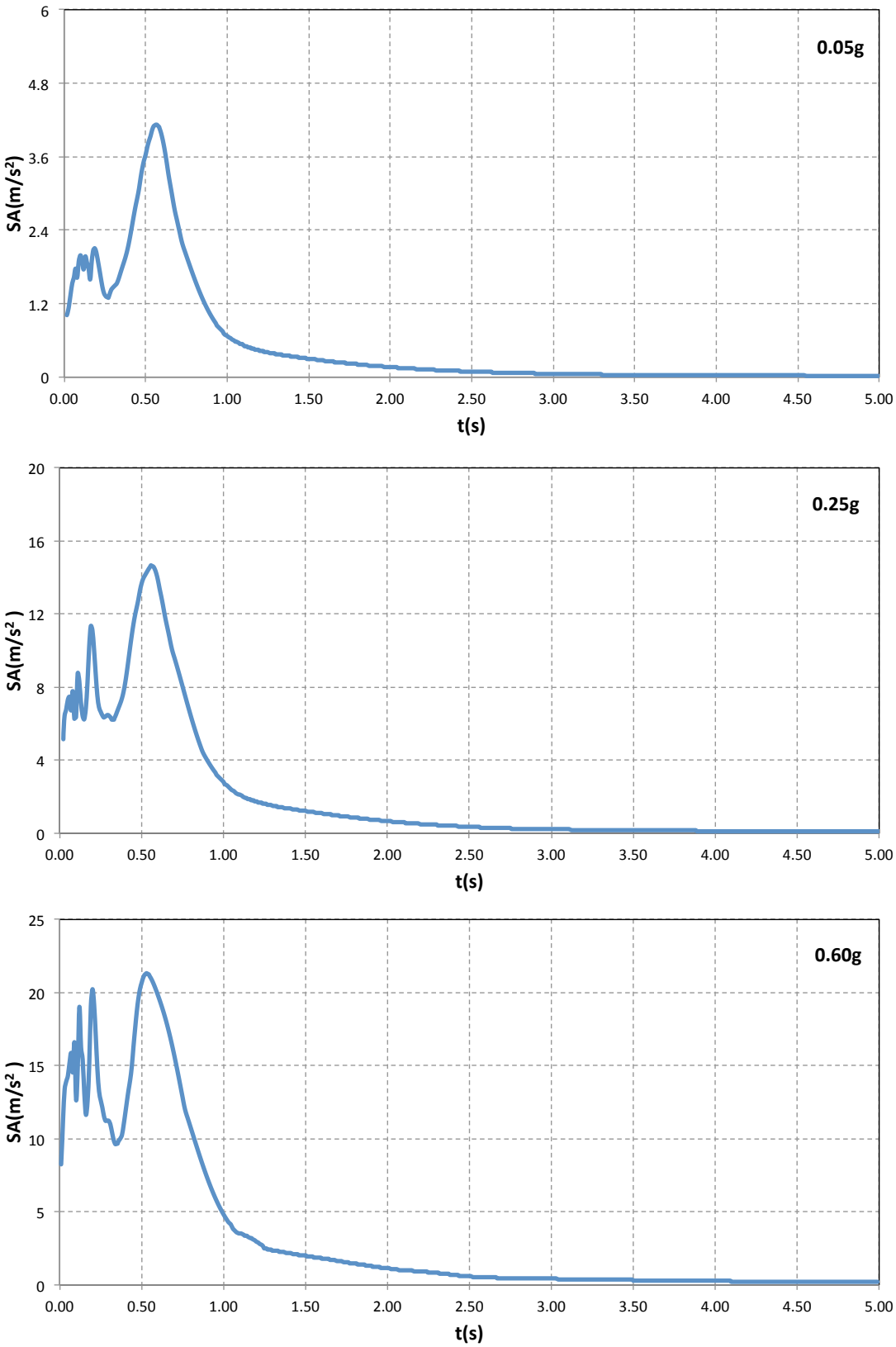

Figure 4.43 PSA Spectrums. *Surface spectrums for the* ***Layered Soil Profile*** *analysed with* ***"UBC3D-PLM"*** *for the* ***Aegion excitation*** *for 0.05g, 0.25g and 0.60g*

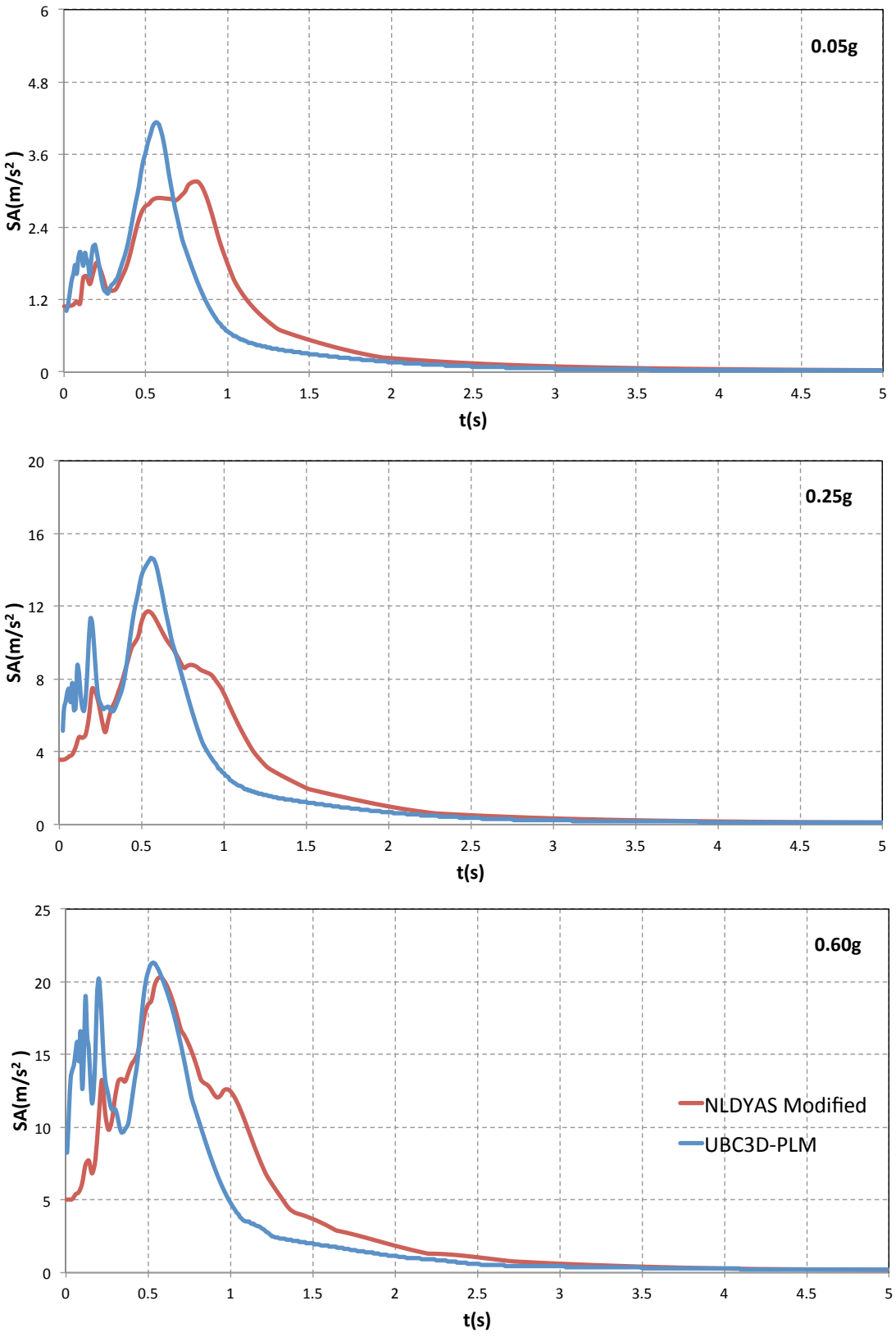

Figure 4.44 PSA Spectrums Comparison. *Comparison between the surface spectrums spectrums for the* ***Layered Soil Profile*** *analysed with* ***"UBC3D-PLM"*** *and* ***"NLDYAS modified"*** *for the* ***Aegion***

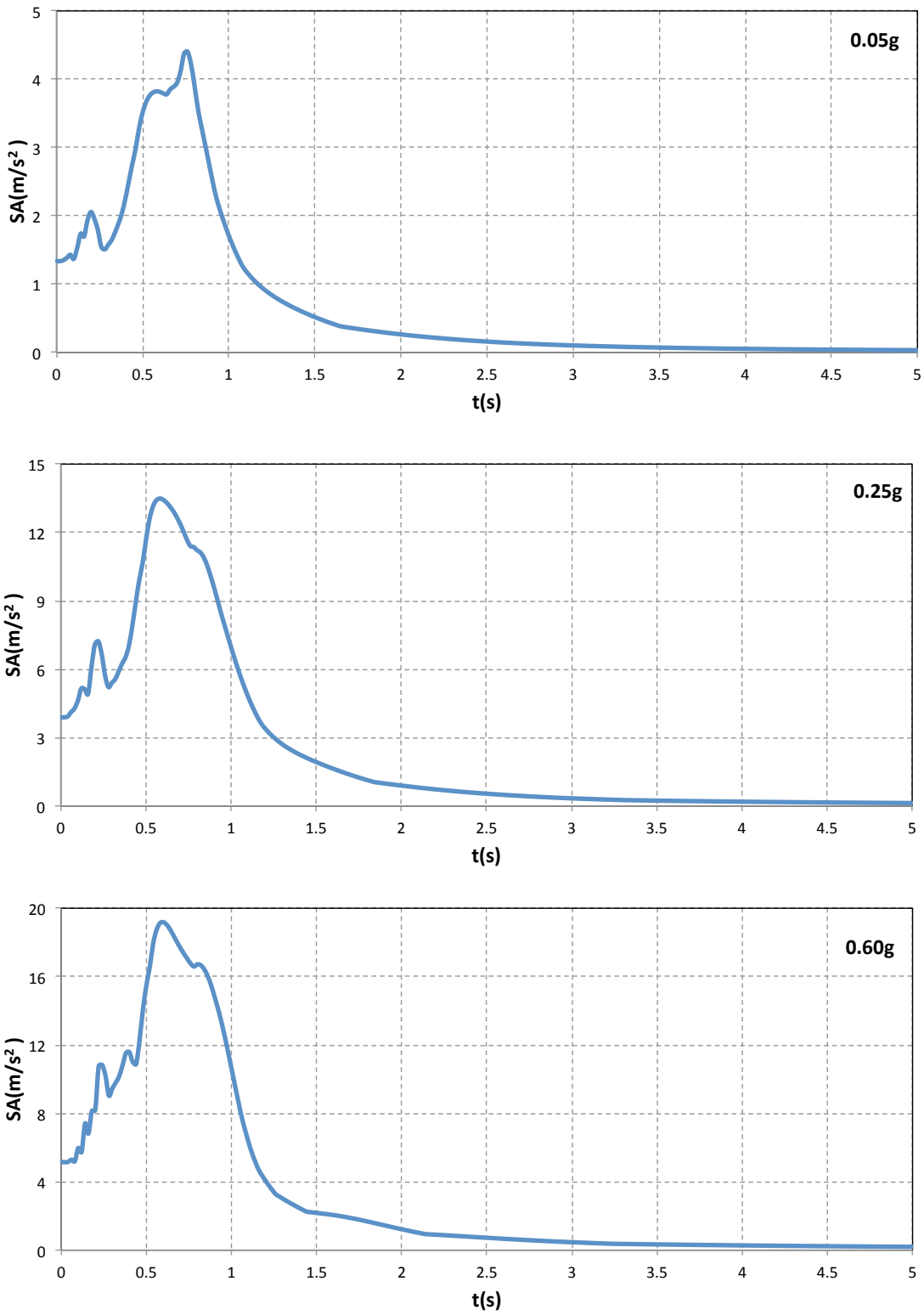

Figure 4.45 PSA Spectrums. *Surface spectrums for the* ***Exponential Soil Profile*** *analysed with* ***"NLDYAS-modified"*** *for the* ***Aegion excitation*** *for 0.05g, 0.25g and 0.60g*

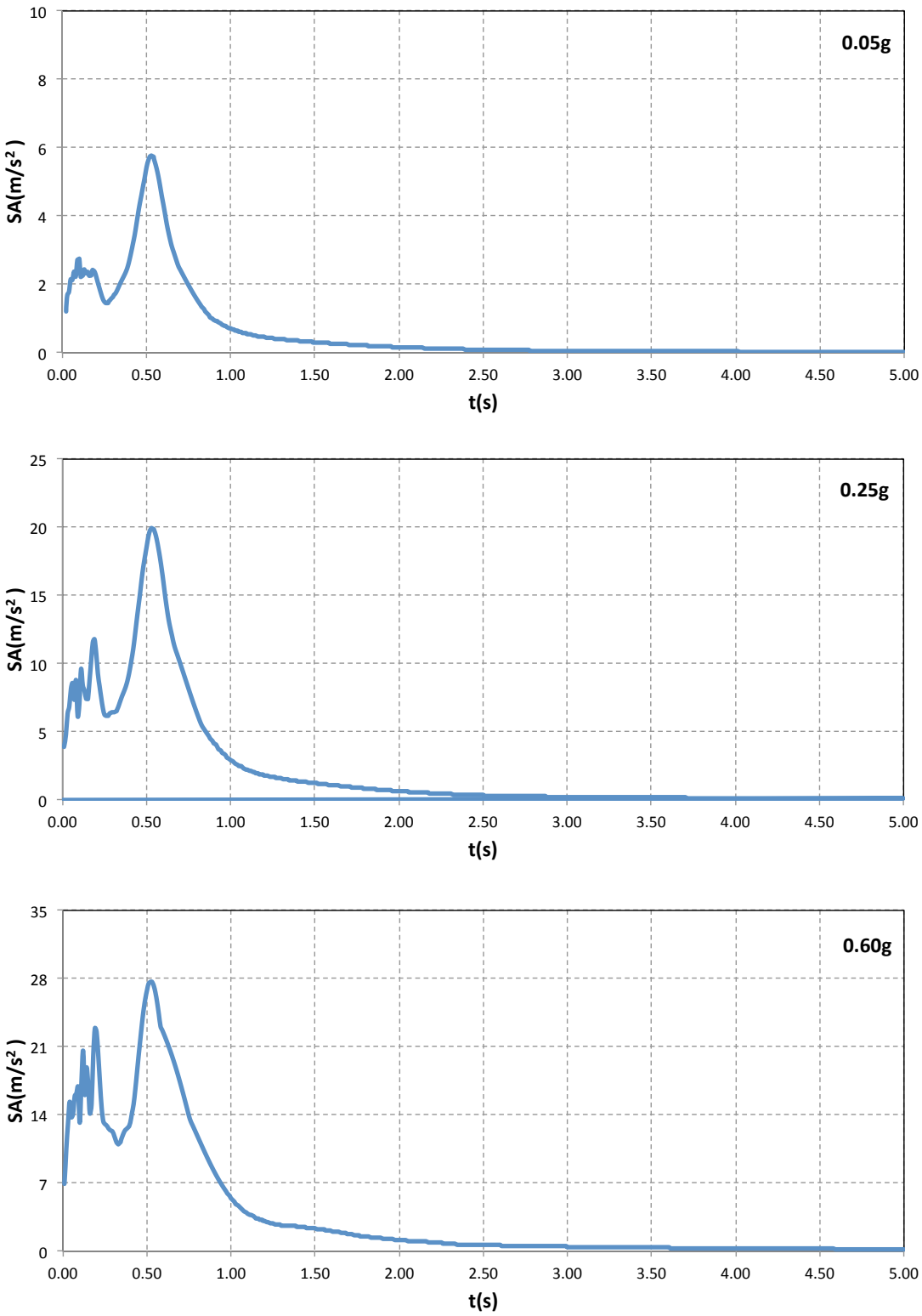

Figure 4.46 PSA Spectrums. *Surface spectrums for the* ***Exponential Soil Profile*** *analysed with* ***"UBC3D-PLM"*** *for the* ***Aegion excitation*** *for 0.05g, 0.25g and 0.60g*

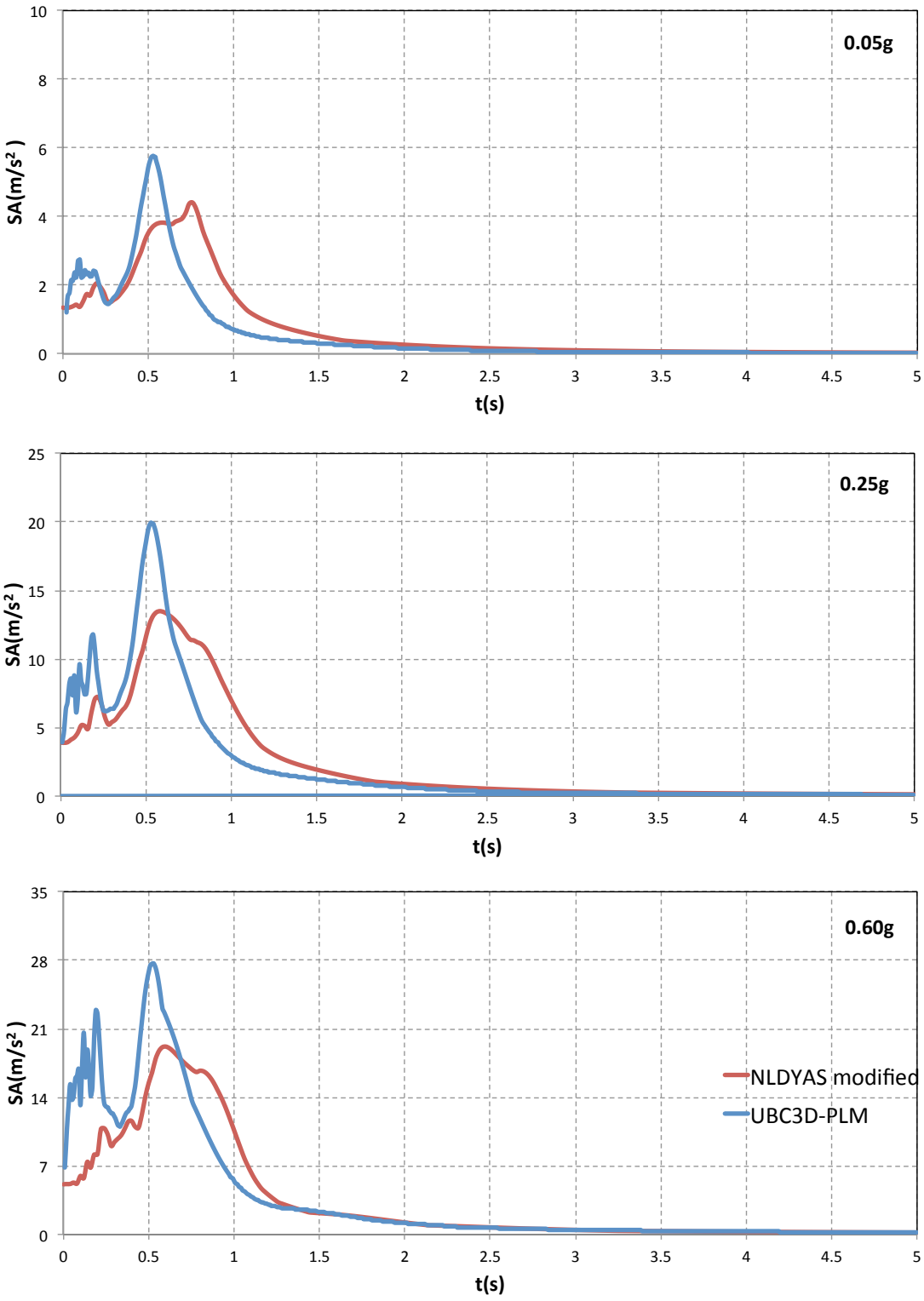

Figure 4.47 PSA Spectrums Comparison. *Comparison between the surface spectrums spectrums for the* ***Exponential Soil Profile*** *analysed with* ***"UBC3D-PLM"*** *and* ***"NLDYAS modified"*** *for the* ***Aegion excitation*** *for 0.05g, 0.25g and 0.60g*

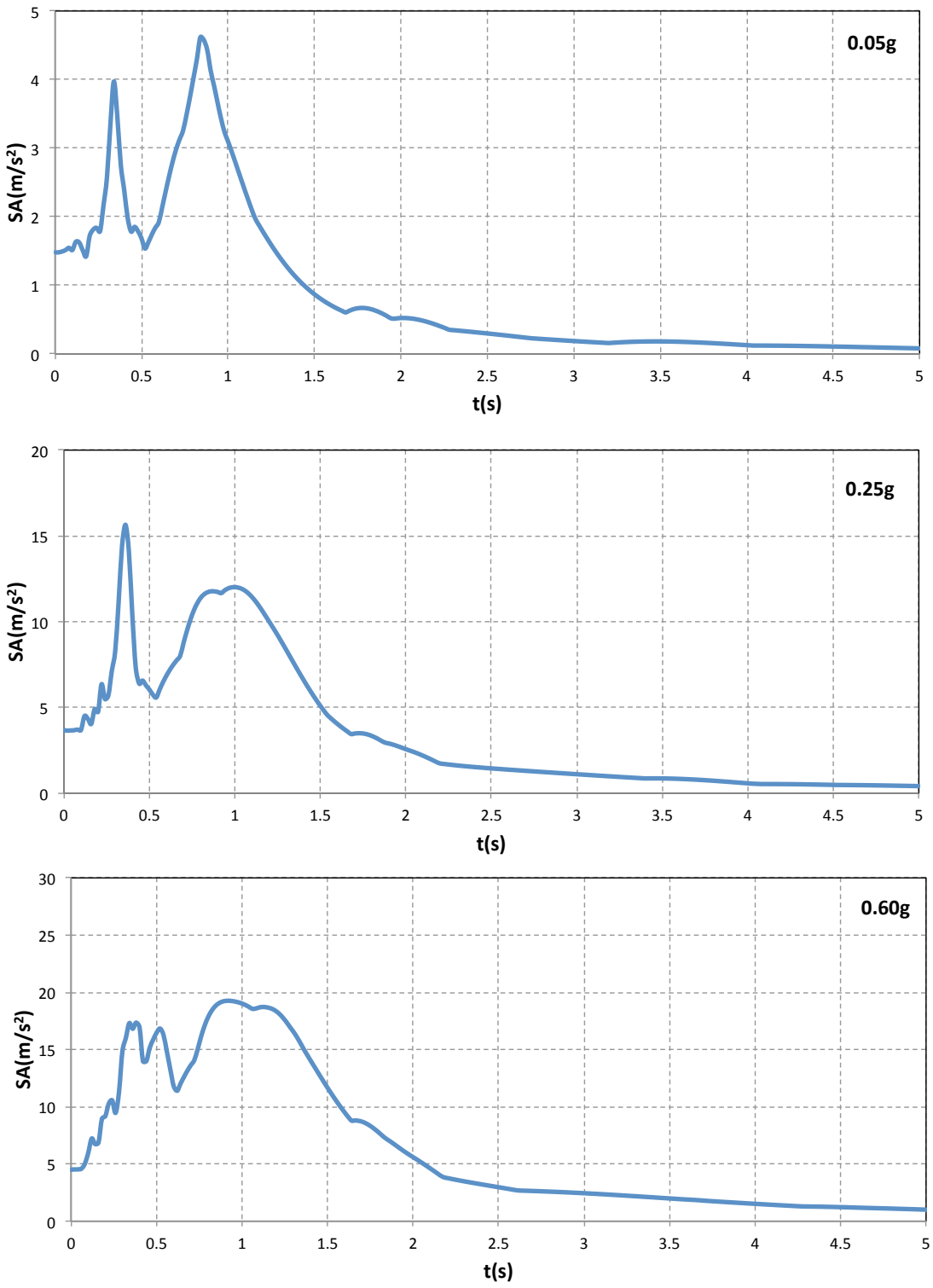

Figure 4.48 PSA Spectrums. *Surface spectrums for the* ***Layered Soil Profile*** *analysed with* ***"NLDYAS-modified"*** *for the* ***Kobe excitation*** *for 0.05g, 0.25g and 0.60g*

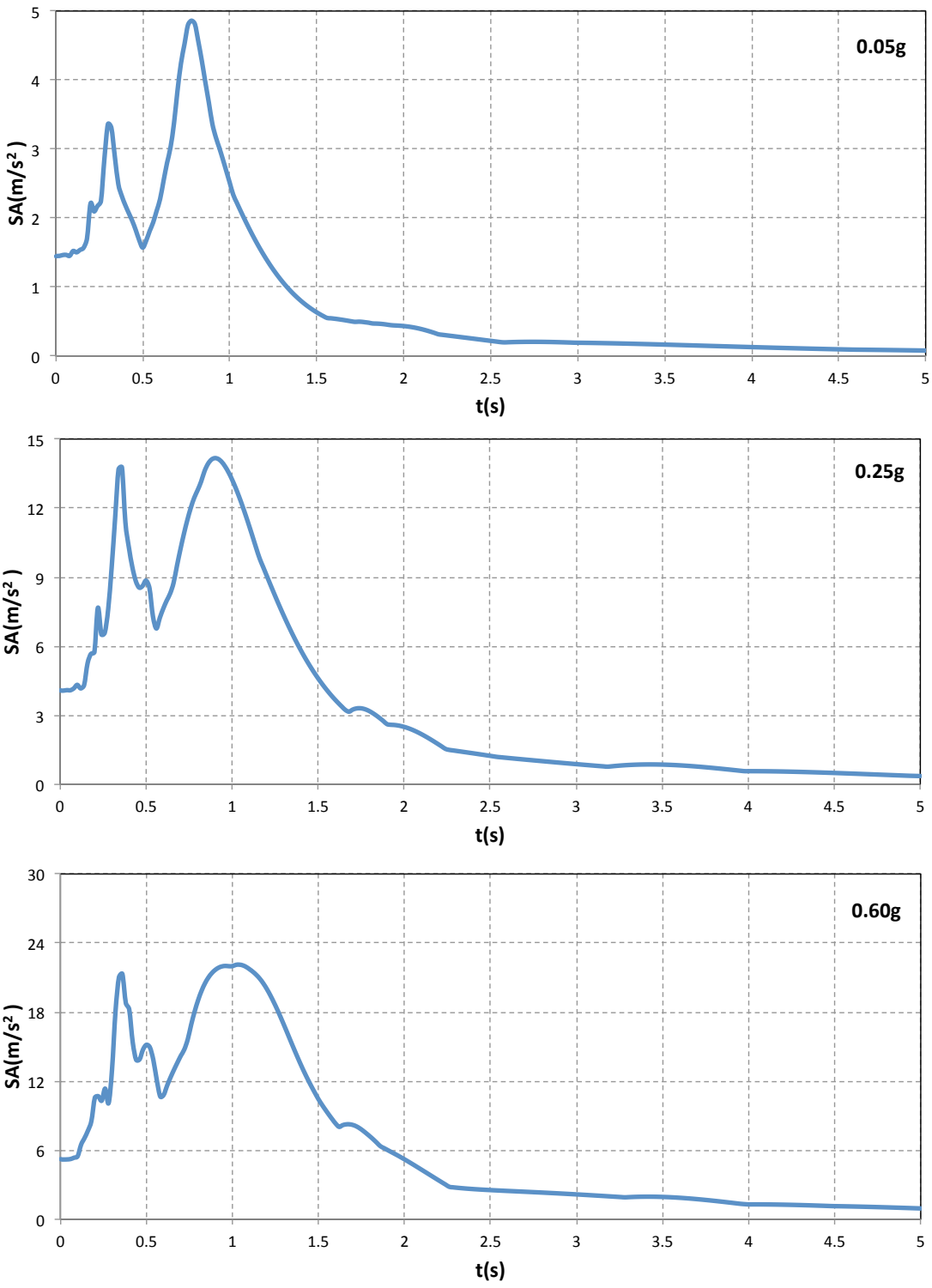

Figure 4.49 PSA Spectrums. *Surface spectrums for the* ***Exponential Soil Profile*** *analysed with* ***"NLDYAS-modified"*** *for the* ***Kobe excitation*** *for 0.05g, 0.25g and 0.60g*

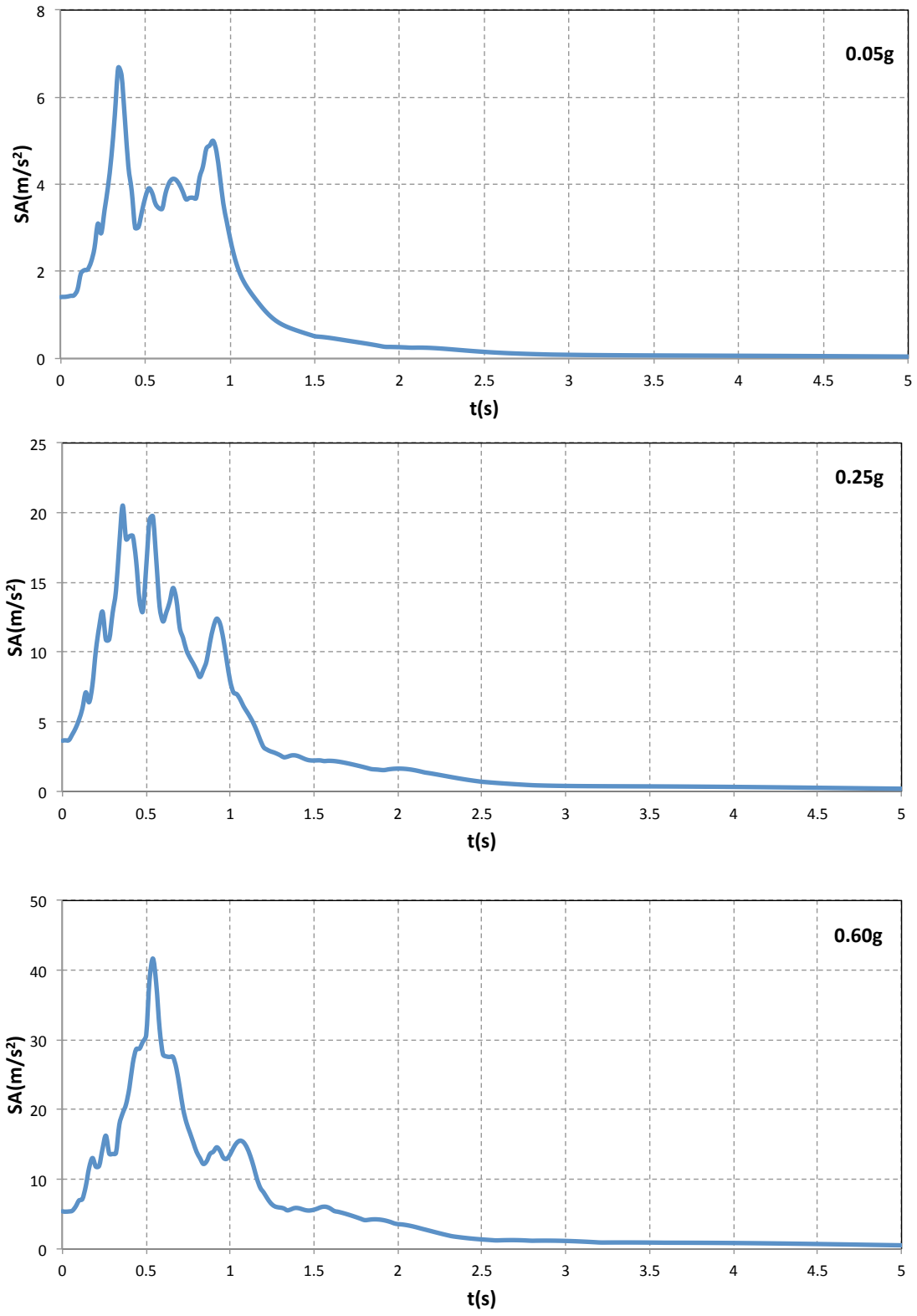

Figure 4.50 PSA Spectrums. *Surface spectrums for the* ***Layered Soil Profile*** *analysed with* ***"NLDYAS-modified"*** *for the* ***Lefkada excitation*** *for 0.05g, 0.25g and 0.60g*

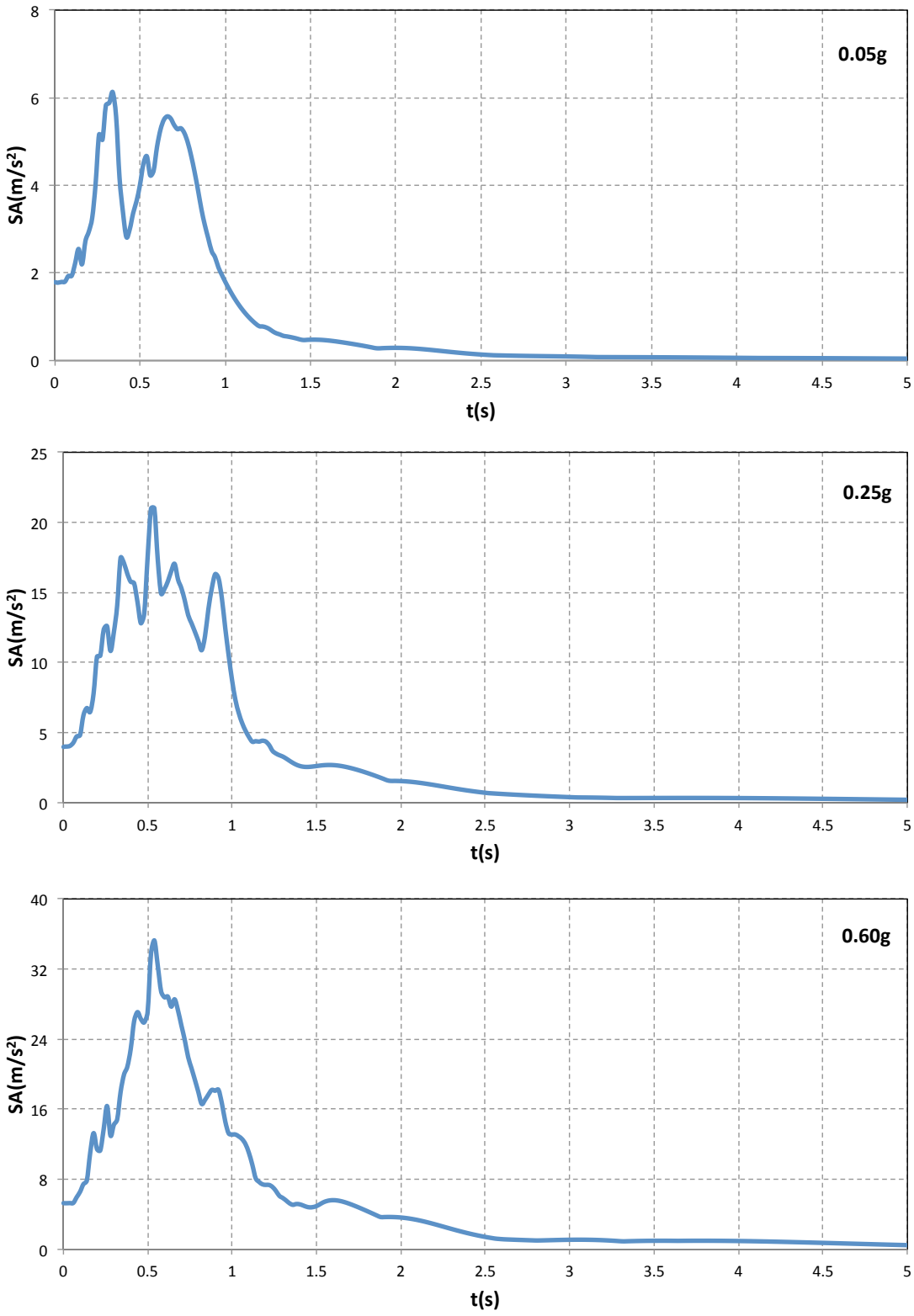

Figure 4.51 PSA Spectrums. *Surface spectrums for the* ***Exponential Soil Profile*** *analysed with* ***"NLDYAS-modified"*** *for the* ***Lefkada excitation*** *for 0.05g, 0.25g and 0.60g*

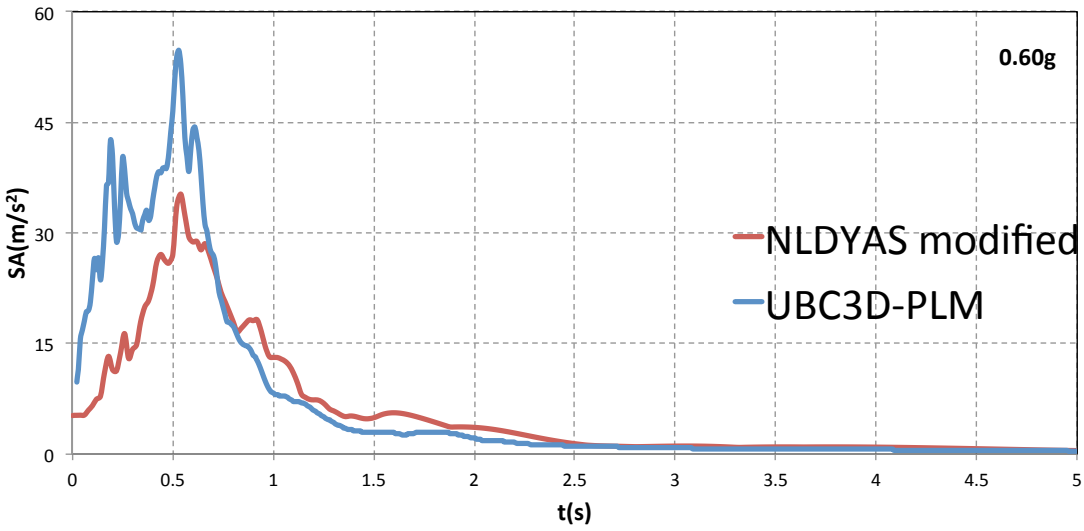

Figure 4.52 PSA Spectrums Comparison. *Comparison between the surface spectrums spectrums for the* ***Exponential Soil Profile*** *analysed with* ***"UBC3D-PLM"*** *and* ***"NLDYAS modified"*** *for the* ***Lefkada excitation*** *for 0.60g*

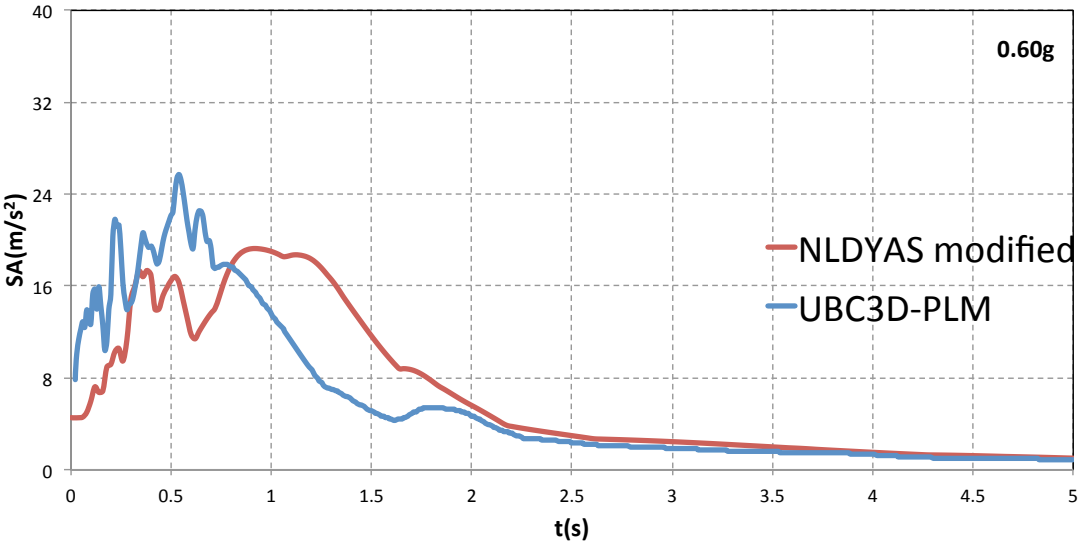

Figure 4.53 PSA Spectrums Comparison. *Comparison between the surface spectrums spectrums for the* ***Layered Soil Profile*** *analysed with* ***"UBC3D-PLM"*** *and* ***"NLDYAS modified"*** *for the* ***Kobe excitation*** *for 0.60g*

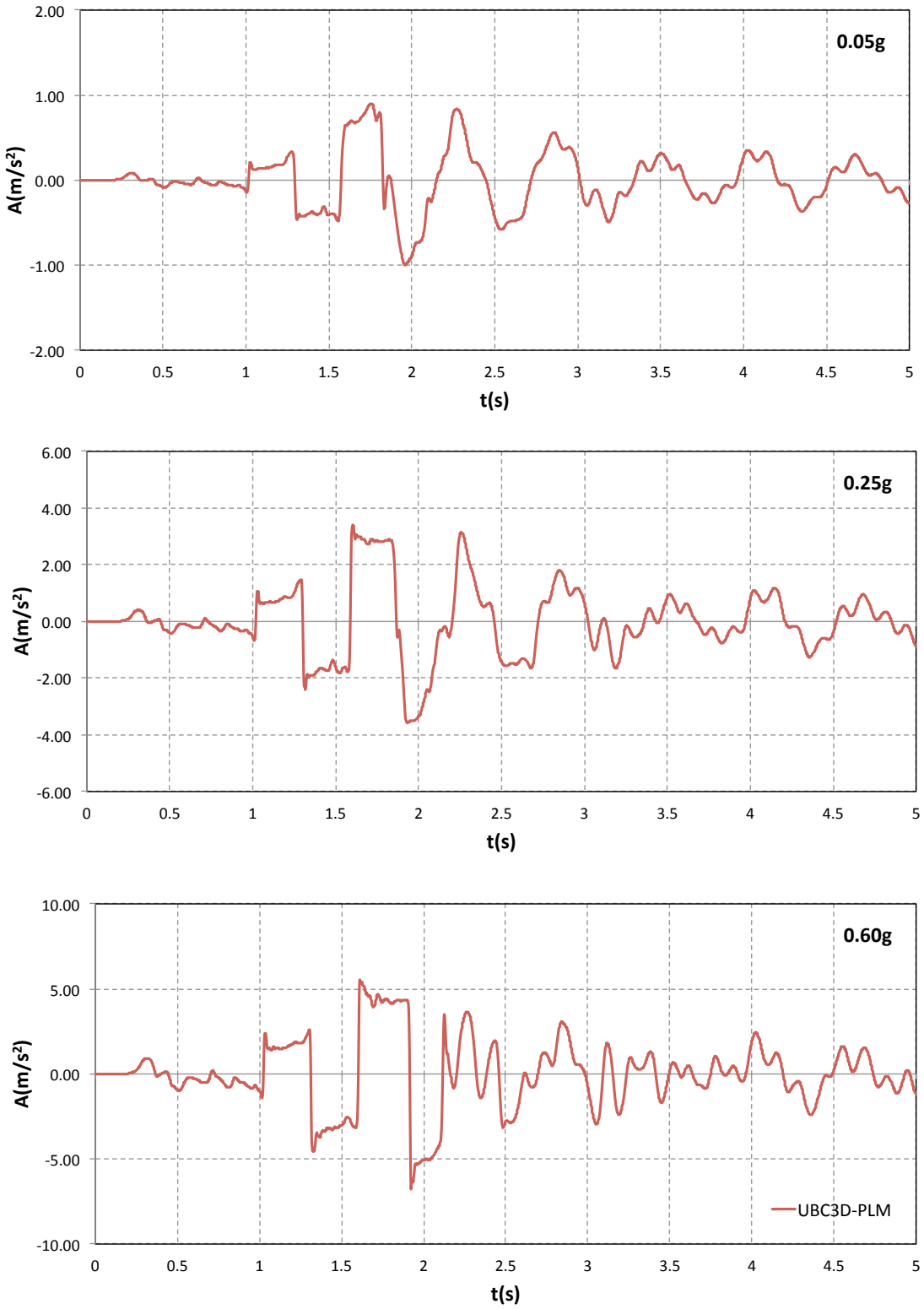

Figure 4.54 Accellerographs. *Accellerographs recorded on the surface of the* ***Layered Soil Profile*** *analysed with* ***"UBC3D-PLM"*** *with the Aegion* ***excitation*** *for 0.05g 0.25g 0.60g*

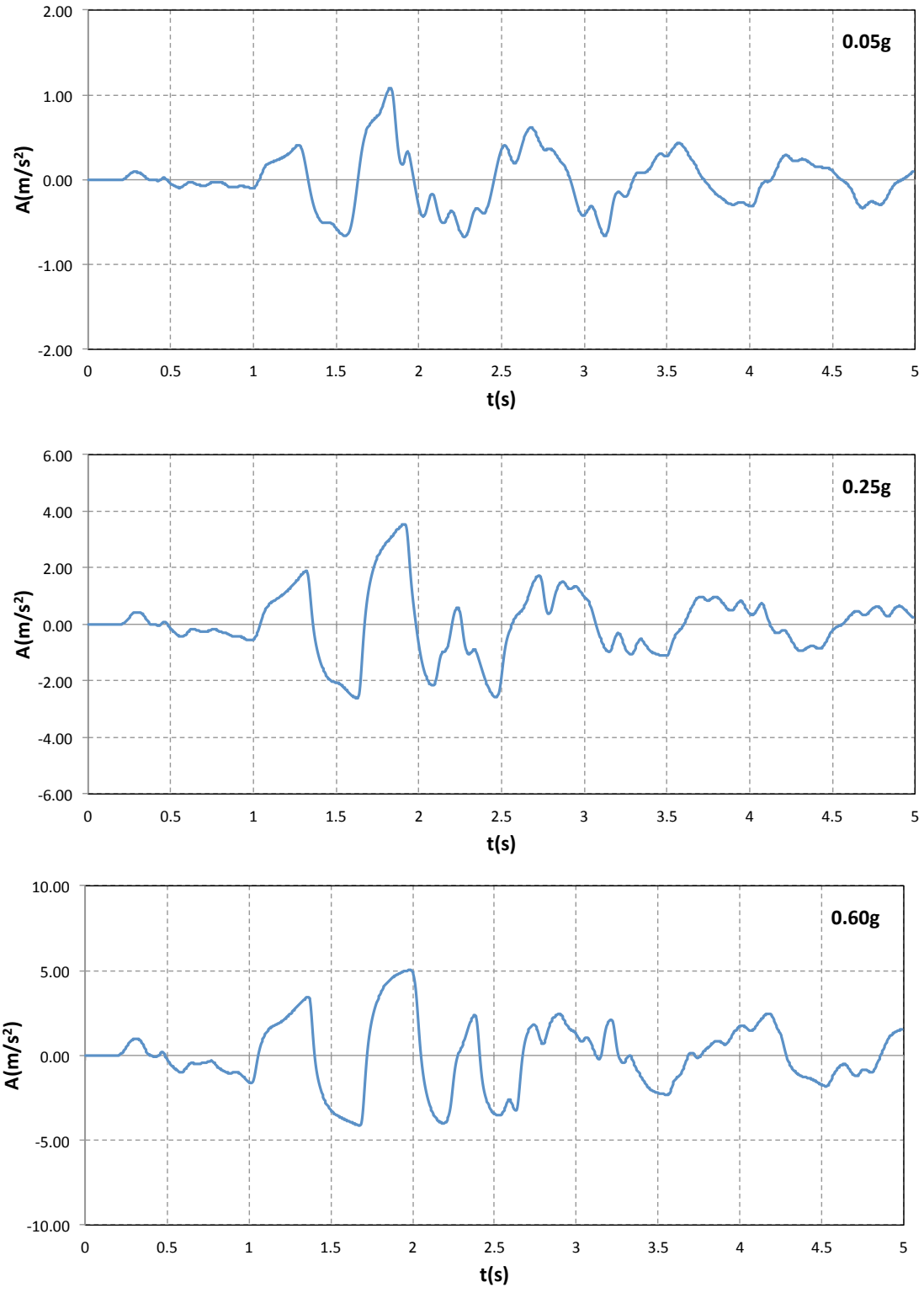

Figure 4.55 Accellerographs. *Accellerographs recorded on the surface of the* ***Layered Soil Profile*** *analysed with* ***"NLDYAS modified"*** *with the Aegion* ***excitation*** *for 0.05g 0.25g 0.60g*

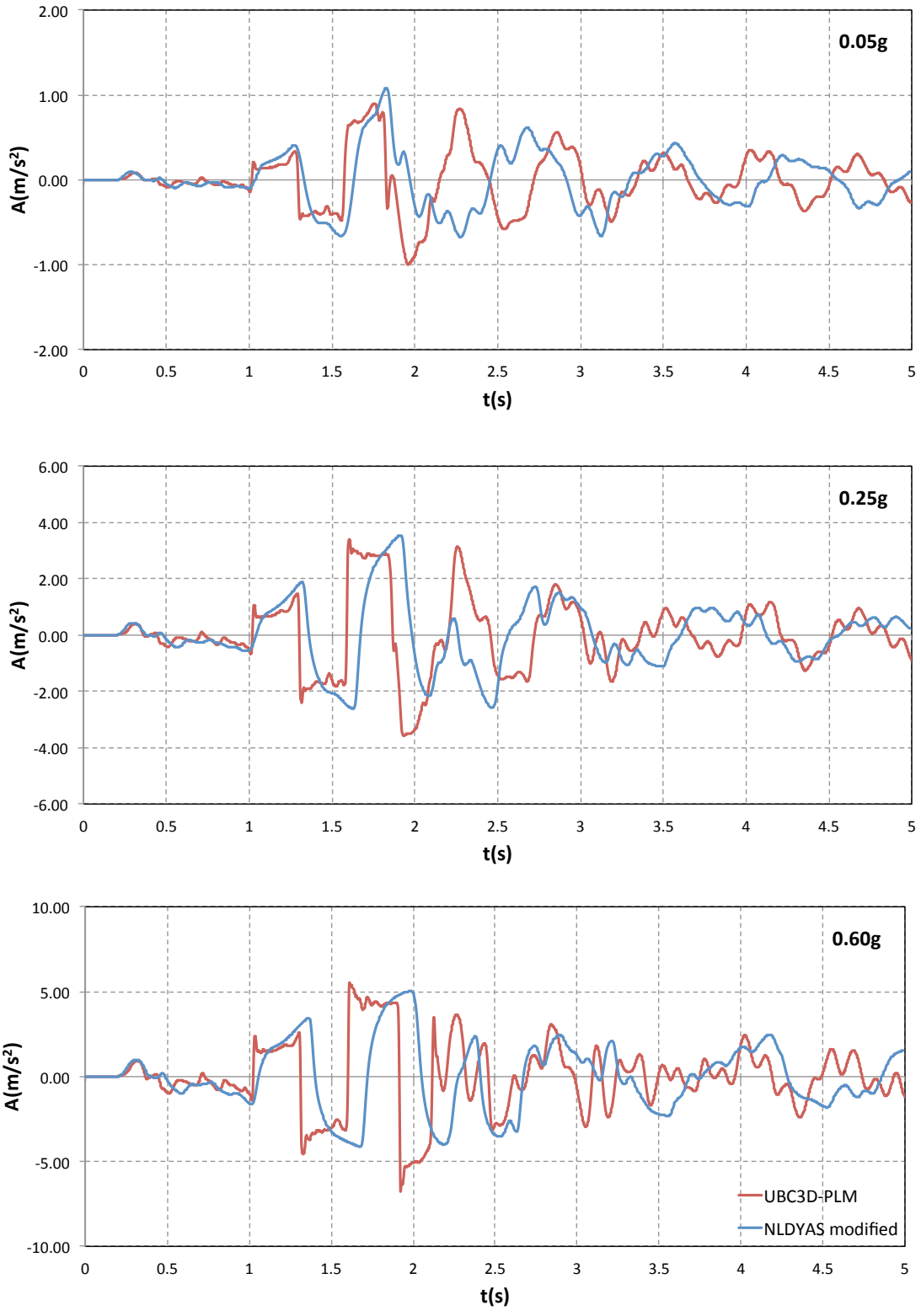

Figure 4.56 Accellerographs Comparison. *Accellerographs recorded on the surface of the* ***Layered Soil Profile*** *comparison analysed with* ***"NLDYAS modified" and "UBC3D-PLM"*** *with the Aegion* ***excitation*** *for 0.05g 0.25g 0.60g*

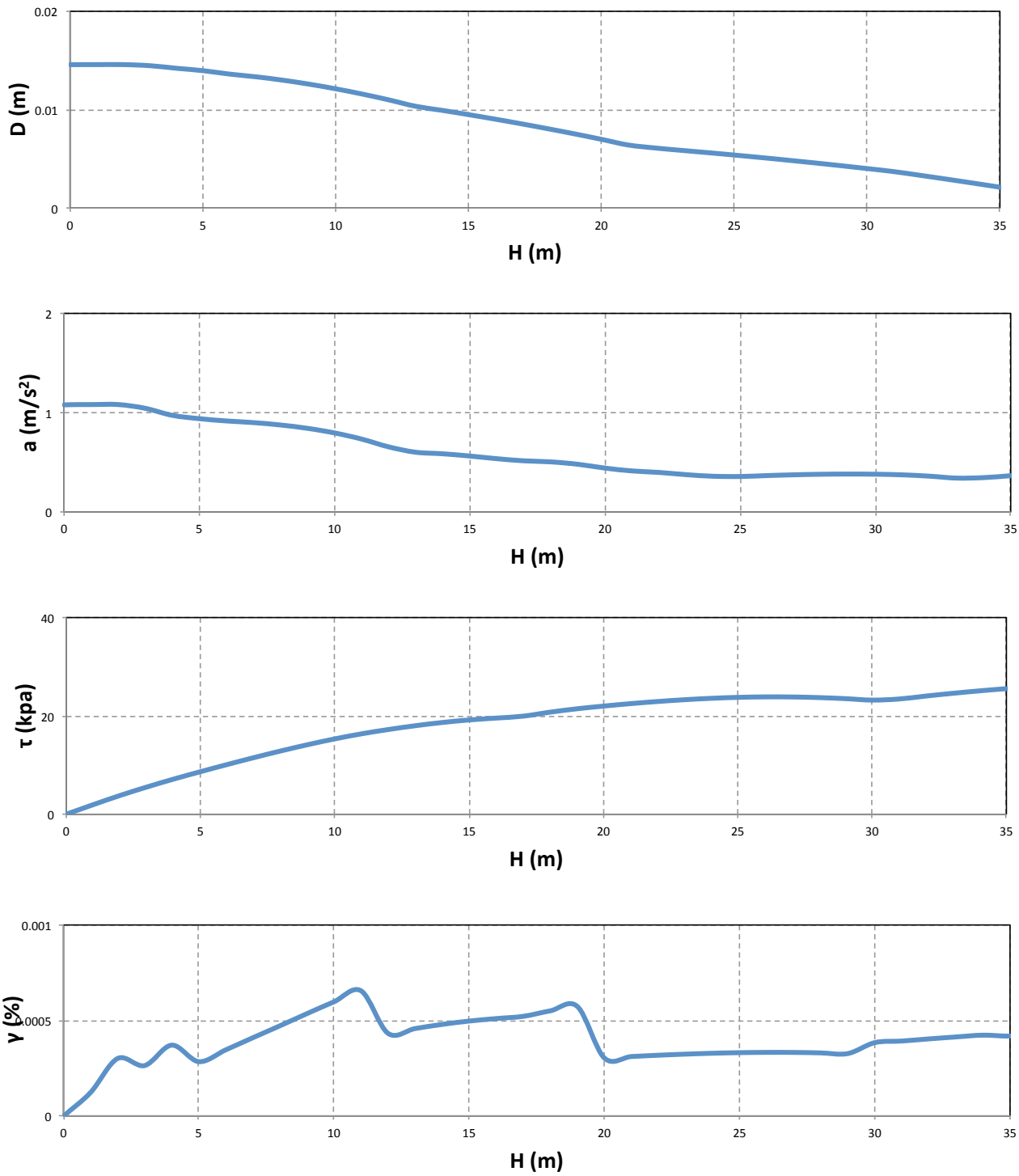

Figure 4.57 Maximums. *Charts featuring the maximum displacement, accelleration, stress and strain of the* ***Layered Soil Profile*** *analysed with* ***"NLDYAS modified"*** *with the Aegion* ***excitation*** *for 0.05g*

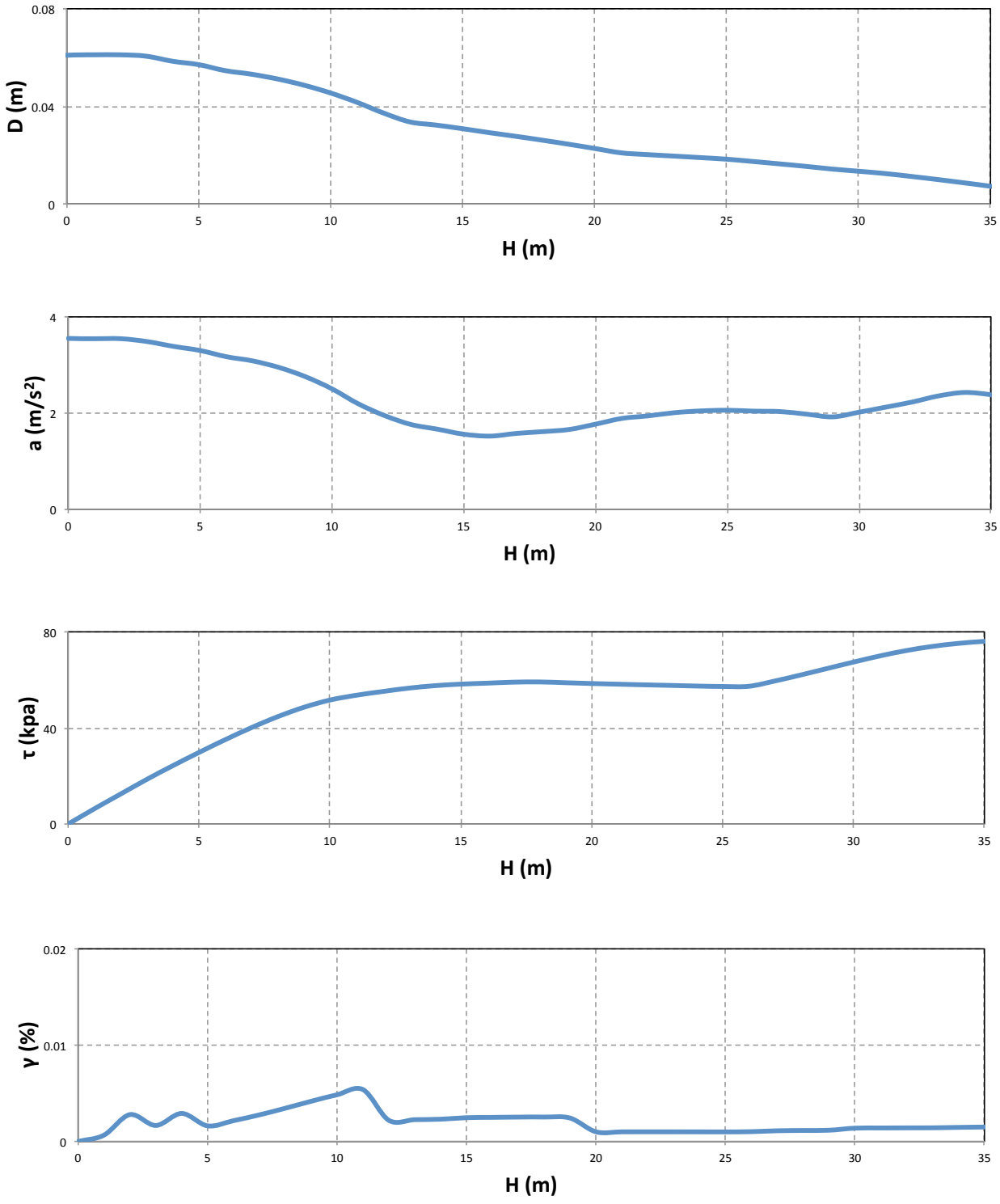

Figure 4.58 Maximums. *Charts featuring the maximum displacement, accelleration, stress and strain of the* ***Layered Soil Profile*** *analysed with* ***"NLDYAS modified"*** *with the Aegion* ***excitation*** *for 0.25g*

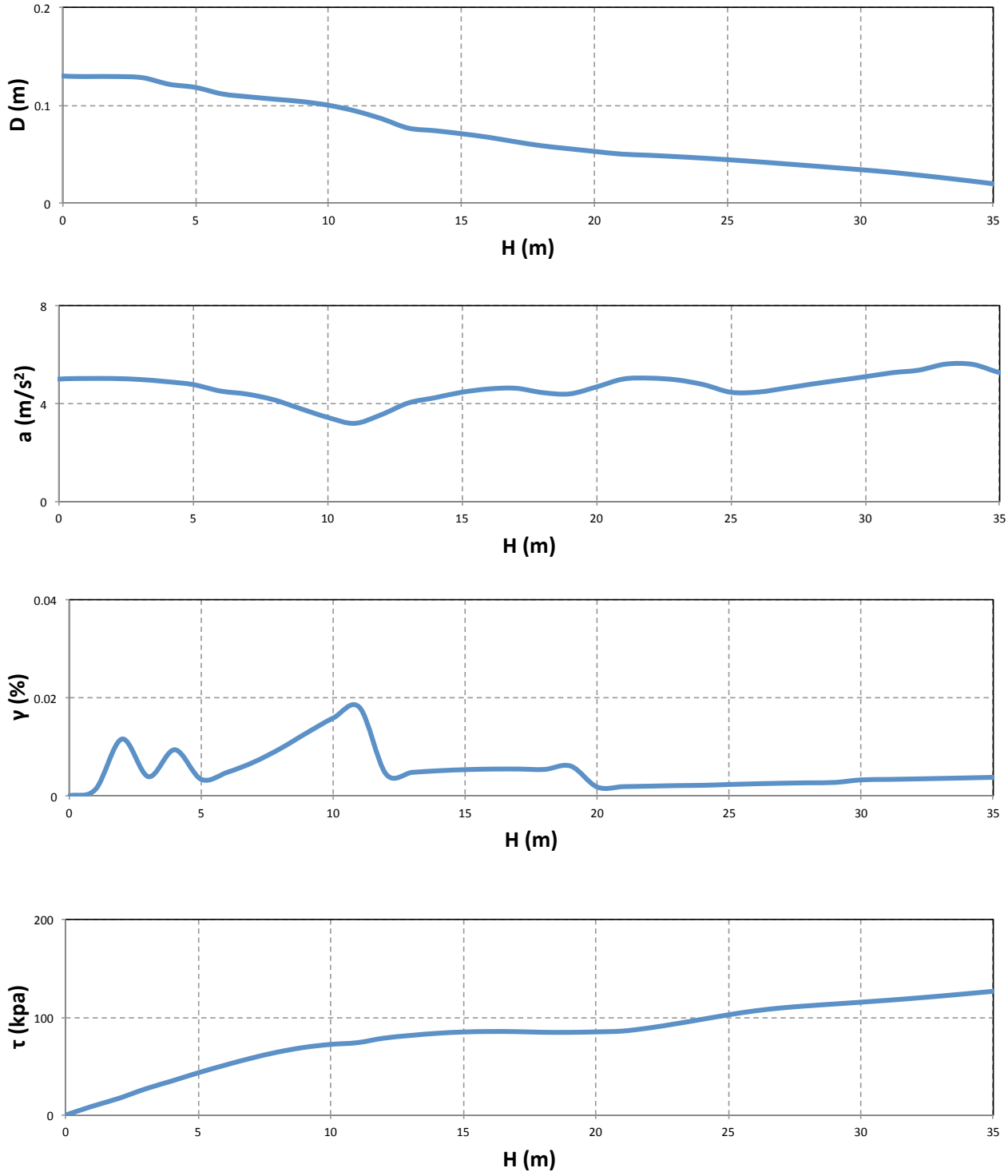

Figure 4.59 Maximums. *Charts featuring the maximum displacement, accelleration, stress and strain of the* ***Layered Soil Profile*** *analysed with* ***"NLDYAS modified"*** *with the Aegion* ***excitation*** *for 0.60g*

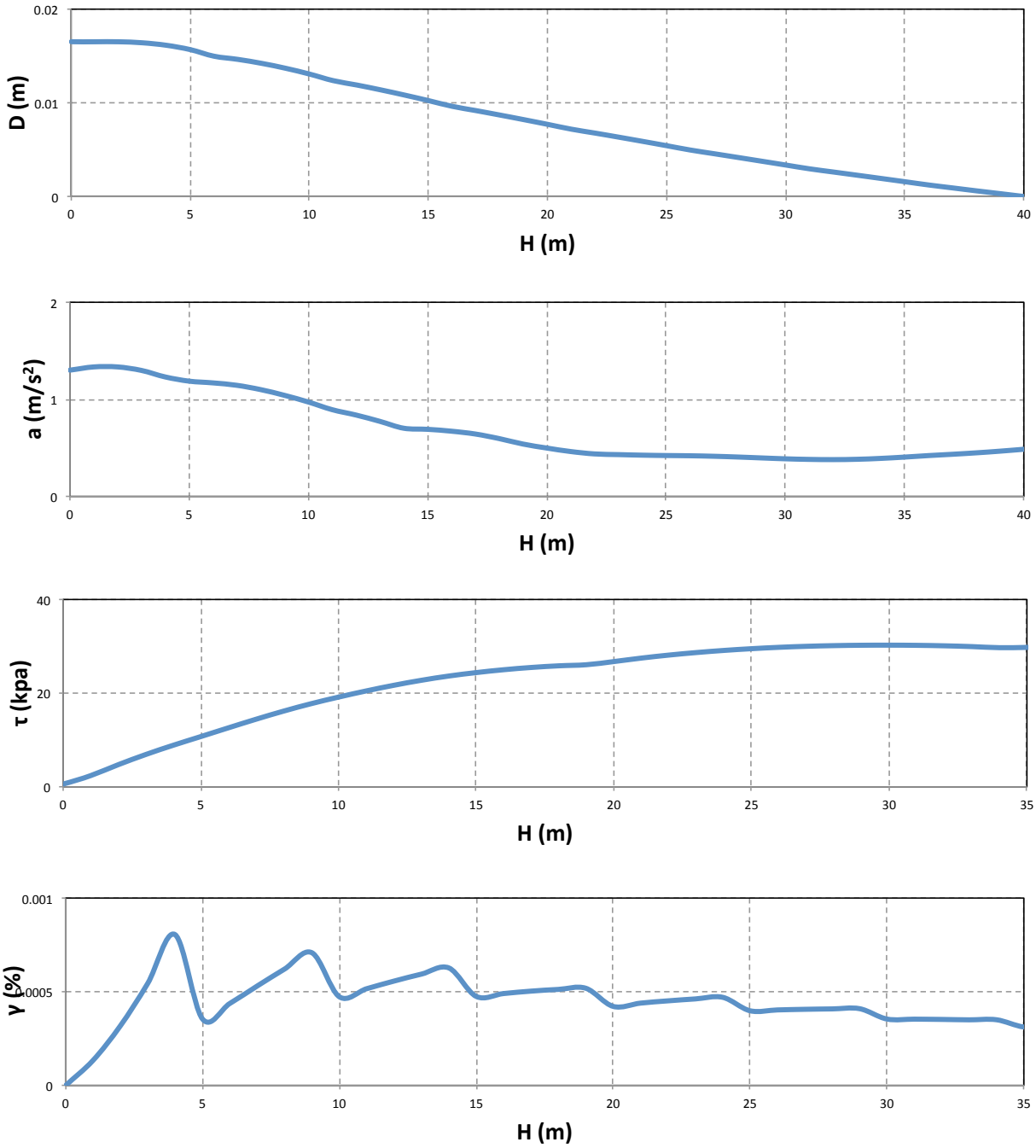

Figure 4.60 Maximums. *Charts featuring the maximum displacement, accelleration, stress and strain of the* ***Exponential Soil Profile*** *analysed with* ***"NLDYAS modified"*** *with the Aegion* ***excitation*** *for 0.05g*

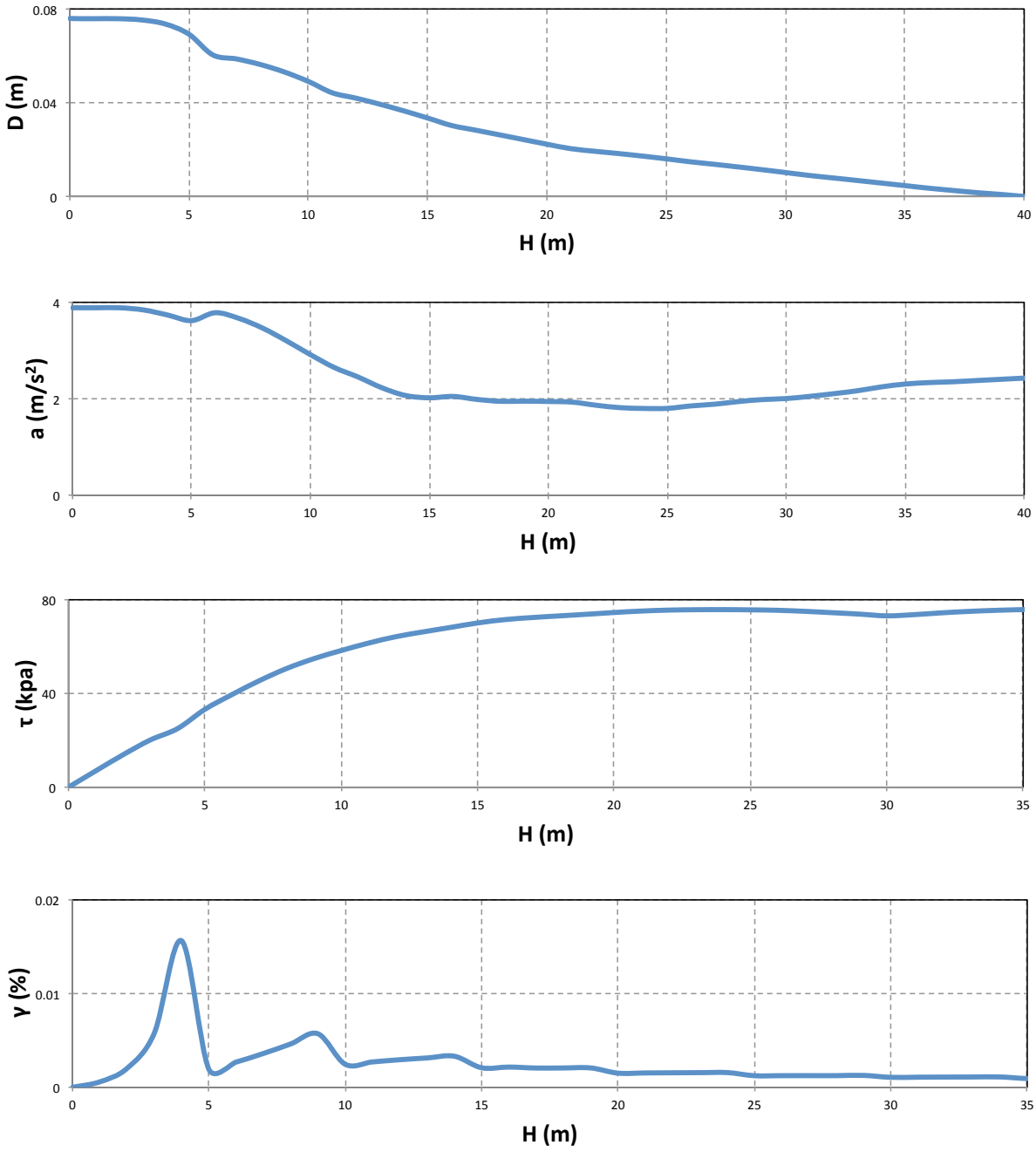

Figure 4.61 Maximums. *Charts featuring the maximum displacement, accelleration, stress and strain of the* ***Exponential Soil Profile*** *analysed with* ***"NLDYAS modified"*** *with the Aegion* ***excitation*** *for 0.25g*

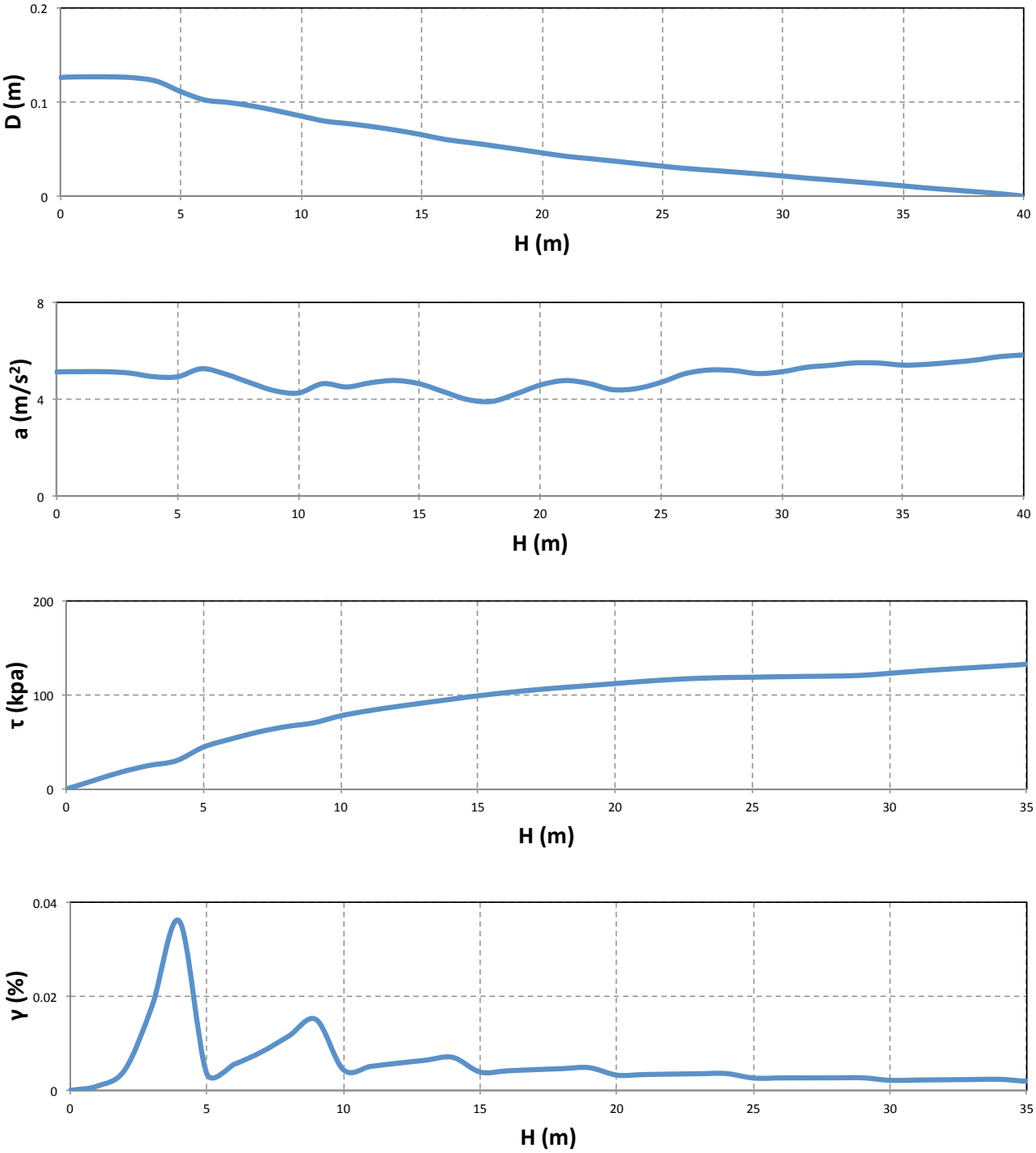

Figure 4.62 Maximums. *Charts featuring the maximum displacement, accelleration, stress and strain of the* ***Exponential Soil Profile*** *analysed with* ***"NLDYAS modified"*** *with the Aegion* ***excitation*** *for 0.60g*

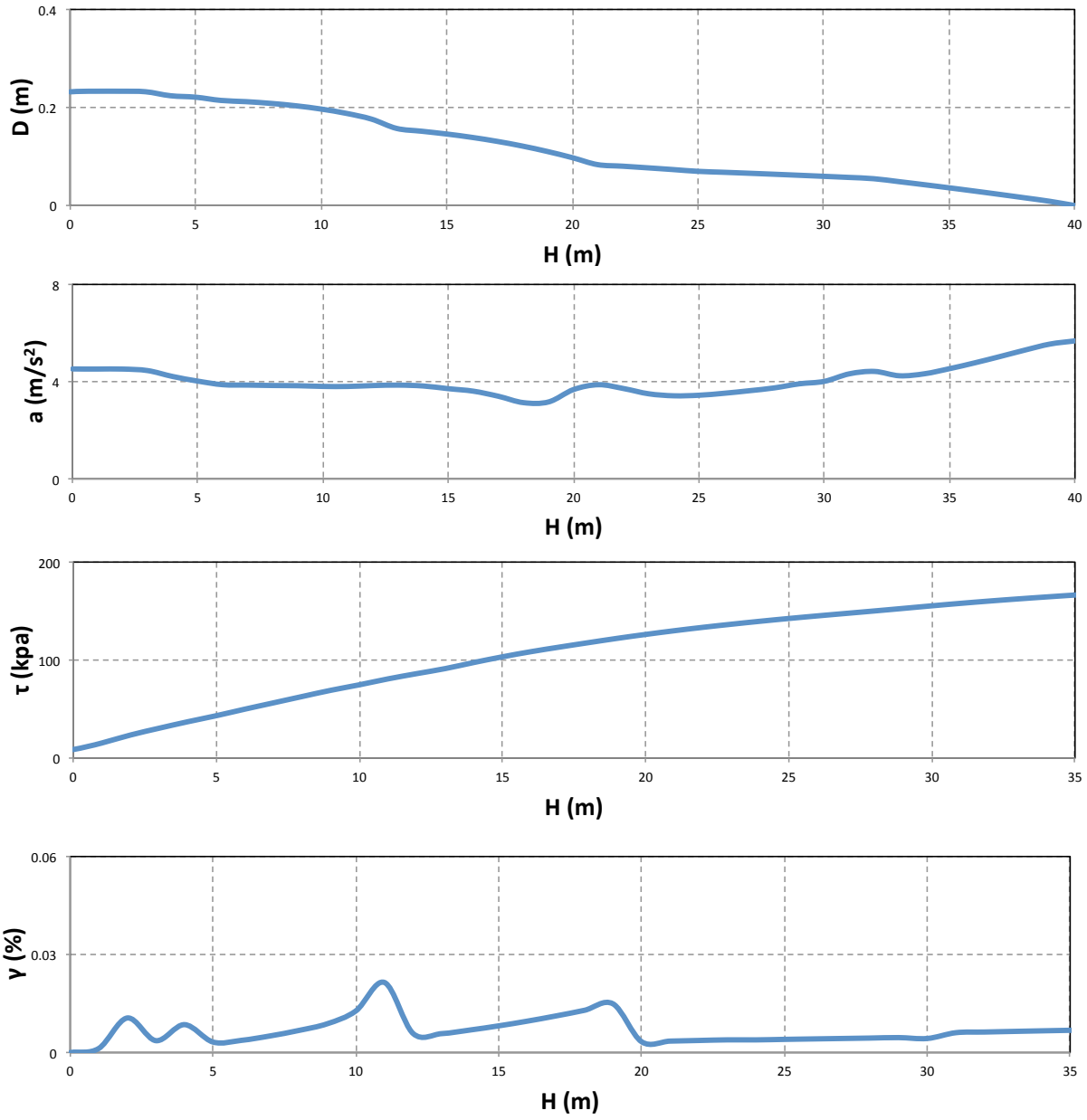

Figure 4.63 Maximums. *Charts featuring the maximum displacement, accelleration, stress and strain of the* ***Layered Soil Profile*** *analysed with* ***"NLDYAS modified"*** *with the* ***Kobe excitation*** *for 0.60g*

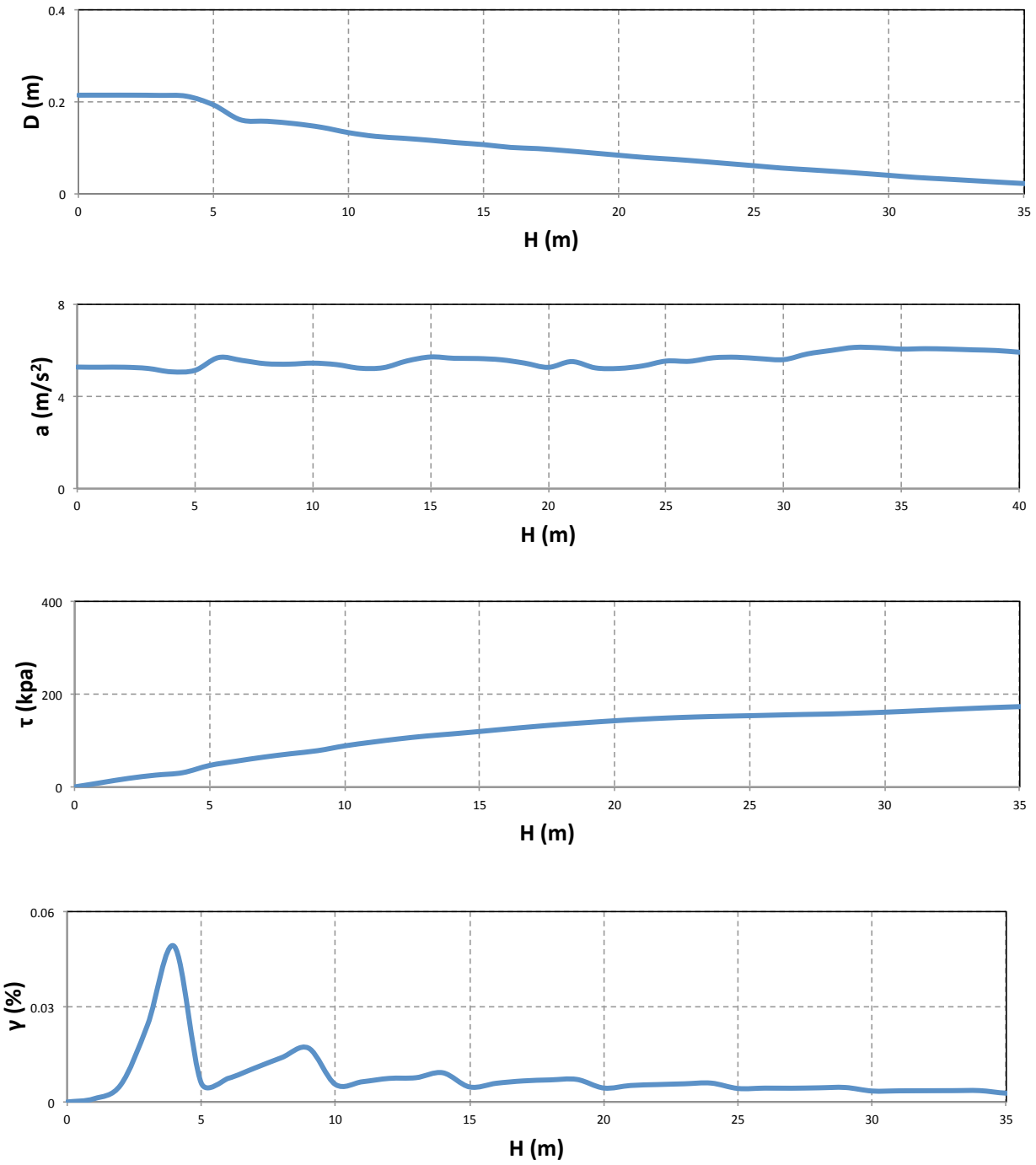

Figure 4.64 Maximums. *Charts featuring the maximum displacement, accelleration, stress and strain of the* ***Exponential Soil Profile*** *analysed with* ***"NLDYAS modified"*** *with the* ***Lefkada excitation*** *for 0.60g*

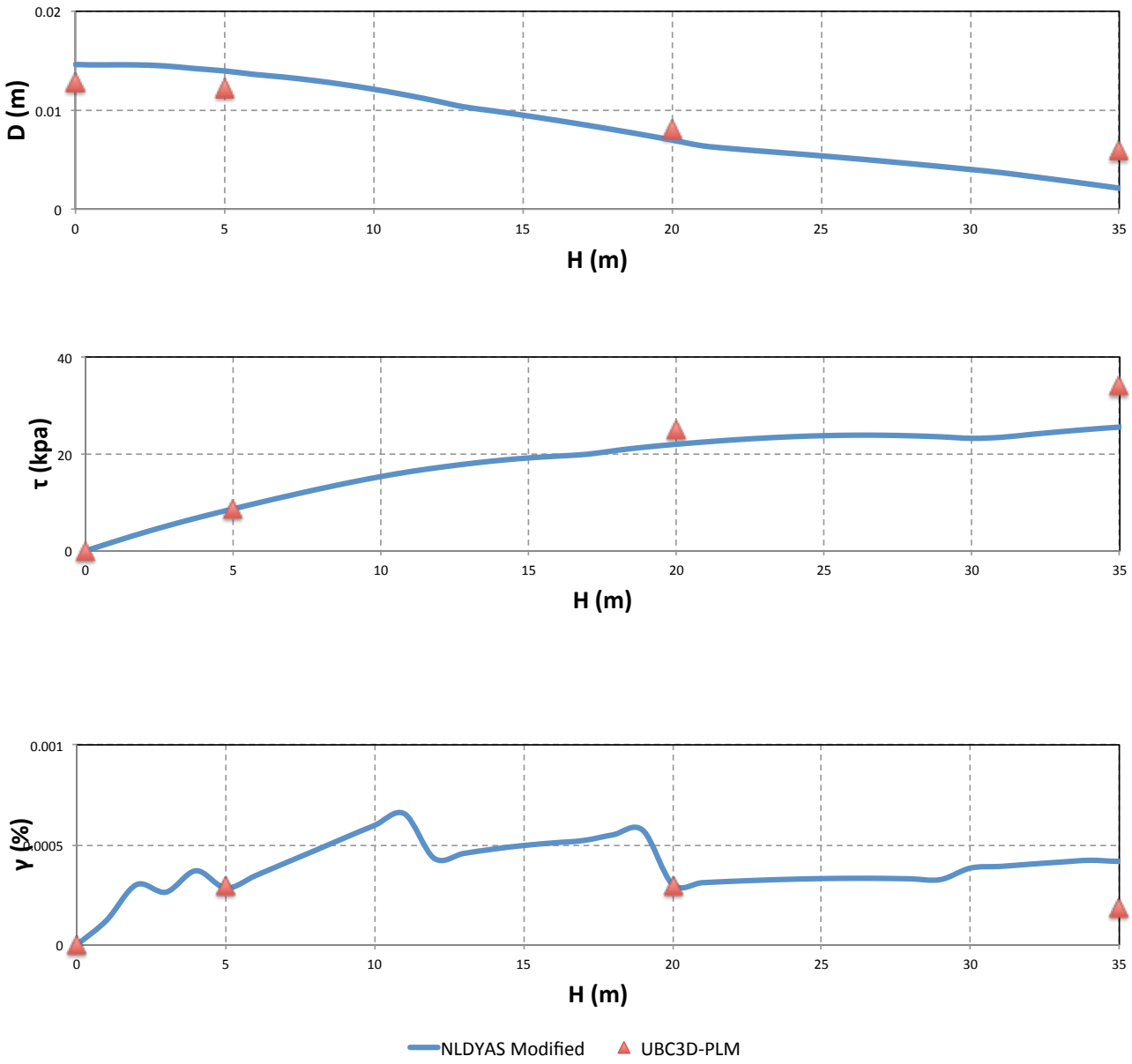

Figure 4.65 Maximums Comparison. *Charts featuring the maximum displacement, accelleration, stress and strain of the* ***Layered Soil Profile*** *analysed with* ***"NLDYAS modified"*** *and* ***"UBC3D-PLM"*** *compared and with the* ***Aegion excitation*** *for 0.05g*

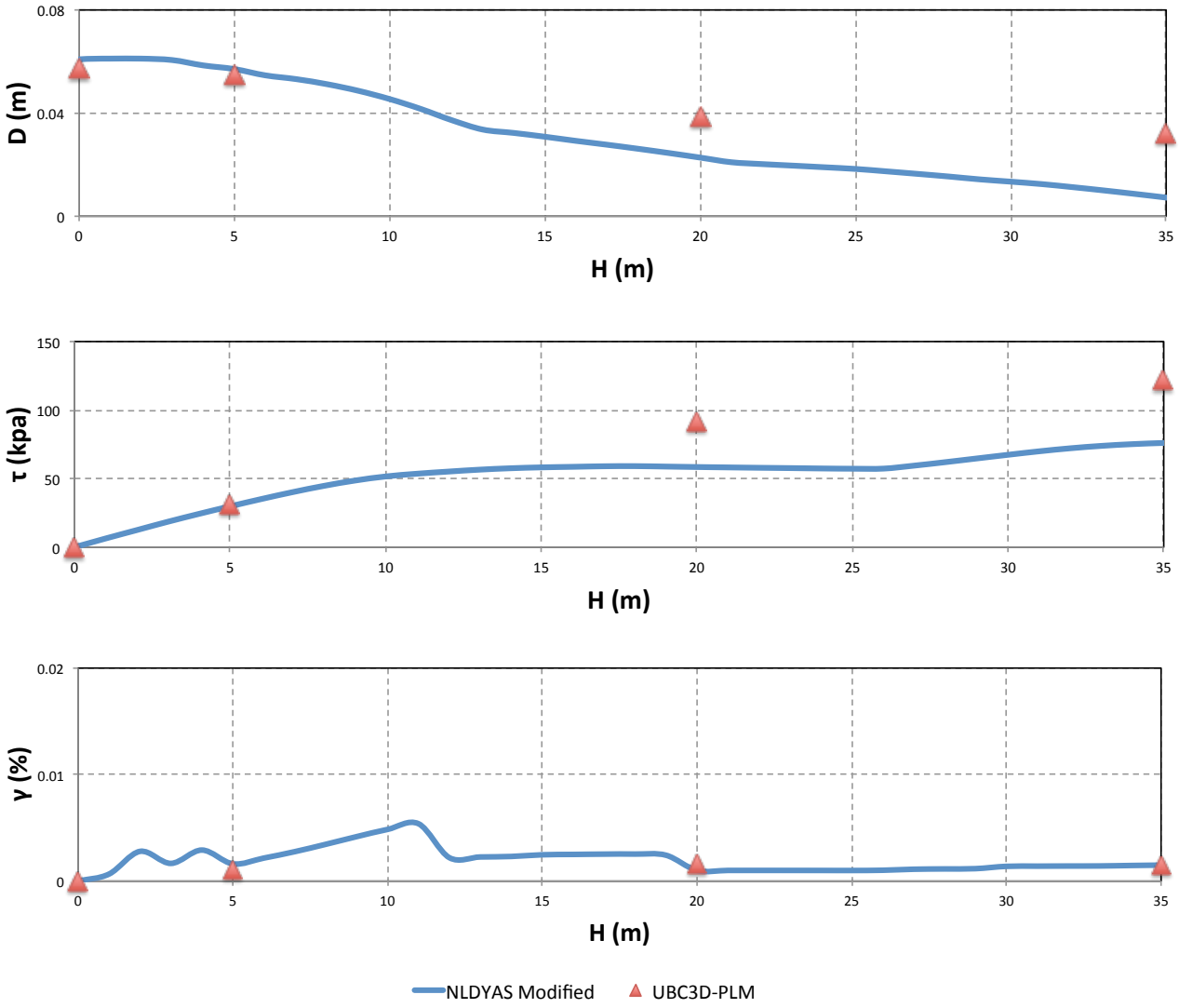

Figure 4.66 Maximums Comparison. *Charts featuring the maximum displacement, accelleration, stress and strain of the* ***Layered Soil Profile*** *analysed with* ***"NLDYAS modified"*** *and* ***"UBC3D-PLM"*** *compared and with the* ***Aegion excitation*** *for 0.25g*

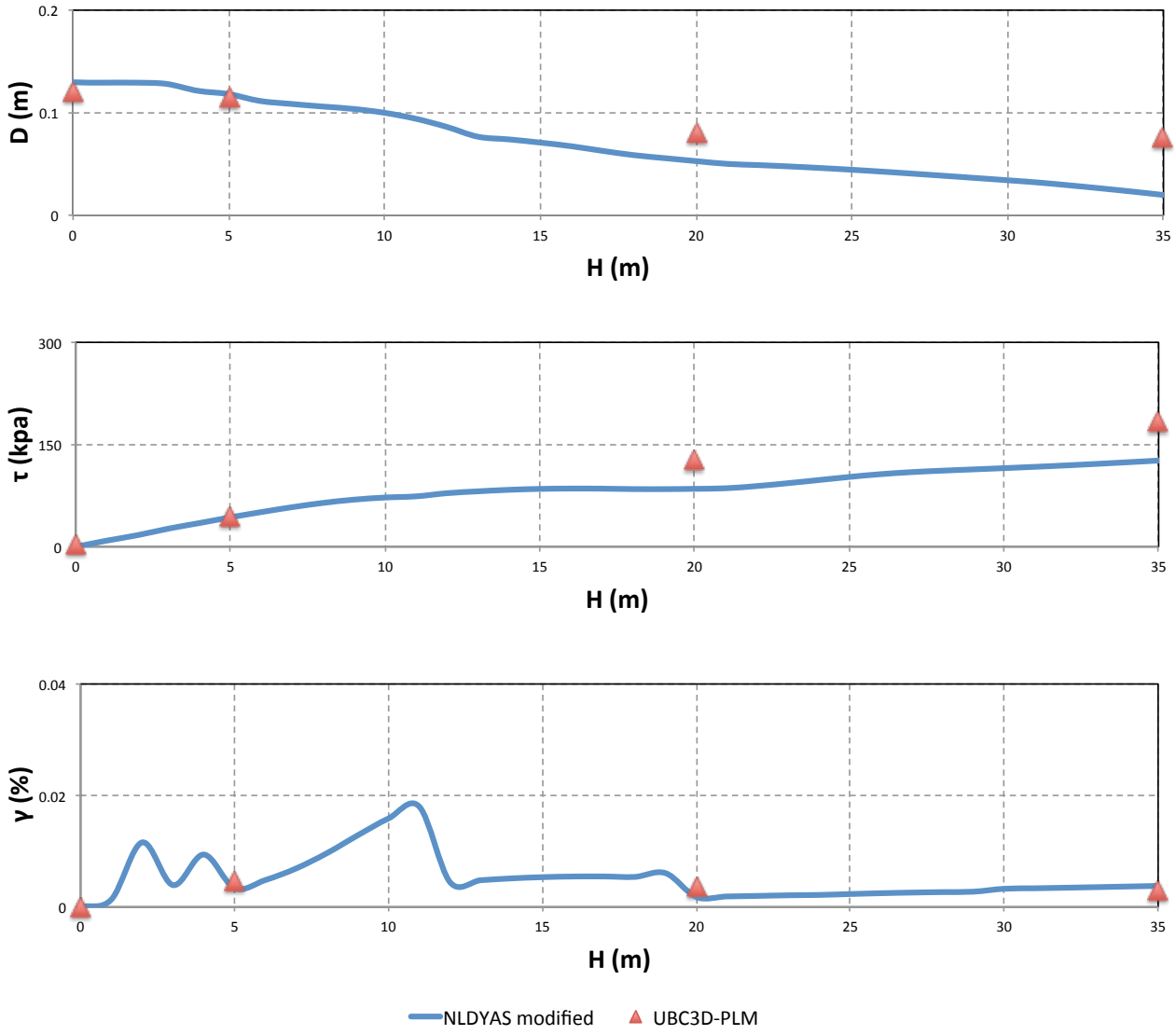

Figure 4.67 Maximums Comparison. *Charts featuring the maximum displacement, accelleration, stress and strain of the* ***Layered Soil Profile*** *analysed with* ***"NLDYAS modified"*** *and* ***"UBC3D-PLM"*** *compared and with the* ***Aegion excitation*** *for 0.60g*

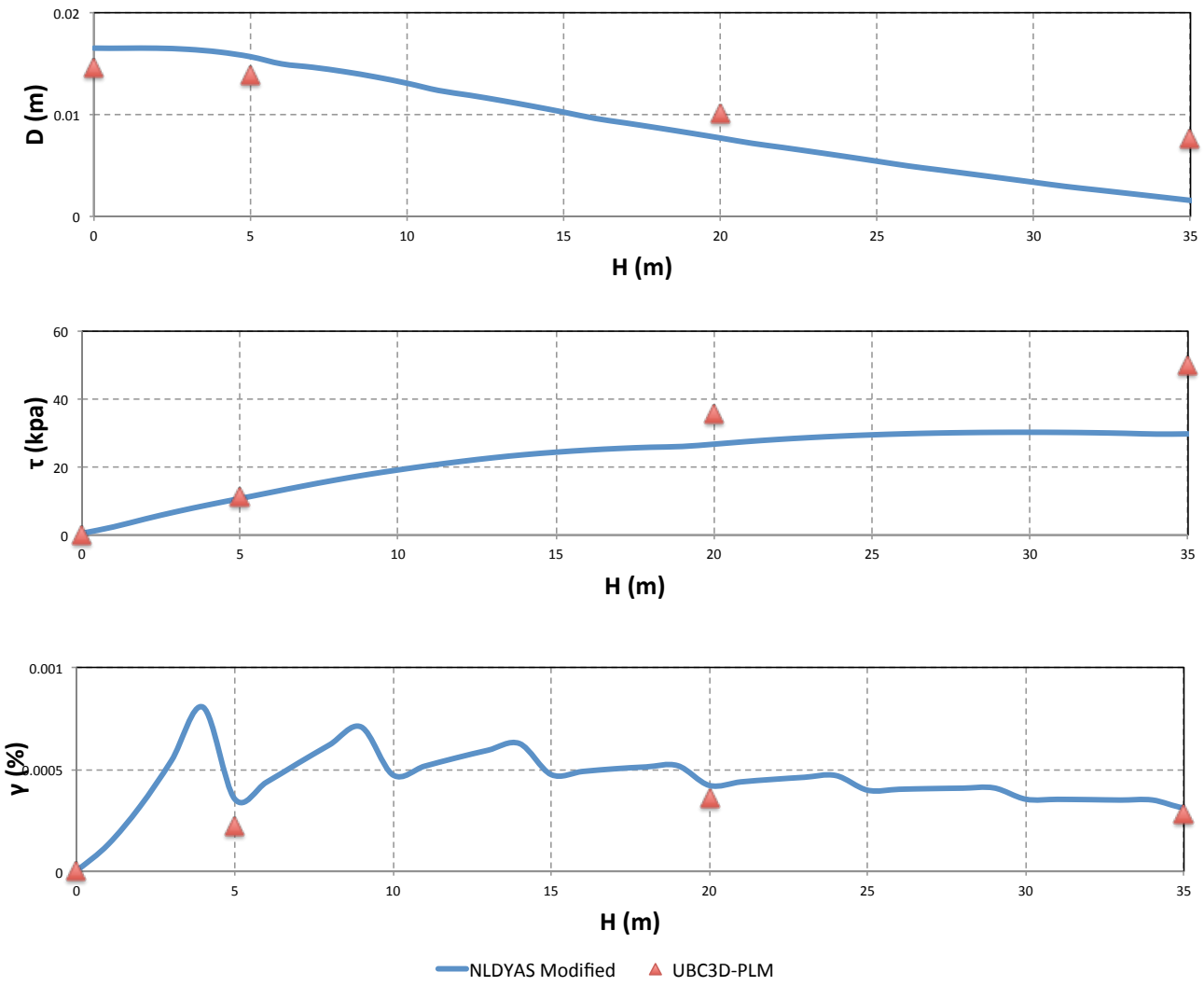

Figure 4.68 Maximums Comparison. *Charts featuring the maximum displacement, accelleration, stress and strain of the* ***Exponential Soil Profile*** *analysed with* ***"NLDYAS modified"*** *and* ***"UBC3D-PLM"*** *compared and with the* ***Aegion excitation*** *for 0.05g*

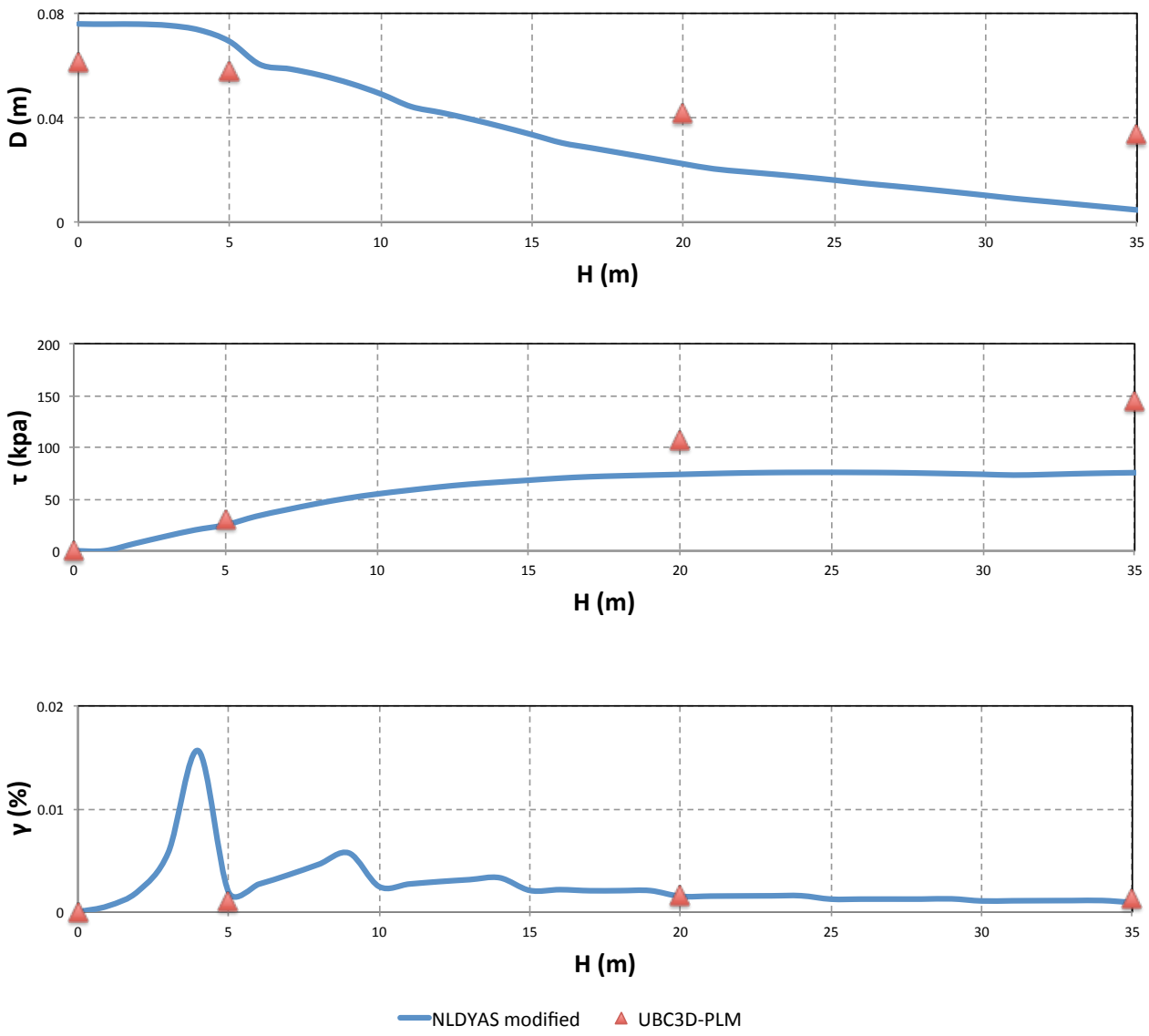

Figure 4.69 Maximums Comparison. *Charts featuring the maximum displacement, accelleration, stress and strain of the* ***Exponential Soil Profile*** *analysed with* ***"NLDYAS modified"*** *and* ***"UBC3D-PLM"*** *compared and with the* ***Aegion excitation*** *for 0.25g*

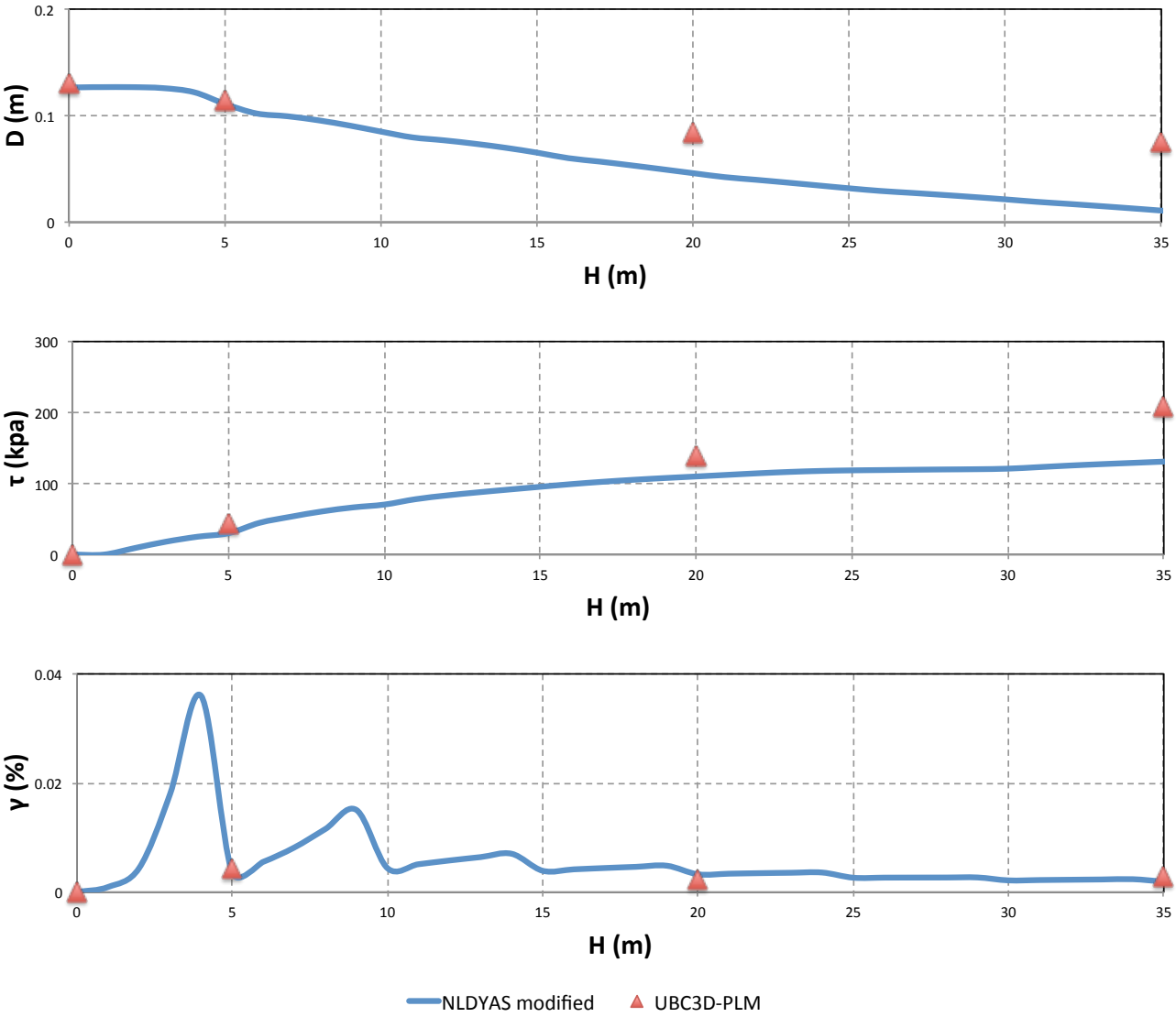

Figure 4.70 Maximums Comparison. *Charts featuring the maximum displacement, accelleration, stress and strain of the* ***Exponential Soil Profile*** *analysed with* ***"NLDYAS modified"*** *and* ***"UBC3D-PLM"*** *compared and with the* ***Aegion excitation*** *for 0.60g*

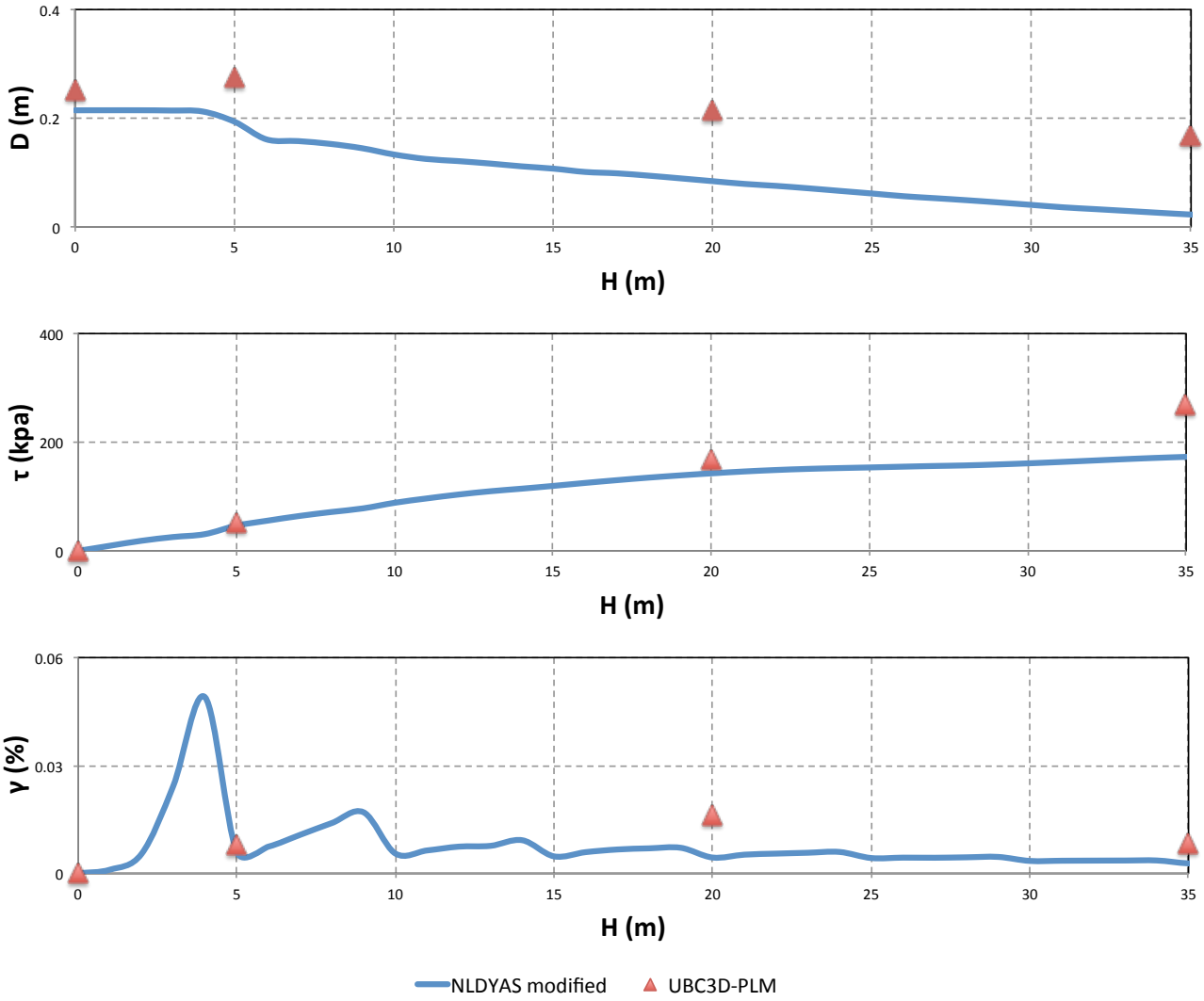

Figure 4.71 Maximums Comparison. *Charts featuring the maximum displacement, accelleration, stress and strain of the* ***Exponential Soil Profile*** *analysed with* ***"NLDYAS modified"*** *and* ***"UBC3D-PLM"*** *compared and with the* ***Lefkada excitation*** *for 0.60g*

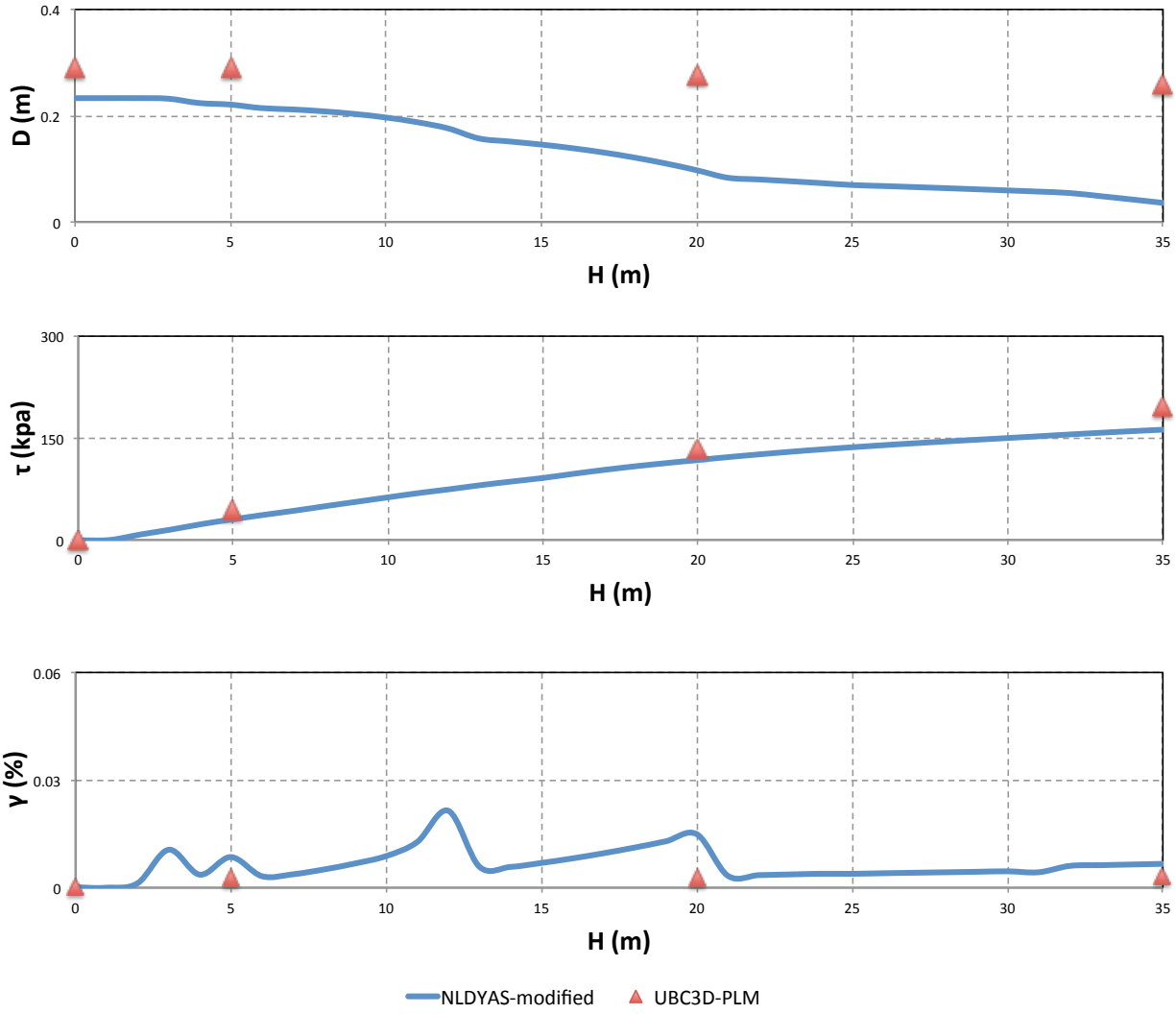

Figure 4.72 Maximums Comparison. *Charts featuring the maximum displacement, accelleration, stress and strain of the* ***Layered Soil Profile*** *analysed with* ***"NLDYAS modified"*** *and* ***"UBC3D-PLM"*** *compared and with the* ***Kobe excitation*** *for 0.60g*

CHAPTER 5

Conclusions & Recommendations

5.1 Final Words

A series of numerical experiments have been carried out in order to compare the non linear seismic responses of two different constitutive models. An optimization process has been proposed under a simplification and equation logic under basic rules that underly the models and verification and validation tests has been carried out subsequently. Experimental soil profiles has been developed in order to put into test the models under different seismic excitations and different seismic scales.

The optimization process is presented and the equation process proposed is described i detail. The process is proposed by taking in mind the specialties and parameters and the need to equate and simplify the two constitutive models in order to be comparable.

The BWGG model was also almost a perfect match under an idealized sinusoidal pulse resulting into same loops than the UBCSAND model for specific parameter choice proving a verification.

It is proven with various tests that on initial loading phase shear modulus is Gmax, while on unloading and on every unloading/reloading phase afterwards shear modulus is always 2*Gmax which is definetely unrealistic cand plays a major role into the discrepancies between the results.

Another discovery is that since UBC3D-PLM is a liquefaction model essentially, it has hardening mechanisms incorporated into it in order to combat overpressures. In order to achieve that it has a hardening modulus incorporated that increases KGp 5

times from 1st cycle and up to 11 times with 1 more time per cycle. This is a weak approach though for non-liquified soils

Even though there are a lot of gray areas since we can not fully equate the two models it is noticed that the two models produce a very close set of displacements. In terms of loops, spectrums and accellerations we dont have a suggestion that really stands out or a remark but since the new smooth hysteresis model achieves a very close curve fitting to bibliography and experimental data and UBCSAND although it has weaknesses in the realistic describing of hysteretic loops this doesnt say much on its abilities of describing nonlinear problems or giving detailed information on the actual soil behavior. At this point with some prejudice seem to be equally usefull on an engineers standpoint but a preference is geared towards the laboratory correct BWGG at least for 1-D problems.

The stress maximums are also very close in the comparison sector.

Even though UBCSAND has the known weakness of elastic unloading till the x-axis and the overcalculation of the damping ration up to the unrealistic levels of 63.7% it is not safe to suggest that its not usefull in non linear analyses. The above analyses have been done in order to clear as much as possible the uncertainties around the use of the two models.

It is understood that also K_G^e/K_G^p ratio plays a vital role into the behavior of the soil. Another optimization process in the future with a different ration than 1 can bring the results closer together. Although the suggestion was that a K_G^e/K_G^p ration equal to 1 is a way to go into the optimization due to reduce the unknow parameters, other ratio values can be used with greater overall success.

Equation the angles $\phi cv=\phi cp$ essentially brings the dilatancy up to zero, that doesnt guaranty that UBC3D-PLM understands it as such, further research is due to that dimension.

The fundamentally different loops show that the soil feels much more stiff in the UBC3D-PLM model, in that order there is a higher stress achieved for less strain. This can only be possible if the two models have the same Gmax at a really small value of strains

and then later UBC3D-PLM alters the loops via some kind of hardening rule that is yet to be defined.

Nevertheless further research and more scenarios must be executed in order to further understand the correlation as well as the validy of our or any optimization method for the models in the future although a thorough work has also been done in this thesis.

References

Gerolymos N., Gazetas G.“NLDYAS user’s manual” (2004)

Drosos V., Gerolymos N., Gazetas G. “Constitutive model for soil amplification of ground shaking: Parameter calibration, comparisons, validation”, Soil Dynamics and Earthquake engineering (2012) pp. 255-272

Petalas A., Vahid Galavi, “Plaxis Liquefaction Model UBC3D-PLM” (2013)

Gerolymos N., Souliotis C., Calibration Methodology for UBC3D-PLM constitutive soil model. Brief report-Part I: Monotonic DSS simulations (2015)

Gerolymos N., Gazetas G.“Constitutive model for 1D cyclic soil behaviour applied to seismic analysis of layered deposits”, Soils and Foundations, vol.45, No.3, 147-159 (2005)

Gerolymos N.PhD “Constitutive model for static and dynamic response of soil, soil–pile andsoil–caisson” chapters 1, 2 and 3

Gazetas G. Soil Dynamics notes N.T.U.A Publications (2007) pp. 43-148

Parpottas A. Gerolymos N. (2014) New smooth hysteresis model for the 1-D analysis of multilayered soil profile seismic response. Diploma Thesis